Analysis of The Inhibitory Activity And Mode of Action of Novel Antimicrobial Organic Nanoparticles

Thesis submitted in accordance with the requirements of the University of Liverpool for the degree of Doctor in Philosophy by Lee Michael Tatham.

September 2011

Table of Contents

List of Figures

List of Equations

List of Tables

Abbreviations

A	adenine
AIDS	acquired immunodeficiency syndrome
ATCC	American type culture collection
ATP	adenosine triphosphate
BAM	binary alignment map
BHI	brain heart infusion
BLAST	basic local alignment search tool
C	cytosine
cDNA	reverse-transcribed ribonucleicacid
CM	*Aspergillus* complete medium
CMC	critical micellisation concentration
DEPC	diethyl polycarbonate
DEX	dextran
dH_2O	distilled water
ddH_2O	double distilled water
DLS	dynamic light scattering
DMSO	dimethyl sulfoxide
DNA	deoxyribonucleicacid
dNTP	deoxynucleotide triphosphate
DOE	design of experiment
dsDNA	double stranded deoxyribonucleicacid
EDTA	ethylenediamine tetra acetic acid
ELS	electrophoretic light scattering
EO	ethylene oxide
G	guanine
HIV	human immunodeficiency virus
HPC	hydroxy propyl cellulose
HPLC	high performance liquid chromatography
HPMC	hydroxy propyl methyl cellulose
IPBC	Iodopropynyl butylcarbamate

LB	Luria broth
MBC	minimum bactericidal concentration
mer	repeat unit
MIC	minimum inhibitory concentration
MOA	mode of action
MLR	multiple linear regression
mRNA	messenger RNA
MWCO	molecular weight cut off
NCBI	national centre for biotechnology information
NGS	next generation sequencing
NNI	national nanotechnology initiative
NRSG	nanotechnology research strategy group
NSTC	national science and technology council
ORF	open reading frame
O/W	oil-in-water
PAGE	polyacrylamide gel electrophoresis
PBS	phosphate buffer saline
PCR	polymerase chain reaction
PEG	poly(ethylene glycol)
PLGA	poly(lactide-co-glycolide)
PLS	projections to latent structures
PO	propylene oxide
PVA	poly(vinyl alcohol)
PVL	Panton-Valentine leukocidin
PVP	poly(vinyl pyrolidone)
QELS	quasi-elastic light scattering
qPCR	quantitative polymerase chain reaction
RIN	RNA integrity number
RNA	ribonucleicacid
RNA-Seq	reverse-transcribed ribonucleicacid sequencing
RPKM	reads per kilobase of exon model per million mapped reads
rRNA	ribosomal ribonucleicacid

RT	reverse-transcription
SAGE	serial analysis of gene expression
SCMC	sodium carboxymethylcellulose
SDC	sodium deoxycholate
SDS	sodium dodecyl sulphate
SEM	scanning electron microscopy
S.E.M	standard error of the mean
SLES	sodium lauryl ether sulphate
SOLiD	sequencing by oligonucleotide ligation and detection
T	thymine
TAE	tris-acetate ethylenediamine tetra acetic acid
TBE	tris-borate ethylenediamine tetra acetic acid
TCA	tricarboxylic acid cycle
TE	tris ethylenediamine tetra acetic acid
TEM	transmission electron microscopy
UV	ultra violet
W/O/W	water-in-oil-in-water
XRD	x-ray diffraction
YEME	yeast extract malt extract

Units

°	degrees
%	percentage
≥	greater than or equal to
≤	less than or equal to
Å	Ångström
bp	base pairs
°C	degrees Centigrade
cfu	colony forming units
Da	Daltons
g	grams
g	1 x gravitational force
h	hours
Kb	kilo base pairs
kV	kilovolt
L	litre
M	moles per litre
m	meter
min	minutes
mg	milligrams
µA	microamperes
mA	milliamperes
µg	micrograms
ml	millilitres
µl	microlitres
µm	micrometres
mm	millimetres
mM	millimoles per litre
mN	millinewtons
mV	millivolts
MW	molecular weight

nA	nanoamperes
ng	nanograms
nm	nanometers
nt	nucleotide
O.D	optical density
pH	percentage hydrogen ion concentration
P_0	optimal partition coefficient
rpm	revolutions per minute
s	seconds
U	one unit of enzyme activity
V	volts
$^{v}/_{v}$	volume/volume
$^{w}/_{v}$	weight/volume
$^{w}/_{w}$	weight/weight

Acknowledgments

Firstly, I would like to thank my academic supervisors, Prof. Clive Edwards, Prof. Alan McCarthy and my supervisors from Iota NanoSolutions Dr. James Long, Prof. Steven Rannard and Dr. Alison Foster for their unwavering help, advice and support throughout my PhD. I am also grateful to Paul Loughnane for providing technical help and advice throughout my lab work, but more importantly, for introducing me to beer festivals.

I am also grateful to Dr. John Kenny for first introducing me to research science as an undergraduate and providing advice and support throughout my PhD. Although I do wonder if my quality of life would have been significantly better if you had told me to stay away from research at times! I am also extremely appreciative to the Biotechnology and Biological Sciences Research Council (BBSRC) and Iota NanoSolutions, who funded this work. I would like to thank Ian Wilson, Kieran Stancombe and Chris Parry who helped with various aspects of the nanoparticle screening work as part of their honours projects.

I would like to thank all the people that have made the office and lab such an interesting and enjoyable place to work over the past four years: Ben Libberton, Marta, Jen, Dave, James Houghton, Ben Baddley, Mark, Jo, Andy, James McDonald, Darren, Jay, Alex, Laura, Chris, Paul, Mike, Rachael, Elena, Azra and Giorgio. Whilst in Liverpool I have made some great friends who always gave me their encouragement and support. In particular I would like to thank Ross, Dave, and Co. for all the great nights out around town and helping me to forget about work!

Finally, a huge thanks to my Mum, Dad and brother Warren for all your encouragement, support and guidance throughout my studies and in everything else I've ever done. Without your support I couldn't have done this and I am eternally grateful.

To Mum and Dad

this is for you.

Abstract

Nanoparticles are difficult to define specifically but usually encompass engineered particles ranging in size from 1 to 1000 nm. The physical and chemical properties of nanoparticles can vary significantly from those of their bulk counterparts largely due to their large surface area to volume ratios. Approximately 40% of antimicrobial agents emerging from development programs exhibit low solubility. This results in inadequate bioavailability, pharmacokinetics and stability. The use of appropriate nano-carriers has been shown to improve the efficacy of antimicrobial agents with the explanation that the biodistribution of the antimicrobial follows that of the carrier rather than being dependent on the physiochemical properties of the compound itself. Therefore characteristics such as solubility and bioavailability can be enhanced.

Here, a range of poorly water-soluble antifungal agents, biocides and an antibiotic were processed using a novel emulsion-evaporation technique to produce organic nanoparticles. These preparations were characterised on the basis of size and zeta potential and tested for inhibitory activity against relevant microorganisms including: *C. albicans*, *E. coli*, *S. aureus* and MRSA. Nanoparticle formulated antimicrobials were usually more inhibitory than the equivalent co-solvent dissolved antimicrobials or water dissolved salt equivalents where available. However, efficacy was dependent on nanoparticle composition.

Optimisation of nanoparticle dichlorophen inhibitory activity was attempted using a generic polymer and surfactant screen. The results were subsequently utilised in a computer modelling design approach. Due to formulation problems, predictive optimisation was not possible. However, nanoparticles of dichlorophen were usually most inhibitory when increased loading ratios of sodium dodecyl sulphate and hydroxy propyl methyl cellulose and reduced loading ratios of dichlorophen and gelatin were used in the preparation. No correlations between particle size, zeta potential and inhibitory activity were identified.

No correlation between the inhibitory activities of blank nanoparticles and active equivalents were identified. A detailed series of controls prepared for one formulation usually produced low MIC values. However, the nanoparticle formulation exhibited the greatest efficacy. This suggested that enhanced activity due to nanoparticle formulation of the antimicrobial was not simply attributed to a synergistic effect between the different materials.

The molecular response of *S. aureus* SH1000 to nanoparticle-formulated ciprofloxacin was investigated using RNA-Seq. All 5 investigated treatments induced differential gene expression. Moreover, comparative analysis between nanoparticle formulated and DMSO dissolved ciprofloxacin treated *S. aureus* SH1000 revealed the differential expression of 61 transcripts. No significant differential expression in DNA repair and replication targets was observed. This suggested that ciprofloxacin may not be more bioavailable to *S. aureus* SH1000 and therefore enhanced efficacy is not attributed to increased bioavailability. However, genes involved in stress response and cell division were shown to be up regulated in response to nanoparticle delivery. The results also revealed that 39 transcripts were differentially expressed due to nanoparticle exposure alone and these included stress response, cell division and virulence-associated genes. The identified differentially expressed transcripts are unlikely to account for the enhanced efficacy associated with nanoparticle delivery.

Nanoparticles represent a novel approach to the delivery of hydrophobic antimicrobials in aqueous dispersions. The advantageous features of nanoparticles are discussed throughout this thesis. The study used a variety of approaches with the aim of elucidating the mechanisms underpinning the observed enhancement in antimicrobial activity. The improved efficacy observed could not be correlated with any physical characteristics of the particles used. The transcriptional profiling results suggested that the improved antimicrobial activity observed was not associated with differential molecular targeting, and challenges current concepts that link enhanced efficacy with increased bioavailability.

Chapter 1

Introduction

1.1 Antimicrobial development and resistance

Antimicrobials are natural or synthetic chemicals that kill or inhibit the growth of bacteria, fungi and viruses (Greenwood *et al.*, 2007). Since the introduction of sulphonamides in the 1930s and penicillin in the 1940s, many new classes of antimicrobial compounds have been developed. The emergence of resistance to these compounds was soon recognised as a considerable clinical problem and during the past 10 – 15 years, numbers of antibiotic resistant organisms have steadily increased (Norrby *et al.*, 2005). Despite these threats to public health, most large pharmaceutical and many biotechnology companies have reduced or closed antibacterial research and development programs (Christoffersen, 2006). Many factors have contributed to this decline; *e.g.* because treatment for bacterial infections is normally only given for a short time period and better return on investments can be made in developing drugs for treating chronic long-lived diseases (Payne *et al.*, 2007). Increased development costs caused, in part, by increased demands from regulatory authorities and stringent price controls mean that the total cost for antimicrobial development is estimated to be €500 – 800 million and is rarely completed in less than 4 to 6 years before administration to humans (Norrby *et al.*, 2005). As a result, very few novel antimicrobial compounds are being developed and therapeutic options for microbial pathogens are currently extremely limited. The situation has forced clinicians to use older, previously discarded drugs that may have significant toxicity and for which there is a lack of data to guide selection of dosage regime or duration of therapy (Boucher *et al.*, 2009).

Biocides play an important role in limiting the potential sources of infection. Resistance to biocides is less common and likely to reflect the multiple targets within the cell as well as the general lack of known detoxifying enzymes (Poole, 2002). However there is concern about the increasing use of biocides in the community leading to resistance

development and the potential for cross-resistance with clinically important antibiotics (Levy, 2000).

Invasive fungal infections are also an increasing threat to human health. In the developed world these infections usually occur when aggressive immunosuppressive therapies are used. The overall mortality for invasive diseases caused by *Candida* spp. and *Aspergillus* spp. is 30-50% despite new diagnostic and therapeutic strategies (Denning & Hope, 2010). The high degree of phylogenetic relatedness between fungi and humans means that there are few differential targets to be exploited for antifungal drug development (Cowen, 2001). Resistance to antifungals is of growing concern in both clinical and agricultural settings, but in contrast with bacteria, resistance cannot be transferred between fungal cells (Norrby *et al.*, 2005).

Fourteen crop plants provide the bulk of food for human consumption and at least 10% of global food production is lost to disease. Globalisation of agriculture has meant that crop plants, often with a narrow genetic base, are now grown far from their centres of origin and therefore far from the pathogens that co-evolved with them. The over-reliance on a narrow range of crops for food production, intensive farming methods and the global transportation of crops, intensifies the risks posed by fungal pathogens and the spread of antifungal resistant strains (Strange & Scott, 2005). Antifungal agents currently used include: polyenes, pyrimidine analogues, allylamines, azoles, echinocandins and strobilurins (Meneau & Sanglard, 2005 ; Denning & Hope, 2010).

The use of antimicrobials for prophylactic or therapeutic purposes in humans or for veterinary or agricultural purposes, has provided the selective pressure favouring the survival and spread of resistant organisms (Bax *et al.*, 2000). Genomics has not yet delivered the anticipated novel target identification and subsequent therapeutics (Payne *et al.*, 2007). A large proportion, ~40%, of new antimicrobial candidates emerging from development programs are either insoluble or poorly soluble in water, which results in inadequate bioavailability, pharmacokinetics and stability (Rabinow, 2004 ; Kingsley *et al.*, 2006). Various research efforts have been undertaken which aim

to overcome these issues, particularly for orally administered antimicrobials, where the free compound often exhibits low systemic bioavailability attributed to premature degradation and inadequate solubility in the gastrointestinal tract (Pandey *et al.*, 2005). The ability to improve solubility of previously discarded, currently used and future antimicrobials may offer some practical answers to the present and growing shortage of usable antimicrobials in clinical, veterinary and agricultural applications.

1.2 Antimicrobial delivery methods

A need has always existed for effective and safe delivery of poorly water-soluble drugs. Insolubility is caused by a molecule's limited ability to hydrogen bond with water (hydrophobicity) or by difficulty in breaking apart molecules in the solid state (high lattice energy). Water has the ability to form molecular clusters that are tightly interlinked through hydrogen bonding. In order to dissolve, a solute must successfully compete with these strong intermolecular and intramolecular interactions. Dissolution therefore requires modification of the solid phase to reduce lattice energy (Kipp, 2004). Conventional approaches used to solubilise, poorly water-soluble antimicrobials include: the use of water soluble salts or esters of the parent substance or the use of excessive amounts of co-solvent to dissolve the antimicrobial. Significant pressure exists to reduce the use of organic co-solvents due to health and environmental toxicity concerns (Tomlin, 1995 ; Allen Jr, 2008 ; Duncalf *et al.*, 2008). Another approach used is the chemical modification of antimicrobials by covalent conjugation with polyethylene glycol (PEG) to improve solubility, a process described as PEGylation (Veronese & Mero, 2008). Many researchers are making efforts to discover new classes of antimicrobial compound, but some studies are focused on improving currently available antimicrobials by chemical modifications. The best prospect for achieving improvements over current therapies will occur through better delivery of existing or as yet undiscovered compounds so that they can overcome the barriers that prevent them reaching their target sites. These novel delivery systems can address and correct problems related to physical characteristics, including solubility and stability (Kabanov *et al.*, 2002). Examples of nano-scale delivery platforms used for antimicrobials include micelles, liposomes, and nanoparticles.

Micellisation occurs when amphiphilic molecules self-assemble into micelles in aqueous solutions. The critical micelle concentration (CMC) is defined as the concentration at which micelles are formed (Heerklotz, 2008). Polymeric micelles (Figure 1.1) are formed by self-assembly of block copolymers consisting of two or more polymer chains with different hydrophobicity. Spontaneous assembly into core-shell micellar structures occurs in an aqueous environment when the CMC is reached, to minimise the system's free energy. The hydrophobic inner core of the micelle can be used to 'solubilise' water insoluble compounds (Zhang *et al.*, 2008b). Micelles have been evaluated and found to be efficient delivery systems in multiple pharmaceutical applications in drug and gene delivery processes. Numerous micelle structures produced from block copolymers have been developed for gene delivery. These molecules react with DNA to produce polymer complexes. The underlying characteristic of these technologies, is that the DNA is condensed, protected from degradation and permitted enhanced transport into the cell, which has been shown to increase trans-gene expression (Kabanov *et al.*, 2002 ; Kabanov *et al.*, 2005). Venne *et al.* (1996) demonstrated that the cytotoxic effects of doxorubicin in tumours with multidrug-resistance phenotypes, increased when mixed with block copolymers.

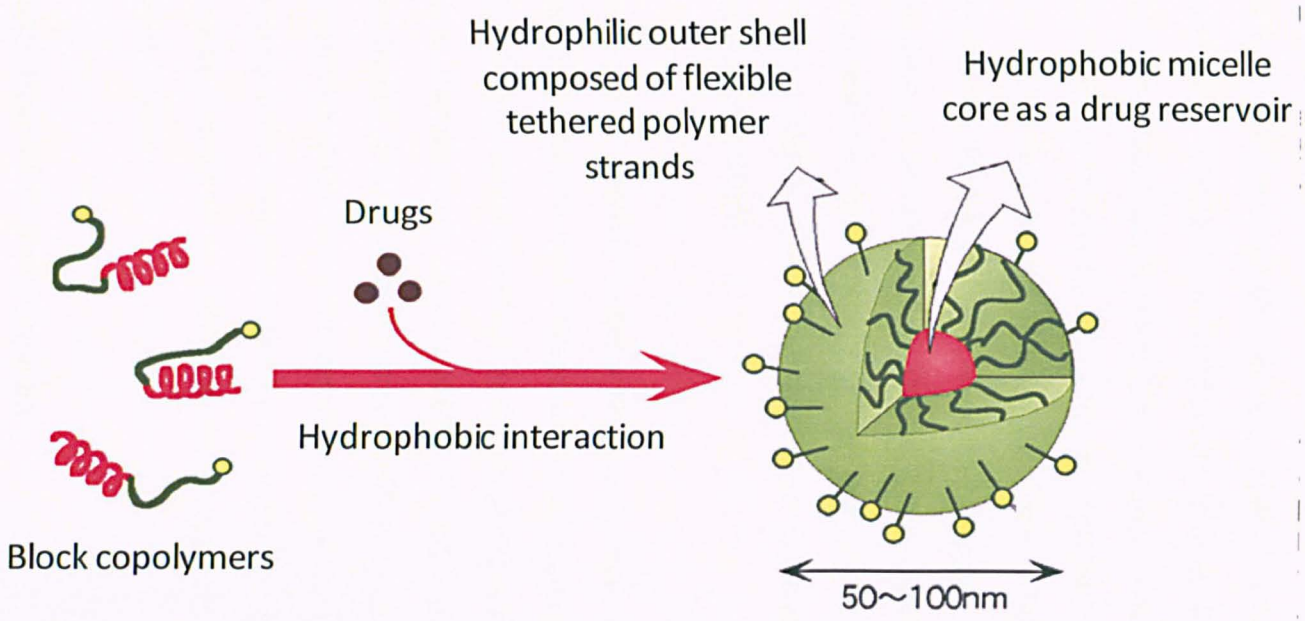

Figure 1.1 Polymeric micelles as carriers for drug delivery. Block copolymers with amphiphilic character spontaneously assemble into polymeric micelles, with a unique core-shell structure in which an inner core, serving as a nanocontainer of hydrophobic drugs, is surrounded by an outer shell of hydrophilic polymers. Adapted from Nishiyama & Kataoka (2006).

Liposomes are spherical vesicles ranging in size from 20 nm to 10 μm in diameter and consist of one or more phospholipid bilayers surrounding an inner water space (Ulrich, 2002). Vesicle formulations are usually based on natural or synthetic phospholipids and cholesterol. Advantages of liposomal formulated antimicrobials include improved pharmacokinetics and bioavailability, decreased toxicity and enhanced activity against intracellular pathogens (Webb *et al.*, 1998). Liposomes can encapsulate both hydrophilic and hydrophobic compounds (Petros & DeSimone, 2010). Numerous antibiotics have been encapsulated in liposomes, and have been shown to be more effective than the free drug. Liposome encapsulated antimycobacterial agents, *e.g.* amikacin and streptomycin, have been used effectively against *Mycobacterium tuberculosis* infections and shown to be more inhibitory than comparable amounts of the free drug in animal models (Salem *et al.*, 2005). Disadvantages of liposomal formulated antimicrobials include short-shelf life, physical instability and expensive preparation methods that are not always possible to scale up (Drulis-Kawa & Dorotkiewicz-Jach, 2010).

Nanoparticle drug delivery systems have gone from scientific curiosities to areas of active research and are now utilised in clinical applications. In particulate delivery, a distinction is made between micro and nanoparticles and usually refers to the particle dimensions (Farokhzad & Langer, 2009). The differences in size, gives each class of particle different properties and therefore different applications. Examples of research using antimicrobial loaded microparticles include the use of novel microbial inhibitors such as propolis, a resin produced by bees (Bruschi *et al.*, 2006), antibiotics such as ciprofloxacin (Arnold *et al.*, 2007) and antifungal compounds such as tebuconazole (Asrar *et al.*, 2004).

1.3 Nanoparticles and Nanotechnology

Nanoparticles are difficult to define; they are usually described as engineered particles ranging in size from 1 to 1,000 nm (Kreuter, 1991 ; Petros, 2010). However others describe nanoparticles as engineered materials at the atomic and molecular scale of 1 to 100 nm (Zhang *et al.*, 2008b ; Farokhzad & Langer, 2009). Nanoparticles can be made of chemically diverse materials. The most common nano-materials include

metals, metal oxides, silicates, non-oxide ceramics, polymers, organics, carbon and biomolecules. Nanoparticles can exist in several different morphologies such as spheres, cylinders and tubes and can be designed with surface modifications to meet the specific applications for which they are intended (Nagarajan, 2008). The physical and chemical properties of nanoparticles vary significantly from those of their bulk counterparts. Nanoparticles have unique properties resulting from their ultra small size that gives a large surface area to mass ratio and hence a high fraction of atoms / molecules, constituting the nanoparticle, on the particle surface rather than in the particle interior, which increases reactivity. These features mean that nanoparticles can often differ functionally from bulk materials of the same composition (Zhang *et al.*, 2008a). Nanoparticles already have significant importance in a range of applications; as dispersion colours (Lvov *et al.*, 2010), they play an important role in the formation of pigments (Meng *et al.*, 2010) and in the production of catalysts; in the production, transportation and storage of energy (Serrano *et al.*, 2009 ; Teki *et al.*, 2009); as quantum dots with special properties for electronic components; in biological applications used in DNA processing (Kanaras *et al.*, 2007); to deliver nanoparticulate forms of pharmaceutically active compounds specifically to the desired site of action in the body (Horn & Rieger, 2001). Nanoparticles can be synthesised by a variety of methods using gas, liquid or solid phase processes. These include high temperature evaporation, microwave irradiation, physical and chemical vapour decomposition synthesis, colloidal or liquid phase methods in which chemical reactions in solvents lead to the formation of colloids, molecular self-assembly and mechanical processes of size reduction including grinding and milling. Details of common methods employed for organic nanoparticle formation processes are outlined in section 1.6. In 2007, more than 470 products included some form of nanotechnology. Many of these products address consumer needs in health-care, electronics and computers, food and beverage, automotive and appliance industries (Nagarajan, 2008). Nanotechnology undoubtedly presents a major opportunity for the economic and technological development of many countries; current predictions estimate the value of global nanotechnology industry at $1 trillion per annum by 2015 (Defra, 2007).

1.3.1 Carbon Nanotubes

Carbon nanotubes and quantum dots are two examples of developing nanotechnologies for multiple applications. Carbon nanotubes are well ordered hollow graphite nanomaterials with lengths from several hundred nanometres to several micrometres and diameters of 0.4-2 nm for single walled nanotubes and 2-100 nm for multi-walled carbon nanotubes (Cheung *et al.*, 2010). The structure of single walled nanotubes can be viewed as wrapping up a graphene sheet into a seamless hollow cylinder. The structure of multi walled nanotubes can be viewed as several co-axially arranged single walled nanotubes of different radii. Carbon nanotubes are the strongest materials yet discovered, have heat transmission capacity greater than natural diamond and semiconducting properties greater than all known semiconductors (Zhou *et al.*, 2005). The densely packed carbon atom structure arranged in a honeycomb lattice can partially explain these unique properties. Carbon nanotubes have also been explored for potential biological applications. With all atoms exposed on the surface of single walled nanotubes, they have an ultrahigh surface area that permits efficient attachment of multiple molecules along the length of the nanotube sidewall. The flexibility of nanotubes may allow them to bend and afford multiple binding sites of a functionalised nanotube material to one cell, leading to a multi-valence effect and improved binding affinity of nanotubes conjugated with targeting ligands (Cheung *et al.*, 2010). Carbon nanotubes have been explored as novel drug delivery devices. Pristine single walled carbon nanotubes have been shown to exhibit an antimicrobial effect in a size-dependent manner, indicating they might be useful as building blocks for antimicrobial therapeutics (Kang *et al.*, 2008). Organic modification of carbon nanotubes can also generate sites for the attachment of bioactive molecules and therefore they have been proposed for use in antimicrobial and antitumor chemotherapy applications. Developments have also been made in the use of carbon nanotube based tissue engineering and regenerative medicine. They can be used as additives to reinforce the mechanical strength of tissue scaffolding and conductivity by dispersing them in a polymer or used to improve the extracellular matrix (Zhang *et al.*, 2010a).

1.3.2 Quantum dots

Luminescent semi-conductor nanocrystals or quantum dots are inorganic fluorescent nanocrystals. As a photon of energy impinges a semiconductor, exciting an electron from the valence band into the conduction band, it generates an electron-hole pair that is weakly bound. For semiconductor nanocrystals with dimensions less than a few nanometres, their energy levels are quantized, which can be controlled by crystal sizes (Nirmal & Brus, 1998). This effect leads to superior optical properties of quantum dots, such as narrow, symmetric and size adjustable emission spectra. The benefits of quantum dots over organic flurorophores or fluorescent proteins include stronger fluorescence and greater fluorescence stability against photo bleaching, which facilitates long term monitoring of intermolecular and intramolecular interactions in cells and organisms. Quantum dots have been utilised for intracellular drug and gene trafficking. For example, functionalised quantum dots have been used as intracellular tracers of plasmid DNA. Quantum dot aptamer doxorubicin conjugate has been developed for simultaneous cancer imaging and traceable drug delivery (Ho & Leong, 2010).

1.3.3 Gold and silver nanoparticles

Materials can be assembled on, encapsulated within, or integrated both inside and on the surface of inorganic nanoparticles using different chemistries and techniques to create multifunctional nanosystems (Sekhon & Kamboj, 2010). After silicon, gold is probably the most frequently used element in nano-scale science, and gold nanoparticles have been used for longer than any other metal. Most current uses of gold nanoparticles in the 1 to 100 nm range utilise ligand-stabilisation usually via thiol moieties. The ability to obtain stable gold nanoparticles and their unique physical and chemical properties has led to widespread use of these systems in life science applications (Hutchings *et al.*, 2008). Gold nanoparticles undergo a localised surface plasmon resonance or electron oscillation with light that can be exploited to generate a colour change or produce localised heating. These features have been exploited in cancer therapy through the selective photo-thermal heating and killing of cancer cells (Sekhon & Kamboj, 2010). Gold nanoparticles have also been shown to be effective in the detection and identification of bacteria through the use of DNA probes based on

the nanoparticle, or functionalised with specific oligonucleotide sequences that allows identification based on colour change processes. Gold nanoparticles are stable, non-toxic platforms on which pharmaceutical compounds can be attached and delivered from. The antibiotics ciprofloxacin, streptomycin, gentamicin, neomycin, ampicillin and vancomycin have been suitably conjugated to gold nanoparticles. Gold nanoparticle conjugates of antimicrobials are often more inhibitory compared with the same concentration of the antibiotics used alone (Pissuwan *et al.*, 2010). Kanaras *et al.* (2007) demonstrated the enzymatic cleavage of DNA-gold nanostructures using restriction enzymes. The authors note that the ability to manipulate DNA enzymatically in these processes is an important proof-of-principle in the development of hierarchical chemical methods of nanoscale assembly, and could find applications in the controlled release of proteins or other biomolecules. The use of gold nanoparticles is evident in a wide range and growing number of biological applications.

Silver has been used in the treatment of burns and chronic wounds for centuries and was the major weapon against wound infections in World War I until the advent of antibiotics. Metallic silver in the form of silver nanoparticles has made a comeback as a potentially important antimicrobial agent that may offer solutions to the problems associated with the development of antimicrobial resistance amongst pathogenic bacteria (Rai *et al.*, 2009). Silver nanoparticles have been synthesised through a range of methods and particle morphologies include spheres, rods, cubes and wires, normally within a size range of <100 nm (Chen & Schluesener, 2008). The antimicrobial activity of silver nanoparticles utilising a range of preparation techniques has been well documented and subsequently, they have emerged in diverse medical applications such as wound dressings, silver coated medical devices and in nanoparticle solutions (Rai *et al.*, 2009 ; Sekhon & Kamboj, 2010). For example, the nano-silver wound dressing product Acticoat™ (Smith & Nephew - www.smith-nephew.com) is available on the market for the treatment of a range of wound infections.

1.4 Organic nanoparticles and delivery of poorly water-soluble compounds

Nanosuspensions consist of sub-micron colloidal particles of active ingredients, which are stabilised by excipients such as surfactants and polymers. If particles in a

nanosuspension approach each other too closely, they will agglomerate. This must be prevented to ensure a stable system. By combining polymers and charged surfactants that complement each other, it should provide the necessary repulsive barrier between two neighbouring particles to prevent particle growth (Rabinow, 2004).

Nanosuspensions can be used for compounds that are water insoluble but soluble in oil (high log P) or for 'brick dust' compounds that are both water and oil insoluble. Although lipid based systems can be used to formulate some of these compounds as well; nanoparticles are the preferred option particularly when no other approach will work (Rabinow, 2004). According to the Noyes-Whitney equation (1.1), reducing a particles size and therefore increasing the surface area, will increase the dissolution rate of poorly water soluble drugs, thereby addressing issues related to poor bioavailability (Hu *et al.*, 2004).

$$\frac{dC}{dt} = \frac{AD\,(Cs - C)}{h} \qquad (1.1)$$

Equation 1.1 The Noyes-Whitney equation to describe the dissolution rate of a particle, where dC/dt is the rate of dissolution, A is the surface area of the particle, D is the diffusion coefficient, Cs is the apparent solubility of the drug in the dissolution medium, C is the concentration of the drug in the dissolution medium at time t and h is the thickness of the diffusion boundary layer. The rate of dissolution can be improved by creating particles that have a high surface area and improved wet-ability or by increasing the solubility of the drug. It is theorised that nanoparticles may be able to supersaturate within the dissolution medium owing to Ostwald ripening. Small droplets of liquid dispersed in a gas-liquid medium evaporate more rapidly than large droplets owing to increased curvature at the droplet surface, which raises the vapour pressure of the liquid. This theory has been suggested to apply to solid-liquid interfaces as well. By decreasing the size of solid particles or by creating a more uniform distribution, the high energy state that is achieved will increase the extent to which it can dissolve owing to an increased dissolution pressure (Williams & Vaughn, 2006).

When two particles with different radii are placed into a solvent, each particle will develop equilibrium with the solvent. The solubility of the smaller particle will be greater than that of the larger particle. Consequently, there would be a net diffusion of solute from the small particle to the larger particles proximity. To maintain equilibrium, solute will deposit onto the surface of the large particle, whereas the small particle has to continue dissolving, to compensate for the amount of solute diffused away. As a result, the small particle gets smaller and the large gets larger a process known as Ostwald ripening. The rate of Ostwald ripening depends on the transport mechanism for molecules from the small particle to reach the large. The process results in abnormal particle growth, leading to inhomogeneous solutions and must be considered when designing particles (Morrison & Ross, 2002 ; Cao, 2004).

Increasing numbers of nanoparticle preparation methods for the delivery of poorly water-soluble drugs aimed at a variety of applications are evident in the literature. The active ingredient in nanosuspensions can be dissolved, entrapped, encapsulated or attached to the nanoparticle matrix depending on the methods of preparation and can be optimised for activity (Soppimath *et al.*, 2001). Several nanoparticle therapeutics, produced principally using mechanical milling or synthesis reactions that generate liposomal and polymeric nanosuspensions, have been successfully introduced for the treatment of cancer, pain and infectious diseases, outlined in Table 1.1, and numerous products are currently under clinical testing or entering pipelines. These therapeutics use the opportunities provided by nanomaterials to target delivery of drugs, to improve their solubility, to extend their half-life, improve therapeutic index and reduce immunogenicity (Petros & DeSimone, 2010).

Table 1.1 Clinically approved nanoparticle based therapeutics. Table adapted from Zhang *et al.*, (2008b).

Composition	Trade name	Company	Indication
Liposomal platforms			
Liposomal amphotericin B	Abelcet	Enzon	Fungal infections
Liposomal amphotericin B	AmBisome	Gilead Sciences	Fungal and protozoal infections
Liposomal cytarabine	DepoCyt	SkyePharma	Malignant lymphomatous meningitis
Liposomal daunorubicin	DaunoXome	Gilead Sciences	HIV related Kaposi's sarcoma
Liposomal IRIV vaccine	Epaxal	Berna Biotech	Hepatitis A
Liposomal morphine	DepoDur	SkyePharma, Endo	Postsurgical analgesia
Liposomal-PEG doxorubicin	Doxil/Caelyx	Ortho Biotech, Schering-Plough	HIV related Kaposi's sarcoma, metastatic ovarian cancer
Polymeric platforms			
Methoxy-PEG-poly(DL-lactide) taxol	Genexol-PM	Samyang	Metastatic breast cancer
PEG-adenosine deaminase	Adagen	Enzon	Severe combined immunodeficiency disease associated with adenosine deaminase deficiency
PEG-anti-vascular endothelial growth factor aptamer	Macugen	OSI Pharmaceuticals	Age-related macular degeneration
PEG-hepatocyte growth factor	Somavert	Nektar, Pfizer	Acromegaly
Poly(allylamine hydrochloride)	Renagel	Genzyme	End stage renal disease
Other platforms			
Albumin bound paclitaxel	Abraxane	Abraxis BioScience, AstraZeneca	Metastatic breast cancer
Nanocrystalline aprepitant	Emend	Elan, Merck	Antiemetic
Nanocrystalline fenofibrate	Tricor	Elan, Abbot	Anti-hyperlipidemic
Nanocrystalline sirolimus	Rapamune	Elan, Wyeth	Immunosuppressant

1.5 Nanoparticle Safety, Regulation and Environmental persistence

The introduction of all new technologies have unexpected consequences, both beneficial and harmful. The ability to control matter at nanometer scales is leading to technological advances in many areas, including energy, medicine and the environment. Developments in nanotechnology also represent potential economic and social benefits. However, the novel behaviour of nanomaterials may also pose risks to human health and the environment. The regulatory authorities of countries that wish to take advantage of nanotechnologies including the UK and USA have developed advisory groups and research strategies to monitor and characterise the potential risks of nanomaterials. In the UK, the Nanotechnology Research Strategy Group (NRSG) draws on expertise from government department and agencies, the research councils, academia and industry. The individual task forces set up, investigate: standardisation of reference materials and monitoring; exposure to nanomaterials; human health hazard and risk assessment; environmental hazard and risk assessment; and the social and economic dimensions of nanotechnologies (Defra, 2007 and DEFRA website). In the USA, The National Science and Technology Council (NSTC) developed The National Nanotechnology Initiative (NNI), an organisation that like the NRSG is a multi-agency group, with the strategic approach of investigating the influence of nanomaterials on: human health and the environment; analytical methods of investigating nanoparticles for setting standards; exposure assessment; risk management (The National Nanotechnology Initiative, 2008). Both groups recognise the need for continued research and monitoring of nanomaterials, if the full advantages of the technologies are to be realised.

Public awareness of nanotechnologies is increasing as a consequence of the, non-specifically regulated, introduction of products containing nanomaterials such as self-cleaning windows and stain resistant clothes. The fear that nanotechnologies would be seriously hindered by pressure groups as observed for genetic engineering technologies has largely failed to develop. However toxicity concerns of manufactured nanoparticles do exist (Sheetz *et al.*, 2005 ; Seaton *et al.*, 2010). The process underlying pathological effects of particles in the lungs and cardiovascular system is inflammation, involved in asthma, chronic obstructive lung disease, pulmonary fibrosis and cancer

(Seaton *et al.*, 2010). Generally, nanoparticles have a more pronounced effect on inflammation, cell damage and cell stimulation than an equal mass of particles of the same material at a greater size (Donaldson *et al.*, 2000). Surface area is thought to be the cause of the pro-inflammatory effects and even low toxicity particle surfaces have the ability to generate free radicals and oxidative stress in cells. For nanotubes it is likely that they conform to small fibre characteristic properties and therefore if single long fibres are likely to be released into the air, they should be treated as asbestos without the need for further toxicology testing. For other engineered nanoparticles, tests for inflammatory potential and endothelial activation need to be developed in order to monitor those that may pose a hazard. The already widespread use of nanoparticles in consumer products is a potential cause for concern especially when they may be inhaled, ingested or applied to the skin. What proportions of nanoparticles are allowed into mixtures, how to measure and label them and how to enforce regulation represents a considerable challenge. The unregulated use of nanoparticles has the potential to cause unexpected toxic effects from inhalation accidents, skin allergies or intestinal problems (Seaton *et al.*, 2010).

The study of nanoparticle fate and impact on the environment is becoming an important issue, due to the discharges of nanoparticles already occuring to the environment and the likely increase of nanowastes emitted due to the rapid growth of the nanoparticle industry (Ju-Nam & Lead, 2008). Nanoparticles are not just one class of potential pollutant, they contain a wide range of materials with different physical, chemical and toxiological properties. Nanoparticles should therefore be broken down into a series of classes and not considered as a single homogeneous group. Nanoparticles can be divided into groups by their core materials, *i.e.* organic and inorganic nanoparticles. Examples of organic nanoparticles include carbon nanotubes and polymeric systems, while inorganic nanoparticles include metals, metal oxides and quantum dots. Unbound nanoparticles may be released from disposed or residue paints, cosmetics or pharmaceuticals. Other nanoproducts such as textiles or coatings may produce nanowastes formed of composites. Metalic nanoparticles may releases toxic ions due to leaching (Ju-Nam & Lead, 2008 ; Bystrzejewska-Piotrowska *et al.*, 2009). The persistence of inorganic nanoparticles, quantum dots and carbon

nanotubes in both aqueous and terrestrial environments means that the long term effects of nanowastes are not yet fully understood (Nowack & Bucheli, 2007).

1.6 Nanoparticle preparation and production

Organic nanodispersed systems can be obtained using a range of techniques that can be broadly divided into two categories;

1. The 'top-down' approach that includes the mechanical milling of raw materials or attrition processes to break down larger materials.

2. The 'bottom-up' approach to build materials through the conversion of products or educts dissolved in suitable solvents into nanodispersed systems by precipitation, condensation or specific synthesis procedures (Horn & Rieger, 2001 ; Cao, 2004).

The classical techniques used to obtain nanoparticles are outlined in Figure 1.2.

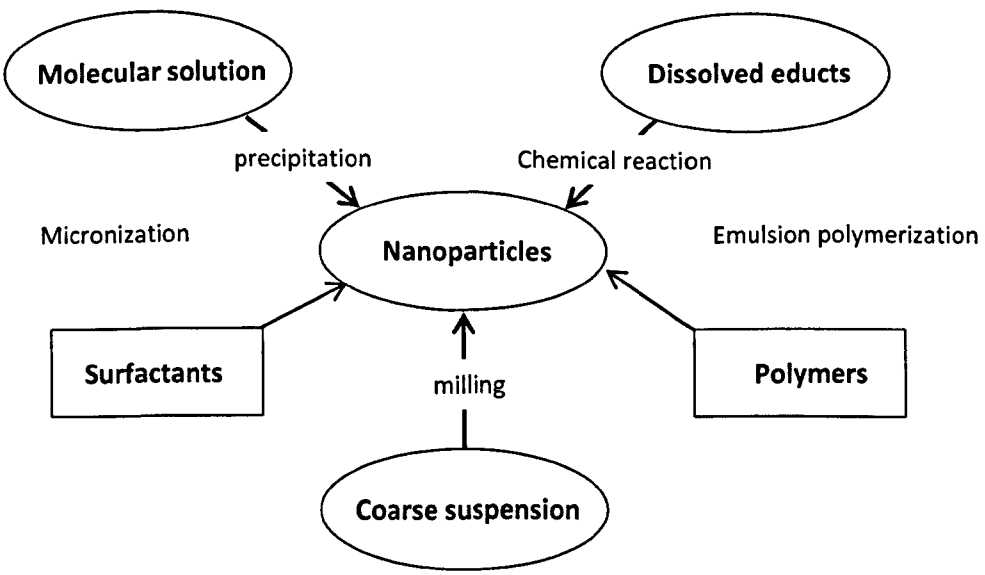

Figure 1.2 Methods for the preparation of nanoparticles adapted from Horn & Rieger, (2001).

1.6.1 Theoretical approaches of particle formation

Multi-component systems exist initially as single phases. Modification of conditions such as temperature and pressure or by homogenous mixing with a further component, induces free energy changes which means phase separation is energetically more favourable. The approach assumes that particles (atoms, molecules or ions) in the phase that is separating out, merge together and nucleate. This is observed for solids in a liquid phase, liquid in a gas phase (condensation), gas in a liquid phase (foaming) and liquids in a liquid phase (emulsion). In colloidal chemistry a further model is used to explain mono-dispersity. As the concentration of a dissolved substance continues to rise until it reaches the critical nucleation concentration, nuclei are formed from the substance, which begin to grow. The concentration momentarily falls below the critical nucleation concentration so that no new nuclei are formed. The nuclei already formed grow until the concentration of the remaining dissolved material has fallen to the equilibrium concentration (Horn & Rieger, 2001). This process describes the building up of nanoparticles from the molecular state, as in precipitation. Nanoparticles can also be formed by breaking larger micron-sized particles down, as in milling. In both processes, a new surface area is formed that necessitates a free-energy cost. The system prefers to reduce the increase in surface area by either dissolving crystalline nuclei, in the case of precipitation, or agglomerating small particles, regardless of their formulation mechanism. These processes are restricted by the addition of surfactants, which permit electrostatic repulsion among particles and limits compression (Rabinow, 2004).

1.6.2 Mechanical milling

Milling is the most common approach used to form particles from poorly soluble drugs in the pharmaceutical industry. An example of where mechanical processes were commercialised for nanoparticle preparation, utilising wet milling technology can be seen at the Elan Corporation. Elan uses NanoCrystal® technology that typically reduces the size of drug particles to less than 2,000 nm (Elan website, 2011). Wet milling is an attrition process in which micron size drug crystals are milled in the presence of grinding media. The poorly water-soluble drug is first dispersed in an aqueous based surfactant solution and the resulting suspension is wet milled with grinding media. The

high shear forces generated during impact of the milling media with the solid drug provide energy to fracture drug crystals into nanometer-sized particles. Limitations of wet milling processes include: contamination of the product by grinding material, batch-to-batch variations in particle size and degree of crystallinity, risk of microbiological contamination and physical limitations of the material that can be processed (Hu *et al.*, 2004).

1.6.3 Polymerisation in miniemulsions

Miniemulsions, also known as microemulsions, consist of small, stable and narrowly distributed droplets in a continuous phase. The miniemulsion process is a versatile technique for the formation of a broad range of polymers and structured materials in confined geometries. These are obtained by high shear processes, such as, ultrasonication or high pressure homogenisation. The stability of the droplets is ensured by the combination of the amphiphilic component, the surfactant and sometimes the use of co-stabilisers that are soluble and homogeneously distributed in the droplet phase; the co-stabiliser has a lower solubility in the continuous phase than the rest of the droplet phase and therefore builds up an osmotic pressure in the droplets. The small droplets can act as nanocontainers in which reactions can take place, either inside or at the surface of the droplets resulting in the formation of nanoparticles suitable for drug delivery (Landfester, 2009).

1.6.4 Emulsification – Evaporation Process

Emulsification-evaporation is the classical method for preparation of water dispersible nanoparticulate materials of water-insoluble active compounds. Preparation of nanoparticles is carried out by dissolving the active compound with an emulsifier in a suitable solvent, then emulsifying with an aqueous solution of a protective colloid (*e.g.*) gelatin, and removing the solvent by evaporation at room temperature or through distillation. The precipitation / crystallisation occurs in the droplet during evaporation / distillation when the solubility limit is crossed. Particle size can be adjusted within wide limits by altering the droplet size distribution of the oil-in-water (O/W) emulsion. This can be achieved by modifying the choice of homogeniser. The main disadvantages of this process are the difficulties in removing all the solvent from

the final product and the general lack of control over droplet size and hence particle size distributions of the final product (Horn & Rieger, 2001).

1.6.5 Emulsification – Diffusion

In this technique, a water-saturated solvent phase containing a polymer and the active compound are emulsified by intensive stirring with a solvent-saturated aqueous phase consisting of a protective colloid or surfactant. The addition of water to the O/W emulsion causes disturbance in the diffusion equilibrium. This induces solvent diffusion into the homogeneous aqueous phase at which point the solubility limits of the polymer and active compound are crossed and particle formation begins. The nanoparticles are stabilised by the protective colloid and the solvent is removed by distillation (Horn & Rieger, 2001).

1.6.6 Nanoparticle production methods utilising antimicrobials

The majority of research has been directed towards the antimicrobial effect of inorganic or "hard" nanoparticles including metallic and ceramic materials, such as silver, zinc oxide, titanium and silica (Morones *et al.*, 2005 ; Cousins *et al.*, 2007 ; Rai *et al.*, 2009 ; Haggstrom *et al.*, 2010). Less focus has been directed towards the formation of organic systems. There are however examples of polymeric organic nanoparticles that utilise a variety of materials, preparative and production methods evident in the literature that differ from the proprietary nanoparticle technology used in this work. Esmaeili *et al.* (2007) produced and evaluated the activity of rifampicin loaded poly(lactide-co-glycolide) nanoparticles that were produced using a modified emulsification-solvent diffusion method. Kisich *et al.* (2007) performed moxifloxacin encapsulation in poly(butyl cyanoacrylate) using polymerisation in the presence of the drug to form nanoparticles. A range of studies have utilised variations in emulsion evaporation processes. The antifungals voriconazole, clotrimazole and econazole were processed into poly(lactide-co-glycolide) loaded nanoparticles (Pandey *et al.*, 2005; Peng *et al.*, 2008). Ciprofloxacin loaded PLGA and polyethylbutylcyanoacrylate (PEBCA) nanoparticles were prepared and evaluated using variations in the emulsion-evaporation process (Page-Clisson *et al.*, 1998 ; Dillen *et al.*, 2004 ; Dillen *et al.*, 2006 ; Jeong *et al.*, 2008). Despite the advantageous features of the aforementioned

preparations and others, antimicrobial loaded polymeric organic nanoparticles have yet to have significance in clinical / agricultural applications.

1.6.7 Iota NanoSolutions™

Iota NanoSolutions Limited is a spinout company from Unilever with the aim of exploiting and developing novel nanodispersion technologies. The company originally developed from a collaboration between the University of Liverpool Department of Chemistry and Unilever (Iota NanoSolutions website, 2011). Iota NanoSolutions™ use five technology platforms to produce organic nanoparticles. The IN-PrESS™ platform was utilised for the production of nanoparticles in this work. The nanoparticle technology used by Iota NanoSolutions™ is unique and patent protected. The new route to aqueous nanodispersions differs from the previously described classifications and other techniques. Zhang *et al.* (2008a) previously generated an oil-in-water (O/W) emulsion using a volatile organic solvent oil phase containing a dissolved organic compound and a continuous aqueous phase containing water-soluble polymers or surfactants. The resulting emulsion was subsequently dripped or atomised onto the surface of a cryogenic liquid, or frozen directly, resulting in the formation of frozen beads, micrometer sized powders or large monolithic structures. Freeze drying was used to remove both the water and organic solvent producing highly porous composite materials that produced nanoparticulate dispersions when dissolved in water. The technology used to produce nanoparticles in this work is a variant of the aforementioned process and detailed in section 2.4 and briefly outlined in Figure 1.3 (Duncalf *et al.*, 2008 ; Zhang *et al.*, 2008a). Spray drying was used to transform the feed from a liquid state into a dry particulate form. Spray drying involves the atomisation of the aqueous feed into a spray and contact between the spray and drying medium (hot air) results in moisture evaporation. The drying of the spray proceeds until the desired moisture content in the dried particles is obtained and the product is removed from the air (Masters, 1985). The nanoparticle preparation and formation processes do not involve any chemical reactions thus eliminating potential complications with by-products or required downstream purification procedures. Chemical modification would result in a final product that was chemically different from the starting material. Chemical modification of drugs occurs, for example when

salt groups are added to chemicals or when they are PEGylated to improve solubility (Zhang *et al.*, 2005 ; Duncalf *et al.*, 2008 ; Zhang *et al.*, 2008a ; Ray, 2009).

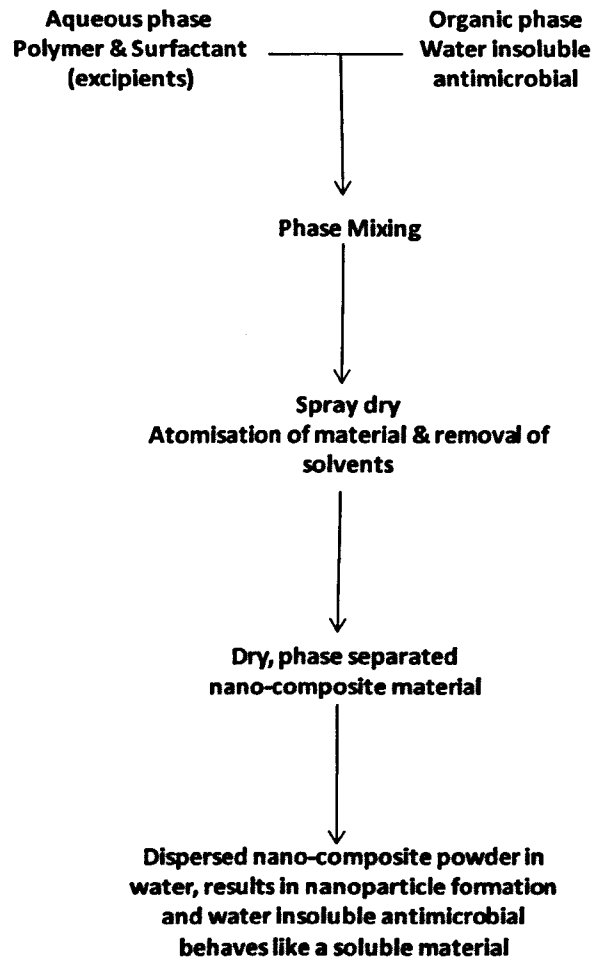

Figure 1.3 Nanoparticle preparation and production using Iota NanoSolutions™ IN-PrESS™ platform.

1.7 Nanoparticle characterisation

A number of nanoparticle characterisation techniques exist and are selected on the basis of application and performance required of the nanosuspension. Common approaches used to characterise nanoparticles include dynamic light scattering (DLS) to measure particle size, electrophoretic light scattering (ELS) to measure zeta potential, scanning electron microscopy (SEM) to investigate particle shape and morphology and X-ray diffraction (XRD) to determine degree of crystallinity.

1.7.1 Particle size

A variety of techniques are used to measure particle-size distribution (Rabinow, 2004). A key to choosing the most suitable particle sizing technique is to find one that is sensitive to those portions of the size distribution that are most significant to pertinent macroscopic properties of the material (Morrison & Ross, 2002). Light scattering techniques have been the main choice for the determination of particle size and distribution as they are ideally suited to analysis of submicron dispersions. Light directed at a particle can be deflected or absorbed by the particle, which is dependent on the size of the particle relative to the wavelength of the light source. Particles significantly larger than the wavelength of light will exhibit diffraction, whereas smaller particles tend to scatter light. One of these techniques is Dynamic Light Scattering (DLS), also known as Quasi-Elastic Light Scattering (QELS) that is suited to nanoparticle measurement because it takes advantage of Brownian motion. The random Brownian motion of particles causes fluctuations in the intensity of the scattered light when observed from a fixed point. The rate of fluctuation in the scattering intensity is proportional to the magnitude of the Brownian motion, with smaller, fast moving particles generating a greater rate of fluctuation in scattering intensity than larger particles. These data allow a correlation function describing the motion of the particles to be constructed and calculation of a particles Brownian motion coefficient. This coefficient is related to the particles size by the Stokes – Einstein equation (Equation 1.2) (Malvern Instruments, 2003 ; Williams & Vaughn, 2006). Viscosity correction values were applied to nanoparticle preparations and average size distributions were determined.

$$D = \frac{kT}{3\pi\eta d} \tag{1.2}$$

Equation 1.2 The Brownian diffusion coefficient D is inversely proportional to particle diameter, as shown by the Stokes-Einstein equation. Where k is the Boltzmann constant, T is the absolute temperature, η is the viscosity of the liquid and d is the diameter of the particle. By measuring the scattering intensity as a function of time, calculating an auto-correction of the data, fitting the data to an exponential and solving the diffusion coefficient, the particle diameter can be accurately calculated (Morrison & Ross, 2002).

1.7.2 Zeta Potential

Particles composed of heteroatomic molecules are either uncharged, or display a surface charge that is positive or negative depending on the orientation and ionization of the particle components. The electrostatic interactions between particles will determine the possibility of aggregation or repulsion (Williams & Vaughn, 2006). However, zeta potential measurements only consider electrostatic and not steric charge effects. Steric charge is less well understood and cannot be directly measured, therefore electrostatic features are emphasised (Cao, 2004). The development of a net charge at the particles surface affects the distribution of ions in the surrounding interfacial region, resulting in an increased concentration of counter ions close to the surface (Figure 1.4). The liquid layer surrounding the particle exists as two parts, an inner region (stern layer), where the ions are strongly bound and an outer diffuse region where they are less firmly attached. Within the diffuse layer there is a notional boundary in which the ions and particles form a stable entity. When a particle moves, ions within the boundary move within it, but any ions beyond the boundary do not move with the particle. This boundary is the surface of hydrodynamic shear and the potential that exists at this boundary is the zeta potential (Wilson *et al.*, 2001). Ideally, particles should have a high net zeta potential compared to the dispersing medium, to prevent aggregation. The dividing line between electrostatically stable and unstable suspensions is usually taken at either +30 or -30 mV. Particle systems with zeta potentials more positive than +30 mV or more negative than -30 mV are considered

electrostatically stable, as a general rule (Malvern Instruments, 2003). The repulsive forces brought on by similar ionic charges on particle surfaces prevent the natural attractive forces determined by hydrogen bonding and van der Waals (Williams & Vaughn, 2006).

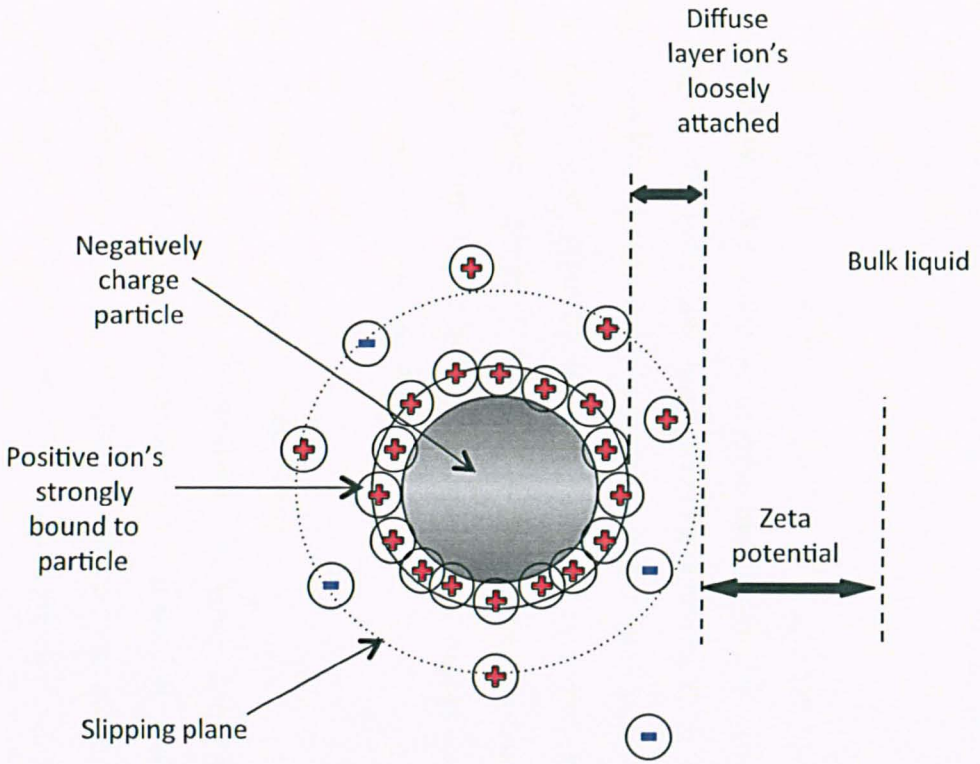

Figure 1.4. A representation depicting the various solvent layers surrounding a nanoparticle resulting in zeta potential (Adapted from Malvern Instruments, 2003).

1.7.3 Particle characterisation

Scanning electron microscopy plays a role in determining the size of a limited number of particles, but more importantly in the evaluation of particle shape and morphology. The technique usually requires a conductivity agent to be applied to the samples surface, typically gold or palladium that is added through sputter coating under high vacuum and acts as conductive medium. High-energy electrons are delivered to the particles surface, reflected and detected to build a sample image. Distributions of sizes are nearly impossible to determine using this method due to the limited number of particles that can be viewed (Dubes *et al.*, 2003).

X-ray diffraction (XRD) is a technique used to characterise the difference between amorphous and crystalline solids. An amorphous solid has short-range molecular order between neighbouring molecules, but unlike crystalline solids, has no long-range order of molecular packing or well-defined molecular confirmation. Amorphous solids have higher solubility and dissolution rates than corresponding crystals. However amorphous solids are generally less stable than corresponding crystals (Yu, 2001). Crystalline solids are preferred by the pharmaceutical industry due to their long-term stability, giving products a greater shelf life.

1.7.4 Critical Micellisation Concentration (CMC)

CMC is the calculation of the concentration at which amphiphiles associate into micellar structures. Spontaneous assembly into core-shell micellar structures occurs in an aqueous environment when the CMC is reached, to minimise the systems free energy (Zhang *et al.*, 2008b). The CMC values of the individual excipients, the antimicrobial loaded and blank nanoparticles of selected preparations were assessed to determine if spontaneous micellisation of these materials occurred around the inhibitory concentrations for these materials. Surface tension measurements were taken to calculate CMC values.

1.8 Antimicrobials

The unwanted effects of microbial growth have long been controlled through the use of chemical agents, whether these are associated with hygiene delivery, preservation or chemotherapy. Antibiotics are generally pharmacologically precise and exert their action at a single physiological target. Biocide formulations, on the other hand, contain antibacterial chemicals that are at sufficient concentrations to affect multiple rather than singular cell targets. Biocides include anticeptics, disinfectants and preservatives but not antibiotics. Biocides are rarely pharmacologically precise and therefore do not usually permit their use as therapeutic agents. Relative to the wealth of data concerning the mode of action of antibiotics, scant attention has been paid to biocidal molecules. However general themes are evident for chemical groups of biocides. Chlorine and oxygen releasing agents exert bactericidal action through oxidation of thiol and other chemical groups represented within a range of membrane-bound and intracellular enzymes. Quaternary ammonium compounds, phenols and substituted phenols induce physical disruption and partial solubilisation of the cell wall and membrane. Alcohols at bactericidal concentrations induce denaturation of cytoplasmic proteins and coagulation of cell contents. A number of mechanisms account for the wide range of sensitivity found for the antibacterial action of antibiotics and biocides. Some organisms lack critical target sites or have an inability to accumulate the agent at target sites. Other organisms undergo phenotypic changes to reflect the conditions they are exposed to such as the temporary expression of efflux pumps or synthesis and export of protective enzymes (Russell & McDonnell, 2000 ; Gilbert & McBain, 2003).

1.8.1 Tebuconazole and propiconazole

Tebuconazole is a systemic broad-spectrum antifungal compound (Figure 1.5A) with low water solubility (32 $\mu g\ ml^{-1}$) and good solubility in a range of organic solvents. Tebuconazole is a popular product in both Europe and the USA (*e.g.*) as Folicur® (Bayer) which is effective against various smut and bunt diseases of cereals and a range of other crops (Asrar *et al.*, 2004 ; Bayer CropScience website, 2011). Propiconazole (Figure 1.5B) is a systemic broad-spectrum fungicide widely used to protect a range of crops including cereals. Propiconazole has a high boiling point and

poor water solubility (100 μg ml^{-1}), but is very soluble in organic solvents. Although propiconazole is no longer accepted as an anti-fungal treatment in the UK, it remains used in a large number of countries worldwide (Tomlin, 1995). Azole antifungals belong to the group of ergosterol biosynthesis inhibitors that inhibit enzymes involved in the post-squalene steps of the fungal sterol biosynthesis pathway. Azoles have a cytochrome P_{450} as a common cellular target in yeast and fungi that is involved in the 14 α-demethylation of lanosterol. The triazole binds to the heme iron of the cytochrome P_{450}, thus inhibiting the enzymatic reactions and ultimately preventing fungal growth (Sanglard *et al.*, 1998).

A

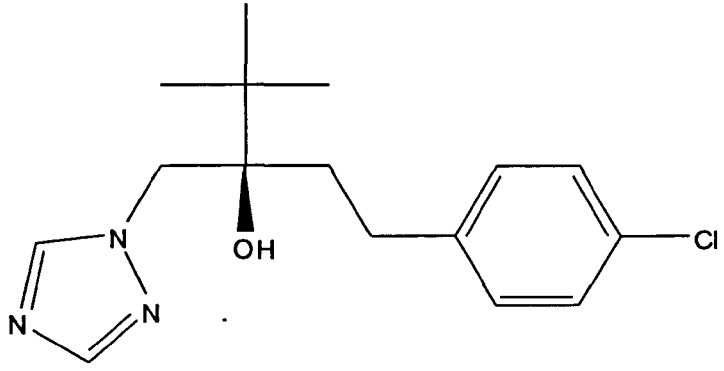

B

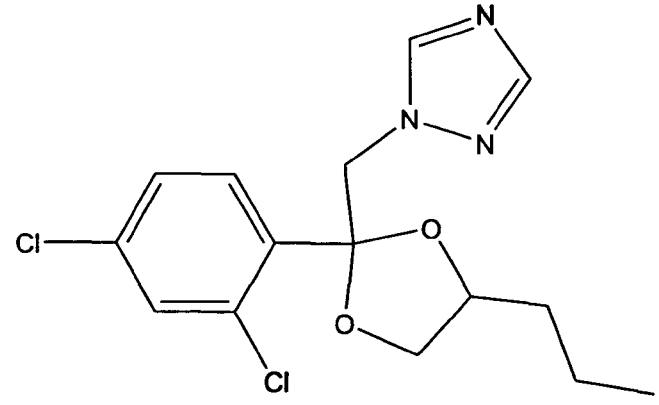

C

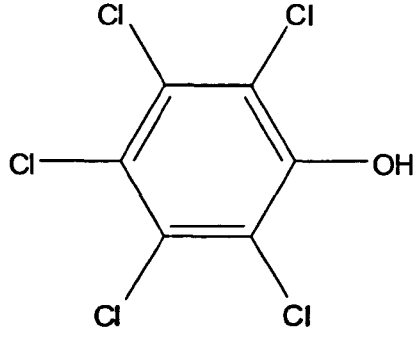

D

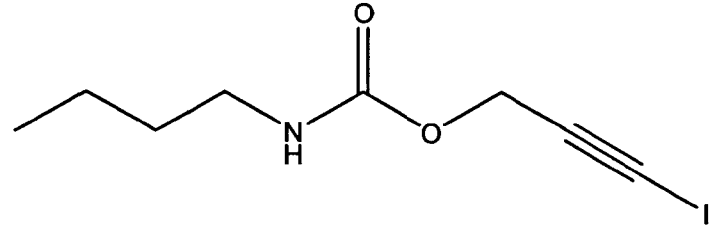

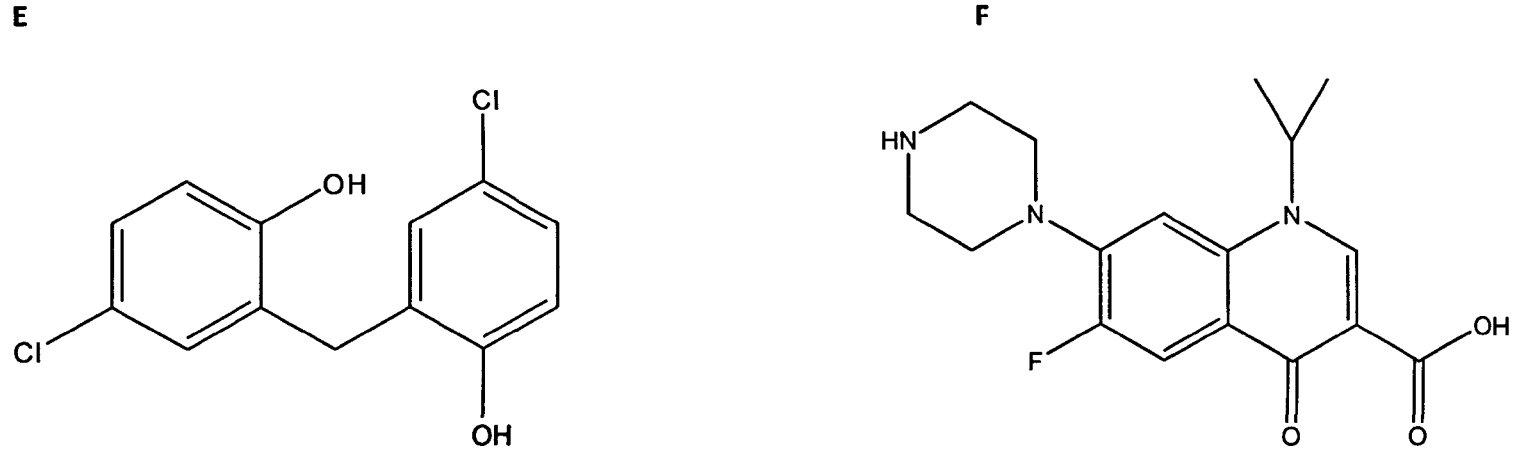

Figure 1.5. Chemical structures of (A) tebuconazole (B) propiconazole (C) pentachlorophenol (D) Iodopropynyl butylcarbamate (IPBC) (E) dichlorophen (F) ciprofloxacin (produced using ChemDraw Ultra 11.0).

1.8.2 Pentachlorophenol

Pentachlorophenol is a broad-spectrum fungicide and bactericide, formerly used to protect wood from fungal rots and used as a general disinfectant (Figure 1.5C). Pentachlorophenol has a melting point of 191^{O}C, poor water solubility (80 μg ml^{-1}), but is stable and soluble in most organic solvents (Tomlin, 1995). Phenols typically target transmembrane pH gradients and affect membrane integrity resulting in leakage of cell materials, disruption of transport processes and inhibition of respiratory and energy coupling mechanisms (Denyer & Stewart, 1998).

1.8.3 Iodopropynyl butylcarbamate (IPBC)

Iodopropynyl butylcarbamate (IPBC) is a halogenated unsaturated carbamate (Figure 1.5D) with widespread application in both occupational and consumer products as a preservative. IPBC is found in paints, coatings, wood preserves, shampoos, baby products, contact lenses and in a range of other applications. IPBC is a highly effective fungicide and bactericide able to inhibit the growth of a variety of fungi, bacteria, algae and viruses (Badreshia & Marks, 2002). IPBC's primary mode of action is not known, it has however been suggested that the anti-fungal property may be related to iodine toxicity, as it consists of a carbamic acid moiety complexed to iodine (Jarrard *et al.*, 2004). It has also been suggested that carbamate antimicrobials act on a range of physiological sites (Adam *et al.*, 2009). IPBC has poor water solubility (≤100 μg ml^{-1}), but exhibits good solubility in a range of organic solvents (Frauen *et al.*, 2001).

1.8.4 Dichlorophen

Dichlorophen (Figure 1.5E) is a commonly used fungicide and bactericide widely employed as an antimicrobial in consumer toiletries such as soaps and cosmetics. It is used to treat fungal infections of the skin and is present in the product Mycota® spray for the treatment and prevention of athlete's foot and is also used as a fungicide in agriculture (Cox *et al.*, 2004 ; Mycota® website, 2011). Like most general biocides, dichlorophen's mode of action is relatively poorly understood (Denyer & Stewart, 1998). Phenoxyethanol and its analogue 2,4-dichlorphenoxyethanol (dichlorophen) affect a range on intracellular targets, dependent on concentration (Gilbert *et al.*, 1977). At sub-lethal biocide levels a variety of concentration dependent processes

take place. These range from actions such as the disruption of potassium:proton antiporters, respiration uncoupling and competitive inhibition of NADH binding by malate dehydrogenase. Additionally, DNA biosynthesis is slowed relative to general anabolism in the cell at sub-MICs (Gilbert *et al.*, 1980; Gilbert & McBain, 2003). Dichlorophen displays poor water solubility (30 $\mu g\ ml^{-1}$), but good solubility in organic solvents (530,000 $\mu g\ ml^{-1}$) in ethanol (Tomlin, 1995).

1.8.5 Ciprofloxacin

Ciprofloxacin is a powerful broad-spectrum fluoroquinolone antibiotic effective against a range of Gram-negative and positive bacteria (Dillen *et al.*, 2006). Ciprofloxacin is insoluble in water ($\leq$ 100 $\mu g\ ml^{-1}$) and many organic solvents which results in poor bioavailability (Figure 1.5F). For example, a current treatment regime of cystic fibrosis associated infection entails oral administration of ciprofloxacin. Typically 0.5-5% of each dose enters the bloodstream and just ~10% of the circulating drug reaches the site of infection (Arnold *et al.*, 2007). Ciprofloxacin must entre the bacterial cell before it can exert an antimicrobial effect. It has been proposed that ciprofloxacin penetrates the envelopes of bacteria by three routes (i) by a hydrophilic pathway through water-filled porin channels; (ii) by a hydrophobic pathway through the lipid bilayer, and (iii) by the self-promoted pathway, which involves the displacement of the divalent cations that bridge adjacent lipopolysaccharide molecules. However, the mechanism by which the self-promoted pathway functions remain unclear and its existence has been questioned (Berlanga *et al.*, 2004).

Bacterial DNA topology is controlled by three enzymes: DNA gyrase, DNA topoisomerase I and DNA topoisomerase IV. Gyrase and topoisomerase IV are related, sharing amino acid similarity (Chen *et al.*, 1996). Ciprofloxacin targets two of these essential intracellular bacterial enzymes, DNA gyrase and topoisomerase IV (Berlanga *et al.*, 2004). Gyrase controls DNA super-coiling and relieves topological stress arising from the translocation of transcription and replication complexes along DNA. Topoisomerase IV has been described as a de-catenating enzyme required for DNA replication. Trapping of gyrase and topoisomerase IV on DNA is also thought to lead to the release of double-stranded DNA breaks. (Refer to Figure 1.6, for representation of

events involved in quinolone mediated cell death with gyrase as the primary target). A similar series of complexes and broken DNA products may form when quinolone compounds interact with topoisomerase IV. Both enzymes are required for cell growth and therefore ciprofloxacin is characterised as a bactericidal antibiotic (Drlica & Zhao, 1997).

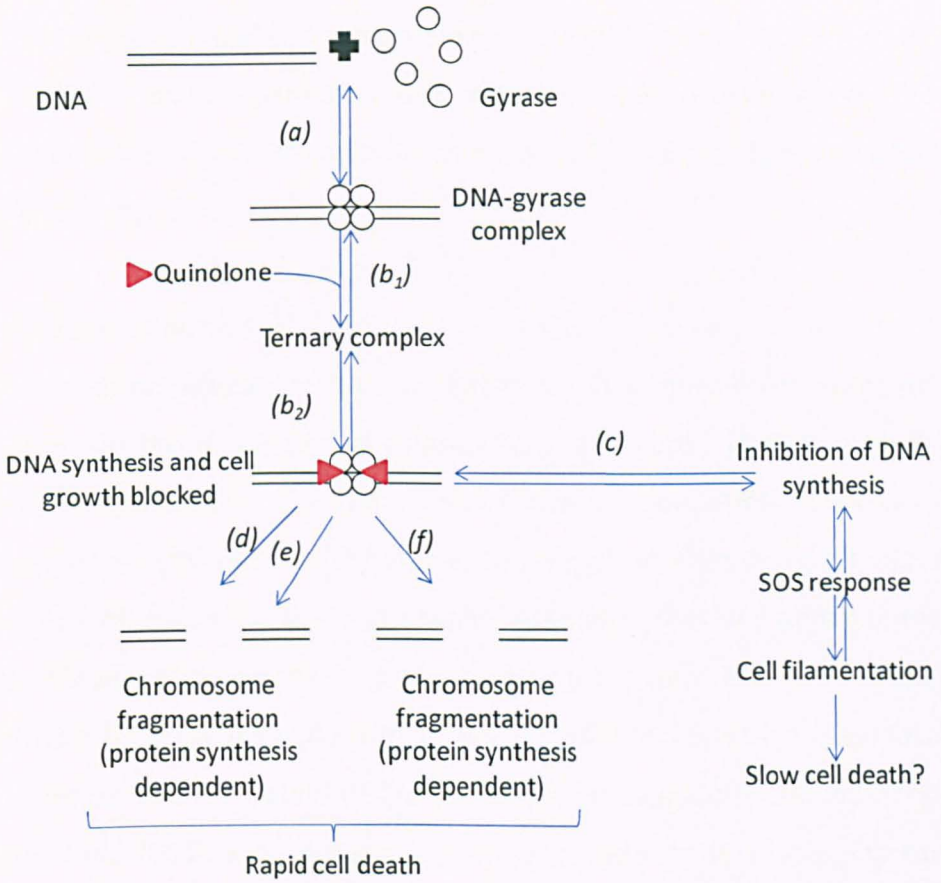

Figure 1.6. Schematic representation of quinolone action with gyrase as the primary target. (Step *a*) Binding of gyrase to DNA. (Step *b*) Reversible formation of quinolone-gyrase-DNA complexes that rapidly block DNA replication. (Step b_1) depicts binding of quinolone to gyrase-DNA complexes before DNA cleavage; (step b_2) represents binding after DNA cleavage. (Step *c*) Inhibition of replication leads to induction of the SOS response and cell filamentation. (Step *d*) Lethal chromosome fragmentation that requires ongoing protein synthesis in aerobic conditions. (Step *e*) Lethal chromosome fragmentation that requires on-going protein synthesis but not aerobic conditions. (Step *f*) Lethal chromosome fragmentation that requires neither ongoing protein synthesis or aerobic conditions (Adapted from Drlica *et al.*, 2008).

1.9 Microorganisms

A range of Gram-positive and Gram-negative bacteria and fungi were selected to test a variety of antimicrobial preparations. The microorganisms chosen represent widely studied model systems with characteristics suitable for screening large numbers of materials for activity.

1.9.1 *Staphylococcus aureus*

S. aureus is a Gram-positive human commensal and opportunistic pathogen. The anterior nares are the major site of colonisation, with about 20-30% of individuals being persistent carriers and 30% intermittent carriers. Colonisation increases the risk of infections when the host defences are compromised (Wertheim *et al.*, 2005). *S. aureus* is one of the main causes of hospital acquired infections affecting the skin, soft tissues, bloodstream and lower respiratory tract. *S. aureus* is also associated with venous catheter bacteraemia and serious deep seated infections such as endocarditis, haemolytic pneumonia and osteomyelitis (Lindsay & Holden, 2004 ; Rooijakkers *et al.*, 2005 ; Plata *et al.*, 2009). *S. aureus* is equipped with a variety of virulence factors that include both structural and secreted products participating in the pathogenesis of infection. Structural products include the numerous surface proteins called 'microbial surface components recognising adhesive matrix molecules' (MSCRAMMs) that mediate attachment to host tissues and initiate colonisation leading to an infection (Plata *et al.*, 2009).

S. aureus secretes several cytolytic toxins including; alpha-hemolysin, beta-hemolysin, gamma-hemolysin, leukocidin and Panton-Valentine leukocidin (PVL). Cytolytic toxins form β-barrel pores in the cytoplasmic membranes and cause leakage of the cell's content and lysis. PVL exhibits affinity for leukocytes and is mostly associated with community acquired meticillin resistant *S. aureus* (CA-MRSA) (Kaneko & Kamio, 2004 ; Foster, 2005). *S. aureus* also generates a group of immune-stimulating toxins implicated in gastroenteritis and toxic shock syndrome. These super-antigens cross-link MHC class II molecules on antigen presenting cells with T-cell receptors. Formation of this complex induces intense T-cell proliferation resulting in massive cytokine

production and release that causes capillary leak, epithelial damage and hypotension (Baker & Acharya, 2004).

Gene expression of virulence factors is regulated in a tightly controlled manner, so that it is complimentary to the biological cycle of *S. aureus*. The production of factors involved in virulence are controlled by quorum sensing. Genes coding for surface proteins are up regulated during early phases of growth, whereas genes that encode secreted proteins are up regulated in late exponential phase. This pattern of gene expression appears to reflect a strategy in which the pathogen first establishes itself in the host and only then attacks it. This regulation is largely imparted by RNA III, a riboregulator that acts as the key effector of the agr quorum sensing system (Novick & Geisinger, 2008 ; Plata *et al.*, 2009).

Meticillin resistant *Staphylococcus aureus* (MRSA) has become a leading cause of infections in healthcare related settings. In several industrialised nations, 40-60% of all hospital reported *S. aureus* infections are now resistant to meticillin (Lindsay & Holden, 2004). MRSA is defined by the presence of a large mobile genetic element (21-67 kb), that is absent from the meticillin susceptible *S. aureus* chromosome, called the staphylococcal cassette chromosome, *mec* (SCC*mec*). This carriers the *mecA* gene that codes for an alternative penicillin binding protein, PBP2a, with low affinity to all β-lactams. The *mecA* gene complex is widely distributed among *S. aureus* species as well as among other staphylococcal species. It has therefore been suggested that *mec* may be freely transmissible among staphylococci (Ito *et al.*, 1999). MRSA infections are treated with vancomycin, but there are reports of vancomycin resistant isolates (VRSA) that have acquired the *vanA* resistance gene from vancomycin resistant enterococci (Hiramatsu, 2001; Lindsay & Holden, 2004). The emergence of MRSA strains in the community (CA-MRSA) causing infections ranging from skin abscesses to pneumonia in otherwise healthy individuals is of growing concern (Shukla, 2005). Inevitably, this focuses research into the development of new, novel agents and methods used to deliver them, to limit *S. aureus* transmission and inhibit growth.

1.9.2 *Escherichia coli*

E. coli represents one of the most frequently and best studied bacterial organisms. *E. coli* is a Gram-negative enteric bacterium that typically colonises the gastrointestinal tract and coexists as a commensal in healthy humans and many animals (Dobrindt, 2005). *E. coli* typically colonises the infant gastrointestinal tract within hours of life, and, thereafter normally remains confined to the intestinal lumen. However, in immune-compromised hosts, or when the gastrointestinal barriers are damaged, even 'non-pathogenic' strains of *E. coli* can cause infection. Like most mucosal pathogens *E. coli* follows a strategy of infection: (i) colonisation of a mucosal site, (ii) evasion of host defences, (iii) multiplication, and (iv) host damage (Nataro & Kaper, 1998). Several highly adapted *E. coli* clones, also exist, that have acquired an increased ability to adapt to new niches and allow them to cause a broad spectrum of disease. Three general clinical syndromes can result from infection: enteric / diarrhoeal disease, urinary tract infections (UTI's) and sepsis / meningitis (Kaper *et al.*, 2004). A highly conserved feature of diarrhoeal disease-causing *E. coli* is the ability to colonise the mucosal surface despite peristalsis and competition for nutrients by the indigenous flora. *E. coli* strains have specific fimbrial antigens that enhance intestinal colonising abilities and allow adherence to the small bowel mucosa. Once colonisation is established *E. coli* utilises a range of mechanisms for the development of diarrheal disease including: enterotoxin production; enterotoxigenic *E. coli* (ETEC) and enteroaggregative *E. coli* (EAEC), invasion; enteroinvasive *E. coli* (EIEC), and/or intimate adherence with membrane signalling; enteropathogenic *E. coli* (EPEC), enterohaemorrhagic *E. coli* (EHEC) and diffusely adherent *E. coli* (DAEC) (Nataro & Kaper, 1998). Each pathotype has distinguishing characteristics related to epidemiology, pathogenesis, clinical manifestation and treatment. The virulence factors that distinguish the various *E. coli* pathotypes have been acquired from numerous sources including; bacteriophages, plasmids and the genomes of other bacteria (Wick *et al.*, 2005).

1.9.3 *Candida albicans*

The polymorphic fungus *Candida albicans* is the most clinically significant member of the *Candida* genus (Ramage *et al.*, 2005). *C. albicans* readily colonises the oral cavity,

gut and female genital tracts as a commensal organism, however it has also emerged as an important opportunistic pathogen and the cause of significant morbidity and mortality (Nucci & Anaissie, 2001 ; Khan *et al.*, 2003). *Candida* spp. are the fourth leading cause of nosocomial infections in the USA, and in patients with candidemia the mortality rate is 35%. Amongst the infections caused by *C. albicans*, one-third occur in patients who experience a course of complicated abdominal surgery. Furthermore, oropharyngeal candidiasis (OPC) occurs in 70% of patients with acquired immunodeficiency (AIDS) and ~70% of all women (with or without AIDS) will experience at least one episode of vaginitis (Calderone & Fonzi, 2001; Khan *et al.*, 2003). Candidiasis may occur as a result of disturbed balance between host immunity and the pathogen. This disorder is not only due to the immunological dysfunction of the host, but also to the fungal ability to adapt to new niches, dependent on the expression of genes associated with infection (Brown *et al.*, 2007). *C. albicans* virulence factors include; the production of hydrolytic enzymes and adhesions. There are also other characteristic properties that influence fungal virulence, including the ability to form biofilms on various surfaces, changes to morphological form and switching between various phenotypes (Karkowska-Kuleta, 2009).

Morphogenesis in *C. albicans* refers to the transition between unicellular yeast cells and filamentous pseudohyphal or hyphal growth. Yeast cells are thought to be responsible for dissemination in the environment and finding new hosts, while hyphae are required for tissue damage and invasion. The transition between these forms is in response to diverse environmental stimuli and virulence is attenuated for regulatory mutants that are confined to yeast or filamentous forms. However, it has been demonstrated that lesions are populated by both morphological forms, suggesting that both have a role in the development and progression of disease. *C. albicans* cells can also change cell surface properties, colony appearance, biochemical and metabolic properties to become more virulent during an infection known as phenotypic switching (Calderone & Fonzi, 2001; Karkowska-Kuleta, 2009). In the white-opaque switch system of *C. albicans*, opaque cells colonise the skin in a cutaneous model more than white phase cells, but are less virulent in an animal model (Kvaal *et al.*, 1999).

Biofilms are protected niches for microorganisms where they are safe from antibiotic treatment and can therefore create a source of persistent infection. During biofilm formation *C. albicans* cells express genes that influence pathogenicity. Properties such as increased adhesion, production of carbohydrates, increased drug resistance through efflux mechanisms and quorum sensing are observed. Biofilm formation on indwelling medical devices remains a significant clinical problem (Chandra *et al.*, 2001).

The production and secretion of hydrolytic enzymes play an important role in tissue damage, dissemination, iron acquisition and overcoming the host immune system. A group of *C. albicans* secreted hydrolytic enzymes are SAPs (secreted aspartyl proteinases), which are regulated at the transcriptional level. Targeted host proteins including: collagen, laminin, fibronectin, mucin, most immunoglobulins, interleukin-1β, salivary lactoferrin and precursors for several blood coagulation factors amongst others (Naglik *et al.*, 2003; Schaller *et al.*, 2005).

1.9.4 *Aspergillus niger*

A. niger is a filamentous fungus that grows aerobically and is a member of the black *Aspergillus* (Schuster *et al.*, 2002 ; Pel *et al.*, 2007). These fungi are ubiquitous worldwide and produce abundant amounts of conidia that are readily dispersed by air currents, thereby facilitating exposure (De Lucca, 2007). *A. niger* is considered a food, grain and chemical spoilage agent (Abarca *et al.*, 2004). It is often associated with damp environments and has been shown to cause adverse health effects when present in damp or mouldy buildings (Fog Nielsen, 2003). Although *A. niger* is a rare opportunistic pathogen, it is known to be problematic in immune-compromised patients and those with severe illness (Schuster *et al.*, 2002). Besides contacting the skin, eyes and ears, the conidia are sufficiently small to be inhaled and lodge in all recesses of the lung, including the alveoli (De Lucca, 2007). *A. niger* is the third most common species associated with invasive pulmonary aspergillosis and is also a causative agent of aspergilloma (farmer's lung). It is frequently isolated on the skin of the external ear canal where it can cause local inflammation (otomycosis) and can be implicated in human mycoses in different locations, occasionally in disseminating infections (Abarca *et al.*, 2004). The risk of allergic hypersensitivity reactions to inhaled

spores or the enzyme dusts produced have also been identified (Schuster *et al.*, 2002). Among the secondary metabolites produced by filamentous fungi, mycotoxins are most relevant from a safety point of view. Some *A. niger* have been reported to synthesis ochratoxin A, a nephrotoxin and carcinogenic mycotoxin (Schuster *et al.*, 2002 ; Pel *et al.*, 2007). A few antifungal agents are available for the treatment of aspergillosis in humans. Theses belong to one of three groups: polyenes, azoles and echinocandins (Meneau & Sanglard, 2005).

1.10 Current understanding of nanoparticle-cell interactions for delivery of active ingredients.

The physical and chemical properties of nanoparticles can vary significantly from those of their bulk counterparts largely as a result of large surface area-to-volume ratio. Although significant numbers of published methodologies and subsequent applications of nanoparticles now exist, little detail is evident either suggesting or demonstrating the mechanisms that determine and account for the differences in activity observed in both prokaryotic and eukaryotic organisms. Most explanations for the observed improvements in activity of nanoparticle formulated active ingredients, including antimicrobials, are suggested on the basis of improved solubility, dissolution rates and due to partition-coefficient effects.

An important physiochemical property of a drug substance is solubility. A balance between aqueous and lipid solubility is important for dissolution (aqueous) and absorption across biological membranes (lipid). Although solubility is normally considered a physiochemical constant, small size increases solubility. Therefore small particles of drugs often display improved dissolution and absorption (Allen Jr, 2008). Increased solubility near the particles surface results in an enhancement in the concentration gradient between the surface and the bulk solution. This high gradient, by Fick's law, must lead to an increased mass flux away from the particle's surface. As particle diameter decreases, its surface area to volume ratio increases, leading to an increased dissolution rate (Kipp, 2004). Studies have indicated that nanoparticle formation of antimicrobials can account for increased rates of dissolution, however it appears to be dependent on particle design and size, to whether burst or biphasic

profiles are observed (Esmaeili *et al.*, 2007; Kisich *et al.*, 2007; Pillai *et al.*, 2008). Mohammadi *et al.* (2010) however, suggested that nanoparticles of the macrolide antibiotic azithromycin had reduced but more sustained, dissolution rates compared to free azithromycin. It was suggested that the rate of release was modified by the presence of an insoluble polymer in the nanoparticle matrix body, which reduced water penetration and therefore dissolution and diffusion of the antimicrobial.

It has been stated that the activity of compounds of various classes increases with oil-water partition coefficient, and that oil-water partitioning simulates the partitioning of compounds between the aqueous and lipophilic receptors (Dearden, 1985). The partition coefficient is commonly used for estimating the permeability potential and lipophilicity of the drug. It is defined as: P = (concentration of drug in octanol)/(concentration of drug in water), where P is dependent on the drug concentration only if the drug molecules have a tendency to associate in solution (Allen Jr, 2008). Haas *et al.* (2009) investigated the effects of nanoencapsulated quinine against *Plasmodium berghei in-vivo*. It was determined that despite nanoencapsulation of quinine presenting a similar plasma profile for that observed for the free drug and similar pharmacokinetic properties, nanoencapsulation increased efficiency of the active compound by 30%. It was therefore suggested that nanocapsules could have increased the drug concentration at the site of action. This was demonstrated using a partition-coefficient investigation, which indicated that nanoencapsulation doubled the drug penetration into red blood cells, and was thus used to justify the improvement in activity observed. However, the experiment did not determine whether the mechanism of increasing partition-coefficient was due to adhesion of the nanoparticles to the erythrocyte membrane and therefore facilitating drug penetration, or increased internalisation of the nanostructures, or both. It has been suggested that optimal partition coefficient (P_0) giving maximal biological response exists, $\log P_0 \sim 6$ for bactericides active against Gram-positive bacteria, while $\log P_0 \sim 4$ for those active against Gram-negative bacteria. Other factors such as charge and size of the active organic molecule, can affect the rate at which molecules arrive at a receptor sites and the ability of the molecules to interact with the target receptors, irrespective of the organism (Dearden, 1985). Limited investigation has been

conducted, classifying the molecular mechanisms that underlie the bacterial response to nanoparticles. Two approaches have been identified:

1. A direct approach that assesses cellular response mechanisms, such as differences in cell viability and cell indicators of stress.

2. A discovery based approach to identify the genetic response of cells to nanoparticles.

Pelletier *et al.* (2010) investigated the effects of Cerium oxide (CeO_2) nanoparticles on bacterial viability and subsequently performed microarray analysis to discover the global transcriptomics of *E. coli* after exposure to CeO_2 nanoparticles. Lok *et al.* (2006) performed a proteomic analysis on the mode of action of silver nanoparticles in *E. coli*. Silver nanoparticles were found to be more inhibitory than unprocessed silver nitrate. Both studies indicated there were no significant changes between the transcriptomes or proteomes of *E. coli* when treated with either nanoparticle preparations or unprocessed equivalents. Although some research effort has been made to determine the mode of action of inorganic nanoparticles at the molecular-cell level, there is no evidence of such research using antimicrobial organic nanoparticles.

1.11 Comparing inhibitory activity

Minimum Inhibitory Concentrations (MIC's) are defined as the lowest concentration of an antimicrobial that will inhibit the visible growth of microorganisms after overnight incubation. Minimum Bactericidal Concentrations (MBC's) are defined as the lowest concentration of antimicrobial that will prevent the growth of an organism after subculture on to antibiotic free media, generally taken as 99.9% killing. MIC's are frequently used as a research tool to determine the *in-vitro* activity of antimicrobials (Andrews, 2001 ; Gilbert & McBain, 2003). Although MIC's and MBC's are considered the 'gold standard' for determining the susceptibility of organisms to antimicrobials, several technical pitfalls are associated with the techniques. MIC and MBC endpoints are based upon arbitrary definitions and can be poorly reproducible even within a particular methodology. Biological variability can mean different MIC and MBC

breakpoints are obtained due to individual interpretation of the data. Dilution methods suffer from several technical problems, such as: antibiotic carryover, bacteria adhering to the surface of the test vessel and the growth phase of the inoculum utilised may affect the MIC and MBC values obtained (Amsterdam, 1990).

As discussed nanoparticle interactions with cells are complex and likely to be interlinked. Therefore a suitable assay was required to determine if nanoparticle formation of antimicrobials influenced the inhibitory activity compared to solvent dissolved forms of the same chemical. Comparisons of inhibitory activity were made using a range of techniques as outlined in section 2.3.

1.12 Optimisation using Design of Experiment modelling

Design of Experiment (DOE) is a widely used tool in formulation processes, but is generic and applicable to a range of applications. DOE involves making a set of experiments representative with regards to a given question. Standard reference experiments are performed usually called a centre point, and subsequent representative experiments are conducted around it to determine the relative significance of each parameter within the experimental system. The model can perform theoretical optimisation to predict the response values for all possible combinations of factors within the experimental region and identify an optimal experimental point. DOE MODDE™ supports multiple linear regression (MLR) and projections to latent structures (PLS) for fitting the model data. The principal advantages of using a DOE process, is the ability to gain large amounts of information, whilst conducting the minimum number of experiments (Eriksson *et al.*, 2008). An example of a simple cube based DOE is outlined in Figure 1.7. Hyper-cubes can be used to model more complex systems, with a large number of experimental parameters.

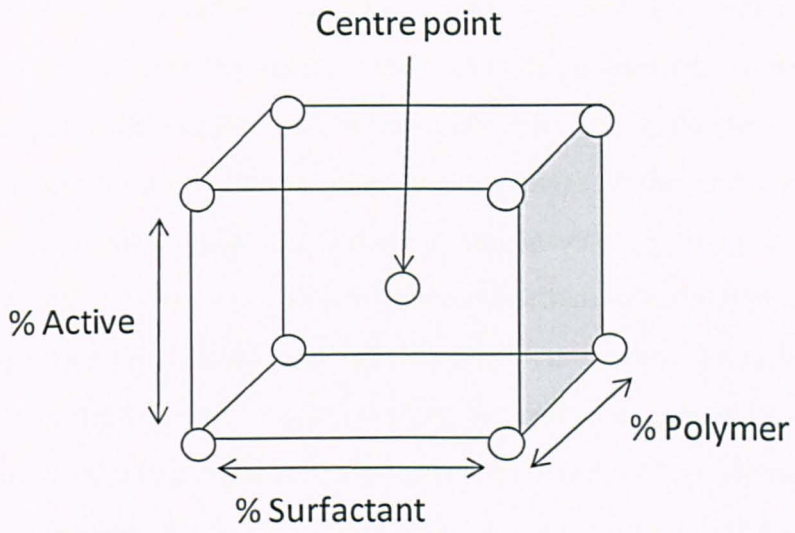

Figure 1.7. Symmetrical distribution of experimental points around a centre point, investigating the relative significance of each parameter; active antimicrobial, surfactant and polymer loading ratios (% $^{w}/_{w}$), based on a simple cube based Design of Experiment model (Adapted from Eriksson *et al.*, 2008).

1.13 Next generation high-throughput sequencing

Over the past four years, there has been a fundamental shift away from the application of 'first-generation' automated Sanger sequencing to newer methods referred to as 'next-generation' sequencing (NGS) for genome analysis (Metzker, 2010). The earliest work using massively parallel sequencing was published in 2000, however the instruments produced by 454 and Solexa established the next generation of sequencers as a reality. Next generation sequencing is currently offered by over 30 companies but is ruled by three main competitors: Roche™ (454 Life Sciences), Illumina® (Genome Analyzer™) and Applied Biosystems™ (SOLiD™). Each of the systems uses a different chemistry and offers unique benefits, but the essential process remains the same: following nucleic acid fragmentation and a series of ligation reactions and amplification steps, sequencing by synthesis is carried out and millions of 35-400 bp reads are created that can be mapped to the genome (Cullum *et al.*, 2011). Next generation sequencing techniques provide high speed and throughput, such that genome sequencing projects that took several years with the Sanger technique can now be completed in weeks. The Applied Biosystems™ SOLiD™ platform was used in this work. The sequencing system was introduced in 2007 and utilises sequencing by

ligation processes as outlined in Figure 1.8. Briefly, a sequencing primer is hybridised to single-stranded copies of the library molecules to be sequenced. A mixture of 8-mer probes carrying four distinct fluorescent labels compete for ligation to the sequencing primer. The fluorophore on the two 3' most nucleotides of the probe is read. Three bases including the dye are cleaved from the 5' end, leaving a 5' free phosphate on the extended primer that is then available for further ligation. After multiple ligations, the synthesised strands are melted and ligation products washed away before a new sequence primer (shifted by one nucleotide) is annealed. Starting from the new sequencing primer the ligation reaction is repeated for three other primers, facilitating the read out of the dinucleotide encoding for each start position in the sequence. The use of specific fluorescent labels means that the dye read outs can be converted to sequence. The system currently allows sequencing of more than 300 million beads in parallel, with a typical read length between 25 and 75 nucleotides (Ansorge, 2009; Kircher & Kelso, 2010).

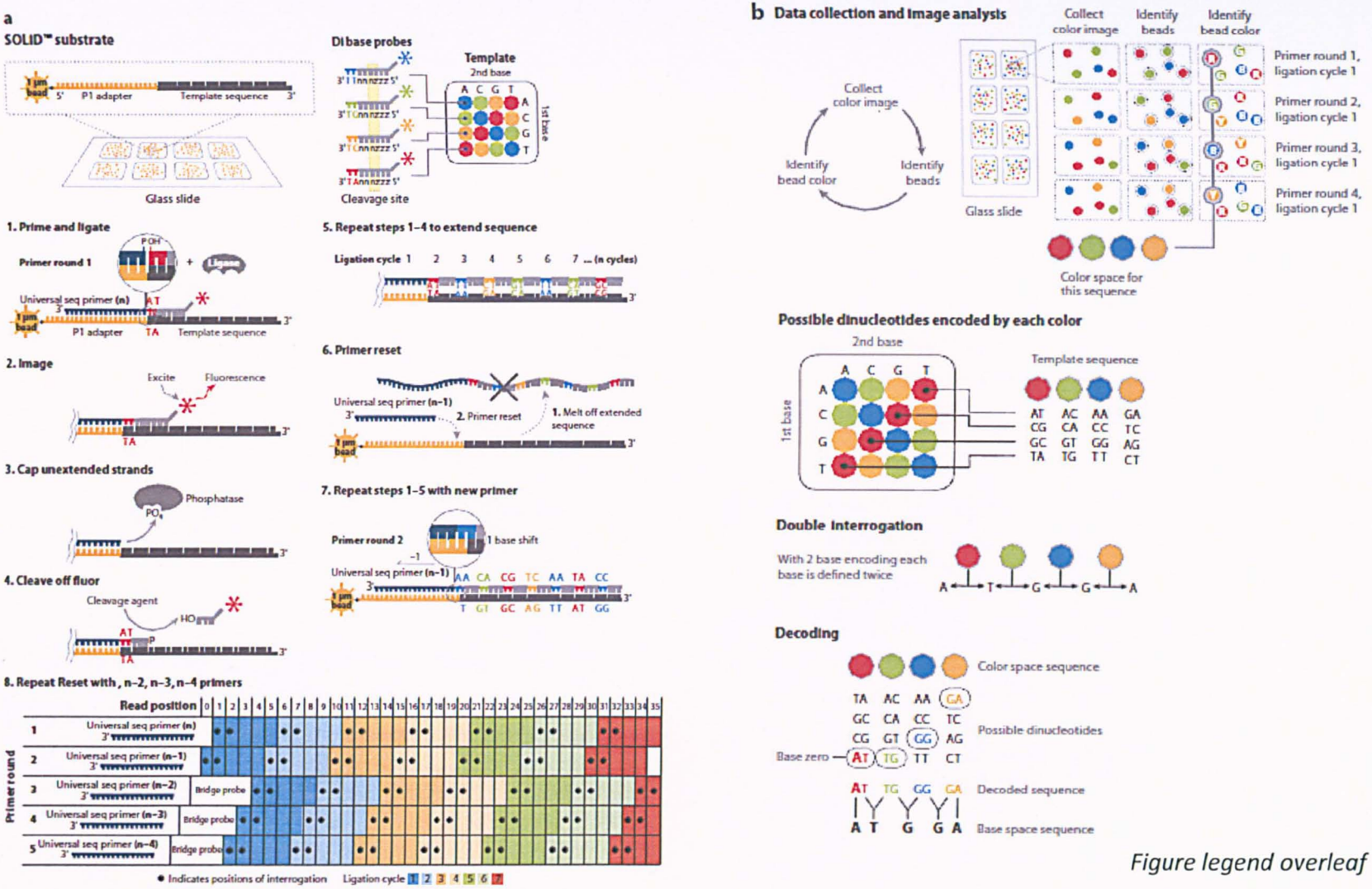

Figure legend overleaf

Figure 1.8. (a) Ligase mediated sequencing approach of the SOLiD™ sequencer. DNA fragments are amplified on the surfaces of 1 μm magnetic beads to provide sufficient signal during the sequencing reactions and then deposited onto a flow cell slide. Ligase mediated sequencing begins by annealing a primer to the adapter sequences on each amplified fragment and then DNA ligase is provided with specific fluorescent labelled 8-mers whose 4^{th} and 5^{th} bases are encoded by the attached fluorescent group. Each ligation step is followed by fluorescent detection and regeneration moves bases from the ligated 8-mer and prepares the extended primer for another round of ligation. (b) Principles of two base encoding. Because each fluorescent group on a ligated 8-mer identifies a two base combination, the resulting sequence reads can be screened for base-calling errors against true polymorphisms by aligning individual reads to known reference sequence. Adapted from Mardis, (2008).

1.14 Comparison of techniques used for assessing bacterial gene expression levels

Changing levels of transcription is one of the primary mechanisms initiating adaptive processes in a cell. Coupled with translation, it can lead to production of new proteins, changes in membrane composition and in cellular machinery (van Vliet, 2010). The transcriptome is the complete set of transcripts in a cell for a specific developmental stage or physiological condition. Understanding the transcriptome is essential for interpreting the functional elements of the genome and revealing the molecular constituents of cells (Wang *et al.*, 2009). The challenge has always been to accurately get and as much information as possible about the transcriptome. Various technologies have been developed to explore and quantify the bacterial transcriptome.

For more than a decade, microarrays have allowed the simultaneous monitoring of expression levels of all annotated genes in cell populations and later generations of the technology consisting of probes designed to interrogate a genome systematically irrespective of any gene annotation were introduced (Marguerat & Bahler, 2010). The rapid development of microarray technologies and subsequent publications, prompted the development of MIAME (Minimum Information About a Microarray Experiment) guidelines that permits transparent comparisons of microarray data from different studies (Brazma *et al.*, 2001). Due to the advances in microarray technology high-density arrays have become widely available largly due to reduced operational costs. However, while microarrays have been instrumental in the understanding of transciption, the technology has relatively limited dynamic range for the detection of transcript levels due to background saturation and spot density and quality. Microarrays need to include sequences from multiple strains as mismatches can significantly affect hybridisation efficiency and hence oligonucleotide probes designed for a single strain may not be optimal for others. This may lead to high background signal due to non-specific hybridisation. The comparsion of transcription levels between experiments, although possible, remains challenging and usually requires complex normalisation methods (Hinton *et al.*, 2004 ; van Vliet, 2010).

SAGE (Serial Analysis of Gene Expression) was one of the first methods used for gene expression profiling. Expressed genes were represented by short tags that quantitatively correlated with gene expression levels. The tags are defined by a common restriction enzyme, which creates the cDNA fragment from the 3' most restriction site in the gene. Tags were cloned and sequenced but the expense of Sanger sequencing meant that the libraries created were rarely sequenced deeply enough. By coupling SAGE with the deep sequencing offered by next generation sequencing, rare transcripts are more likely to be represented and reproducibility is improved (Cullum *et al.*, 2011).

RNA-Seq is perhaps one of the most complex next-generation applications but has advantages over the aforementioned approaches. Unlike hybridisation based technologies, RNA-Seq is not limited to the detection of known transcripts. Low background signal and the absence of upper limit quantification means a larger dynamic range of expression can be detected. RNA-Seq data also show high levels of reproducibility for both technical and biological replicates (Costa *et al.*, 2010). In addition to the technical challenges posed by RNA-Seq experiments, the rapid increase in knowledge gained from such studies requires consideration. Like other breakthroughs in functional genomics, the development of RNA-Seq has been accumpanied by new problems.

The library preparation is a key step of RNA-Seq, because it determines how closely the cDNA sequence data reflects the original RNA population. To perform a whole transcriptome analysis, not limited to annotated mRNAs, the selective depletion of abundant rRNA molecules (16S, 23S) is required. Hybridisation with rRNA specific oligonucleotide probes and subsequent removal using magnetic beads is the main procedure used to selectively deplete large rRNA molecules from total isolated RNA. However, it remains unknown what effect this has on the composition of the mRNA fraction. With further advances in library preparation and sequencing technologies, it may not be necessary to remove rRNA and tRNA. Thus allowing for the development of more representative cDNA libraries with improved quality (Costa *et al.*, 2010; van Vliet, 2010).

In classical next generation sequencing protocols, which have been developed for the analysis of genomic DNA, protocols have been adapted to sequence cDNA. The most straightforward approach is to synthesise double stranded cDNA from RNA, to which adapters can be ligated. This robust protocol was widely used in the original RNA-Seq experiments. However, the loss of information on transcriptional direction was a drawback. Additional protocols have been developed that retain strand specificity. They differ in how the adapter sequences are inserted into the cDNA, for example, by direct ligation of RNA adapters to the RNA sample before reverse transcription. Following reverse transcription using a reverse transcriptase and random hexamers, size selection of cDNA products using denaturing polyacrylamide gel electrophoresis (PAGE) was performed and subsequenty amplified using PCR. Despite using cycle limiting PCR reactions, any amplification of the cDNA using the SOLiD™ sequencing primers, has the potential to introduce an over-representation of shorter transcripts in the cDNA library. Such amplification is not required in the construction of cDNA libraries for microarray experiments and is therefore considered an advantage of this technique. Sequencing was conducted as outlined in section 1.13. (Costa *et al.*, 2010; Marguerat & Bahler, 2010; van Vliet, 2010).

Like other next-generation sequencing technologies RNA-Seq faces informatics challenges including the development of efficient methods to store, retrieve and process large amounts of data that must be overcome to reduce errors in image analysis, base-calling and remove low quality reads (Wang *et al.*, 2009). The resulting RNA-Seq reads are individually mapped to the source genome and counted to obtain the number and density of reads corresponding to RNA from each known exon, splice event or new candidate gene. The sensitivity of RNA-Seq is a function of both molar concentration and transcript length. Transcript levels can be quantified in reads per kilobase of exon model per million mapped reads (RPKM). The RPKM measure of read density reflects the molar concentration of a transcript in the starting sample by normalising for RNA length and for the total read number in the measurement. This facilitates transparent comparison of transcript levels both within and between samples (Mortazavi *et al.*, 2008). However, the distribution of these normalised read counts no longer possesses the advantageous feature of an equal mean and varaince

value. Therefore shorter genes develop greater degress of variance than larger ones. As a result, statistical power to detect differential expression becomes a function of gene length. This is an inherent feature of RNA-Seq data because there are larger sample sizes for longer genes. The RPKM value has also been shown to display bias in GC content and dinucleotide frequencies. It has been demonstrated that these bias patterns are specific to experimental protocols and not specific to biological sources. This suggested that such features are technical artefacts rather than biologically relevant patterns (Zheng *et al.*, 2011). More recently developed methods to estimate levels of gene expression from RNA-Seq studies have been published *e.g.* Hansen *et al.*, 2010; Li *et al.*, 2010 and Zheng *et al.*, 2011. Improved uniformity and reduced statistical associated bias from RNA-Seq data have been reported, however, these techniques remain at present experimental.

The rapid increase in microarray datasets promoted the standardisation of methods and database access through the release of the MIAME (Minimum Information About a Microarray Experiment) guidelines. This estabilshed the minimum requirements for publication of microarray datasets. Similar guidelines for RNA-Seq data do not exist at present. Therefore interpretation of such experimental datasets is usually performed on the guidelines set by individual research groups or institutions and therefore interpretaion and the comparison of RNA-Seq datasets can be challenging and requires standardisation (van Vliet, 2010).

Despite the described limitations of RNA-Seq, Fu *et al.* (2009) reported that RNA-Seq provided better estimates of absolute transcript levels compared to comparative microarray experiments, when using protein expression measurements to evaluate the accuracy of the two methods (Fu *et al.*, 2009). As a result, increasing numbers of RNA-Seq experiments exploring various aspects of the bacterial transcriptome are evident in the published literature. For example, Passalacqua *et al.* (2009) investigated the transcriptome of *Bacillus anthracis* throughout the organism's lifecycle exposing it to eight conditions in which transcript diversity was expected to be maximised. Data from the RNA-Seq study highlighted a very high level of correlation between technical replicates, while data from separate samples at different stages of growth showed

significant differences, reflective of the diverse growth conditions sampled. The authors noted that RNA-Seq has the potential to be an extremely powerful tool for studying bacterial gene expression that can be used to map transcriptional boundaries and operon structure on a genome wide scale to identify previously unrecognised elements in the genome.

1.15 Aims and objectives

The overall aim of the project is to design, characterise and test nanoparticle formulated antimicrobials against a selection of model microorganisms for inhibitory activity and reference these against conventional forms of solvent dissolved delivery. To undertake molecular based techniques to elucidate mechanisms that may account for differences in activity between treatments using leading edge transcriptomic approaches.

The project has the following specific aims:

- To determine how applicable the nanoparticle formulation process technology is to a range of poorly water-soluble antifungals and antibacterials.
- To investigate the inhibitory effects of the prepared antimicrobial loaded nanoparticles against Gram-negative and Gram-positive bacteria and fungi that have different molecular targets.
- To investigate the influence of nanoparticle design on inhibitory activity, including the types and loading ratio's of excipients and loading ratio of antimicrobial.
- To characterise nanoparticle preparations on the basis of size and zeta potential and investigate if such features influence inhibitory activity.
- To investigate the use of mathematical software modelling for optimising inhibitory activity of antimicrobial loaded nanoparticles.
- To identify a suitable mode of action (MOA) analysis that would provide a comprehensive tool to assess if differences between nanoparticle treated and conventionally treated *S. aureus* cells exists.
- To design a suitable protocol investigating the influence of ciprofloxacin loaded nanoparticles and necessary controls for a comparative transcriptional profiling investigation using *S. aureus*.

Chapter 2

Materials and Methods

2.1 Microorganisms and growth media

Details of bacterial and fungal strains used in this study and the growth media used routinely to culture them are presented in Table 2.1. Yeast Extract Malt Extract (YEME) comprised 20 g glucose (BDH), 10 g yeast extract (Merck), 10 g malt extract (Lab M) and 1 g bacterial peptone (Difco) dissolved in 1 L dH_2O. *Aspergillus* Complete Medium 1.5% was prepared using 10 g glucose (BDH), 2 g peptone (Difco), 1 g yeast extract (Merck), 10 ml casamino acids solution (Difco) 20 ml *Aspergillus* salts solution (Table 2.2), 10 ml vitamin solution (Table 2.2) and 1.5% agar (Merck) if required, made up to 1 L with dH_2O.

2.2 Chemicals and Reagents

Antimicrobials were selected for investigation using a number of criteria; the antimicrobial had to exhibit poor water solubility or insolubility ($\leq$ 100 $\mu g\ ml^{-1}$) to test the described technology, be available in sufficient quantities to process into nanoparticles (preferably greater than 1 g of antimicrobial) and Iota NanoSolutions had to have the rights to process the material, *i.e.* proprietary compounds produced by third part companies were not available for study. On the basis of the aforementioned criteria, six antimicrobials were selected with differing modes of action and applications. The antimicrobials were processed using the described technology (section 2.4) into nanoparticles.

Dichlorophen, ciprofloxacin, pentachlorophenol and iodopropynyl butylcarbamate (IPBC) were obtained from Sigma-Aldrich Chemical Co. (St. Louis, USA). Tebuconazole was supplied by Arch Timber Protection Chemicals (Castleford, UK). Propiconazole was provided as an industrial sample (95%) by Zhejiang Heben Pesticide & Chemical Company (Zhejiang, China). Ciprofloxacin HCl was obtained from VWR (Biochemica, Germany). Sodium lauryl ether sulphate (SLES) was a gift from Unilever R&D

department (Port Sunlight, UK). All other polymers and surfactants were obtained from Sigma-Aldrich Chemicals Co. (St. Louis, USA).

Table 2.1 Bacterial and fungal strains used in this study

Species / Strain	Source[a]	Growth media
Aspergillus niger ATCC 1015	ATCC	*Aspergillus* Complete Medium 1.5%
Candida albicans ATCC 18804	ATCC	Yeast Extract Malt Extract
Escherichia coli MC1061	UoL	Luria Burtani (Merck)
Meticillin Resistant *Staphylococcus aureus* 252	UoL	Brain Heart Infusion (Lab M)
Staphylococcus aureus SH1000	UoL	Brain Heart Infusion (Lab M)

[a]UoL = University of Liverpool Culture Collection, ATCC = American Type Culture Collection

Table 2.2 Components of *Aspergillus* vitamin and salt solutions used to produce *Aspergillus* Complete Medium 1.5%

***Aspergillus* vitamin solution**	**Trace elements solution**	***Aspergillus* salts solution**
PABA* – 160 mg	di-Sodium tetraborate – 40 mg	Potassium chloride – 26 g
Inositol – 160 mg	Cupric sulphate - 400 mg	Magnesium sulphate – 26 g
Nicotinic acid – 40 mg	Ferrous (II) sulphate – 800 mg	Potassium phosphate – 76 g
Pantothenic acid – 240 mg	Manganese sulphate – 800 mg	Trace element solution 50 ml
Pyridoxine – 100 mg	Sodium molybdate – 800 mg	Chloroform – 2 ml
Riboflavin – 40 mg	Zinc sulphate – 8 g	dH_2O to 1 L
Choline chloride – 560 mg	dH_2O to 1 L and autoclaved	
Putrescine – 800 mg		
Biotin (100 µg ml^{-1} solution) – 8 ml		
dH_2O to 400 ml and autoclaved		

* Para-aminobenzoic acid

2.3 Inhibition assays

Suitable assays were developed to determine if nanoparticle formulated antimicrobials were more inhibitory than the unprocessed free form of the same chemical. Nanoparticle preparations were compared for activity with organic co-solvent dissolved antimicrobials. Organic co-solvent dissolved delivery represents one of the most common methods of delivering poorly water-soluble antimicrobials and would provide a dissolved compound comparison. The solvent used to dissolve the antimicrobials for comparison had to fulfil a number of criteria: to be water miscible so as to produce a single phase homogeneous solution when mixed with the aqueous liquid growth media; be a good solvent for the active compound so as to prevent precipitation when diluted; have a relatively high boiling point to avoid evaporation during incubation steps; induce limited toxicity to the test organism being investigated. Ethylene glycol appeared to have the potential to meet all these requirements.

If aqueous salt dissolved forms of the active compounds were available, comparisons of activity were made with the nanoparticle preparation. Due to the aqueous route of delivery that the aforementioned nanoparticle technology permits, a water 'dissolved' comparison was required. This was achieved through the addition of the active compound until complete theoretical water saturation was achieved. Although this control would never be utilised in practice, it represents a direct comparison for activity with the aqueous dissolved nanoparticle and aqueous dissolved free active. Blank nanoparticle preparations composed of the polymer and surfactant at equal ratios and produced using identical process methods were compared for activity with the antimicrobial loaded nanoparticles.

2.3.1 Minimum Inhibitory Concentration (MIC)

MIC values were determined by broth micro-dilution in 96 well plates (Greiner) and used to measure the inhibitory activity of unprocessed and nanoparticle formulated antimicrobials and their necessary controls. MIC assays for *S. aureus* SH1000 and MRSA-252 were conducted using Brain Heart Infusion (BHI) broth, Luria Burtani (LB) broth for *E. coli* and using yeast extract malt extract (YEME) broth for *C. albicans*. Briefly, a concentration range was generated across the 96 well plates to a volume of

100 µl and inoculated with 100 µl of a $O.D_{550}$ 0.2 adjusted culture of either *S. aureus* SH1000, MRSA-252, *E. coli* or *C. albicans*, to final concentrations as outlined in Figure 2.1. Wells D11 and H11 contained 100 µl of the appropriate liquid growth medium, plus 100 µl of adjusted culture and served as positive controls. Wells D12 and H12 contained 100 µl of the liquid test suspension, 100 µl of the appropriate growth medium and served as negative controls. The 96 well plates were incubated at 37°C for 24 hours under static conditions. Subsequently, optical density readings were taken using a Wallac Victor^3 1420, 96 well plate reader (550 nm) and negative control values subtracted from the test values to determine relative inhibition imposed by each treatment condition. The MIC was determined as the concentration at which no growth occurred over the 24 hours. Each experiment was conducted in triplicate.

	1	2	3	4	5	6	7	8	9	10	11	12
A	500	250	125	62.5	31.25	15.63	7.81	3.91	1.95	0.98	0.49	0.24
B	218.6	109.3	54.65	27.33	13.66	6.83	3.42	1.71	0.85	0.43	0.21	0.11
C	183.3	91.65	45.83	22.91	11.46	5.73	2.86	1.43	0.72	0.36	0.18	0.09
D	150.0	75.0	37.50	18.75	9.38	4.69	2.34	1.17	0.59	0.29	+ve	-ve
E	500	250	125	62.5	31.25	15.63	7.81	3.91	1.95	0.98	0.49	0.24
F	218.6	109.3	54.65	27.33	13.66	6.83	3.42	1.71	0.85	0.43	0.21	0.11
G	183.3	91.65	45.83	22.91	11.46	5.73	2.86	1.43	0.72	0.36	0.18	0.09
H	150.0	75.0	37.50	18.75	9.38	4.69	2.34	1.17	0.59	0.29	+ve	-ve

Figure 2.1. Concentration range of antimicrobials across the 96 well plates (μg ml^{-1})

(+ve) positive control

(-ve) negative control

2.3.2 Minimum Bactericidal Concentration (MBC) assays

MBC experiments were conducted when MIC determination was not possible due to the physical characteristics of the test solution being investigated. Conical flasks of BHI and either nanoparticle formulated ciprofloxacin, blank nanoparticle, DMSO dissolved ciprofloxacin, DMSO only or sterile ddH_2O were adjusted to $O.D_{550}$ of 0.2 using an overnight culture to a final volume of 50 ml. The prepared flasks were incubated at 37°C with shaking at 120 rpm for 24 hours. Samples were extracted, serially diluted using Phosphate Buffer Saline (PBS) (Melford) and spot plated onto antibiotic-free BHI agar plates. Following overnight incubation at 37°C, colony counts were taken and relative inhibition imposed by each test condition was determined as the percentage re-growth of cells exposed to each condition compared to the uninhibited control. MBC values were determined as the concentration at which no re-growth of colonies was observed on agar plates. Each experiment was conducted in triplicate.

2.3.3 Growth effects

The effects of different antimicrobial and control treatments on the growth of cells were assessed to determine if any inhibition occurred with time. Conical flasks of Brain Heart Infusion (BHI) and either antimicrobial containing or blank treatment solutions or sterile ddH_2O were adjusted to $O.D_{550}$ 0.2 using an overnight culture to a final volume of 50 ml. The flasks were incubated at 37°C with shaking at 120 rpm. Samples were taken over a period of time and measured spectrophotometrically (550 nm) to analyse relative cell growth and any imposed inhibition. Each experiment was conducted in triplicate.

2.3.4 Disk diffusion susceptibility assay

To investigate the inhibitory activity of various processed and unprocessed antimicrobials against *A. niger*, a disk diffusion assay was utilised. Spore suspensions of *A. niger* were prepared by washing confluent growth *A. niger* on agar plates with 5 ml ddH_2O / 5% Tween-20 solution (Sigma-Aldrich). The resulting hyphal / spore suspension was subsequently passed through an 11 µm pore diameter filter (Millipore) to produce an inoculum mainly composed of spores and adjusted to ~$2x10^6$ spores ml^{-1} using ddH_2O (Petrikkou *et al.*, 2001). The spore suspension (100 µl) was spread onto

CM 1.5% agar plates to produce confluent lawns. The sterile filters were prepared by the addition of 10 µl of either: nanoparticle formulated tebuconazole (10 % $^{w}/_{w}$ tebuconazole, 30% $^{w}/_{w}$ SDS, 60% $^{w}/_{w}$ PVA) or iodopropynyl butylcarbamate (10 % $^{w}/_{w}$ IPBC, 50% $^{w}/_{w}$ SDS, 40% $^{w}/_{w}$ HPMC), blank nanoparticle (30% $^{w}/_{w}$ SDS, 60% $^{w}/_{w}$ PVA) or (50% $^{w}/_{w}$ SDS, 40% $^{w}/_{w}$ HPMC) or acetone dissolved antimicrobial at either 0.01% $^{w}/_{v}$, 0.1% $^{w}/_{v}$ or 1.0% $^{w}/_{v}$. Formulations consisted: 1 µg ml^{-1} at 0.01% $^{w}/_{v}$, 10 µg ml^{-1} at 0.1 $^{w}/_{v}$ or 100 µg ml^{-1} at 1.0% $^{w}/_{v}$ of tebuconazole or iodopropynyl butylcarbamate in the antimicrobial containing preparations. The blank and antimicrobial loaded preparations were produced and tested at comparable concentrations and volumes. The negative control consisted of an equal volume of ddH_2O added to the filter disks. After allowing the filters to air dry they were added to the inoculated agar surface using aseptic technique throughout. The plates were sealed and incubated at 30°C for 96 hours, after which zones of inhibition were recorded.

2.4 Nanoparticle preparation

Nanoparticles were produced using a novel modified emulsion-evaporation technique, developed by Iota NanoSolutions Ltd. Briefly, a water insoluble antimicrobial was dissolved in a suitable non-aqueous solvent or mixture of non-aqueous solvents. The oil phase was subsequently mixed with an aqueous phase containing a water-soluble polymer and surfactant (together termed excipients). The resulting mixture comprised a single phase material in which the water-soluble carrier and water insoluble antimicrobial were dissolved. It was subsequently fed through a spray dryer (Büchi, B-290^{TM}), operated under negative pressure. The operating conditions were: pump rate (20%, 7.2 ml min^{-1}), inlet temperature 150°C, aspiration 100% and maximum nitrogen flow for atomisation (approximately 55 L hr^{-1}). The resulting powder passed through a cyclone and dropped into a collection vessel. Dry composite materials were obtained for all preparations. Upon mixture of the dry nano-composite material with ddH_2O, the water-soluble excipients dissolve and the water-insoluble antimicrobial behaves like a soluble material through the formation of nanoparticles. Unless stated otherwise stock nanoparticle solutions were produced at 2 mg ml^{-1} of the antimicrobial immediately prior to use. The resulting nanoparticulate dispersion can resemble a transparent

molecular solution and 'insoluble' antimicrobials can be delivered as an aqueous suspension (Duncalf *et al.*, 2008 ; Zhang *et al.*, 2008a).

2.5 Nanoparticle characterisation

All nanoparticle preparations were characterised by size determination using dynamic light scattering (DLS) and zeta potential using electrophoretic light scattering (ELS). Selected preparations were examined using scanning electron microscopy (SEM) to investigate particle shape and morphology. X-ray diffraction (XRD) was used to determine the degree of crystallinity within the individual constituent components and processed nanoparticle preparations.

2.5.1 Size and zeta potential

All size measurements were conducted using a Malvern Zetasizer Nano^{TM} dynamic light scattering (DLS) instrument fitted with a 633 nm 4 mW laser. Samples were dispersed to a concentration of 2 mg ml^{-1} and were analysed with detection angles of 173° (back scatter) and 12° (forward scatter). Standard optical quality disposable UV cuvettes were used to contain the samples. Results were displayed as Z-average diameters of the mean of 5 consecutive measurements. All viscosity measurements were made using a Hydramotion viscolite 700 instrument, and size results adjusted accordingly.

Zeta potential was determined using Electrophoretic Light Scattering (ELS) in which the velocity of charged particles under the influence of an applied electric field is measured by monitoring the frequency shift of the scattered light from the particles. Samples were prepared at 2 mg ml^{-1}, ~800 µl was injected into a capillary cell and measured on a Malvern Zetasizer Nano^{TM} with the detector positioned at a 17° scattering angle (Malvern Instruments). The data were analysed and interpreted using Malvern software version 6.1. All charges were recorded as the mean of 5 consecutive measurements.

2.5.2 Critical Micellisation Concentration (CMC)

CMC calculates the concentration at which amphiphiles associate into micellar structures. Serial dilutions of nanoparticle and excipient materials were produced in standard flat bottom 96 well plates using ddH_2O. The last column of the plate was reserved for a control of ddH_2O to which the measurement of each sample was quantified. Following sample dilution, 50 µl was transferred into a Teflon coated Kibron 96 well measurement plate (Kibron Inc.). Surface tension measurements were conducted on a Delta-8 multichannel microtensionmeter (Kibron Inc.). The instrument utilises eight parallel microbalances to determine surface tension based on the Du Nouy method; the maximum force exerted by the surface tension is recorded as the probes are withdrawn from the solutions. The surfaces of the probes were cleaned between measurements using a furnace. The data were combined and analysed using Kibron Delta-8 software.

2.5.3 High Performance Liquid Chromatography (HPLC) methods

HPLC analysis was conducted to determine the actual loading of active ingredients in nanoparticle formulations and to monitor the rate of dissolution of dichlorophen. All analysis was conducted using a Perkin Elmer 200 series instrument fitted with an auto-sampler and a diode array detector. Separation was achieved using a 5 µm Sunfire column, 4.6 mm i.d. x 150 mm o.d. All measurements were conducted in duplicate. A linear calibration was determined for dichlorophen over a concentration range of 1.025 µg ml^{-1} to 205 µg ml^{-1} (R^2 0.9976) under the following operating conditions; isocratic mobile phase 75:25 methanol:water, flow rate 1 ml min^{-1}, injection volume of 20 µl and detector acquisition set at 205 nm. All samples were prepared in or diluted with the mobile phase. Each measurement was conducted over 10 minutes and the peak corresponding to the dichlorophen eluted after 5.76 minutes.

A linear calibration was determined for ciprofloxacin over a concentration range of 1 µg ml^{-1} to 100 µg ml^{-1} (R^2 0.9925) under the following operating conditions; gradient elution, mobile phase 10:90 acetonitrile:acetic acid, flow rate 1 ml min^{-1}, injection volume of 30 µl and detector acquisition set at 280 nm. All samples were prepared in a

5:95 mix of glacial acetic acid:acetonitrile. Each measurement was conducted over 6 minutes with the peak corresponding to the ciprofloxacin eluting after 0.8 minutes.

2.5.4 SEM

Field emission scanning electron microscopy (SEM) was conducted using a Hitachi S-4800™ instrument. Nanoparticle preparations were dispersed at 1 mg ml^{-1} and mounted onto sample stubs and gold coated for 2 minutes at 25 μA using a sputter-coater (Emitech K550X) prior to imaging. SEM images were produced using the following microscope settings: accelerator voltage, 3000 V; working distance, 8400 μm; emission current, 10600 nA; magnification settings ranging from x 500 to x 50000.

2.5.5 X-ray Diffraction (XRD) analysis

XRD was performed to identify whether a preparation of nanoparticle formulated ciprofloxacin (50/27/55) was present in amorphous or crystalline states. XRD analysis was carried out on ciprofloxacin loaded and blank nanoparticles, and individual excipients using an R-AXIS IV++™ Xray diffractometer (Rigaku). Samples (~5 mg) were loaded onto hollow glass rods and adjusted onto the instrument's stage. The operating conditions were as follows: detection distance, 200 mm; rotation angle, 10°; exposure time, 3 min; optic type, multilayer; collimation type, 0.5 pinhole; focus, 0.07; voltage, 40 kV; current, 20 mA; conducted at 20°C. Image analysis was carried out using CrystalClear™ 1.3.6 software.

2.6 Design of Experiment (DOE)

Computer modeling was used to identify trends in nanoparticle design of significance to inhibitory activity. A simple cube based DOE was used for the purpose of screening and optimisation of nanoparticle design in this work, as outlined in Figure 1.7. Initial material screening provided the details of input parameters to investigate. The parameters set were: loading ratios of dichlorophen (5% - 20% $^{w}/_{w}$), loading ratios of HPMC (0% - 85% $^{w}/_{w}$), loading ratios of gelatin (0% - 85% $^{w}/_{w}$) and loading ratios of SDS (10% - 50% $^{w}/_{w}$). Experimental points suggested by the model were produced and screened for activity against *S. aureus* SH1000, MRSA, *E. coli* and *C. albicans*.

2.7 Agarose gel electrophoresis

Nucleic acid extracts were visualized using agarose gel electrophoresis. Gels were comprised of 1% $^{w}/_{v}$ agarose in 1 x TAE (Tris-acetate EDTA) buffer diluted with ddH_2O from a 50 x stock of TAE (2 M Tris, 57.1 ml L^{-1} glacial acetic acid, 0.05 M EDTA, pH 8.0). Ethidium bromide (0.25 μg ml^{-1}) was added to the agarose gel. Electrophoresis was conducted in a tank containing 1 x TAE buffer for 45 min at 100 volts. Nucleic acid was visualised using UV trans-illumination (254 nm) on the Gene Genius bio imaging system (Syngene). Nucleic acid fragment size was determined by comparison to an appropriate size marker.

2.8 Sample and library preparation for SOLiD™ RNA Sequencing

RNA-Seq was identified as a suitable experimental procedure to investigate whether transcriptional differences existed in co-solvent dissolved antimicrobial delivery, antimicrobial-loaded nanoparticle delivery and control solution treated cells. The Applied Biosystems™ SOLiD™ platform was used for the purpose of this investigation and the processes used are outlined in Figure 2.2.

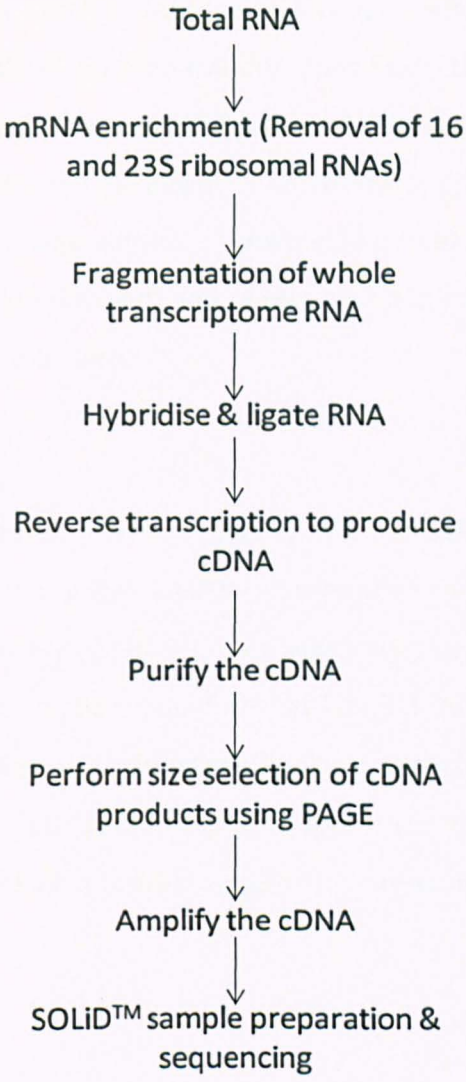

Figure 2.2 Processes in whole transcriptome library preparation for SOLiD™ sequencing. (Adapted from SOLiD™ Total RNA-Seq kit protocol, 2010)

2.8.1 Sample preparation for transcriptional analysis

To ascertain the transcriptional response of *S. aureus* SH1000 to the nanoparticle formation of ciprofloxacin, an overnight culture (16 hour) of SH1000 was used to inoculate conical flasks containing BHI (Lab M) to $O.D_{550}$ 0.2. These 50 ml cultures were placed in a shaking water bath at 37°C at 125 rpm and incubated until the $O.D_{550}$ reached ~0.6. To each 250 ml conical flask, equal volumes (390 µl) of nanoparticle formulated ciprofloxacin solution (preparation 50/27/55), ciprofloxacin dissolved in DMSO, blank nanoparticle, DMSO or ddH_2O were added to each mid-exponential

phase culture. The final ciprofloxacin concentration was 15.63 µg ml^{-1} for both nanoparticle and DMSO dissolved preparations. Specifically the nanoparticle test flasks comprised 15.63 µg ml^{-1} ciprofloxacin, 42.9 µg ml^{-1} PVP and 19.5 µg ml^{-1} Pluronic F127. An equal concentration of blank nanoparticle solution comprising 42.9 µg ml^{-1} PVP and 19.5 µg ml^{-1} Pluronic F127 was utilised. Following 20 min exposure to each treatment condition, the cells were lysed as outlined in section 2.8.2; each treatment and control culture was performed in triplicate.

2.8.2 Cell lysis

Three ml of mid-exponential phase *S. aureus* SH1000 culture were centrifuged at 5,000 x *g* for 2 min, and the cell pellet re-suspended in 2 volumes of RNA*later*® (Ambion) and incubated overnight at 4°C. The tubes were centrifuged at 5, 000 x *g* for 10 min, supernatant was removed and the cell pellet re-suspended in 420 µl TE containing 600 µg ml^{-1} RNase-free lysostaphin (Sigma-Aldrich), 400 U ml^{-1} mutanolysin (Sigma-Aldrich) and 40 µg ml^{-1} proteinase K (Qiagen). The cells and lysis reaction mix were incubated at 37°C for 60 min with occasional gentle mixing. Adapted from Kenny *et al.*, (2009).

2.8.3 RNA extraction

Glassware was rendered RNase free by washing followed by baking at 250°C for at least four hours. All plastic ware was certified RNase free. Solutions were prepared with 0.1% $^{v}/_{v}$ diethyl polycarbonate (DEPC) (Sigma-Aldrich) prior to autoclaving, unless this was not possible due to cross reactivity with certain chemicals. In such cases, the solutions were produced with DEPC treated water that had been autoclaved prior to addition of RNase-free dry chemicals. All apparatus, pipettes and work surfaces were treated with RNase Zap™ (Ambion) prior to extraction. All extracts were stored at -80°C until use.

2.8.4 RNeasy mini kit™ (Qiagen)

RNA was extracted from samples following the manufacturer's protocol. Briefly, successive 700 µl volumes of sample were transferred to the spin column and centrifuged for 15 s at ≥ 10,000 rpm and the flow-through discarded after each

centrifugation. After processing, 50 µl RNase-free water was applied directly to the spin column membrane and centrifuged for 1 min at ≥ 10,000 rpm to elute the RNA and repeated using the same 50 µl aliquot. Following RNA elution, 10 units of RNasin® Ribonuclease Inhibitor (Promega) was added to each sample according to the manufacturer's protocol. RNA quantification was performed using a Qubit™ fluorometer and the RNA assay kit Quant-iT™ (Invitrogen).

2.8.5 DNaseI treatment of RNA extracts (Ambion)

Following RNA extraction, DNA was removed by DNaseI treatment. For each reaction, no more than 200 µg ml^{-1} of nucleic acid was included, 2 µl rDNase I and 5 µl 10X Reaction buffer (Ambion) were made up to 50 µl with nuclease-free water. The reaction mix was incubated at 37°C for 30 min and a further 2 µl rDNase I (Ambion) was added. The reaction mix was incubated for a further 30 min. Following incubation, the reaction mix was made up to 300 µl with nuclease-free water. RNA was extracted with 300 µl phenol: chloroform: isoamyl alcohol (25:24:1) (Sigma-Aldrich) with brief vortexing, and centrifuged at 10,000 x *g* for 5 min. The aqueous layer was added to a fresh tube and RNA precipitated with 750 µl ice cold 100% ethanol and 30 µl of 3M sodium acetate pH 5.2. Following overnight incubation at -20°C, samples were centrifuged at full speed for 15 min. The supernatant was removed and the pelleted RNA washed with 500 µl ice cold 70% ethanol. After further centrifugation at full speed, the supernatant was removed and the pelleted RNA air-dried and resuspended in 15 µl TE. RNA was quantified using a Qubit™ fluorometer (Invitrogen), RNA integrity was measured using a 2100 Bioanalyzer (Agilent), and the RNA preparation stored at -80°C until use.

2.8.6 mRNA enrichment

Following DNase I treatment of RNA, mRNA was enriched using a Microb*express*™ Kit (Ambion) according to the manufacturer's protocol. Briefly, the enriched mRNA was precipitated at -20°C overnight and resuspended in 10 µl TE. RNA was quantified using a Qubit™ fluorometer (Invitrogen), RNA integrity was measured using a 2100 Bioanalyzer (Agilent) and the RNA preparation stored at -80°C until use.

2.8.7 Fragmentation of whole transcriptome RNA

Following mRNA enrichment, RNA was fragmented using RNase III (Ambion) according to the manufacturer's protocol. For each sample, ~0.5-1.0 µg of rRNA-depleted RNA, 1 µl RNase III Reaction Buffer and 1 µl RNase III were assembled and incubated at 37°C for 10 min. After incubation, 90 µl of nuclease-free water was added to each reaction mix and RNA subsequently cleaned up using components from the RiboMinus™ Concentration Module (Invitrogen) according to the manufacturer's protocol. The fragmented RNA was eluted in 20 µl nuclease-free water, quantified using a Qubit™ fluorometer (Invitrogen), RNA integrity measured using a 2100 Bioanalyzer (Agilent) and the RNA preparation stored at -80°C until use.

2.8.8 Reverse-transcription of RNA

Following fragmentation and clean up, 90 ng of each RNA sample was hybridized and ligated using components from the SOLiD™ Small RNA Expression Kit (Ambion) according to the manufacturer's protocol. Briefly, each hybridization mix was incubated at 65°C for 10 min, 16°C for 5 min and then mixed with RNA ligation reagents and incubated at 16°C for a further 16 h. Following ligation, reverse transcription was performed using ArrayScript™ reverse transcriptase, 2.5 mM dNTP mix and 10 X RT buffer (Ambion). 20 µl of each reverse transcription master mix was added to each 20 µl ligation reaction and incubated at 42°C for 30 min. The cDNA was subsequently purified using the MinElute® PCR Purification Kit (Qiagen) and stored at -20°C until use.

2.8.9 Size selection of cDNA product

The cDNA product for each sample was size selected on Novex® 6% TBE-Urea 1 mM gels (Invitrogen) using a XCell *SureLock*™ Mini-Cell (Invitrogen). The DNA ladder HyperLadder™ V (Bioline) was diluted to 40 ng μl^{-1} with RNase-free water, and 5 µl was mixed with an equal volume of 2X Novex® TBE-Urea Sample Buffer (Invitrogen) for each sample run. Equal volumes of the cDNA samples were prepared and mixed with 2X Novex® TBE-Urea Sample Buffer (Invitrogen). The cDNA and DNA ladder samples were incubated at 95°C for 3 min and subsequently snap-cooled on ice. The Novex® 6% TBE-Urea 1.0 mM gels (Invitrogen) were prepared and cDNA samples run according to

the manufacturer's protocol. The gels were stained with SYBR® Gold nucleic acid stain (Invitrogen) for 20 min with gentle agitation, and the reaction products were visualised using a UV transilluminator. Gel material containing 100-200 nt DNA was excised and split vertically in-to 4 pieces using a sterile scalpel blade, and stored at -20°C until use.

2.8.10 Amplification of cDNA

Following size selection, the cDNA was amplified using components from the SOLiD™ Small RNA Expression Kit and SOLiD™ RNA Barcoding Kit (Ambion) according to the manufacturer's protocol. Briefly, two PCR reactions were prepared for each sample to generate sufficient cDNA to perform subsequent template bead preparation. Each PCR reaction consisted: PCR buffer, 25 µM of each SOLiD™ PCR primers (1-10), 2.5 mM dNTP mix. AmpliTaq™ DNA polymerase and one excised gel piece. The thermal cycling conditions used are outlined in Table 2.3. After amplification, the DNA products were purified using the PureLink™ PCR Micro Kit (Invitrogen) according to the manufacturer's protocol. The yield and size distribution of the amplified DNA was measured using a 2100 Bioanalyzer (Agilent) and stored at -20°C until required.

Table 2.3 Thermal cycling conditions for cDNA amplification

Stage	Temperature °C	Time
Hold	95	5 min
Cycle (15 cycles)	95	30 sec
	62	30 sec
	72	30 sec
Hold	72	7 min

2.8.11 SOLiD™ sequencing

Following library construction, template bead preparation was performed. Each library template was clonally amplified on SOLiD™ P1 DNA beads by emulsion PCR following the manufacturer's protocol (SOLiD™ 3 Plus System, Template Bead Preparation) and quantified using a KAPA™ Library Quantification Kit (KAPA Biosystems). After PCR and enrichment of the template beads, they were deposited onto a full titanium slide providing ~ 420 million usable beads and sequenced on a SOLiD™ 3 Plus System (Applied Biosystems). Template bead preparation, library quantification and SOLiD™ sequencing were performed by The Liverpool Centre for Genomic Research.

2.8.12 Bioinformatic analysis of SOLiD™ RNA-Sequencing data

Bioinformatic analysis of the raw SOLiD™ sequence data was conducted by The Liverpool Centre for Genomic Research. Briefly, reads for each sample were mapped to the reference genome *S. aureus* 8325 (NCBI) using BioScope™ software (version 1.2, Applied Biosystems) resulting in a Binary Alignment Map (BAM) representing alignment information for all mapped reads. Uniquely mapping reads that mapped to only one location, were then used to produce a separate BAM file. Subsequently, Reads Per Kilobase of exon model per Million of mapped reads (RPKM) values were generated, based on the annotations provided by the reference genome and the coverage data produced from the BAM file. Expression analysis of the RPKM values was performed using the DESeq package scripts (Anders & Huber, 2010) provided through Bioconductor (www.bioconductor.org) using the R statistical computing language (www.r-project.org) to estimate the variance and test for differential expression in the data. Subsequently, genes were filtered on expression level, with only those genes that changed by at least 2 fold with a maximum significance cut off at p=0.05 considered biologically significant. The genome browsers and annotation tools Artemis (Rutherford *et al.*, 2000) and Integrative Genomics Viewer (IGV) (Robinson *et al.*, 2011) were used for visualisation of the transcriptomes to permit greater understanding of each feature within its genomic context. Annotations of identified features were conducted using The Seed (www.theseed.org) (Overbeek *et al.*, 2005) and KEGG: Kyoto Encyclopedia of Genes and Genomes (www.genome.jp/kegg) (Kanehisa & Goto, 2000).

2.9 Dissolution assay

Dissolution assays were performed to investigate the rate of dichlorophen released when nanoparticle formulated (DOE/97/03 consisting: 15% $^{w}/_{w}$ dichlorophen, 50% $^{w}/_{w}$ SDS, 40% $^{w}/_{w}$ HPMC) and prepared as a water stirred equivalent. The final concentration of each component in both nanoparticle and water stirred preparations was: 250 mg dichlorophen, 250 mg SDS and 1166 mg HPMC. Dialysis membranes with a molecular weight cut off (MWCO) of 12-14000 Daltons (Medicell International Ltd) were prepared by boiling 12 cm lengths in ddH_2O and subsequently filling the dialysis tube with 40 ml of the nanoparticle or water stirred mixture of dichlorophen, SDS and HPMC at equal quantities. The dialysis membrane was sealed and placed into a 1 L beaker of 460 ml pre-heated ddH_2O at 37°C and stirred at 200 rpm. A feedback loop temperature probe and heating plate were used to ensure the temperature remained constant. Samples (0.5 ml) were taken periodically from the water and replaced with equal volumes of fresh ddH_2O. Samples were mixed with equal volumes of acetonitrile prior to HPLC analysis using a Perkin Elmer 200 series as outlined in section 2.5.3.

Chapter 3

Nanoparticle formation of antifungals and biocides for comparisons of inhibitory activity

3.1 Introduction

Fungal pathogens pose a particular challenge in antimicrobial development because they are eukaryotes that share close evolutionary histories with their hosts. The number of drug classes that have distinct targets in fungi is limited and the usefulness of most antifungal compounds is compromised due to either host toxicity or diminished efficacy in killing fungal pathogens (Odds *et al.*, 2003 ; Cowen, 2008). Invasive fungal infections are an increasing threat to human health. In the developed world these infections usually occur when aggressive immunosuppressive therapies are used. The overall mortality for invasive diseases caused by *Candida spp.* and *Aspergillus spp.* is 30-50% (Denning & Hope, 2010). *Candida spp.* are the fourth leading cause of nosocomial infections in the USA with *Candida albicans* being the most clinically significant (Calderone & Fonzi, 2001 ; Ramage *et al.*, 2005). *Aspergillus niger* is a rare opportunistic pathogen but is known to be problematic in immune-compromised patients and those with severe illness (Schuster *et al.*, 2002).

Fungal pathogens not only pose a direct threat to human health, but also to agricultural crops that are essential to maintaining global food supplies (Strange & Scott, 2005). *A. niger* is also recognised as a crop, food and chemical spoilage agent (Abarca *et al.*, 2004). The globalisation of agriculture has meant that crop plants, often with a narrow genetic basis, are now grown far from their centres of origin and the pathogens that co-evolved with them. The over-reliance on a narrow range of crop plants for food production, intensive farming methods and the global transportation of crops, intensifies the risks posed by fungal pathogens and the spread of antifungal resistant strains (strange & Scott, 2005). Resistance to antifungals is of growing concern in both clinical and agricultural settings, leading to increased mortality and lower crop yields (Norrby *et al.*, 2005).

A range of antifungals and general biocides with known antifungal properties, which all display poor water solubility, ($\leq$ 100 $\mu g\ ml^{-1}$), that were available in sufficient quantities to formulate and that have a variety of applications, were processed into nanoparticles as described in section 2.4. Comparisons of inhibitory activity between nanoparticle formulated antifungals and biocides were made with organic co-solvent dissolved forms of delivery as described in sections 2.3, 2.3.1 and 2.3.4.

The two azoles propiconazole and tebuconazole were investigated for inhibitory activity. The azole group of antifungals display action against diverse fungi and have been one of the most widely used classes of antifungals for decades. The azoles target lanosterol 14α demethylase (encoded by *ERG11*) and block the production of ergosterol (Figure 3.1) which is the predominant membrane component this leads to the accumulation of toxic sterol intermediates and ultimately prevents fungal growth (Lupetti *et al.*, 2002 ; Cowen, 2008).

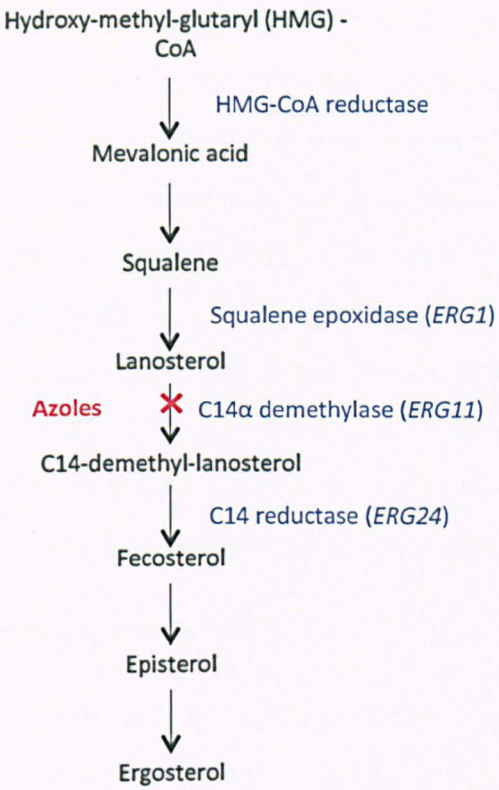

Figure 3.1. The mode of action of azole antifungals affecting the ergosterol biosynthetic pathway (adapted from Lupetti *et al.*, 2002).

Tebuconazole is widely used in Europe and the USA as Folicur® (Bayer) which is effective against various smut and bunt diseases of cereals and a range of other crops (Asrar *et al.*, 2004 ; Bayer CropScience website, 2011). Propiconazole is also a systemic broad-spectrum fungicide widely used in agriculture. Pentachlorophenol is a broad-spectrum fungicide formally used to protect wood from fungal rots (Tomlin, 1995). Iodopropynyl butylcarbamate (IPBC) is a highly effective fungicide with widespread application in both occupational and consumer products where it is used as a preservative (Badreshia & Marks, 2002). Dichlorophen is a commonly used fungicide widely employed in consumer toiletries such as soaps and cosmetics. For example, it is used to treat fungal infections of the skin and is present in the product Mycota® spray for the treatment and prevention of athlete's foot and is also used in agriculture as a fungicide (Cox *et al.*, 2004 ; Mycota website, 2011).

A range of studies have utilised variations in the emulsion evaporation process to form organic nanoparticles. Patel *et al.* (2010) produced poly(lactic-co-glycolic) nanoparticles containing the hydrophobic antifungal itraconazole using an oil-in-water emulsion evaporation technique. The prepared nanoparticles were tested for inhibitory activity against *Aspergillus flavus* and found to be more inhibitory than water-dissolved and Triton X-100-emulsified itraconazole preparations. Peng *et al.* (2008) produced voriconazole loaded poly(lactide-co-glycolide) nanoparticles using an emulsion-evaporation technique and showed the nanoparticle preparation was more inhibitory against *C. albicans* than an equivalent solvent-dissolved voriconazole preparation. The materials, preparative and production methods used to produce these nanoparticles differ from those used in this investigation.

The chapter has the following specific aims:

- To investigate if the poorly water soluble antifungals propiconazole, tebuconazole, pentachlorophenol, dichlorophen and iodopropynyl butylcarbamate could be formulated into nanoparticles.
- To investigate the inhibitory efficacy of the nanoparticle formulated antifungals that have varying molecular targets against *C. albicans* and *A. niger* using MIC and filter disk diffusion assays.
- To investigate the influence of nanoparticle design on the expressed size and zeta potential of the formulation.
- To investigate the influence of nanoparticle design on nanoparticle efficacy of inhibition and to determine if a correlation exists between nanoparticle physical characteristics and efficacy.

The specific aims identified in this chapter address some of the broader aims identified in section 1.15 including; the investigation into the overall scope of the nanoparticle formulation process, the influence of antifungal and excipient types and loading ratios on nanoparticle efficacy, and the relationship between nanoparticle physical characteristics and inhibition.

3.2 Propiconazole

Nanoparticles of propiconazole (14/22/04, refer to Table 3.1) were produced and subsequently characterised on the basis of size and zeta potential using a Malvern Zetasizer Nano^{TM} as outlined in section 2.5.1. The prepared propiconazole nanoparticles were tested against *C. albicans* in 96-well plate assays (refer to section 2.3.1) and the inhibitory effects compared with water saturated, co-solvent dissolved propiconazole and blank nanoparticles that were processed using the same protocol as the propiconazole loaded nanoparticles (Figure 3.2).

Table 3.1. Nanoparticle formulated propiconazole and subsequent characterisation.

Preparation code	Nanoparticle composition (% $^{w}/_{w}$)	Size (nm)	Zeta potential (mV)
14/22/04	10% propiconazole 20% SLES 70%PEG	2.98	-32.03

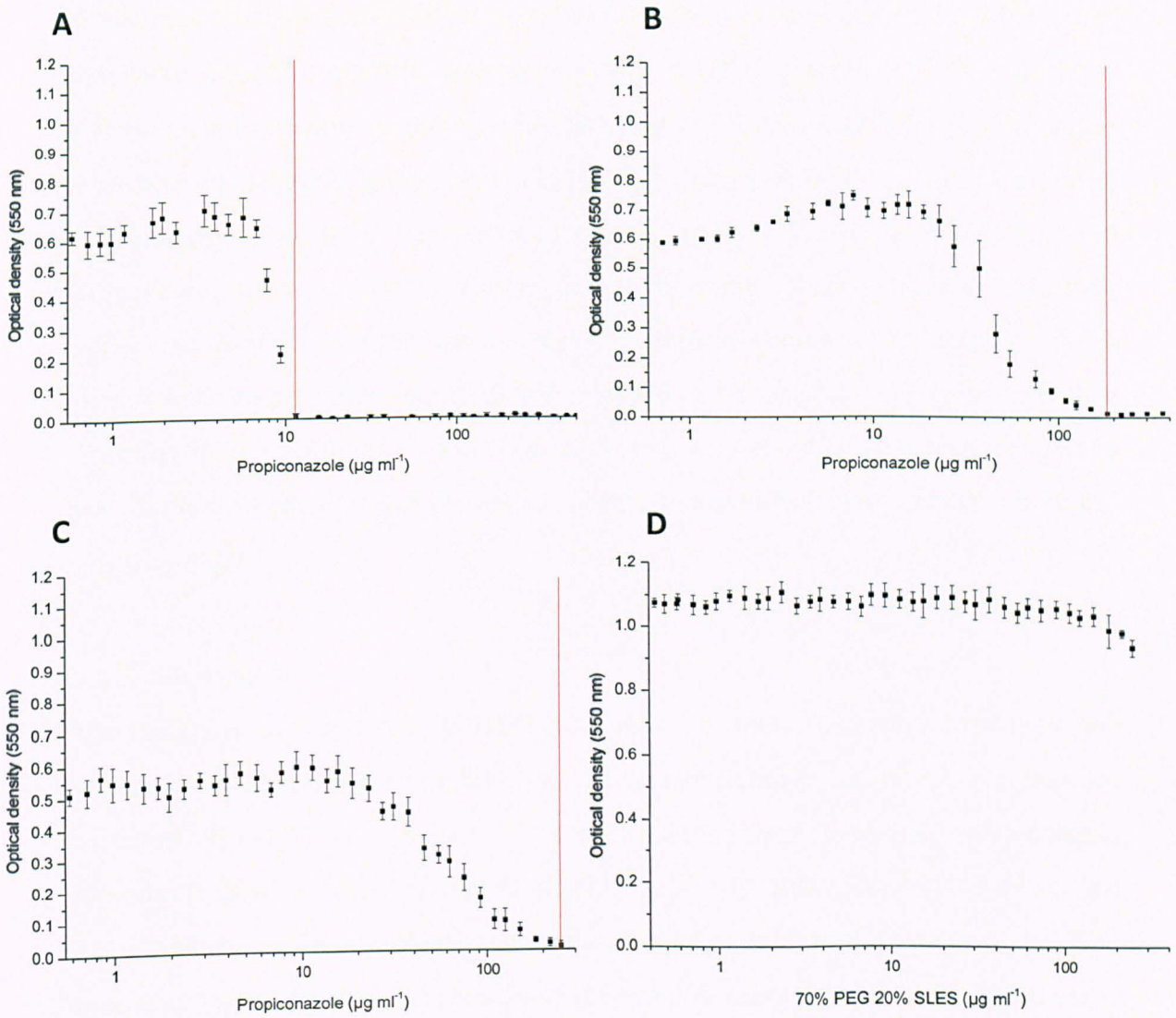

Figure 3.2. The inhibitory effects of propiconazole and controls on *C. albicans* in 96 well plate assays after 24 hours incubation the red line marks the determined MIC. (A) nanoparticle formulated propiconazole (14/22/04), (B) ethylene glycol dissolved propiconazole (C) water saturated propiconazole (D) blank nanoparticle (20% $^{w}/_{w}$ SLES 70% $^{w}/_{w}$ PEG) treated cells. Values are averages from three independent experiments. Error bars indicate standard errors of the mean.

The results in Table 3.1 show that nanoparticles of propiconazole were produced with an average size of 2.98 nm and an average zeta potential of -32.03 mV after viscosity correction. The optically clear and stable nanoparticle preparation was subsequently tested against *C. albicans* for inhibitory activity. The results in Figure 3.2 suggest that nanoparticle formulated propiconazole was more effective at inhibiting the growth of

C. albicans than the conventional co-solvent dissolved form of delivery and the water saturated control. The MIC was determined at 11.46 μg ml^{-1} (S.E.M 1.69^{-3}) for nanoparticle formulated propiconazole, 183.3 μg ml^{-1} (S.E.M 3.88^{-3}) for propiconazole dissolved in ethylene glycol and 250 μg ml^{-1} (S.E.M 6.26^{-2}) for water-saturated propiconazole. The blank nanoparticles comprising 70% $^{w}/_{w}$ PEG and 20% $^{w}/_{w}$ SLES prepared in the same manner and applied at the same concentrations as the active equivalent, produced no MIC value across the concentration range investigated. These results indicate an approximate 16-fold increase in efficacy when using nanoparticle formulated propiconazole compared with the convectional co-solvent dissolved preparation, and an approximate 21 fold improvement over water saturated propiconazole.

3.3 Tebuconazole

Nanoparticles of tebuconazole (25/21/01, refer to Table 3.2) were produced and subsequently characterised on the basis of size and zeta potential using a Malvern Zetasizer Nano™ as outlined in section 2.5.1. The prepared tebuconazole nanoparticles were tested against *C. albicans* in 96 well plate assays (refer to section 2.3.1) and the inhibitory effects compared with water saturated, co-solvent dissolved tebuconazole and blank nanoparticles that were processed using the same protocol as the tebuconazole loaded nanoparticles (Figure 3.3).

Table 3.2. Nanoparticle formulated tebuconazole and subsequent characterisation.

Preparation code	Nanoparticle composition (% $^{w}/_{w}$)	Size (nm)	Zeta potential (mV)
25/21/01	10% Tebuconazole 30% SDS 60% PVA	5.46	-36.19

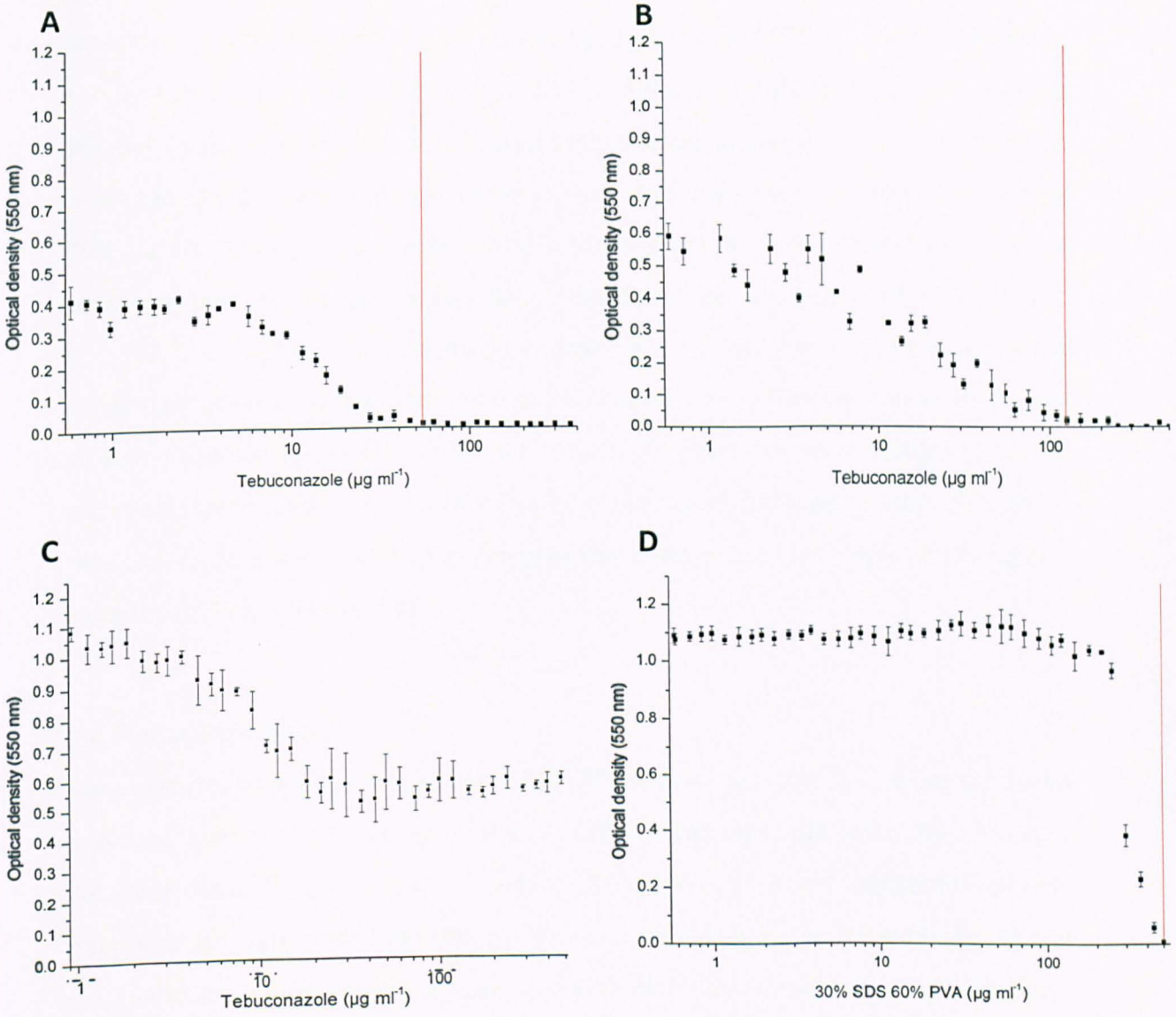

Figure 3.3. The inhibitory effects of tebuconazole and controls on *C. albicans* in 96 well plate assays after 24 hours incubation, the red line marks the determined MIC. (A) nanoparticle formulated tebuconazole (25/21/01), (B) ethylene glycol dissolved tebuconazole (C) water saturated tebuconazole (D) blank nanoparticle (30% $^{w}/_{w}$ SDS 60% $^{w}/_{w}$ PVA) treated cells. Values are the averages from three independent experiments. Error bars indicate standard errors of the mean.

The results in Table 3.2 show that nanoparticles of tebuconazole were produced with an average size of 5.46 nm and an average zeta potential of -36.19 mV after viscosity correction. The optically clear and stable nanoparticle preparation was subsequently tested against *C. albicans* for inhibitory activity. The results in Figure 3.3 suggest that nanoparticle formulated tebuconazole was more effective at inhibiting the growth of

C. albicans than the conventional co-solvent dissolved form of delivery and the water saturated control. The MIC was determined at 54.65 μg ml^{-1} (S.E.M 0) for nanoparticle formulated tebuconazole, 125 μg ml^{-1} (S.E.M 3.00^{-3}) for tebuconazole dissolved in ethylene glycol, and the water-saturated tebuconazole data highlighted no MIC value over the concentration range investigated. The blank nanoparticles comprising 30% $^{w}/_{w}$ SDS and 60% $^{w}/_{w}$ PVA prepared in the same manner and applied at the same concentrations as the active equivalent, produced an MIC value of 500 μg ml^{-1} (S.E.M 2.7^{-2}). These results indicate an approximate 2.3 fold increase in efficacy when using nanoparticle formulated tebuconazole compared with the conventional co-solvent dissolved preparation. The data also highlighted the poor killing efficacy of water-saturated tebuconazole. This may be explained by the lower water solubility of tebuconazole compared with propiconazole that produced an MIC value of 250 μg ml^{-1} against *C. albicans* (Figure 3.2).

3.4 Pentachlorophenol

Nanoparticles of pentachlorophenol (25/PCP/01, refer to Table 3.3) were produced and subsequently characterised on the basis of size and zeta potential using a Malvern Zetasizer Nano™ as outlined in section 2.5.1. The prepared pentachlorophenol nanoparticles were tested against *C. albicans* in 96 well plate assays (refer to section 2.3.1) and the inhibitory effects compared with water saturated, co-solvent dissolved, a salt derivative of pentachlorophenol and blank nanoparticles that were processed using the same protocol as the pentachlorophenol loaded nanoparticles (Table 3.4).

Table 3.3 Nanoparticle formulated pentachlorophenol and subsequent characterisation.

Preparation code	Nanoparticle composition (% $^{w}/_{w}$)	Size (nm)	Zeta potential (mV)
25/PCP/01	10% pentachlorophenol 30% SDS 60% PVA	5.15	-34.91

Table 3.4 The inhibitory effects of pentachlorophenol and controls on *C. albicans* in 96 well plate assays after 24 hours incubation. Values are the averages from three independent experiments, with standard errors of the mean shown.

Preparation	MIC ($\mu g\ ml^{-1}$)	S.E.M
Nanoparticle pentachlorophenol – 25/PCP/01	15.63	5.0^{-3}
Pentachlorophenol in ethylene glycol	18.75	1.0^{-2}
Water saturated pentachlorophenol	>500	-
Blank nanoparticle (30% SDS 60% PVA)	500	2.7^{-2}
Water dissolved sodium pentachlorophenol	37.5	1.6^{-2}

The results in Table 3.3 show that nanoparticles of pentachlorophenol were produced with an average size of 5.15 nm and an average zeta potential of -34.91 mV after viscosity correction. The optically clear and stable nanoparticle preparation was subsequently tested against *C. albicans* for inhibitory activity. The results in Table 3.4 suggest that nanoparticle formulated pentachlorophenol was only slightly more effective at inhibiting the growth of *C. albicans* than the conventional co-solvent dissolved form of delivery and the salt derivative of the base chemical sodium pentachlorophenol. These results indicate an approximate 1.2 fold increase in efficacy when using nanoparticle formulated pentachlorophenol compared with the convectional co-solvent dissolved preparation. They also indicated an approximate 2.4 fold increase in efficacy when using the nanoparticle preparation compared with the water-soluble salt derivative of the base chemical, sodium pentachlorophenol. The water saturated base pentachlorophenol produced no MIC across the concentration range investigated. These results highlight the improvement in inhibitory activity that are afforded to base antimicrobials due to nanoparticle formation compared to water saturated preparations of the base chemical, which would otherwise not be inhibitory to the growth of *C. albicans*. Although the water soluble, sodium pentachlorophenol was more inhibitory than the base pentachlorophenol preparation, it produced a higher MIC value than the equivalent ethylene glycol dissolved preparation. The differences in chemical structure between sodium pentachlorophenol and the base chemical possibly account for the differences in activity observed as it is anticipated that the mode of action will vary between preparations.

3.5 Dichlorophen

A range of dichlorophen nanoparticles (refer to Table 3.5) were produced with either: different polymers, different surfactants or variations in surfactant ratio to determine if such parameters influence inhibitory activity when tested against *C. albicans* in 96-well plate assays. The inhibitory effects of nanoparticle formulated dichlorophen were compared with water saturated, co-solvent dissolved dichlorophen and blank nanoparticles that were processed using the same protocol as the dichlorophen loaded nanoparticles (Table 3.6).

Table 3.5 Nanoparticle formulated dichlorophen preparations and subsequent characterisation.

Preparation code*	Nanoparticle composition (% $^{w}/_{w}$)	Size (nm)	Zeta potential (mV)
Modifications to surfactant ratio			
25/97/01	10% dichlorophen 20% SDS 70% PVA	14.48	-26.78
25/97/02	10% dichlorophen 30% SDS 60% PVA	19.59	-29.96
25/97/03	10% dichlorophen 50% SDS 40% PVA	6.39	-40.15
Modifications to polymer type			
25/97/04	10% dichlorophen 20% SDS 70% HPMC	6.56	-59.07
25/97/05	10% dichlorophen 20% SDS 70% DEX	285.58	-32.71
25/97/06	10% dichlorophen 20% SDS 70% PVP-K30	33.18	-20.78
25/97/07	10% dichlorophen 20% SDS 70% HPC	13.70	-74.03
25/97/08	10% dichlorophen 20% SDS 70% PEG	93.87	-49.01
25/97/10	10% dichlorophen 20% SDS 70% SCMC	494.95	-102.35
25/97/13	10% dichlorophen 20% SDS 70% gelatin	66.46	-10.28
25/97/15	10% dichlorophen 20% SDS 70% PVP	12.32	-36.19
Modifications to surfactant type			
25/97/17	10% dichlorophen 20% sodium deoxycholate 70% PVA	39.27	-15.06
25/97/19	10% dichlorophen 20% SLES 70% PVA	30.84	-33.54

Polymer and surfactant key: SDS-sodium dodecyl sulphate, SLES-sodium lauryl ether sulphate, SDC-sodium deoxycholate, PEG – poly(ethylene glycol), PVA – poly(vinyl alcohol), HPMC – hydroxy propyl methyl cellulose, DEX – dextran, PVP – poly(vinyl pyrolidone), HPC – hydroxy propyl cellulose, SCMC – sodium carboxymethylcellulose.
* Preparations that did not either form an adequate emulsion prior to spray drying or did not re-disperse to form nanoparticles are not shown or used in the study.

Table 3.6 The inhibitory effects of dichlorophen preparations and controls on *C. albicans* in 96 well plate assays after 24 hours incubation. Values are the averages from three independent experiments, with standard errors of the mean shown.

Preparation	MIC ($\mu g\ ml^{-1}$)	S.E.M
25/97/01	11.46	1.77^{-2}
Blank-20% SDS 70% PVA	> 500	-
25/97/02	7.81	1.62^{-3}
Blank-30% SDS 60% PVA	500	2.73^{-2}
25/97/03	6.83	5.31^{-3}
Blank-50% SDS 40% PVA	250	5.00^{-3}
25/97/04	7.81	4.19^{-3}
Blank-20% SDS 70% HPMC	> 500	-
25/97/05	13.66	8.32^{-3}
Blank-20% SDS 70% DEX	125	1.93^{-3}
25/97/06	4.69	6.20^{-3}
Blank-20% SDS 70% PVP-K30	> 500	-
25/97/07	> 500	-
Blank-20% SDS 70% HPC	> 500	-
25/97/08	9.38	1.41^{-2}
Blank-20% SDS 70% PEG	218.6	4.65^{-3}
25/97/10	18.75	6.34^{-3}
Blank-20% SDS 70% SCMC	300	4.71^{-3}
25/97/13	7.81	7.80^{-3}
Blank-20% SDS 70% Gelatin	218.6	7.62^{-3}
25/97/15	109.3	2.54^{-2}
Blank-20% SDS 70% PVP	300	9.81^{-3}
25/97/17	45.83	1.79^{-3}
Blank-20% SDC 70% PVA	> 500	-
25/97/19	11.46	4.96^{-3}
Blank-20% SLES 70% PVA	> 500	-
Dichlorophen in ethylene glycol	11.46	2.21^{-2}
Water saturated dichlorophen	> 500	-

Polymer and surfactant key: SDS-sodium dodecyl sulphate, SLES-sodium lauryl ether sulphate, SDC-sodium deoxycholate, PEG – poly(ethylene glycol), PVA – poly(vinyl alcohol), HPMC – hydroxy propyl methyl cellulose, DEX – dextran, PVP – poly(vinyl pyrolidone), HPC – hydroxy propyl cellulose, SCMC – sodium carboxymethylcellulose.

The results obtained for the dichlorophen loaded nanoparticles indicated that 8 preparations produced either the same or lower MIC values than the conventional ethylene glycol dissolved dichlorophen preparation when tested against *C. albicans*. The blank nanoparticles produced using only excipient materials, but processed using identical techniques usually produced high MIC values ≥ 500 μg ml^{-1}. There are however examples of blank nanoparticle preparations that do impart an inhibitory effect across the concentration range investigated, *e.g.* the blank nanoparticle for preparation 25/97/05 comprising 20% $^{w}/_{w}$ SDS 70% $^{w}/_{w}$ dextran produced an MIC value of 125 μg ml^{-1} and it can therefore be inferred that the excipient materials were likely to have imparted an inhibitory effect within the active nanoparticle preparation in this instance. However, the co-solvent used to dissolve the dichlorophen also imparted an inhibitory effect and produced an MIC value of 183.3 μg ml^{-1}, and is therefore likely to have imparted inhibition in the co-solvent dissolved delivered dichlorophen.

The results in Table 3.6 indicated that lower MIC values were obtained as the surfactant ratio increased within the dichlorophen loaded nanoparticles, despite a constant dichlorophen-loading ratio of 10% $^{w}/_{w}$ in all the preparations. As anticipated, the zeta potential of the particles became more negative in expressed charge as the ratio of anionic surfactant increased within the preparations. Modifications to the type of polymer used within the nanoparticle was shown to have a significant impact on the inhibitory activity of the dichlorophen loaded nanoparticle, with MIC's ranging from 4.69 μg ml^{-1} for preparation 25/97/06 comprising 10% $^{w}/_{w}$ dichlorophen 20% $^{w}/_{w}$ SDS 70% $^{w}/_{w}$ PVP-K30 to ≥ 500 μg ml^{-1} for preparation 25/97/07 comprising 10% $^{w}/_{w}$ dichlorophen 20% $^{w}/_{w}$ SDS 70% $^{w}/_{w}$ HPC. The polymers used in the nanoparticle preparations are widely available hydrophilic polymers with no identifiable characteristics that would account for the variations in the activity of the antimicrobial loaded nanoparticle.

The results in Table 3.6 also indicated that modifications in surfactant type influenced inhibitory activity against *C. albicans*. The preparations 25/97/01 and 25/97/19 consisting of the surfactants SDS and sodium lauryl ether sulphate (SLES) respectively,

produced the same MIC value of 11.46 μg ml^{-1} whereas 25/97/17 consisting of the surfactant sodium deoxycholate produced an MIC of 45.83 μg ml^{-1}. The MIC results show that no correlation exists between the inhibitory activity of the dichlorophen loaded nanoparticle and the blank nanoparticle preparations, suggesting the excipient materials processed into nanoparticles alone does not account for the enhanced efficacy of particular preparations.

3.5.1 Influence of nanoparticle size and zeta potential on MIC

Previous studies have shown correlations between the size of antimicrobial loaded nanoparticles and inhibitory activity (Belesti *et al.*, 2005 ; Jiang *et al.*, 2008). However the methods used to prepare and process the particles differ from those described in this study. To determine if such parameters influenced inhibitory activity in *C. albicans* when treated with dichlorophen loaded nanoparticles, the MIC values obtained in Table 3.6 were plotted against the size and zeta potential values outlined in Table 3.5.

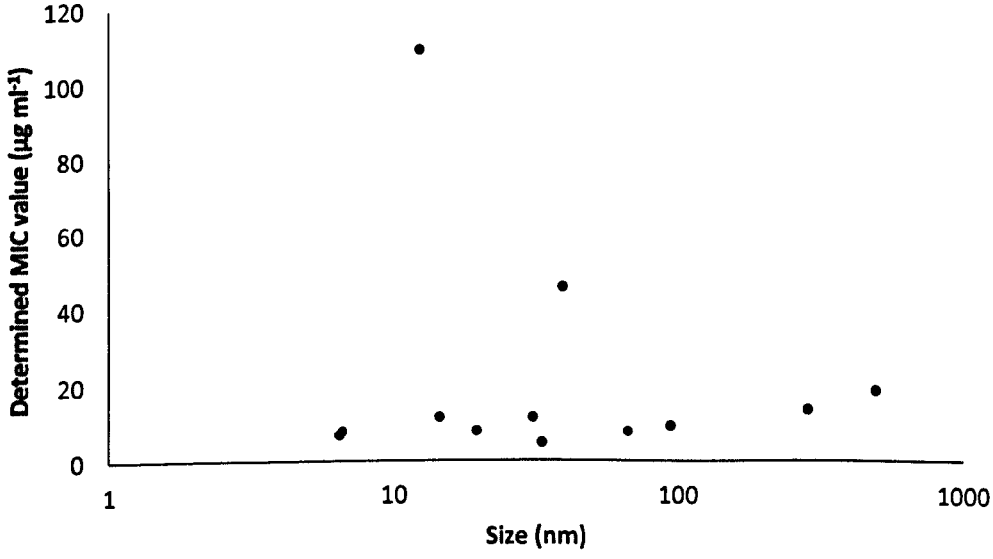

Figure 3.4. Average determined MIC values in *C. albicans* against average nanoparticle size using the MIC and particle sizing data outlined in Tables 3.5 and 3.6 for dichlorophen loaded nanoparticles.

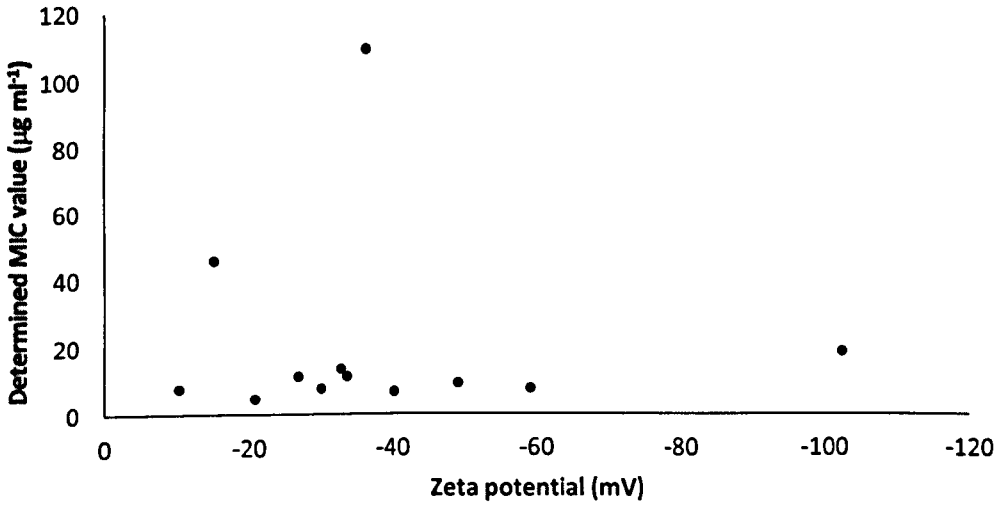

Figure 3.5. Average determined MIC values in *C. albicans* against average nanoparticle zeta potential using the MIC and zeta potential data outlined in Tables 3.5 and 3.6 for dichlorophen loaded nanoparticles.

The results outlined in Figures 3.4 and 3.5 suggest that no correlation exists between the average size of the particles within the nanoparticle suspension, the zeta potential expressed by the nanoparticles and efficacy of inhibition of the individual preparations against *C. albicans*. The results show that inhibitory activity of prepared nanoparticles as a function of the expressed physical characteristics of that preparation is over-simplistic within the multi-component nanoparticles.

3.6 Disk diffusion susceptibility assays against *A. niger*

Filter disk diffusion assays using the antifungal tebuconazole and the biocide iodopropynyl butylcarbamate (IPBC) were conducted as outlined in section 2.3.4. The aims of the work were to determine if the nanoparticle preparations remained stable when applied to filters and agar surfaces, and permitted assessment of the inhibitory activity of prepared nanoparticles compared with co-solvent dissolved equivalents using an alternative technique.

(A)

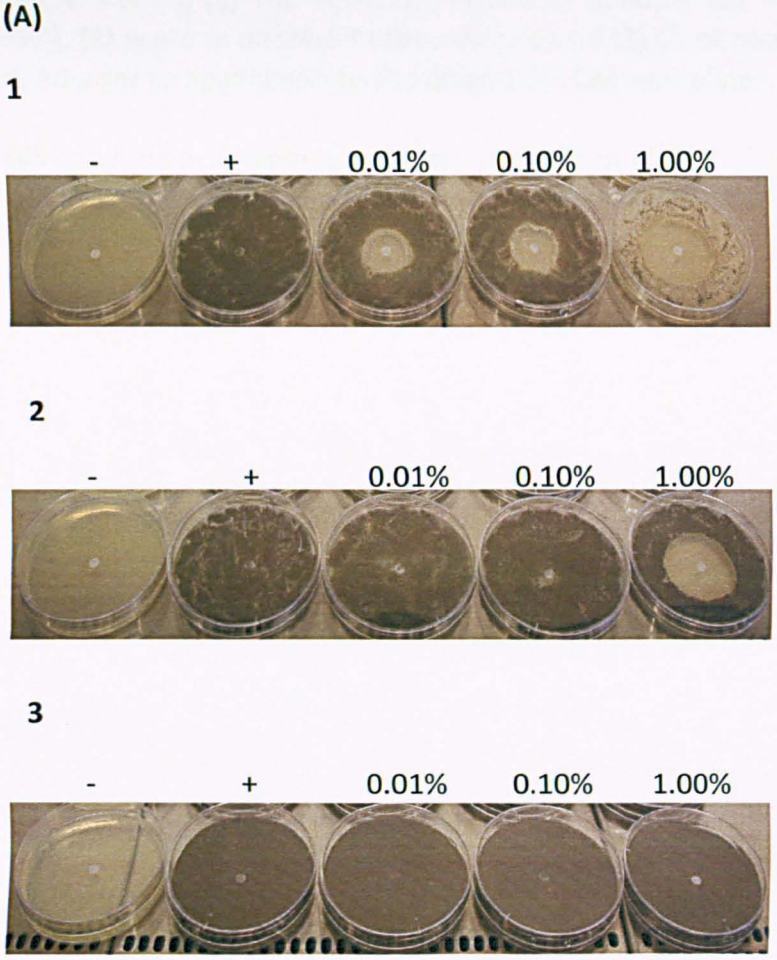

(B)

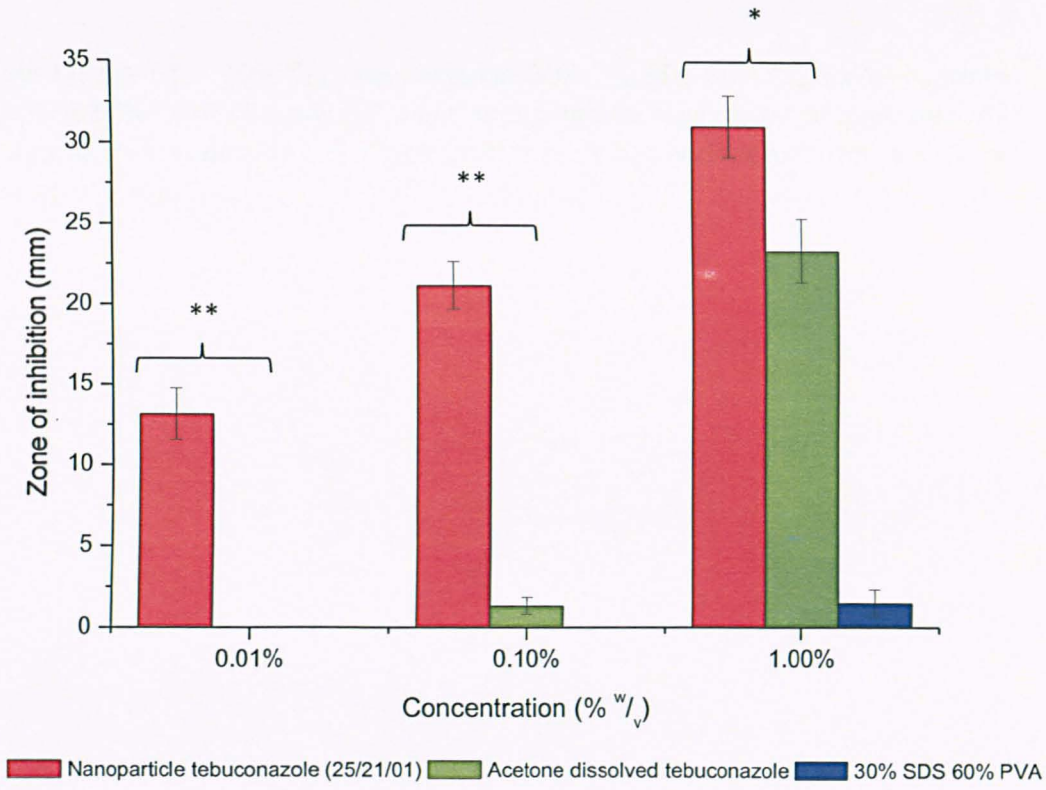

Figure legend overleaf

Figure 3.6. (A) (1) The inhibitory effects of nanoparticle formulated tebuconazole (25/21/01 – 10% $^{w}/_{w}$ tebuconazole 30% $^{w}/_{w}$ SDS 60% $^{w}/_{w}$ PVA), **(2)** acetone dissolved tebuconazole and **(3)** blank nanoparticles consisting 30% $^{w}/_{w}$ SDS 60% $^{w}/_{w}$ PVA against *A. niger*. All filters were fully dried prior to application to the dried 1.5% CM agar plates.

(B) The inhibitory effects of nanoparticle formulated tebuconazole (25/21/01 – 10% $^{w}/_{w}$ tebuconazole 30% $^{w}/_{w}$ SDS 60% $^{w}/_{w}$ PVA), acetone dissolved tebuconazole and blank nanoparticles consisting 30% $^{w}/_{w}$ SDS 60% $^{w}/_{w}$ PVA against *A. niger* measured through zones of inhibition. All filters were fully dried prior to application to the dried 1.5% CM agar plates. Values are averages from three independent experiments. Error bars indicate standard errors of the mean. $^{**}p<0.01$, $^{*}p<0.05$ by Student's t test.

(A)

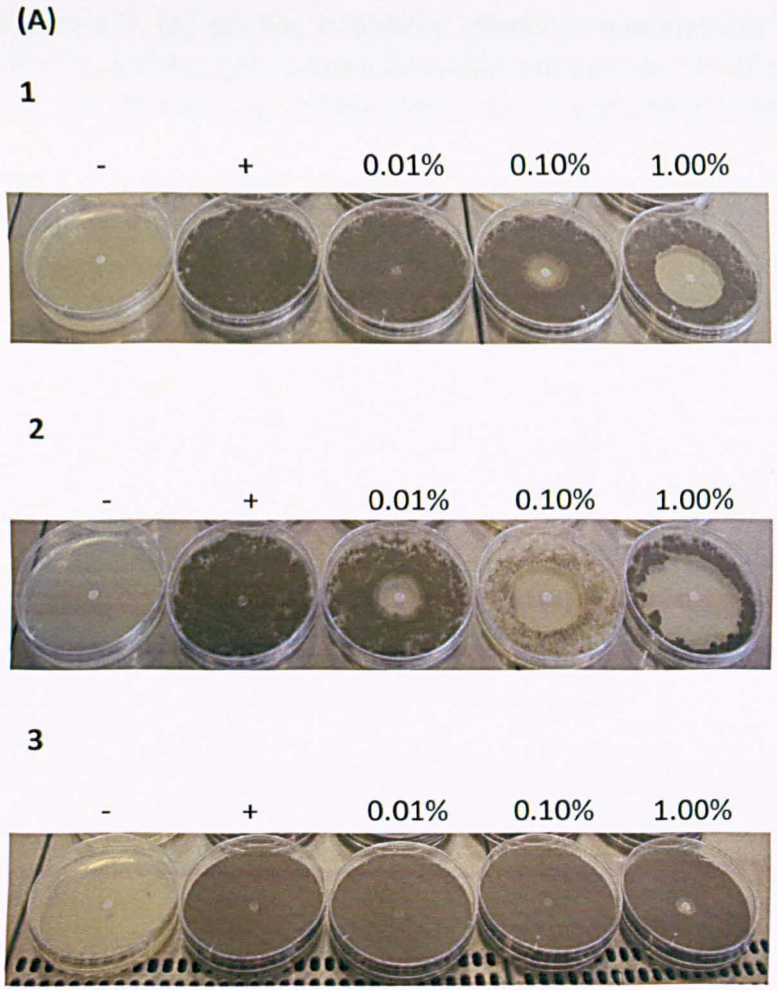

(B)

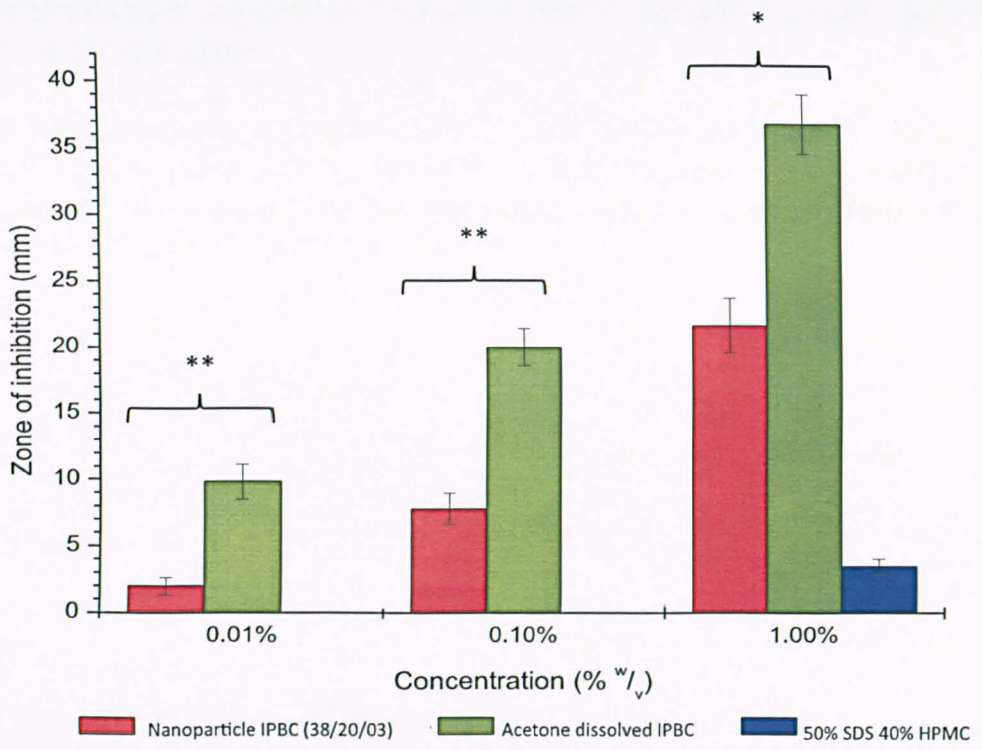

Figure legend overleaf

Figure 3.7. (A) (1) The inhibitory effects of nanoparticle formulated iodopropynyl butylcarbamate (38/20/03 – 10% $^{w}/_{w}$ IPBC 50% $^{w}/_{w}$ SDS 40% $^{w}/_{w}$ HPMC), **(2)** acetone dissolved iodopropynyl butylcarbamate and **(3)** blank nanoparticles consisting 50% $^{w}/_{w}$ SDS 40% $^{w}/_{w}$ HPMC against *A. niger*. All filters were fully dried prior to application to the dried 1.5% CM agar plates.

(B) The inhibitory effects of nanoparticle formulated iodopropynyl butylcarbamate (38/20/03 – 10% $^{w}/_{w}$ IPBC 50% $^{w}/_{w}$ SDS 40% $^{w}/_{w}$ HPMC), acetone dissolved iodopropynyl butylcarbamate and blank nanoparticles consisting 50% $^{w}/_{w}$ SDS 40% $^{w}/_{w}$ HPMC against *A. niger* measured through zones of inhibition. All filters were fully dried prior to application to the dried 1.5% CM agar plates. Values are averages from three independent experiments. Error bars indicate standard errors of the mean. **$p<0.01$, *$p<0.05$ by Student's t test.

The results in Figure 3.6 (A & B) indicate that nanoparticle formulated tebuconazole produced the greatest zones of inhibition against *A. niger* on 1.5% CM agar plates. The advantage of using the nanoparticle preparation of tebuconazole was demonstrated clearly at 0.01% $^{w}/_{v}$ where an average zone of inhibition of 13.17 mm (S.E.M 2.60) was recorded compared to no zone of inhibition obtained for acetone-dissolved tebuconazole. The blank nanoparticle preparation only produced a limited zone of inhibition of 1.5 mm (S.E.M 0.84) at 1.00% $^{w}/_{v}$.

The IPBC nanoparticle preparation 38/20/03 displayed an average size of 6.99 nm and zeta potential of -40.38 mV. The results in Figure 3.7 (A & B) comparing the inhibitory activity of IPBC formulated nanoparticles, acetone dissolved IPBC and blank nanoparticles indicated the opposite trends. It was shown that the acetone dissolved IPBC produced larger zones of inhibition at all the concentrations investigated. The blank nanoparticle preparation produced a limited zone of inhibition at 1.00% $^{w}/_{v}$ of 3.5 mm (S.E.M 0.55). Interestingly however, when nanoparticle IPBC (38/20/03) was tested against *C. albicans* in 96 well plates as outlined in section 2.3.1 an MIC value of 5.73 $\mu g\ ml^{-1}$ (S.E.M 5.13^{-3}) was obtained compared to an MIC value of 15.63 $\mu g\ ml^{-1}$ (S.E.M 8.26^{-3}) for ethylene glycol dissolved IPBC, while the blank nanoparticle preparation produced an MIC value of 250 $\mu g\ ml^{-1}$ (S.E.M 9.47^{-3}). The results suggest that nanoparticle IPBC was less active than co-solvent dissolved IPBC when applied to a surface and tested against *A. niger* but was more inhibitory against *C. albicans* when present as a suspension. The results therefore show that either the type of antimicrobial used in the nanoparticle system or design of the nanoparticle is important when considering what applications the suspension would be utilised for and how it would be applied.

3.7 Discussion

Many antifungals and biocides display poor water solubility (≤ 100 μg ml^{-1}). Conventional approaches used to solubilise poorly water-soluble antifungals include the use of water soluble salts or esters of the parent substance or the use of excessive amounts of co-solvent to dissolve the antifungal (Tomlin, 1995 ; Duncalf *et al.*, 2008). A range of poorly water-soluble antifungals and biocides were formulated using a novel nanoparticle preparation and processing technique as outlined in section 2.4. The resulting nanosuspensions were characterised for physical properties and when dispersed in water resembled transparent molecular solutions, therefore 'insoluble' antimicrobials could be delivered as aqueous suspensions.

These nano-scale delivery platforms were shown to increase the efficacy of inhibition of antimicrobials against *C. albicans* and *A. niger* compared to conventional co-solvent dissolved delivery utilising both 96 well plate micro-dilution assays and filter disk diffusion assays on agar. Nanoparticle formulated pentachlorophenol was also shown to induce greater inhibitory efficacy than the water-soluble sodium pentachlorophenol preparation. Previous studies have investigated the development of organic nanoparticles using emulsion-evaporation processes and shown that nanoparticle formation of antifungals increases efficacy of inhibition compared to alternative delivery methods (Peng *et al.*, 2008 ; Patel *et al.*, 2010). However, no studies identified from the literature indicate such a range of applications of a described nanoparticle formulation technology as outlined in this work where a variant of the novel technology developed by Zhang *et al.* (2008a) was used.

If particles in a nano-suspension approach each other too closely, they will agglomerate. This must be prevented to ensure a stable system. Combining polymers and charged surfactants should provide the necessary repulsive barriers between two neighbouring particles to prevent particle growth (Rabinow, 2004). To investigate if such parameters influenced inhibitory activity, a range of dichlorophen nanoparticle preparations were produced with a constant dichlorophen loading ratio of 10% $^{w}/_{w}$ and either varying ratios of surfactant, type of surfactant or type of polymer (Table 3.5). These preparations were tested against *C. albicans* and found to induce

significant variations in inhibitory activity (Table 3.6). As anionic surfactant ratio increased, the expressed particle zeta potential and obtained MIC value decreased. Several explanations may account for the observed increase in inhibitory activity with increased surfactant ratio. Firstly, surfactants can reduce surface and interfacial tensions by accumulating at the interface of immiscible components and increase the mobility of hydrophobic compounds. Due to these properties, surfactants can interact with microbial proteins and can modify enzyme conformation that alters activity, stability and specificity. Therefore surfactants are potentially toxic to microbes and increasing the ratio of surfactant potentially increased the antimicrobial activity of the preparation (Singh *et al.*, 2007). Secondly, an increased ratio of surfactant in a preparation may be expected to produce a greater number of particles containing the antimicrobial. Increased efficacy corresponding to a possible increase in particle number supports the concept that a greater number of particles reduced MIC. However accurate particle number studies were not possible due to the small size of the particles obtained (<20 nm) there is no current technology available to count particles within this range and therefore this theory could not be substantiated. Electrostatic repulsion would be expected between the anionic nanoparticle and surface of the net negatively charged microbial cell (Dillen *et al.*, 2008 ; McCarron *et al.*, 2004). It would therefore be anticipated that optimal inhibitory activity would occur in preparations that are stable but do not express high degrees of electro-negativity as increased repulsion would be expected, with reduced amounts of antimicrobial reaching the cells. The results in Figure 3.5 suggested that no correlation exists between the average zeta potential expressed by the nanoparticle preparation and the determined MIC value.

Reducing a particle's size and therefore increasing the surface area, will increase the dissolution rates of poorly water soluble antimicrobials, thereby addressing problems related to poor bioavailability (Hu *et al.*, 2004). It has previously been suggested that smaller nanoparticles are more efficient at delivering active compounds to cells (Belesti *et al.*, 2005 ; Jiang *et al.*, 2008). The results outlined in Figure 3.4 suggest that no correlation exists between the size of the dichlorophen nanoparticles used and the inhibitory activity exhibited against *C. albicans*.

The results in Figure 3.6 (A & B) indicated that nanoparticle formation of tebuconazole was more inhibitory and therefore produced greater zones of inhibition than acetone dissolved tebuconazole against *A. niger*. However, the opposite trends were observed for IPBC (Figure 3.7 A & B). This result is difficult to explain because nanoparticle IPBC was shown to be more inhibitory than ethylene glycol dissolved IPBC when tested against *C. albicans* using a micro-dilution technique. It is possible that the difference in efficacy observed was due to the formulation used. The tebuconazole loaded nanoparticles consisted of the polymer PVA and the IPBC loaded nanoparticles consisted of the polymer HPMC. It is possible that cellulosic HPMC 'sticks' to the filter and prevents migration and diffusion across and into the agar. The IPBC preparation may have been less stable when applied to the filter disk, or was unable to deliver IPBC as effectively to the cells. The physical characteristics for both preparations were however similar with average sizes for the tebuconazole and IPBC at 5.46 nm and 6.99 nm respectively and expressed zeta potentials of -36.19 mV and -40.38 mV respectively. These results are further evidence that nanoparticle design and the application of the nano-suspension are significant to the overall inhibitory activity exhibited by a particular formulation. Previous studies have investigated the immobilisation of the widely used antifungal amphotericin (AmB) using a chemical adhesive into non-leaching silica nanoparticles that were shown to be more inhibitory than nanoparticle preparations of silver. These authors note that such antifungal nanoparticle conjugates may be useful to render medical devices with antifungal properties (Paulo *et al.*, 2010).

The aims of this chapter were: to investigate if the poorly water soluble antifungals could be formulated into nanoparticles, to investigate the inhibitory efficacy of the nanoparticle formulated antifungals that have varying molecular targets against *C. albicans* and *A. niger*, to investigate the influence of nanoparticle design on the expressed size and zeta potential of the formulation, to investigate the influence of nanoparticle design on nanoparticle efficacy of inhibition and to determine if a correlation exists between nanoparticle physical characteristics and efficacy.

These specific aims were fulfilled by the results presented in this chapter and are further explored and built upon in Chapter 4 where nanoparticle formulated antimicrobials are tested against Gram-negative and Gram-positive bacteria and a systematic design process subsequently undertaken to fulfil the broader aims of the project. Although the presented results highlight the advantages of using a nanoparticle based delivery approach for antifungals, no clear trends were observed in the data to suggest why certain preparations were more inhibitory than others.

Chapter 4

Nanoparticle formation of antibacterial compounds for comparisons of inhibitory activity and design optimisation

4.1 Introduction

Very few novel antimicrobial compounds are currently being developed and therapeutic options for microbial pathogens are becoming extremely limited (Boucher *et al.*, 2009). The use of antimicrobial agents for prophylactic or therapeutic purposes has provided the selective pressure favouring the survival and spread of resistant organisms (Bax *et al.*, 2000). Antibiotics are generally pharmacologically precise and exert their actions at a single physiological target. Biocides play an important role in limiting the potential sources of infection and usually affect multiple rather than single cell targets and therefore are not usually used as therapeutic agents (Gilbert & McBain, 2003). Resistance to biocides is therefore less common (Poole, 2002). A large proportion of new antimicrobial candidates emerging from development programs are either insoluble or poorly soluble in water resulting in inadequate bioavailability, therefore limiting the potential use and applications of such compounds (Rabinow, 2004 ; Kingsley *et al.*, 2006). Conventional approaches used to solubilise poorly water-soluble antimicrobials include the use of salt derivatives of the parent compound or the use of excessive amounts of co-solvent to dissolve the antimicrobial (Tomlin, 1995 ; Allen Jr, 2008 ; Duncalf *et al.*, 2008). A variety of novel antimicrobial delivery systems are being developed including micelles, liposomes, and nanoparticles. These novel delivery systems can ameliorate problems associated with poor solubility (Kabanov *et al.*, 2002).

A variety of antibacterial compounds, which all display poor water solubility, ($\leq 100\ \mu g\ ml^{-1}$), that were available in sufficient quantities to formulate and that have a

range of applications, were processed into nanoparticles as described in section 2.4. Comparisons of inhibitory activity between nanoparticle formulated antibacterial agents were made with organic co-solvent dissolved forms of delivery as described in sections 2.3, 2.3.1 and 2.3.2.

Pentachlorophenol is a broad-spectrum bactericide used as a general disinfectant with poor water solubility (80 μg ml^{-1}), but is stable and soluble in most organic solvents (Tomlin, 1995). Pentachlorophenol's mode of action is poorly described, however phenols typically target transmembrane pH gradients and affect membrane integrity (Denyer & Stewart, 1998). Dichlorophen is a bactericide widely used as an antimicrobial in consumer toiletries and cosmetics (Cox *et al.*, 2004). Dichlorophen is poorly water soluble (30 μg ml^{-1}) but displays good solubility in organic solvents such as ethanol (530,000 μg ml^{-1})(Tomlin, 1995). Ciprofloxacin is a powerful broad-spectrum fluoroquinolone antibiotic that is insoluble in water ($\leq$ 100 μg ml^{-1}) and many organic solvents. Ciprofloxacin targets two essential intracellular enzymes, DNA gyrase and topoisomerase IV that are associated with the control of DNA topology (Chen *et al.*, 1996 ; Berlanga *et al.*, 2004). Initiation of replication after the blocking of DNA synthesis leads to the induction of the SOS response and cell filamentation (Drlica *et al.*, 2008). These antimicrobials were tested for inhibitory activity against *S. aureus*, a Gram-positive human commensal and opportunistic pathogen, (Plata *et al.*, 2009) and the Gram-negative enteric bacterium *E. coli* (Dobrindt, 2005).

The generic screening of a range of different nanoparticle dichlorophen formulations for inhibitory activity was outlined in chapter 3 and will be further built upon in this chapter. These data were subsequently utilised in a systematic design approach with the aim of identifying the relative significance of each nanoparticle component on inhibitory activity, to determine an optimum nanoparticle composition. Design of Experiment (DOE MODDE™) is a widely used computer application for formulation design processes. The program supports multiple linear regression (MLR) and projections to latent structures (PLS) to identify a series of reference experiments. These experiments are based on a centre point, and subsequent representative experiments are conducted around it to determine the relative significance of each

parameter within the experimental system. Theoretical optimisation is then possible based on predictions for all the possible combinations of variables within the experimental region, therefore potentially reducing the number of experiments required (Eriksson *et al.*, 2008). A simple cube based DOE was used in this work to investigative the variables: percentage $^{w}/_{w}$ loading of antimicrobial; surfactant; and polymer on inhibitory activity (refer to Figure 1.7).

Previous studies investigated the use of the emulsion evaporation process to form ciprofloxacin loaded poly(lactide-co-glycolide) and polyethylbutylcyanoacrylate (PEBCA) organic nanoparticles (Page-Clisson *et al.*, 1998 ; Dillen *et al.*, 2004 ; Dillen *et al.*, 2006 ; Jeong *et al.*, 2008). The aminoglycoside antibiotic gentamicin has potent antibacterial activity against a range of bacteria however, it exhibits poor cellular penetration that limits the antibiotics potential use against intracellular pathogens. Encapsulation of gentamicin into poly(lactide-co-glycolide) nanoparticles was demonstrated and shown to cause no change in the *in-vitro* bactericidal activity against the intracellular pathogen *Brucella melitensis* suggesting a possible application of the nanoparticle preparation (Imbuluzqueta *et al.*, 2011). The materials and production methods used to produce these nanoparticles differ from those outlined in this study.

The chapter has the following specific aims:

- To investigate if the poorly water soluble antibacterials pentachlorophenol, ciprofloxacin and dichlorophen could be formulated into nanoparticles.
- To further investigate the influence of dichlorophen nanoparticle design on inhibitory efficacy against *S. aureus* SH1000 and *E. coli* MC1061.
- To further investigate if size and zeta potential of the prepared nanoparticles influences efficacy of inhibition when tested against *S. aureus* SH1000 and *E. coli* MC1061.
- To investigate the effects of material combinations in the form of feedstock and micellisation solutions, to determine if synergy of components accounts for

enhanced antimicrobial activity in *C. albicans*, *S. aureus* SH1000 and *E. coli* MC1061.

- To use the computer based application Design of Experiment (DOE MODDE™) to investigate the relative significance of % $^{w}/_{w}$ dichlorophen, SDS, HPMC and gelatin loading ratio on inhibitory efficacy and perform design optimisation.
- To perform a dissolution assay to investigate the rate of dichlorophen released through a dialysis membrane when nanoparticle formulated or processed as a water stirred dichlorophen and excipient equivalent.

4.2 Pentachlorophenol

Nanoparticles of pentachlorophenol (25/PCP/01, refer to Table 3.3) were produced and subsequently characterised on the basis of size and zeta potential using a Malvern Zetasizer Nano™ as outlined in section 2.5.1. The prepared pentachlorophenol nanoparticles were tested against *S. aureus* SH1000 in 96 well plate assays (refer to section 2.3.1) and the inhibitory effects compared with water saturated, co-solvent dissolved, a salt derivative of pentachlorophenol and blank nanoparticles that were processed using the same protocol as the pentachlorophenol loaded nanoparticles (Table 4.1).

Table 4.1 The inhibitory effects of pentachlorophenol and controls on *S. aureus* SH1000 in 96 well plate assays after 24 hours incubation. Values are the averages from three independent experiments, with standard errors of the mean shown.

Preparation	MIC ($\mu g\ ml^{-1}$)	S.E.M
Nanoparticle pentachlorophenol – 25/PCP/01	27.33	1.30^{-3}
Pentachlorophenol in ethylene glycol	27.33	0
Water saturated pentachlorophenol	>500	0
Blank nanoparticle (30% SDS 60% PVA)	54.65	7.00^{-3}
Water dissolved sodium pentachlorophenol	6.83	1.22^{-2}

The results in Table 3.3 show that nanoparticles of pentachlorophenol (25/PCP/01) were produced with an average size of 5.15 nm and an average zeta potential of -34.91 mV after viscosity correction. The optically clear and stable nanoparticle preparation was subsequently tested against *S. aureus* SH1000 for inhibitory activity. The results in Table 4.1 suggest that nanoparticle formulated pentachlorophenol was equally as active as the co-solvent dissolved form of delivery. The results indicate an approximate 4-fold increase in efficacy when using the salt derivative of the base chemical, sodium pentachlorophenol compared with the nanoparticle and co-solvent dissolved form of delivery. The water saturated base pentachlorophenol produced no MIC across the concentration range investigated. Interestingly, the blank nanoparticle preparation induced relatively significant levels of inhibition. These results contrast with those obtained when the same preparations were tested against *C. albicans* (Table 3.4) which showed an approximate 1.2 fold increase in efficacy when using

nanoparticle formulated pentachlorophenol compared with the conventional co-solvent dissolved preparation and an approximate 2.4 fold increase in efficacy compared with sodium pentachlorophenol. The blank nanoparticle preparation produced an MIC of 500 μg ml^{-1} against *C. albicans* contrasting with the relatively low MIC obtained when tested against *S. aureus* SH1000. These results highlight that the conventional delivery method of sodium pentachlorophenol was more inhibitory than the nanoparticle delivered pentachlorophenol when tested against *S. aureus* SH1000. The results also indicate significant differences in efficacy of the preparations between *S. aureus* SH1000 and *C. albicans* suggesting that individual nanoparticle formulations may require designing for different organisms.

4.3 Ciprofloxacin

A range of ciprofloxacin nanoparticles (Table 4.2) were produced and subsequently characterised on the basis of size and zeta potential using a Malvern Zetasizer Nano™ or a Malvern Mastersizer™ as outlined in section 2.5.1 (Futi, 2009). The prepared ciprofloxacin nanoparticles were tested against *S. aureus* SH1000 using Minimum Bactericidal Concentration (MBC) assays as outlined in section 2.3.2. MBC assays were used because the larger nanoparticle size caused turbidity in the growth media on addition and therefore accurate MIC determination was not possible. The inhibitory effects of nanoparticle formulated ciprofloxacin were compared with water saturated, DMSO dissolved, a salt derivative of ciprofloxacin and one preparation compared with blank nanoparticles that were processed using the same protocol as the ciprofloxacin loaded nanoparticles (Table 4.3).

Table 4.2 Nanoparticle formulated ciprofloxacin preparations and subsequent characterisation.

Preparation code	Nanoparticle composition (% $^{w}/_{w}$)	Size (nm)	Zeta potential (mV)
41/27/44	5% ciprofloxacin 25% pluronic (F127) 70% PVP	545.2	3.78
41/27/45	10% ciprofloxacin 25% pluronic (F127) 65% PVP	679.6	1.38
41/27/67	10% ciprofloxacin 20% SDS 70% PVA	435.3	-14.7
41/27/68	5% ciprofloxacin 40% SDS 55%PVA	365.6	-18.2
50/27/55	20% ciprofloxacin 25% pluronic (F127) 55% PVP	293	7.9

Polymer and surfactant key: SDS - sodium dodecyl sulphate, PVP – poly(vinyl pyrolidone), PVA – poly(vinyl alcohol)

Table 4.3 The inhibitory effects of ciprofloxacin preparations and controls on *S. aureus* SH1000 determined using Minimum Bactericidal Concentration (MBC) assays. Values are the averages from three independent experiments, with standard errors of the mean shown.

Preparation	MBC (μg ml^{-1})	S.E.M
41/27/44	500	1.5
41/27/45	250	0
41/27/67	62.5	0
41/27/68	15.63	0
50/27/55	31.25	0
Blank-25% pluronic (F127) 55% PVP	>500	0
Ciprofloxacin dissolved in DMSO	62.5	0
DMSO only	500	0
Water dissolved ciprofloxacin hydrochloride	15.63	0

The results presented in Table 4.2 indicated that nanoparticles of ciprofloxacin were produced with a range of particle sizes and zeta potentials. These particle preparations were selected from a particle screen study as they exhibited the greatest stability and processing reproducibility (data not shown) (Futi, 2009). Preparations 41/27/44, 41/27/45 and 50/27/55 were produced using the amphiphilic block copolymer Pluronic F127 that consists of ethylene oxide (EO) and propylene oxide (PO) blocks. The hydrophobic core formed by PO chains provides a suitable microenvironment for the incorporation of water-insoluble drugs while the hydrophilic shell formed by the EO chains maintains dispersion stability (Li *et al.*, 2011). The excipient materials used in these preparations are non-ionic however the nanoparticle formulations exhibited a positive zeta potential. This was due to the small positive charge exhibited by the ciprofloxacin itself. The particles were deemed stable from observational evidence of the nanoparticle dispersion over time. This suggested steric rather than electrostatic stabilisation of the preparation. Due to the formulation processes used, complete antimicrobial entrapment efficiency was anticipated. HPLC analysis confirmed that the ciprofloxacin-loading ratio of 50/27/55 was 20.21% $^{w}/_{w}$ (S.E.M 8.5^{-2}).

The results presented in Table 4.3 indicated significant variation in the antimicrobial activity exhibited by the nanoparticle formulated ciprofloxacin preparations. The results further suggested that nanoparticle design is significant to the activity of particular formulations however, as previously shown no correlation could be sought between nanoparticle size, zeta potential and antimicrobial activity (Appendix 1). Three nanoparticle preparations were shown to produce MBC values equivalent to or lower than those obtained for DMSO dissolved ciprofloxacin treated *S. aureus*. Preparations 50/27/55 and 41/27/68 were shown to produce MBC values 2 and 4 fold lower than DMSO dissolved delivered ciprofloxacin respectively. The water dissolved salt derivative of the base chemical ciprofloxacin hydrochloride produced a low MBC value equivalent to that observed for 41/27/68 however ciprofloxacin HCl is chemically different to the base ciprofloxacin that produced no MBC value across the concentration range investigated and that was processed into the nanoparticle preparations outlined in Table 4.2. These results highlighted the improvements in inhibitory activity that are afforded to the base ciprofloxacin preparation due to

nanoparticle formation, which otherwise would not be inhibitory to the growth of *S. aureus* at the concentrations tested. Preparation 50/27/55 was subsequently used in a mode of action study to determine if nanoparticle formation of ciprofloxacin induced changes at the molecular level that may account for enhanced antimicrobial activity compared to the DMSO dissolved ciprofloxacin.

4.4 Dichlorophen – nanoparticle materials screen

A range of dichlorophen nanoparticles (refer to Table 3.5) were produced with either: different polymers, different surfactants or variations in surfactant to polymer ratio to determine if such parameters influence inhibitory activity when tested against *S. aureus* SH1000 and *E. coli* MC1061 in 96 well plate assays. The inhibitory effects of nanoparticle formulated dichlorophen were compared with water saturated, co-solvent dissolved dichlorophen and blank nanoparticles that were processed using the same protocol as the dichlorophen loaded nanoparticles (Table 4.4).

Table 4.4 The inhibitory effects of dichlorophen preparations and controls on *S. aureus* SH1000 and *E. coli* MC1061 in 96 well plate assays after 24 hours incubation. Values are the averages from three independent experiments, with standard errors of the mean shown.

Preparation	Nanoparticle composition	*S. aureus* SH1000 MIC ($\mu g\ ml^{-1}$)	S.E.M	*E. coli* MC1061 MIC ($\mu g\ ml^{-1}$)	S.E.M
25/97/01	10% dichlorophen 20% SDS 70% PVA	3.91	8.0^{-3}	31.25	1.0^{-3}
Blank - 25/97/01	20% SDS 70% PVA	218.6	6.0^{-2}	>500	-
25/97/02	10% dichlorophen 30% SDS 60% PVA	3.42	5.0^{-3}	62.5	4.0^{-3}
Blank - 25/97/02	30% SDS 60% PVA	54.65	7.0^{-3}	>500	-
25/97/03	10% dichlorophen 50% SDS 40% PVA	2.86	5.0^{-3}	54.65	3.0^{-3}
Blank - 25/97/03	50% SDS 40% PVA	45.83	9.0^{-3}	>500	-
25/97/04	10% dichlorophen 20% SDS 70% HPMC	2.86	3.0^{-3}	2.86	6.0^{-3}
Blank - 25/95/04	20% SDS 70% HPMC	125	1.9^{-3}	>500	-
25/97/05	10% dichlorophen 20% SDS 70% DEX	5.73	0	>500	-
Blank - 25/97/05	20% SDS 70% DEX	109.3	9.0^{-3}	>500	-
25/97/06	10% dichlorophen 20% SDS 70% PVP-K30	>500	-	5.73	2.0^{-3}
Blank - 25/97/06	20% SDS 70% PVP-K30	75	4.0^{-3}	>500	-
25/97/07	10% dichlorophen 20% SDS 70% HPC	>500	-	62.5	5.8^{-2}
Blank - 25/97/07	20% SDS 70% HPC	437.2	1.3^{-2}	>500	-
25/97/08	10% dichlorophen 20% SDS 70% PEG	3.42	5.0^{-3}	5.73	1.0^{-2}
Blank - 25/97/08	20% SDS 70% PEG	91.65	5.0^{-3}	>500	-
25/97/10	10% dichlorophen 20% SDS 70% SCMC	6.83	2.1^{-2}	75	2.0^{-3}
Blank - 25/97/10	20% SDS 70% SCMC	91.65	6.0^{-3}	>500	-
25/97/13	10% dichlorophen 20% SDS 70% gelatin	3.42	1.2^{-2}	27.33	5.0^{-3}
Blank - 25/97/13	20% SDS 70% Gelatin	125	2.4^{-2}	500	6.0^{-3}
25/97/15	10% dichlorophen 20% SDS 70% PVP	4.69	4.0^{-3}	5.73	4.0^{-3}
Blank - 25/97/15	20% SDS 70% PVP	75	6.0^{-3}	>500	-

25/97/17	10% dichlorophen 20% sodium deoxycholate 70% PVA	27.33	6.0^{-3}	22.91	6.0^{-3}
Blank - 25/97/17	20% SDC 70% PVA	>500	-	>500	-
25/97/19	10% dichlorophen 20% SLES 70% PVA	13.66	5.0^{-3}	13.66	1.4^{-2}
Blank - 25/97/19	20% SLES 70% PVA	>500	-	>500	-
Dichlorophen in ethylene glycol	-	13.66	1.4^{-3}	27.33	6.0^{-3}
Water saturated dichlorophen	-	>500	-	>500	-
Ethylene glycol only	-	218.6	2.0^{-3}	183.3	5.0^{-3}

Polymer and surfactant key: SDS-sodium dodecyl sulphate, SLES-sodium lauryl ether sulphate, SDC-sodium deoxycholate, PEG – poly(ethylene glycol), PVA – poly(vinyl alcohol), HPMC – hydroxy propyl methyl cellulose, DEX – dextran, PVP – poly(vinyl pyrolidone), HPC – hydroxyl propyl cellulose, SCMC – sodium carboxy methyl cellulose.

The nanoparticle formulated dichlorophen preparations outlined in Table 3.5 that were tested for inhibitory activity against *C. albicans* (Table 3.6), were subsequently tested against *S. aureus* SH1000 and *E. coli* MC1061 to determine if similar trends in activity were observed. The results in Table 4.4 indicated that 10 of the nanoparticle preparations were more inhibitory than the conventional ethylene glycol dissolved dichlorophen solution when tested against *S. aureus* SH1000 and 7 were more inhibitory when tested against *E. coli* MC1061. The results also highlight the poor killing efficacy of water-saturated dichlorophen that caused no inhibition of the three microorganisms across the concentration range investigated. As previously observed for *C. albicans* a significant range in MIC values was demonstrated despite the dichlorophen loading ratio remaining constant at 10% $^{w}/_{w}$. The MIC values obtained for *S. aureus* SH1000 ranged from 2.86 μg ml^{-1} for preparations 25/97/03 and 25/97/04 to >500 μg ml^{-1} for 25/97/06 and in *E. coli* ranged from 2.86 μg ml^{-1} for preparation 25/97/04 to >500 μg ml^{-1} for 25/97/05. The blank nanoparticles produced using only excipient materials, but processed using identical techniques usually produced high MIC values when tested against *E. coli* >500 μg ml^{-1}, but produced a range of values when tested against *S. aureus* SH1000. As observed in *C. albicans* no correlation between the inhibitory activity of the blank nanoparticles and the dichlorophen loaded nanoparticles was shown, suggesting the excipient materials processed into nanoparticles alone does not account for the enhanced efficacy of particular preparations.

In order to ascertain the effects of changing surfactant ratio on the corresponding MIC, three formulations were produced with a constant dichlorophen loading at 10% $^{w}/_{w}$ but modified SDS to PVA ratios. The increase in surfactant ratio from 20% $^{w}/_{w}$ in preparation 25/97/01 to 50% $^{w}/_{w}$ in preparation 25/97/03 caused an approximate 1.4 and 1.7 fold decrease in MIC against *S. aureus* SH1000 and *C. albicans* (Table 3.6) respectively. The same trend was not observed in *E. coli* that produced the lowest MIC value at 20% $^{w}/_{w}$ SDS loading ratio.

Modifications to the type of polymer used in the nanoparticle formulation, were shown to have a significant impact on the inhibitory activity of the dichlorophen

loaded nanoparticle (Table 4.4). Nanoparticle preparations consisting of the polymers hydroxy propyl methyl cellulose (25/97/04), poly(ethylene glycol) (25/97/08) and gelatin (25/97/13) were most inhibitory against *S. aureus*. Preparations consisting hydroxy propyl methyl cellulose (25/97/04) and poly(vinyl pyrolidone) (25/97/06) were most inhibitory against *E. coli* and preparations consisting hydroxy propyl methyl cellulose (25/97/04), gelatin (25/97/13) and poly(vinyl pyrolidone) (25/97/06) were most inhibitory against *C. albicans* (Table 3.6). The results therefore suggested that nanoparticles produced using the polymers hydroxy propyl methyl cellulose, gelatin and poly(ethylene glycol) were generically the most inhibitory. Nanoparticles consisting of hydroxy propyl cellulose (25/97/07) were the least inhibitory in *S. aureus* and *C. albicans*, and preparations consisting of dextran (25/97/05) or sodium carboxy methyl cellulose (25/97/10) were the least inhibitory against *E. coli*. All the polymers used in this investigation are widely available hydrophilic materials with no identifiable characteristics that would account for the variations in inhibitory activity. However, these results and those obtained for *C. albicans* appeared to indicate that some polymers were more inhibitory than others across different organisms that all have very different cell wall compositions.

The results in Table 4.4 indicated that modifications in surfactant type also influenced inhibitory activity against *S. aureus* and *E. coli*. The results suggested that nanoparticle preparations consisting of the surfactant sodium dodecyl sulphate were most inhibitory against both *S. aureus* and *C. albicans* (Table 3.6) but was the least inhibitory surfactant modified nanoparticle formulation against *E. coli*. Nanoparticles consisting of the surfactant sodium lauryl ether sulphate produced the lowest MIC value against *E. coli* when comparing surfactant modified nanoparticle formulations.

These results and those outlined for *C. albicans* suggested that nanoparticle design was significant in the overall inhibitory activity of particular formulations. They also highlight that some polymers and surfactants were generically more inhibitory than others against the organisms investigated. Surfactant ratio also appeared significant to inhibitory activity, with increased SDS ratio being optimal for activity against *S. aureus* and *C. albicans*. The preparations were also tested for inhibitory activity against

Pseudomonas aeruginosa however no inhibition was observed across the concentration range investigated regardless of dichlorophen delivery method. Therefore *P. aeruginosa* was treated with dichlorophen at twice the standard concentration range utilised however this led to precipitation of components due to interactions with the growth media. The results obtained were considered unreliable and are not shown.

4.4.1 Influence of nanoparticle size and zeta potential on MIC

To determine if the size and zeta potential of the dichlorophen loaded nanoparticles influenced inhibitory activity against *S. aureus* and *E. coli*, the MIC values obtained in Tables 4.4 were plotted against the size and zeta potential values that were obtained from the materials screen formulations outlined in Table 3.5.

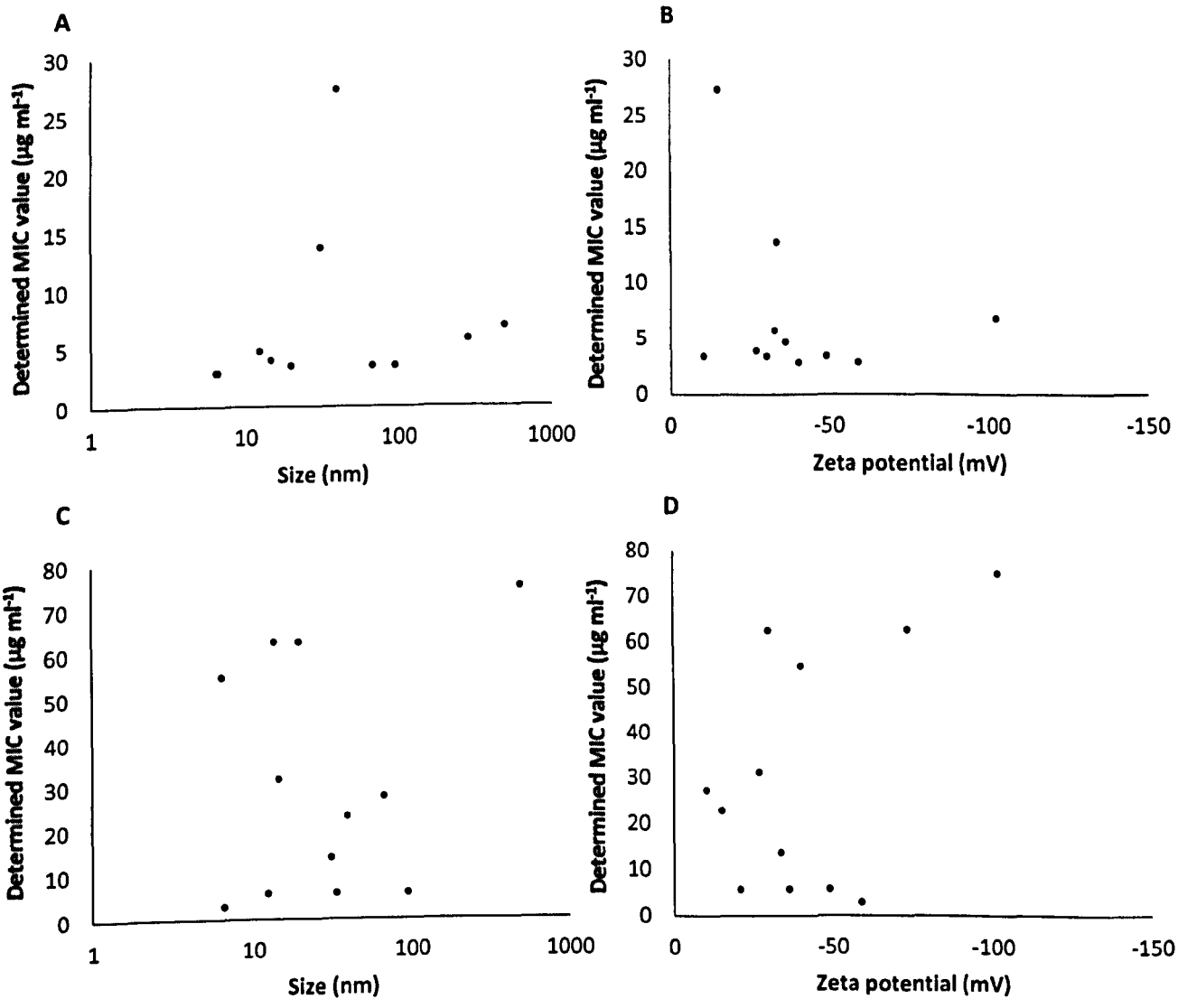

Figure 4.1 Average determined MIC values in *S. aureus* SH1000 (A & B) and *E. coli* MC1061 (C & D) against average nanoparticle size and zeta potential using the data outlined in Tables 3.5 and 4.2.

The results outlined in Figure 4.1 suggested that no correlation exists between the average size of the particles within the nanoparticle suspension, the zeta potential expressed by the nanoparticles and efficacy of inhibition of the individual preparations against *S. aureus* and *E. coli*. The same trends were observed in Figures 3.4 and 3.5 when comparing size and zeta potential values against the obtained MIC values for *C. albicans*. These results add further evidence that inhibitory activity as a function of the expressed physical characteristics of the prepared nanoparticles is an over-simplistic explanation for why certain preparations are more inhibitory than others.

4.5 Effects of material combinations to determine if synergy of components accounts for enhanced antimicrobial activity in *C. albicans, S. aureus,* and *E. coli*.

A series of defined control materials, based on preparation 25/97/04, were produced (Table 4.5) to complement the previously described control datasets that were used to determine if dichlorophen nanoparticles were more inhibitory than conventional delivery methods. These included a micellisation control consisting of equal ratios of the active nanoparticle components, water stirred for 1 week at room temperature to determine if spontaneous micellisation occurred between the material combinations. A feedstock solution consisting of the active nanoparticle components was prepared in either an oil (50% ethylene glycol) or water (50%) phase and subsequently mixed at room temperature to produce a homogeneous solution. This feedstock solution was comparable to the solution used to make the dry nano-composite materials prior to atomisation in the spray drier. A blank feedstock solution was also produced using the same technique without the addition of dichlorophen. The compositions of the defined control materials are outlined in Table 4.5 with the MIC values obtained for each, when tested against *C. albicans*, *S. aureus* and *E. coli* as outlined in section 2.3.1. The results in Table 4.5 indicated that some control preparations did induce significant levels of inhibition, however the engineered nanoparticle suspension consistently gave the lowest MIC value. The micellisation control induced inhibition in *C. albicans* (11.46 $\mu g\ ml^{-1}$) and *S. aureus* (4.69 $\mu g\ ml^{-1}$) but interestingly did not induce inhibition across the concentration range investigated when tested against *E. coli*. The inhibition induced by the micellisation control when tested against *S. aureus* and *C. albicans* suggested that some spontaneous micellisation between the materials was possible.

However, the resulting cloudy suspension after lengthy mixing, with dichlorophen remaining un-dissolved indicated this process was limited. The results show that it was possible to match the MIC value obtained for the micellisation control with the conventional co-solvent dissolved dichlorophen preparation when tested against *C. albicans*. The differences in inhibitory efficacy of the micellisation control solutions between the organisms tested may reflect differences in cell wall compositions. The feedstock solution produced a lower MIC value than ethylene glycol dissolved dichlorophen when tested against *C. albicans* and *S. aureus* but not *E. coli*. The results therefore suggested that combing SDS and hydroxy propyl methyl cellulose into a co-solvent dissolved preparation of dichlorophen increases the efficacy of inhibition, therefore a synergistic effect of the materials was possible. The results in Table 4.5 also indicated that the same MIC value was obtained for the micellisation and feedstock controls when tested against *S. aureus*. This would suggest that a synergy between the materials occurred in the micellisation control however, the same trends were not replicated when tested against *E. coli* and *C. albicans* and therefore a synergy can only be suggested. The difference in inhibitory efficacy of the nanoparticle and control solutions between *C. albicans*, *S. aureus* and *E. coli* may reflect the differences in the cell wall composition between the organisms and the organisms degree of sensitivity to each of the individual components that are used to make the nanoparticle or controls. The delivery of antimicrobials using the described micellisation and feedstock preparations would be considered impractical due to the required preparation times and ability to handle large volumes of unstable solutions. The feedstock solutions also contain large volumes of organic solvent and would therefore not be permitted for use in both clinical and agrochemical applications. These controls are therefore purely of academic interest. The ability of the nanoparticle preparation 25/97/04 to produce the lowest MIC value compared to a detailed series of controls suggests that although some synergistic effect between materials may account for improvements in activity, nanoparticle formation of the materials appeared to further enhance the antimicrobial properties of dichlorophen.

Table 4.5 Inhibitory activity of control preparations compared with the dichlorophen loaded nanosuspension 25/97/04 tested against *C. albicans, S. aureus* and *E. coli.* Values are the averages from three independent experiments, with standard errors of the mean shown.

Preparation	Ratio of dichlorophen ($\%^{w}/_{w}$)	Ratio of SDS ($\%^{w}/_{w}$)	Ratio of HPMC ($\%^{w}/_{w}$)	*C. albicans* MIC ($\mu g\ ml^{-1}$)	S.E.M	*S. aureus* MIC ($\mu g\ ml^{-1}$)	S.E.M	*E. coli* MIC ($\mu g\ ml^{-1}$)	S.E.M
25/97/04[1]	10%	20%	70%	7.81	4.19^{-3}	2.86	3.0^{-3}	2.86	6.0^{-3}
Micellisation[2]	10%	20%	70%	11.46	1.28^{-3}	4.69	7.0^{-3}	>500	-
Feedstock[3]	10%	20%	70%	9.38	4.16^{-3}	4.69	1.0^{-3}	45.83	1.3^{-2}
Blank Feedstock[4]	0%	20%	70%	27.33	6.43^{-3}	54.65	8.0^{-3}	54.65	5.0^{-3}
Dichlorophen in ethylene glycol	-	-	-	11.46	2.21^{-2}	13.66	1.4^{-3}	27.33	6.0^{-3}

[1] 10% $^{w}/_{w}$ dichlorophen, 20% $^{w}/_{w}$ SDS, 70% $^{w}/_{w}$ HPMC processed into nanoparticles

[2] 10% $^{w}/_{w}$ dichlorophen, 20% $^{w}/_{w}$ SDS, 70% $^{w}/_{w}$ HPMC stirred in water at room temperature

[3] 10% $^{w}/_{w}$ dichlorophen, 20% $^{w}/_{w}$ SDS, 70% $^{w}/_{w}$ HPMC stirred in 50% water 50% ethylene glycol at room temperature

[4] 20% $^{w}/_{w}$ SDS, 70% $^{w}/_{w}$ HPMC stirred in 50% water 50% ethylene glycol at room temperature

4.6 Design of Experiment (DOE MODDE^{TM})

The data obtained from the generic screening of nanoparticle formulations for inhibitory activity (Tables 3.6 & 4.4) were subsequently utilised in a systematic design approach with the aim of identifying the relative significance of each design variable on inhibitory activity and ultimately determine an optimum nanoparticle composition. This was carried out using the computer-based application Design of Experiment (DOE MODDE^{TM}) the details of which are outlined in section 1.12. A simple cube based DOE was designed and the following parameters set: dichlorophen 5% $^{w}/_{w}$ – 20% $^{w}/_{w}$, sodium dodecyl sulphate 10% $^{w}/_{w}$ – 50% $^{w}/_{w}$, hydroxy propyl methyl cellulose 0% $^{w}/_{w}$ – 85% $^{w}/_{w}$ and gelatin 0% $^{w}/_{w}$ – 85% $^{w}/_{w}$. The model suggested 12 nanoparticle formulations requiring investigation (Table 4.6) in order to determine which parameters were most significant for inhibitory activity. The suggested materials were tested against *S. aureus* SH1000, MRSA-252, *E. coli* MC1061 and *C. albicans* as outlined in section 2.3.1. Physical characterisation of the nanoparticle preparations was also conducted on the basis of size and zeta potential to determine if a correlation between these parameters and inhibitory activity could be sought (Table 4.6).

Table 4.6. Design of Experiment suggested nanoparticle compositions formulated and subsequently characterised.

Preparation code	Nanoparticle composition (% $^{w}/_{w}$)	Size (nm)	Zeta potential (mV)
DOE/97/01	5% dichlorophen 10% SDS 85% HPMC	223.7	-10.8
DOE/97/02	5% dichlorophen 10% SDS 85% gelatin	52.7	-38.4
DOE/97/03*	15% dichlorophen 15% SDS 70% HPMC	295.2	-17.7
DOE/97/04*	15% dichlorophen 15% SDS 70% gelatin	288.7	-37.7
DOE/97/05	5% dichlorophen 50% SDS 45% HPMC	11.04	-36.2
DOE/97/06	5% dichlorophen 50% SDS 45% gelatin	14.03	-47.3
DOE/97/07	20% dichlorophen 50% SDS 30% HPMC	214.3	-49.5
DOE/97/08	20% dichlorophen 50% SDS 30% gelatin	413.2	-41.0
DOE/97/09	12.5% dichlorophen 30% SDS 57.5% gelatin	13.4	-35.2
DOE/97/10	12.5% dichlorophen 30% SDS 28.75% HPMC 28.75% gelatin	332.4	-43.9
DOE/97/11	12.5% dichlorophen 30% SDS 28.75% HPMC 28.75% gelatin	201.0	-43.1
DOE/97/12	12.5% dichlorophen 30% SDS 28.75% HPMC 28.75% gelatin	28.8	-45.8

*DOE/97/03 and DOE/97/04 – model initially suggested 20% $^{w}/_{w}$ dichlorophen and 10% $^{w}/_{w}$ SDS however the preparations did not re-disperse adequately therefore the preparations were adjusted as outlined in Table 4.6.

Polymer and surfactant key: SDS – sodium dodecyl sulphate, HPMC – hydroxy propyl methyl cellulose

Table 4.7. The inhibitory effects of Design of Experiment dichlorophen preparations and controls on *S. aureus* SH1000, MRSA-252, *C. albicans*, and *E.coli* MC1061 in 96 well plate assays after 24 hours incubation. Values are the averages from three independent experiments, with standard errors of the mean shown.

Preparation code	*S. aureus* SH1000	S.E.M	MRSA-252	S.E.M	*C. albicans*	S.E.M	*E. coli* MC1061	S.E.M
	MIC ($\mu g\ ml^{-1}$)							
DOE/97/01	3.91	1.9^{-2}	1.95	3.0^{-3}	3.91	5.0^{-3}	2.86	1.0^{-2}
Blank-10% SDS 85% HPMC	>500	-	>500	-	>500	-	>500	-
DOE/97/02	7.81	1.2^{-2}	3.42	3.0^{-3}	7.81	2.0^{-3}	27.33	3.0^{-3}
Blank-10% SDS 85% gelatin	>500	-	>500	-	>500	-	>500	-
DOE/97/03	2.86	3.0^{-3}	3.42	8.0^{-3}	7.81	1.0^{-3}	11.46	0
Blank-15% SDS 70% HPMC	300	1.0^{-3}	250	3.0^{-3}	>500	-	>500	-
DOE/97/04	2.86	6.0^{-3}	3.42	1.0^{-3}	6.83	3.0^{-3}	22.91	1.0^{-3}
Blank-15% SDS 70% gelatin	300	0	250	1.73^{-3}	>500	-	>500	-
DOE/97/05	3.42	1.3^{-2}	1.95	5.0^{-3}	3.42	5.0^{-3}	91.65	2.0^{-3}
Blank-50% SDS 45% HPMC	300	5.79^{-3}	125	0	218.6	0	>500	-
DOE/97/06	3.91	7.0^{-3}	1.95	7.0^{-3}	3.91	5.0^{-3}	27.33	6.0^{-3}
Blank-50% SDS 45% gelatin	300	4.7^{-3}	250	2.0^{-3}	366.6	4.0^{-3}	>500	-
DOE/97/07	6.83	5.0^{-3}	3.42	3.0^{-3}	6.83	2.0^{-3}	250	2.0^{-3}
Blank-50% SDS 30% HPMC	300	1.09^{-3}	250	1.4^{-3}	437.2	1.2^{-3}	>500	-

DOE/97/08	6.83	7.0^{-3}	2.86	3.0^{-3}	6.83	2.0^{-3}	22.91	5.0^{-3}
Blank-50% SDS 30% gelatin	250	5.65^{-3}	300	0	366.6	3.0^{-4}	500	1.56^{-3}
DOE/97/09	6.83	3.0^{-3}	3.91	0	6.83	2.0^{-3}	109.3	0
Blank-30% SDS 57.5% gelatin	250	6.09^{-3}	300	1.16^{-3}	366.6	3.0^{-4}	>500	-
DOE/97/10	6.83	5.0^{-3}	3.91	0	5.73	4.0^{-3}	11.46	4.0^{-3}
Blank-30% SDS 28.75% HPMC 28.75% gelatin	250	2.07^{-3}	300	3.75^{-3}	500	8.0^{-4}	>500	-
DOE/97/11	6.83	2.0^{-3}	3.91	3.0^{-3}	6.83	0	13.66	8.0^{-3}
Blank-30% SDS 28.75% HPMC 28.75% gelatin	250	3.0^{-3}	300	2.0^{-3}	500	1.0^{-4}	>500	-
DOE/97/12	6.83	2.0^{-3}	3.91	3.0^{-3}	6.83	0	11.46	3.0^{-3}
Blank-30% SDS 28.75% HPMC 28.75% gelatin	250	1.8^{-3}	300	0	500	8.2^{-3}	>500	-
Water saturated dichlorophen	>500	-	>500	-	>500	-	>500	-
Dichlorophen in ethylene glycol	13.66	1.4^{-3}	13.66	4.0^{-3}	11.46	2.2^{-2}	27.33	6.0^{-3}
Ethylene glycol only	218.6	2.0^{-3}	183.3	3.0^{-3}	183.3	1.1^{-2}	183.3	5.0^{-3}

Polymer and surfactant key: SDS – sodium dodecyl sulphate, HPMC – hydroxy propyl methyl cellulose

A

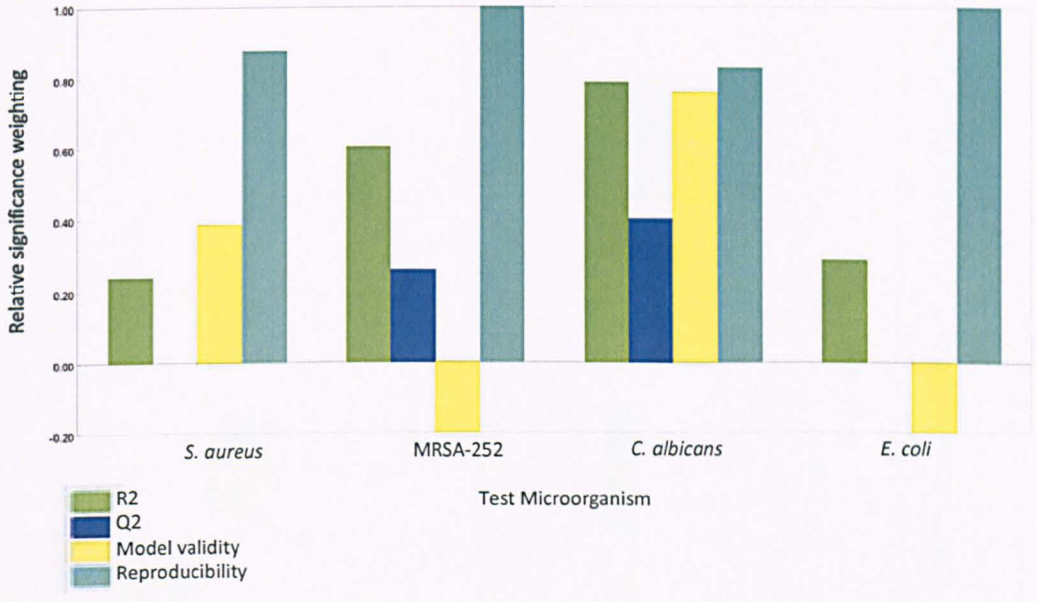
Relative significance weighting
1.00
0.80
0.60
0.40
0.20
0.00
-0.20
S. aureus
MRSA-252
C. albicans
E. coli
Test Microorganism
R2
Q2
Model validity
Reproducibility

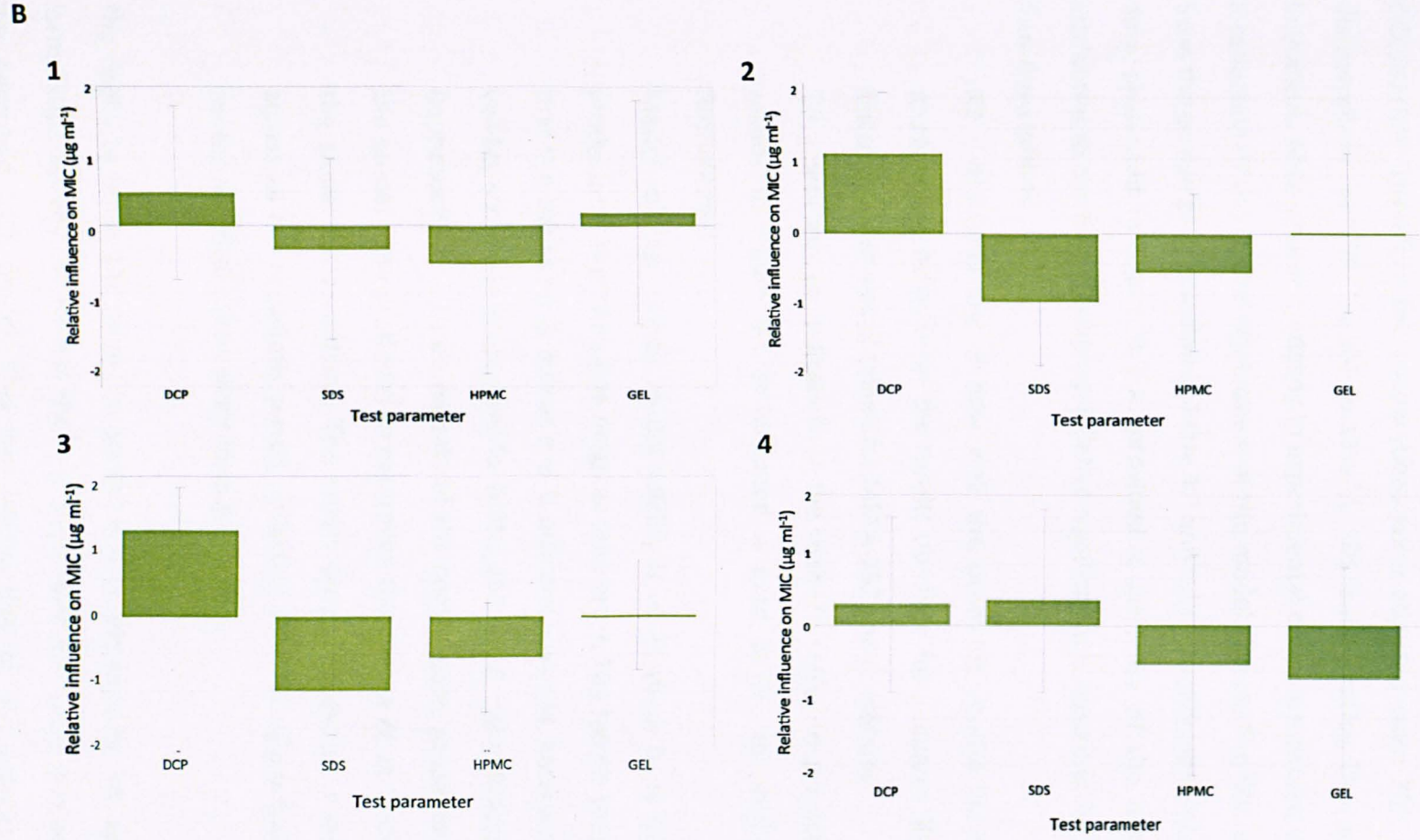

Figure 4.2 DOE MODDE™ model outputs. (A) Summary of the relative significance of the model output that determines the overall ability to predict optimal formulations, details of the figure are outlined in the following text. (B) The relative significance of each test parameter (DCP = dichlorophen; SDS = sodium dodecyl sulphate; HPMC = hydroxy propyl methyl cellulose; GEL = gelatin) on the inhibitory activity of the nanoparticle preparations tested against (1) *S. aureus* SH1000 (2) MRSA-252 (3) *C. albicans* (4) *E. coli* MC1061.

The results presented in Table 4.6 indicated that nanoparticle formulations of dichlorophen were produced. However two preparations suggested by the DOE software did not re-disperse adequately on mixing with water (DOE/97/03 and DOE/97/04). Therefore the preparations were adjusted from 20% $^{w}/_{w}$ to 15% $^{w}/_{w}$ dichlorophen and 10% $^{w}/_{w}$ SDS to 15% $^{w}/_{w}$ SDS loading ratios. This demonstrated the limitations of computer modeling in experimental design processes, which resulted in a reduction in the overall significance of the model output. The MIC values generated from the screen are presented in Table 4.7 and subsequently input into the model. The data presented in Figure 4.2 A. provided a summary of the overall significance attributed to the models output. Relative significance is described by the model using four descriptions:

R2 - is a measure of how well the predicted model fits the data, which appeared to be poor for the results obtained for *S. aureus* SH1000 and *E. coli* but a better fit was obtained for MRSA-252 and *C. albicans*.

Q2 - provides an indication of the model's ability to predict new data. The results in Figure 4.2 A indicated a poor ability to predict new optimal formulations.

Model validity – when model validity is >0.25 there is no lack of fit *i.e.* the model error is in the same range as pure error. The results therefore suggested that the values for *S. aureus* and *C. albicans* are valid, however negative model validity scores were obtained for MRSA-252 and *E. coli* indicating poor validity.

Reproducibility – three repeats of the centre point preparation suggested by the model were produced to determine the degree of variation in response to the same test conditions. The model output suggested good reproducibility across all the organisms tested, reflecting the MIC values that were obtained for the identical centre point formulations.

The ability to utilise the model to predict trends and identify 'hot spots' for optimal formulation activity *i.e.* achieve the lowest possible MIC value was not possible using the described DOE model. This was largely due to the modifications made to DOE/97/03 and DOE/97/04 that reduced the model's significance weighting.

The results presented in Figure 4.2 B are the general trends observed when investigating the relative significance of each parameter on inhibitory activity. The results highlighted that an increase in the dichlorophen loading ratio within the nanoparticle formulation caused an increase in MIC value in all four organisms tested. An increase in SDS loading ratio caused a reduction in MIC values in all the organisms except *E. coli* that displayed an increase in MIC with increased SDS ratio (Figure 4.2 B4). An increase in the loading ratio of the polymer hydroxy propyl methyl cellulose in the nanoparticle preparations generally decreased the MIC value obtained, and an increase in the gelatin loading ratio caused a small increase in the MIC values for *S. aureus* SH1000, MRSA-252 and *C. albicans* but this was shown to cause a reduction in MIC in *E. coli*. Although the model displayed poor overall significance, the results presented in Figure 4.2 B indicated generic trends in nanoparticle design for the optimisation of antimicrobial activity that were also evident when manually interpreting the MIC results outlined in Table 4.7.

The results presented in Table 4.7 indicated that the optimal nanoparticle compositions for inhibitory activity against *S. aureus* SH1000 were DOE/97/03 and DOE/97/04. These formulations produced an MIC approximately 4.8 fold lower compared to the dichlorophen dissolved in ethylene glycol solution. DOE/97/01, DOE/97/05 and DOE/97/06 produced MIC's approximately 7 fold lower compared to the solvent dissolved dichlorophen treated MRSA-252. Preparation DOE/97/05 was shown to produce an MIC approximately 3.3 fold lower than the ethylene glycol dissolved dichlorophen solution against *C. albicans*. Preparation DOE/97/01 was the most inhibitory when tested against *E. coli* with an approximate 9.5 fold decrease in MIC compared to the ethylene glycol dissolved dichlorophen solution. These optimal nanoparticle compositions consisted of low dichlorophen loading ratios and SDS loading ratios ranging from 10% $^{w}/_{w}$ to 50% $^{w}/_{w}$. The preparations DOE/97/01 and DOE/97/05 appeared to be the most consistently inhibitory and therefore offered the broadest range of activity against the microorganisms investigated. Although the variation in MIC values was reduced when using the model, high degrees of variation between certain preparations were still evident for example; DOE/97/01 produced an MIC of 2.86 μg ml^{-1} whereas DOE/97/07 produced an MIC of 250 μg ml^{-1} when tested

against *E. coli*. This highlighted the significant variance in efficacy of activity between nanoparticle designs.

Although further predictive optimisation of nanoparticle design was not possible using the DOE model, several trends were identified that permitted enhanced antimicrobial activity against Gram-negative and Gram-positive bacteria and fungi. No correlation was found between the expressed zeta potential and size of the nanoparticle preparations and inhibitory activity (Appendix 2). This again suggested that antimicrobial efficacy of nanoparticles as a function of the expressed physical characteristics of that preparation is over-simplistic. No correlation was identified between the inhibitory activity of the dichlorophen loaded nanoparticles and the blank nanoparticle preparations, suggesting that the excipient materials processed into nanoparticles alone does not account for enhanced antimicrobial activity of particular formulations.

4.7 Dissolution assay

As particle diameter decreases, its surface area to volume ratio increases, leading to an increased dissolution rate (Kipp, 2004). Previous studies have indicated that nanoparticle formation of antimicrobials can account for increased rates of dissolution, however this appeared to be dependent on particle design, to whether burst or biphasic profiles are observed (Esmaeili *et al.*, 2007; Kisich *et al.*, 2007; Pillai *et al.*, 2008). Dissolution assays were performed to investigate the rate of dichlorophen released when formulated into nanoparticles, using preparation DOE/97/03 and comparing this with an unformulated dichlorophen preparation consisting of water stirred dichlorophen, SDS and HPMC at equal quantities. The dissolution assays were conducted as outlined in section 2.9 and the concentration of dichlorophen released was determined using HPLC as outlined in section 2.5.3.

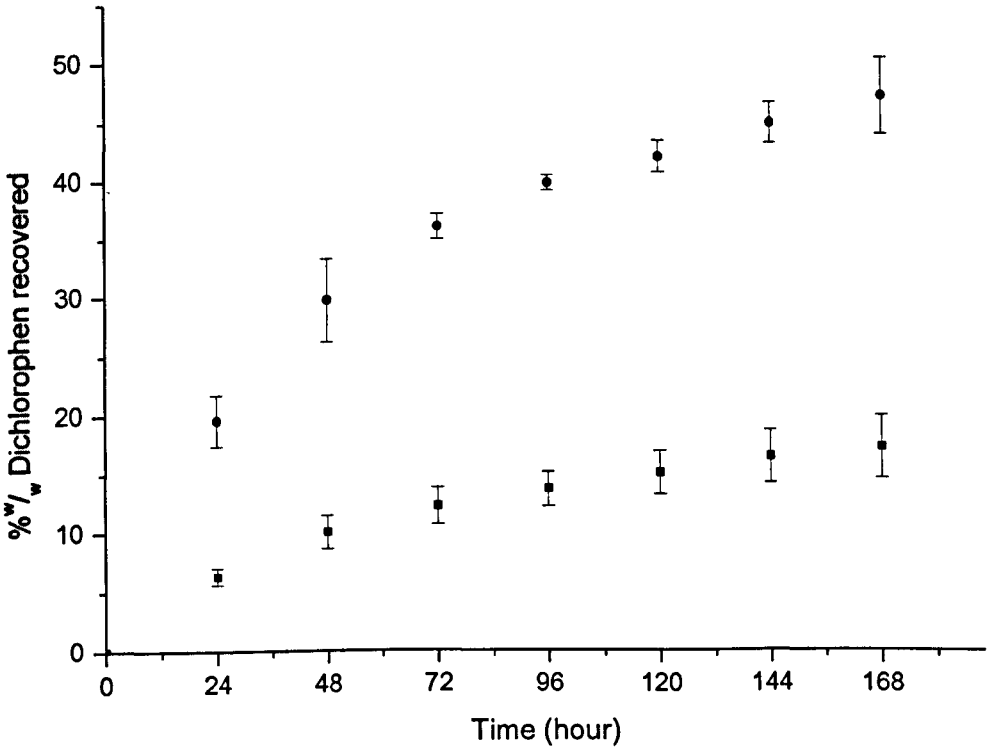

Figure 4.3 Dissolution assay comparing the rate of dichlorophen released from a dialysis membrane (donor compartment) when formulated as either nanoparticles (DOE/97/03 – 15% $^{w}/_{w}$ dichlorophen, 15% $^{w}/_{w}$ SDS, 70% $^{w}/_{w}$ HPMC) (●) or dichlorophen, SDS and HPMC water stirred (■) at equal ratios and concentrations comparable to the nanoparticle formulated preparation. Final total dichlorophen concentration was 250,000 μg. Samples taken at 24-hour intervals over 168 hours and assayed for dichlorophen recovered from the water stirred acceptor compartment using HPLC. Values are averages from three independent experiments. Error bars indicate standard errors of the mean.

The results presented in Figure 4.3 indicated that the rate and total amount of dichlorophen released from the dialysis membrane (the donor compartments) when nanoparticle formulated was greater than that observed for the water stirred dichlorophen and excipient mixture. Both profiles indicated that the most rapid rate of dichlorophen release was within the first 24 hours with an average of 19.62% and 6.34% being recovered from the nanoparticle formulated and water stirred preparations (acceptor compartments) respectively, indicating a small 'burst' effect profile. The rate of release was subsequently shown to decline with 17.29% of the dichlorophen being recovered from the dichlorophen and excipient mixture test and an average of 47.18% of the dichlorophen being recovered from the nanoparticle

formulated dissolution after 168 hours. Dichlorophen has a quoted water solubility of 30 μg ml^{-1} (Tomlin, 1995). Interestingly, these results indicated that after 168 hours of being water stirred an average of 86.45 μg ml^{-1} of dichlorophen was recovered from the dichlorophen and excipient mixture and 235.9 μg ml^{-1} of dichlorophen was recovered from the nanoparticle formulated dissolution test. The ability to recover dichlorophen at a concentration greater than its theoretical water solubility suggested that some spontaneous micellisation might have occurred with the excipients materials therefore enhancing solubility limits within the dichlorophen and excipient mixture test. However, the cloudy suspension both within the dialysis membrane and in the sampled acceptor compartment solution, and the ability to identify remaining un-dissolved dichlorophen within the dialysis membrane suggested this process was limited. The ability to recover an average of 235.9 μg ml^{-1} of dichlorophen a concentration approximately 7.9 fold greater than the solubility limits of the antimicrobial in water, suggested that nanoparticle formation enhanced dissolution rates. This may therefore improve dichlorophens bioavailability possibly explaining the enhanced antimicrobial activity observed when using a nanoparticle preparation.

4.8 Discussion

Formulation methodologies, applications and advantageous features of organic nanoparticles for the delivery of antimicrobials are increasingly being described in the published literature (Page-Clisson *et al.*, 1998 ; Dillen *et al.*, 2004 ; Dillen *et al.*, 2006 ; Jeong *et al.*, 2008 ; Imbuluzqueta *et al.*, 2011). This study utilised a novel emulsion-evaporation process first described by Zhang *et al.* (2008a) to produce water dispersible organic nanoparticles from the poorly water soluble antibacterial compounds pentachlorophenol, ciprofloxacin and dichlorophen. The nanoparticle preparations were usually shown to be more inhibitory than conventional organic co-solvent dissolved delivery and provides further evidence for the potential scope of the described technology.

Previous studies have investigated how nanoparticle design or the preparative methods used to formulate nanoparticle preparations influenced the physical characteristics and therefore the potential applications of the formed nanoparticles. Das *et al.* (2010) investigated the design of Eudragit RL100 nanoparticles using a solvent displacement or nano-precipitation method for optimising ocular delivery of the antifungal amphotericin-B. The study indicated that particle size and drug release rates were a function of drug to polymer ratio. The antifungal displayed equivalent activity against *Fusarium solani* as the control preparation, but was optimised for ocular delivery *i.e.* caused reduced irritation and displayed prolonged release profiles. Bozkir & Saka (2005) investigated the optimisation of a nano-precipitation – solvent displacement technique for the nanoparticle formation of 5-fluorouracil loaded poly(lactide-co-glycolide) nanoparticles in which the type of surfactant, amount of acetone used in the preparation procedure and molecular weight of the polymer used in the nanoparticle design was modified in order to determine the influence of such parameters on nanoparticle size, entrapment efficiency and release kinetics. Dillen *et al.* (2004) investigated the influence of viscosifying agents as a dispersion media on ciprofloxacin HCl release from poly(lactide-co-glycolide) nanoparticles that were prepared using a W/O/W emulsion-solvent evaporation method. The influence of polymer type incorporated into the nanoparticle preparations and the subsequent influence on particle size, ciprofloxacin release rates and the rheological behaviour of

the particles were investigated, with the aim of identifying an optimal design for ciprofloxacin activity. The results suggested the choice of polymer influenced the rheological behaviour of nanoparticle solutions with some exhibiting Newtonian and others non-Newtonian characteristics. The choice of polymer was also shown to influence the rate of ciprofloxacin released from the nanoparticle and it was therefore suggested that the polymer used in the nanoparticle design should be selected on the basis of the application required of the nanosuspension (Dillen *et al.*, 2004).

The results presented in this study also indicated that nanoparticle design influenced the physical characteristics and inhibitory activity exhibited by the nanoparticle preparations. The particles used in this study are novel and therefore the ability to cross reference design trends with previous studies is limited. The generic screening of materials highlighted that the choice and ratio of surfactant and the choice of polymer used in the nanoparticle formulation was significant to antimicrobial activity despite the dichlorophen loading ratio remaining constant at 10% $^{w}/_{w}$. These results were subsequently used to form the basis of a Design of Experiment (DOE MODDE^{TM}) model to identify the relative significance of each parameter on inhibitory activity. The aim was to perform theoretical design optimisation based on all the possible combinations of variables within the developed experimental region to improve efficacy of inhibition (Eriksson *et al.*, 2008). The results presented in Figure 4.2 indicated poor model significance and therefore theoretical design optimisation was not possible. The model is likely to have failed due to the inability to produce nanoparticles from two of the suggested preparations. This skewed the test statistics and therefore significantly reduced the models fit and ability to predict an optimal formulation. Another possible cause of the models failure could be associated with the degree of variability associated with data generated from biological experiments and therefore reduced ability to predict outcomes from such experiments compared with data produced from the physical sciences which DOE MODDE^{TM} is primarily targeted at. However, several trends were identified when manually interpreting the data. As the loading ratio of dichlorophen was reduced, the MIC (per unit mass of active) also decreased (Table 4.7, Figure 4.2 B). Although this result would appear unusual, the quantity of excipients is higher in these low antimicrobial loading preparations. It is suggested that particle

number is likely to increase with a reduced loading ratio of antimicrobial. It was also shown that an increase in surfactant ratio generally decreased MIC values that may also be attributed to increased particle numbers. More nanoparticles containing a smaller load of the antimicrobial are suggested to improve efficacy of inhibition because a greater number of nanoparticle – cell interactions is anticipated, thus allowing the antimicrobial to reach targets more efficiently. However, accurate particle number studies were not possible due to the small particle sizes obtained and therefore this theory could not be substantiated. Previous studies have also suggested that smaller nanoparticles are more efficient at delivering active compounds to cells (Belesti *et al.*, 2005 ; Jiang *et al.*, 2008).

The results presented in this study indicated that no correlation between the physical characteristics of the prepared nanoparticle suspensions on the basis of size or zeta potential were linked to the antimicrobial efficacy of particular preparations for all the antimicrobials investigated. Another possible explanation for variation in inhibitory activity between nanoparticle preparations is the affinity of the nanoparticles to interact with the cells that would largely be based on charge or chemical interaction. The ability to monitor and quantify such interactions would not however be possible at present.

No correlation was identified between the antimicrobial activity of the blank nanoparticles and the antimicrobial loaded equivalents therefore suggesting the enhanced efficacy of particular formulations was not attributed to the processed excipients. The series of defined control preparations produced in Table 4.5 indicated that nanoparticle formation of dichlorophen enhanced the antimicrobial activity even though the feedstock and micellisation solutions did induce significant levels of inhibition in most test conditions. The micellisation control was shown to produce the same MIC value as the feedstock solution when tested against *S. aureus,* which suggested a synergy between dichlorophen and the excipients materials had occurred. However, the same trend was not replicated when tested against *C. albicans* and *E. coli.* The feedstock solution was also shown to produce lower MIC values than the conventional solvent dissolved dichlorophen when tested against *S. aureus* and

C. albicans. However, the feedstock solution was less inhibitory than the nanoparticle formulation in all three organisms tested. Collectively, the results suggested a synergy between the individual nanoparticle constituent components was not the only explanation for enhanced dichlorophen efficacy. All the presented data suggests that nanoparticle formation of antimicrobials affords the materials additional properties over non-nanoparticle formulated equivalents in addition to the ability to use an organic co-solvent free delivery system. This suggested that nanoparticle formation of dichlorophen permitted enhanced efficacy compared to conventional delivery and the control chemical preparations. A series of detailed controls as outlined in this work has not been identified in the published literature. No physical features linked to modifications in nanoparticle design could be attributed to variations in activity. Nanoparticles produced using the described method should therefore be designed and optimised for the intended application in order to achieve optimal efficacy.

A feature of nanoparticle suspensions is the increase in saturation solubility and consequently an increase in the dissolution rate of the active compound. This increase in the dissolution rate is in addition to that caused by the greater surface area exhibited by nanoparticles. In general, solubility is a compound specific constant which is temperature dependent (Kocbek & Krisl, 2006). However, due to greater dissolution pressure, the saturation solubility increases below a particle size of approximately 1 μm (Muller & Keck, 2004). By decreasing the size of solid particles or by creating a more uniform distribution, the high-energy state achieved will increase the extent to which it can dissolve (Williams & Vaughn, 2006). The results presented in Figure 4.3 suggested that the nanoparticle preparation DOE/97/03 displayed an increase in dissolution rate compared to a water mixed dichlorophen and excipient comparison. The ability to recover dichlorophen at an average concentration of 86.45 μg ml^{-1} after 168 hours when the water solubility limit of dichlorophen is quoted at 30 μg ml^{-1} (Tomlin, 1995) suggested that some spontaneous micellisation of the water stirred dichlorophen and excipient mixture had occurred. However, the cloudy suspensions contained in both the donor and acceptor compartments and the visibly un-dissolved dichlorophen remaining in the donor dialysis tube suggested this process was limited. These observations contrast with those made for the nanoparticle formulated

preparation DOE/97/03 in which both the donor and acceptor compartments remained optically clear and no un-dissolved dichlorophen was evident in the donor compartment. The small size of the particles means they do not scatter enough light to make their dispersions appear cloudy. Dichlorophen was recovered at 235.9 $\mu g\ ml^{-1}$ a concentration 7.9 fold greater than the saturated solubility limits of dichlorophen in water. However, only 47.18 % of the dichlorophen was recovered in the acceptor compartment after 168 hours. This may be explained by the inability of some of the nanoparticles to pass through the pores of the dialysis membrane. No direct correlation exists between 2-dimensional metric length and 3-dimensional molecular size. However, the dialysis membrane used had a molecular weight cut off ranging between 12-14000 Daltons and therefore a pore size ranging between 2-3 nm. The nanoparticle preparation DOE/97/03 exhibited an average particle size of 295.2 nm. It is therefore anticipated that a significant proportion of the nanoparticles were unable to migrate through the dialysis membrane into the sampled acceptor compartment. The heterogeneity of the preparation is likely to have allowed for passing of the smaller particles and any leached components through the membrane. The observed increase in dissolution rate may favourably affect bioavailability and account for the improvements in antimicrobial activity of the nanoparticle delivered dichlorophen.

It has been stated that the activity of compounds from various classes improves with oil-water partition coefficient and that oil-water partitioning stimulates the movement of compounds between aqueous and lipophilic receptors (Dearden, 1985). The release rate of drugs is governed by the partition coefficient and the rate of diffusion across membranes (Leo *et al.*, 2004). Previous studies have demonstrated the advantages of nanoparticle function for enhanced drug penetration or internalisation of the nanostructure, due to the suggested increase in drug concentration at the site of action (Haas *et al.*, 2009). An investigation was undertaken to determine if dichlorophen dissolved in a range of ethylene glycol to water ratios and therefore solvent polarities, influenced antimicrobial activity. It was suggested that when dichlorophen was dissolved in less polar solutions, it would induce greater degrees of inhibition because the antimicrobial would be less stable in solution, undergo partitioning and interact with the cell. However, no substantial trends were observed

from the investigation because of the varying degrees of ethylene glycol induced inhibition that skewed the results (data not shown).

The results presented in this chapter have shown that it is possible to produce nanoparticle preparations of poorly water-soluble antibacterial agents and subsequently deliver them using an aqueous route. Nanoparticle delivered antimicrobials usually induced greater degrees of inhibition than an equivalent solvent dissolved solution. A generic screen of nanoparticle formulated dichlorophen materials was further developed using the computer application DOE MODDE^{TM}. The initial aims were to determine the relative significance of each design parameter % $^{w}/_{w}$ dichlorophen, SDS, hydroxyl propyl methyl cellulose and gelatin loading ratios on inhibitory efficacy. Although several trends were identified, the model output indicated a poor fit and ability to predict from the data. This was likely to be due to the inability to produce two of the suggested nanoparticle preparations and the limitations associated with modelling in biological systems. These factors were the likely cause of model failure and therefore conclusive trends and the ability to predict optimal formulations was not possible.

A dichlorophen dissolution assay was performed to investigate the rate of dichlorophen released through a dialysis membrane when nanoparticle formulated or prepared as a water stirred mixture of dichlorophen, SDS and hydroxy propyl methyl cellulose. The results indicated that dichlorophen was released at a greater rate when formulated as nanoparticles compared with an unformulated dichlorophen excipient mixture with 2.7 fold more dichlorophen being recovered after 168 hours. A range of ciprofloxacin nanoparticles were produced, characterised and subsequently investigated for inhibitory activity against *S. aureus* SH1000. Nanoparticle formulation of ciprofloxacin was more challenging due to the antibiotics poor solubility in water and many organic co-solvents. However, selected preparations were shown to be more inhibitory than an equivalent DMSO dissolved form of delivery. It was determined that a detailed physical characterisation and molecular mode of action study using a ciprofloxacin formulation may identify why nanoparticles are more

inhibitory. Preparation 50/27/55 was selected for this analysis and the results are presented in chapter 5.

Chapter 5

Characterisation of nanoparticle formulated ciprofloxacin and subsequent mode of action analysis in *S. aureus* SH1000 using RNA Sequencing (RNA-Seq).

5.1 Introduction

The physical and chemical properties of nanoparticles can vary significantly from those of their bulk counterparts largely as a result of their large surface area-to-volume ratio. It was demonstrated that nanoparticle formation of a range of antimicrobials with differing molecular targets usually increased efficacy of inhibition compared to the equivalent solvent dissolved delivery (chapters 3 & 4). In particular, the nanoparticle formulated ciprofloxacin preparation 50.27.55 (20% $^{w}/_{w}$ ciprofloxacin, 55% $^{w}/_{w}$ PVP, 25% $^{w}/_{w}$ pluronic F127) was shown to produce an MBC value half that of the equivalent solvent dissolved preparation when tested against *S. aureus* SH1000 (Table 4.3).

A detailed study of the physical characteristics of the ciprofloxacin nanoparticle preparation and subsequent mode of action analysis was performed to determine if nanoparticle formation of ciprofloxacin causes differential gene expression. Ciprofloxacin was chosen because it is insoluble in water and many organic solvents and therefore described as a 'brick-dust' material that ultimately results in poor antimicrobial bioavailability. Moreover, ciprofloxacin has a well characterised mode of action (Drlica & Zhao, 1997 ; Berlanga *et al.*, 2004 ; Cirz *et al.*, 2007) and is widely available.

Tests for the quality of nanosuspensions were selected on the basis of the application and the required performance of the preparation (Rabinow, 2004). Critical micellisation concentration (CMC) analysis was performed to determine if spontaneous micellisation of the ciprofloxacin loaded nanoparticle, blank nanoparticle and individual constituent components occurred around the inhibitory concentrations of

these materials. CMC is the calculation of the concentration at which amphiphiles spontaneously associate into core-shell micellar structures and can be calculated using microtensionmeters to identify changes in the surface tension of a liquid, a feature indicative of micellisation (Zhang *et al.*, 2008b). Scanning electron microscopy (SEM) is an important method for the evaluation of nanoparticle shape and morphology (Dubes *et al.*, 2003). X-ray diffraction (XRD) is used to measure inter-particle spacing's resulting from interference between waves reflecting from different crystal planes. XRD can identify differences between amorphous and crystalline solids. Amorphous solids have higher solubility and dissolution rates than corresponding crystals. However, crystalline solids are preferred by the pharmaceutical industry due to their long term stability (Yu, 2001 ; Hassellöv, 2008). XRD and SEM were performed alongside size and zeta potential determination to fully characterise the physical properties that make up the multi-component ciprofloxacin loaded nanoparticle and how these might influence their mode of action.

There is a significant and expanding number of published methodologies and applications of nanoparticles. However, little work has been carried out to elucidate the mechanisms that account for the advantageous features of nanoparticles compared with their bulk counterparts. A greater understanding of how nanoparticles interact with both prokaryotic and eukaryotic organisms will undoubtedly be required, due to the introduction of products that contain nanomaterials and the remaining uncertainties regarding toxicity and environmental persistence of such materials (Sheetz *et al.*, 2005 ; Nowack & Bucheli, 2007 ; Seaton *et al.*, 2010). Two main approaches have been identified for characterising the microbial response to nanoparticles. The first type of analysis assesses cell viability, many examples of which are evident in the literature (Dillen *et al.*, 2004 ; Esmaeili *et al.*, 2007 ; Pissuwan *et al.*, 2010 ; Rai *et al.*, 2009). This approach was also used in the results presented in chapters 3 and 4. The second type of analysis is a discovery-based approach to identify the molecular response of cells to nanoparticles. Very few studies have used such methods, but there are examples where microarrays have been used to ascertain the transcriptional response of *E. coli* to Cerium oxide (CeO_2) nanoparticles (Pelletier *et al.*, 2010) and a proteomic analysis was done in *E. coli* exposed to silver nanoparticles (Lok

et al., 2006). Although some attempts have been made to characterise the mode of action of inorganic nanoparticles at the molecular-cell level, there is no published evidence of such research using polymeric antimicrobial loaded organic nanoparticles.

To ascertain the response of *S. aureus* SH1000 to nanoparticle formulated ciprofloxacin, transcriptional profiling was performed 20 minutes post exposure to growth limiting concentrations of the antibiotic (15.63 $\mu g\ ml^{-1}$), using next generation RNA sequencing. To determine if transcriptional differences exist between nanoparticle and solvent dissolved ciprofloxacin, five test conditions were investigated: nanoparticle bound ciprofloxacin, ciprofloxacin dissolved in DMSO, blank nanoparticle consisting of excipient materials, DMSO only and uninhibited cells. The overall aims of the investigation were:

1. To determine if transcriptional variation occurs when *S. aureus* SH1000 cells are treated with equal concentrations of ciprofloxacin either delivered as a nanoparticle suspension or dissolved in DMSO.
2. To determine if nanoparticle formation of ciprofloxacin induces greater transcriptional variation in known ciprofloxacin target genes.
3. To determine if the presence of nanoparticles induces differential expression when transcriptional features associated with ciprofloxacin, excipients and DMSO are removed.

Analysis of the *S. aureus* transcriptomic response to ciprofloxacin loaded organic nanoparticles should dramatically increase our knowledge and understanding of how prokaryotes respond to such drug delivery systems.

5.2 Critical Micellisation Concentration (CMC)

CMC is the calculation of the concentration at which amphiphiles associate into micellar structures. Analysis of the CMC results revealed that the nanoparticle preparation (50.27.55), blank nanoparticle (minus ciprofloxacin) and nanoparticle constituent components did not form into spontaneous core-shell micellar structures at concentrations close to the determined MBC values for these materials (Figure 5.1). The Kibron microtensionmeter software indicated that no spontaneous micellisation occurred across the concentration range investigated for the ciprofloxacin loaded nanoparticle preparation (50.27.55) as no significant change in surface tension was identified. The blank nanoparticle produced a CMC value of 560 $\mu g\ ml^{-1}$ and the pluronic F127 a CMC of 137 $\mu g\ ml^{-1}$, however visual inspection of data in Figure 5.1. suggested that the CMC was greater than 10,000 $\mu g\ ml^{-1}$. No CMC value was identified from the analysis of the polymer PVP. The MBC value of 50.27.55 against *S. aureus* SH1000 was 31.25 $\mu g\ ml^{-1}$ and was used at 15.63 $\mu g\ ml^{-1}$ for the transcriptional profiling analysis. As the data show that they do not behave as typically micellised materials, the preparation was confirmed to be engineered nanoparticles. Also as a standard test, the components that made up the nanoparticle preparation were stirred in water for several days. The ciprofloxacin remained un-dissolved adding observational evidence that the materials did not micellise when mixed.

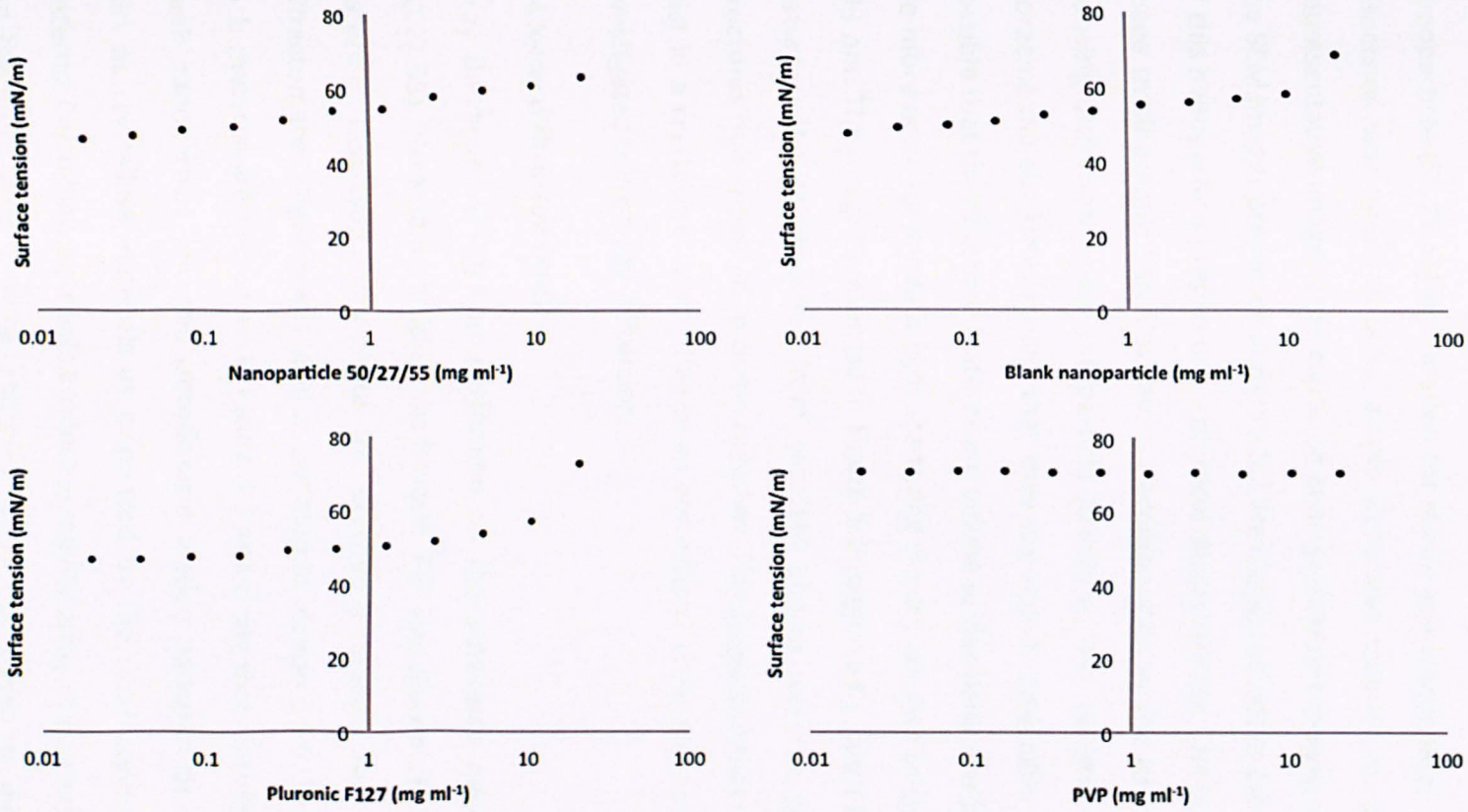

Figure 5.1. Critical Micellisation Concentration (CMC) readings of nanoparticle formulated ciprofloxacin (50/27/55), blank nanoparticle, pluronic F127 and PVP determined using a Kibron multichannel microtensionmeter. Solutions were contained within Teflon coated 96 well plates (Kibron Inc). The CMC values were identified using Kibron Delta-8 software.

5.3 Scanning Electron Microscopy (SEM)

Field emission scanning electron microscopy (SEM) was conducted using a Hitachi S-4800™ instrument as outlined in section 2.5.4 to evaluate the ciprofloxacin loaded nanoparticle (50.27.55) preparation for shape and morphology. A dilute nanoparticle dispersion was mounted onto sample stubs and coated with gold prior to imaging. Representative images were captured at magnifications ranging from x 500 to x 50000. The SEM images presented in Figure 5.2 are suggested not to provide a clear indication of this nanoparticle preparation's physical characteristics. The high energy required to image small organic particles causes decomposition of the labile organic compounds inducing distortion within the particle structure. The robustness usually found with inorganic nanoparticles means that they are readily amenable to SEM analysis. It is possible that the observed features are unique to this particular preparation. However, the more accurate dynamic light scattering result indicated an average particle size of 293 nm. The images presented in Figure 5.2 suggested a much larger particle size. A feature that was identified from the SEM images was the apparent 'needle like' structures that appeared to clump together. This suggested that the nanoparticles may exist in a crystalline rather than in an amorphous state and consequently they were investigated using X-ray diffraction.

5.4 X-ray diffraction (XRD)

X-ray diffraction (XRD) was performed on the powdered nanoparticle preparation (50.27.55), blank nanoparticle, ciprofloxacin, PVP and pluronic F127 to determine if the materials displayed amorphous or crystalline states. An R-AXIS IV++™ Xray diffractometer (Rigaku) was used as outlined in section 2.5.5. The individual traces for each material are presented in Figure 5.3 and show that ciprofloxacin, pluronic F127, blank nanoparticle and the ciprofloxacin loaded nanoparticle (50/27/55) materials exist as crystalline materials as evidenced by the clear banding on the diffraction patterns. Crystalline materials produce a regular array of scatters from the fixed point and therefore clear banding. The polymer PVP produced no distinct banding on the diffraction pattern and can therefore be classified as an amorphous material. The combined effects of each material were analysed in Figure 5.4 by comparing quadrants of each. The results highlight the multi-component nature of the nanoparticle

preparation 50.27.55. The diffraction pattern for ciprofloxacin, pluronic F127 and PVP match the banding pattern for the nanoparticle preparation explaining the crystalline morphology of the nanoparticle observed in Figure 5.4 image A quadrant 1 and the 'needle like' structures observed in the SEM images (Figure 5.2.). The blank nanoparticle material clearly showed the distinct banding pattern obtained from the pluronic F127 and the background scatter obtained from the amorphous PVP in Figure 5.4 image B quadrant 1. No anomalies in the diffraction patterns were observed, with each signature pattern of the nanoparticle and blank nanoparticle accounted for.

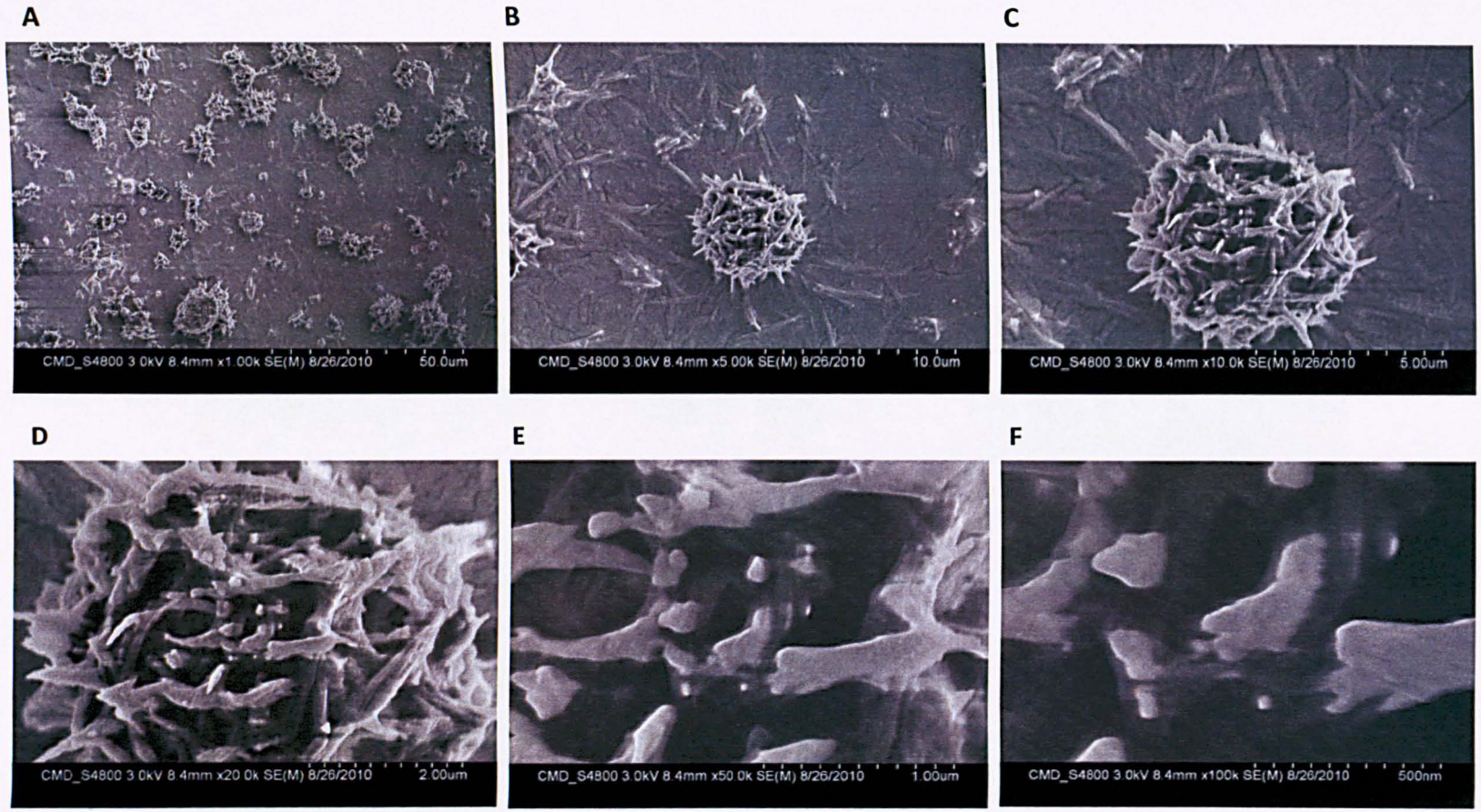

Figure 5.2. Scanning Electron Microscopy (SEM) of nanoparticle formulated ciprofloxacin (50/27/55, 20% $^{w}/_{w}$ ciprofloxacin, 55% $^{w}/_{w}$ PVP, 25% $^{w}/_{w}$ pluronic F127) conducted using a Hitachi S-4800^{TM}. A – x 500 magnification, B – x 1000 magnification, C – x 5000 magnification, D - x 10000 magnification, E – x 20000 magnification and F – x 50000 magnification.

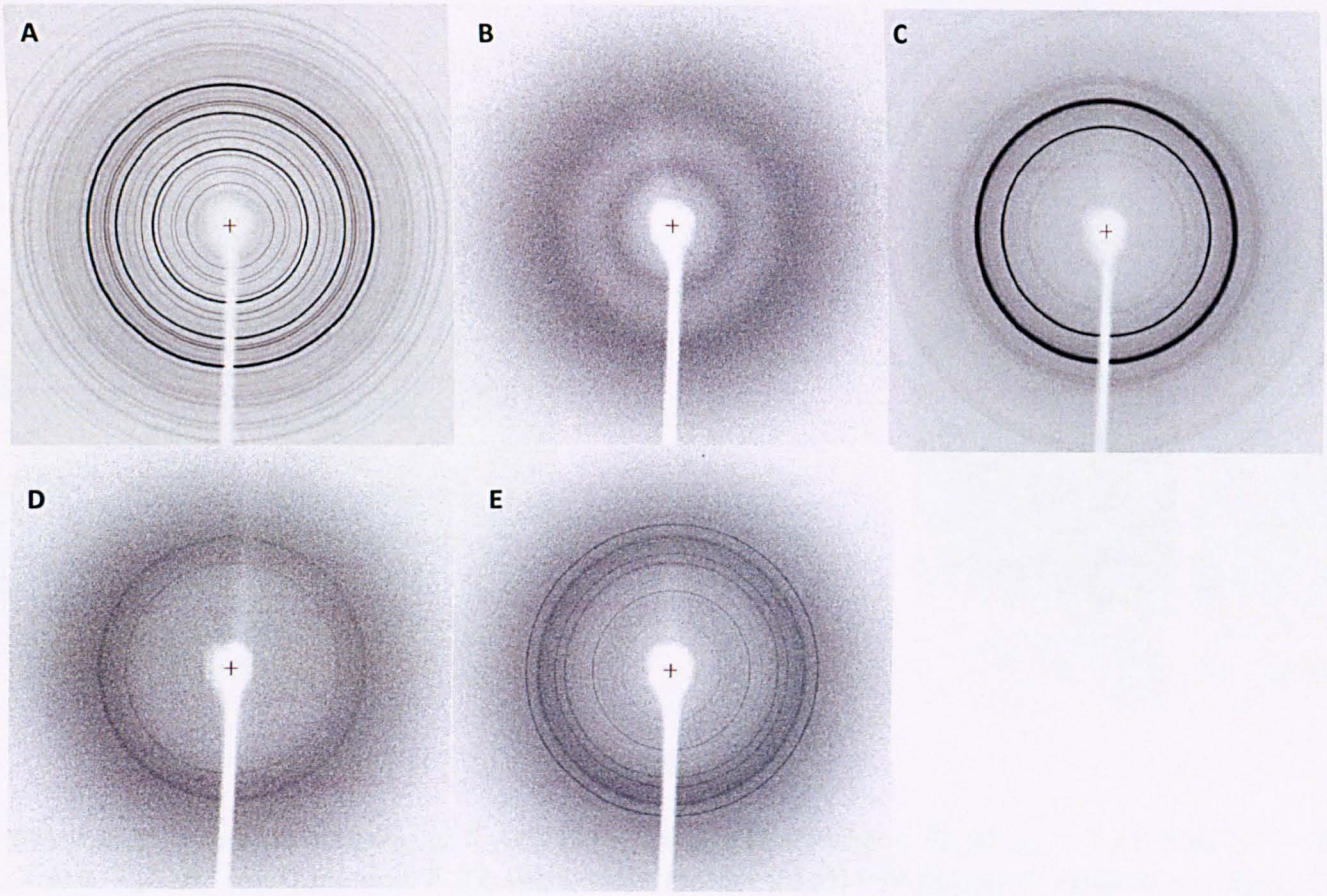

Figure 5.3. X-ray diffraction (XRD) perfomed using an R-AXIS IV++^{TM} Xray diffractometer (Rigaku) of: (A) ciprofloxacin, (B) PVP poly(vinyl pyrolidone), (C) pluronic F127, (D) Blank 50/27/55 – 25% $^{w}/_{w}$ pluronic F127 55% $^{w}/_{w}$ PVP, (E) 50/27/55 - 20% $^{w}/_{w}$ ciprofloxacin 25% $^{w}/_{w}$ pluronic F127 55% $^{w}/_{w}$ PVP.

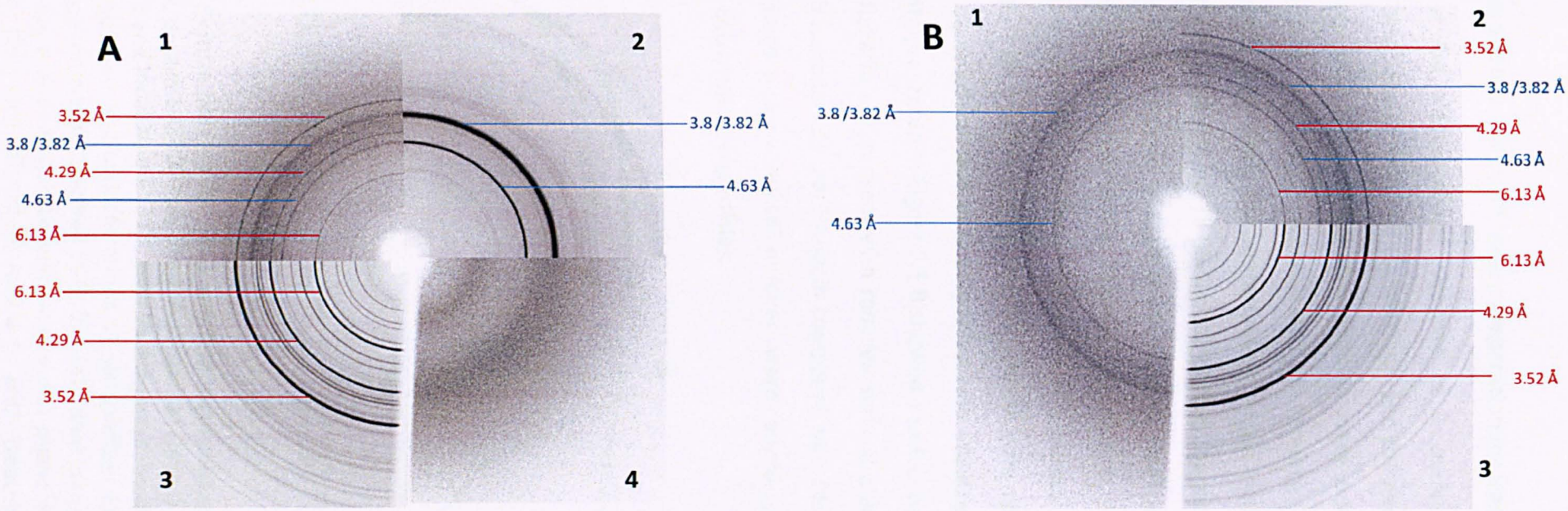

Figure 5.4. . X-ray diffraction (XRD) perfomed using an R-AXIS IV++^{TM} Xray diffractometer (Rigaku) of: (A)(1) 50/27/55 - 20% $^{w}/_{w}$ ciprofloxacin 25% $^{w}/_{w}$ pluronic F127 55% $^{w}/_{w}$ PVP, (A)(2) pluronic F127, (A)(3) ciprofloxacin (A) (4) PVP poly(vinyl pyrolidone). (B) (1) Blank 50/27/55 - 25% $^{w}/_{w}$ pluronic F127 55% $^{w}/_{w}$ PVP (B) (2) 50/27/55 - 20% $^{w}/_{w}$ ciprofloxacin 25% $^{w}/_{w}$ pluronic F127 55% $^{w}/_{w}$ PVP (B) (3) ciprofloxacin. Å = Ångström length units (1 Ångström = 0.1 nm).

5.5 *S. aureus* SH1000 and cDNA library preparation for transcriptional profiling

To ascertain the transcriptional response of *S. aureus* SH1000 to nanoparticle formulated and solvent dissolved ciprofloxacin and the necessary controls, a range of concentrations and times of solution addition were tested (data not shown). To identify a growth profile that demonstrated the variance in growth imparted by each treatment while permitting the extraction of a high yield and quality of RNA. The addition of ciprofloxacin at 15.63 μg ml^{-1} either nanoparticle formulated, DMSO dissolved or equal volumes of control solutions as outlined in section 2.8.1 produced the growth profiles observed in Figures 5.5 A & B. The data in Figure 5.5 A demonstrated a reduction in the growth rate of *S. aureus* SH1000 when ciprofloxacin was present, with marginal reductions in growth rate observed when nanoparticle formulated ciprofloxacin was used compared with DMSO dissolved ciprofloxacin. The kill curve data presented in Figure 5.5 B showed a reduction in the viable cell numbers when ciprofloxacin was present with reduced survival observed when the cells were treated with nanoparticle ciprofloxacin compared with DMSO dissolved ciprofloxacin. Slight reductions in recovered cell numbers were counted when the cells were treated with DMSO and blank nanoparticles.

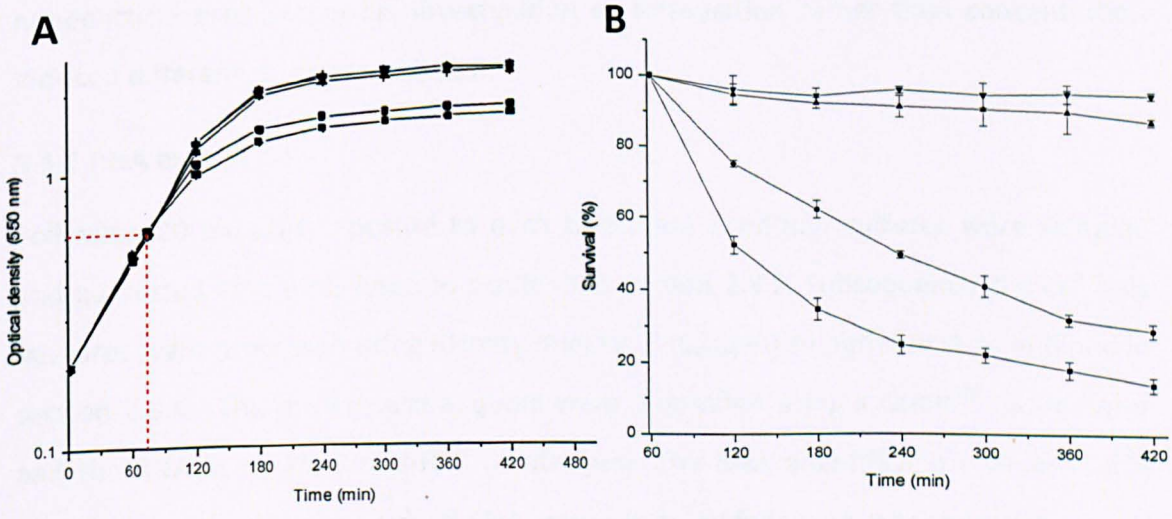

Figure 5.5. Culture preparation for transcriptional profiling analysis. (A) An overnight culture of *S. aureus* SH1000 was used to inoculate conical flasks containing 50 ml BHI to $O.D_{550}$ 0.2 and incubated at 37°C with shaking until the $O.D_{550}$ reached ~0.6. To each flask equal volumes and concentrations of nanoparticle formulated ciprofloxacin (■), (50.27.55), ciprofloxacin dissolved in DMSO (●), blank nanoparticle (▼), DMSO (▲) or ddH_2O (◆) were added to each mid-exponential phase culture (marked by the red dotted line). Following 20 min exposure to each treatment condition a sample of

culture was taken and processed to extract RNA. (B) Percentage re-growth of *S. aureus* SH1000 compared to the ddH_2O treated cells. Test conditions and figure symbols as outlined in 5.5 A. The values from each treatment and control culture are the mean of three experiments. Error bars indicate standard errors of the mean and are within the symbols.

The use of equal concentrations of ciprofloxacin in both nanoparticle and DMSO dissolved tests permitted the investigation of formulation rather than concentration induced effects on the transcriptome of *S. aureus* SH1000. However, as observed in Table 4.3 the formulation of ciprofloxacin into nanoparticles caused a reduction in MBC value compared to the DMSO dissolved ciprofloxacin treated cells. The observed MBC values were 31.25 $\mu g\ ml^{-1}$ and 62.5 $\mu g\ ml^{-1}$ respectively. An alternative method, could have investigated the transcriptional response of *S. aureus* to half the respective MBC values for each formulation. This would have permitted the investigation of each formulation at comparative levels of imposed ciprofloxacin induced inhibition on *S. aureus*. However, it was determined that comparison of each formulation at equal concentrations, despite imposing differing levels of inhibition, would provide a greater insight into the mechanisms that allowed for enhanced efficacy associated with the nanoparticle preparation *i.e.* investigation of formulation rather than concentration induced differences on transcription.

5.5.1 RNA extraction

Following 20 minutes exposure to each treatment condition cultures were sampled and harvested cells were lysed as outlined in section 2.8.2. Subsequently the cell lysis mixtures were processed using RNeasy mini kit™ (Qiagen) to purify RNA as outlined in section 2.8.4. The nucleic acid aliquots were quantified using a Qubit™ fluorometer and the RNA assay kit Quant-iT™ (Invitrogen). The RNA quantification values (Table 5.1.) suggested sufficient yields of RNA were extracted following cell treatment.

Table 5.1. Quantification of extracted RNA from *S. aureus* SH1000 following various ciprofloxacin and control treatments, using a Qubit™ fluorometer and the RNA assay kit Quant-iT™ (Invitrogen).

***S. aureus* SH1000 RNA extract**	**Replicate**	**Calculated RNA concentration***
Nanoparticle ciprofloxacin (50.27.55)	1	254
	2	389
	3	423
DMSO dissolved ciprofloxacin	1	787
	2	471
	3	398
Blank nanoparticle	1	749
	2	404
	3	936
DMSO	1	823
	2	978
	3	828
Uninhibited	1	702
	2	421
	3	854

*(ng μl^{-1}), eluted in 50 µl

5.5.2 DNaseI treatment of extracted RNA

Following RNA extraction and confirmation that sufficient yield was obtained from each sample (Table 5.1), DNA was removed using rDNaseI (Ambion) as outlined in section 2.8.5. RNA integrity was measured using a 2100 Bioanalyzer (Agilent) (Fig. 5.6 and Table 5.2) and quantified using a Qubit™ fluorometer (Invitrogen) (Table 5.2). DNase treatment resulted in the removal of genomic DNA and strong bands of RNA were visible in the electrophoresis gels of the cleaned-up RNA (Fig 5.6). The concentration of RNA ranged from 136 – 2000 ng μl^{-1} within the samples. The 23/16S rRNA ratios, the RNA integrity values and flat base-lines observed in the Bioanalyzer traces (data not shown), together provide an indication of the RNA preparation quality, that were considered sufficient to allow progression to the mRNA enrichment process.

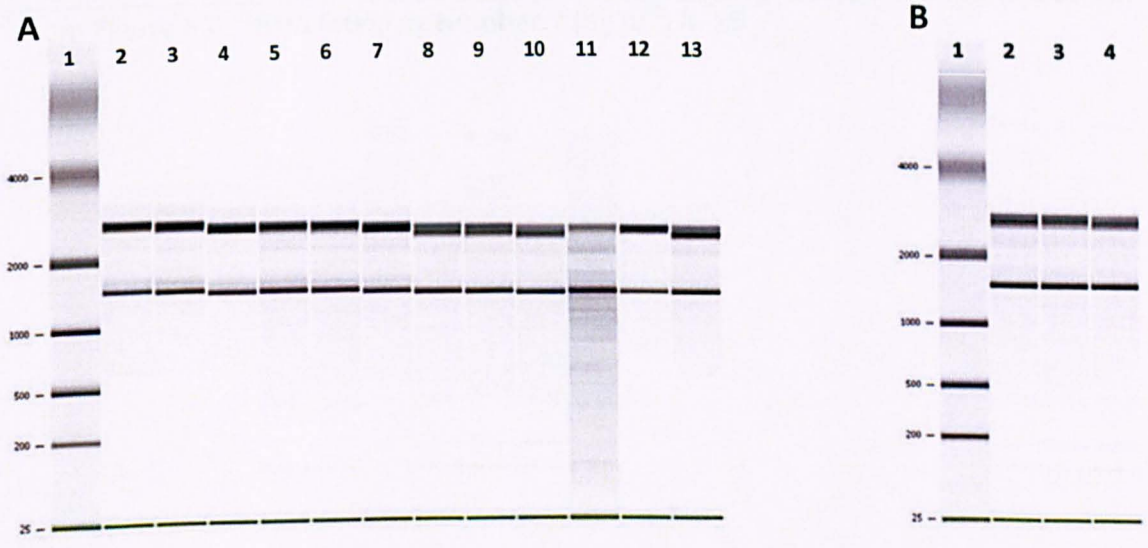

Figure 5.6. Bioanalyzer (Agilent) electrophoresis analysis of DNaseI treated RNA extracts.

A. Lane 1 – ladder, Lanes 2 to 4 – DNaseI treated RNA extracted from nanoparticle (20% $^{w}/_{w}$ ciprofloxacin 55% $^{w}/_{w}$ PVP 25% $^{w}/_{w}$ pluronic F127 - 50.27.55) exposed *S. aureus* SH1000, Lanes 5 to 7 - DNaseI treated RNA extracted from DMSO dissolved ciprofloxacin exposed *S. aureus* SH1000, Lanes 8 to 10 - DNaseI treated RNA extracted from blank nanoparticle (55% $^{w}/_{w}$ PVP 25% $^{w}/_{w}$ pluronic F127) exposed *S. aureus* SH1000, Lanes 11 to 13 - DNaseI treated RNA extracted from DMSO exposed *S. aureus* SH1000. **B.** Lane 1 – ladder, Lanes 2 to 4 DNaseI treated RNA extracted from uninhibited *S. aureus* SH1000.

Table 5.2. Bioanalyzer (Agilent) electrophoresis of DNaseI treated RNA extracts, 23/16S rRNA ratio, RNA integrity number (RIN) and RNA quantification of extracts using a Qubit™ fluorometer.

***S. aureus* SH1000 RNA extract**	**Gel lane [a]**	**23/16S rRNA Ratio**	**RIN [b]**	**Calculated RNA concentration [c]**
Nanoparticle ciprofloxacin (50.27.55)	2	1.6	10	617
	3	1.3	10	274
	4	1.6	10	353
DMSO dissolved ciprofloxacin	5	1.2	9.6	652
	6	1.4	9.9	604
	7	1.5	10	136
Blank nanoparticle	8	1.6	9.9	883
	9	1.3	10	1100
	10	1.4	10	608
DMSO	11	1.6	10	2000
	12	1.3	9.2	641
	13	1.4	9.8	653
Uninhibited	B2	1.5	9.7	406
	B3	1.3	9.5	592
	B4	1.3	9.6	761

[a] From Figure 5.6. [b] RNA Integrity Number. [c] (ng μl^{-1}) in 15 µl.

5.5.3 mRNA enrichment of total RNA samples

The selective depletion of abundant 16S and 23S ribosomal RNA molecules from total RNA is required in the process of cDNA library construction. mRNA enrichment was conducted using the Microb*express*™ kit (Ambion) as outlined in section 2.8.6, which employs a modified sandwich capture hybridisation method for the recovery of specific nucleic acid molecules. The results presented in Figure 5.7 and Table 5.3 indicated that sufficient rRNA was depleted from the majority of samples as demonstrated by the loss of banding associated with these nucleic acid molecules on the electrophoresis traces and subsequent reduction in the 23/16S rRNA ratio. However, lanes 2, 3, 4 (50.27.55 treated), 8 (blank nanoparticle treated) and 11 (DMSO treated) extracts were not sufficiently rRNA depleted indicated by the remaining clear bands on the electrophoresis trace (Fig 5.7) and the high 23/16S rRNA ratios (Table 5.3). These samples were therefore processed through a second round of mRNA enrichment in which sufficient rRNA depletion was achieved (Fig 5.8 and Table 5.4). With satisfactory mRNA enrichment, equal concentrations of samples from each treatment group were pooled.

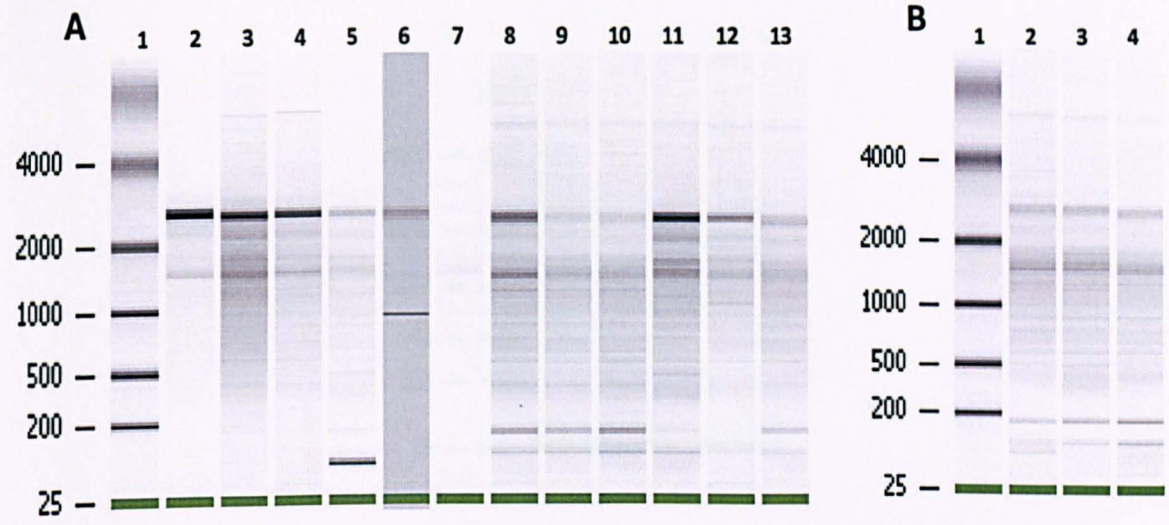

Figure 5.7. Bioanalyzer (Agilent) electrophoresis analysis of mRNA enriched RNA extracts.

A. Lane 1 – ladder, Lanes 2 to 4 – mRNA enriched RNA extracted from nanoparticle (20% $^{w}/_{w}$ ciprofloxacin 55% $^{w}/_{w}$ PVP 25% $^{w}/_{w}$ pluronic F127 - 50.27.55) exposed *S. aureus* SH1000, Lanes 5 to 7 - mRNA enriched RNA extracted from DMSO dissolved ciprofloxacin exposed *S. aureus* SH1000, Lanes 8 to 10 - mRNA enriched RNA extracted from blank nanoparticle (55% $^{w}/_{w}$ PVP 25% $^{w}/_{w}$ pluronic F127) exposed *S. aureus* SH1000, Lanes 11 to 13 - mRNA enriched RNA extracted from DMSO exposed *S. aureus* SH1000. **B.** Lane 1 – ladder, Lanes 2 to 4 mRNA enriched RNA extracted from uninhibited *S. aureus* SH1000.

Table 5.3. Bioanalyzer (Agilent) electrophoresis of mRNA enriched RNA extracts, 23/16S rRNA ratio and quantification of extracts using a Qubit™ fluorometer.

***S. aureus* SH1000 RNA extract**	**Gel lane [a]**	**23/16S rRNA Ratio**	**Calculated RNA concentration [b]**
Nanoparticle ciprofloxacin (50.27.55)	2	8.6	88.3
	3	4.2	31
	4	4.5	28.6
DMSO dissolved ciprofloxacin	5	1.3	43.1
	6	0.1	78.6
	7	0	5.97
Blank nanoparticle	8	1.8	45.5
	9	0.3	26.3
	10	0.4	29.2
DMSO	11	5.1	49.5
	12	1.5	40.9
	13	0.8	40.3
Uninhibited	B2	1.2	35
	B3	1.6	43.4
	B4	1.3	25.5

[a] From Figure 5.7. [b] (ng μl^{-1}) in 10 μl.

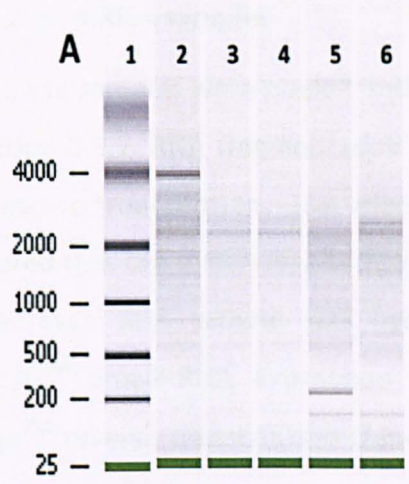

Figure 5.8. Bioanalyzer (Agilent) electrophoresis analysis of mRNA enriched RNA extracts.

Lane 1 – ladder, Lanes 2 to 4 – mRNA enriched RNA extracted from nanoparticle (20% $^{w}/_{w}$ ciprofloxacin 55% $^{w}/_{w}$ PVP 25% $^{w}/_{w}$ pluronic F127 - 50.27.55) exposed *S. aureus* SH1000, Lane 5 - mRNA enriched RNA extracted from blank nanoparticle (55% $^{w}/_{w}$ PVP 25% $^{w}/_{w}$ pluronic F127) exposed *S. aureus* SH1000, Lane 6 - mRNA enriched RNA extracted from DMSO exposed *S. aureus* SH1000.

Table 5.4. Bioanalyzer (Agilent) electrophoresis of repeated mRNA enrichment from RNA extracts, 23/16S rRNA ratio and quantification of extracts using a Qubit™ fluorometer.

***S. aureus* SH1000 RNA extract**	**Gel lane [a]**	**23/16S rRNA Ratio**	**Calculated RNA concentration [b]**
Nanoparticle ciprofloxacin	2	0	40.5
	3	0	19.4
	4	0	18.3
Blank nanoparticle	5	0	36.5
DMSO	6	0	29.1

[a] From Figure 5.8. [b] (ng μl^{-1}) in 10 μl.

5.5.4 Fragmentation of enriched mRNA samples

Following mRNA enrichment, the samples were pooled and fragmented using RNase III (Ambion) as outlined in section 2.8.7. RNA fragmentation improves the hybridization kinetics associated with reverse-transcription. The electrophoresis gel and trace images (Fig 5.9 A & B) indicated that the mRNA was sufficiently fragmented. Following sample clean-up, 90 ng of each RNA sample was hybridized and ligated using components from the SOLiD™ Small RNA Expression Kit (Ambion) and reverse transcribed using ArrayScript™ reverse transcriptase (Ambion) as outlined in section 2.8.8.

5.5.5 Size selection and amplification of cDNA

The cDNA products resulting from reverse transcription were size selected on Novex® 6% TBE-Urea 1 mM gels (Invitrogen) as outlined in section 2.8.9 and gel material containing 100-200 nt DNA was excised as shown in Figure 5.10. The selected gel material was split vertically into 4 pieces using a sterile scalpel blade. Subsequently, two PCR reactions were prepared for each sample and one excised gel piece transferred to each as outlined in section 2.8.10. The thermal cycling conditions used for cDNA amplification are outlined in Table 2.3. Bioanalyzer traces of the size selected and amplified cDNA products from each treatment sample are presented in Figure 5.11 and display a narrow nucleic acid size distribution, mostly in the 100 – 200 nt size range and low levels of background scatter. The Liverpool Centre for Genomic Research performed template bead preparation with the amplified cDNA, library quantification and sample sequencing using a SOLiD™ 3 Plus System as outlined in 2.8.11.

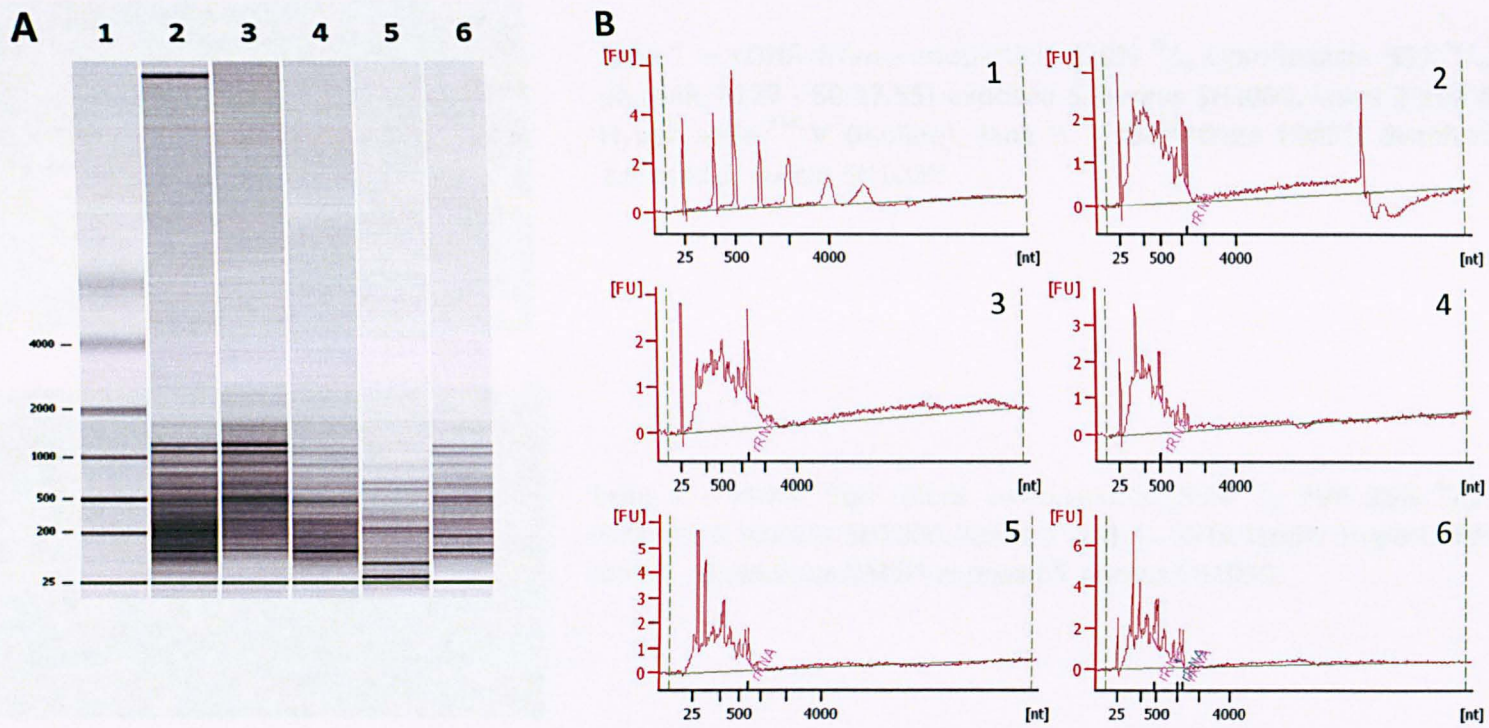

Figure 5.9. A. Lane 1 – ladder, Lane 2 – fragmented mRNA from nanoparticle (20% $^{w}/_{w}$ ciprofloxacin 55% $^{w}/_{w}$ PVP 25% $^{w}/_{w}$ pluronic F127 - 50.27.55) exposed *S. aureus* SH1000, Lane 3 - fragmented mRNA extracted from DMSO dissolved ciprofloxacin exposed *S. aureus* SH1000, Lane 4 - fragmented mRNA extracted from DMSO exposed *S. aureus* SH1000, Lane 5 - fragmented mRNA extracted from blank nanoparticle (55% $^{w}/_{w}$ PVP 25% $^{w}/_{w}$ pluronic F127) exposed *S. aureus* SH1000, Lane 6 - fragmented mRNA extracted from uninhibited *S. aureus* SH1000.

Figure 5.9. B. Graph 1 – ladder, Graph 2 – fragmented mRNA from nanoparticle (20% $^{w}/_{w}$ ciprofloxacin 55% $^{w}/_{w}$ PVP 25% $^{w}/_{w}$ pluronic F127 - 50.27.55) exposed *S. aureus* SH1000, Graph 3 - fragmented mRNA extracted from DMSO dissolved ciprofloxacin exposed *S. aureus* SH1000, Graph 4 - fragmented mRNA extracted from DMSO exposed *S. aureus* SH1000, Graph 5 - fragmented mRNA extracted from blank nanoparticle (55% $^{w}/_{w}$ PVP 25% $^{w}/_{w}$ pluronic F127) exposed *S. aureus* SH1000, Graph 6 - fragmented mRNA extracted from uninhibited *S. aureus* SH1000.

A

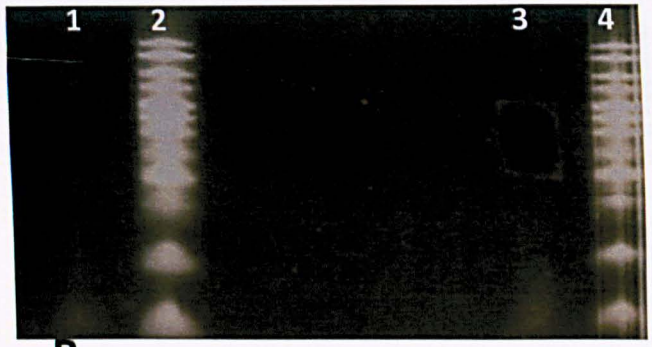

Lane 1 – cDNA from nanoparticle (20% $^{w}/_{w}$ ciprofloxacin 55% $^{w}/_{w}$ PVP 25% $^{w}/_{w}$ pluronic F127 - 50.27.55) exposed *S. aureus* SH1000, lanes 2 and 4 - DNA ladder HyperLadder™ V (Bioline), lane 3 - cDNA from DMSO dissolved ciprofloxacin exposed *S. aureus* SH1000.

B

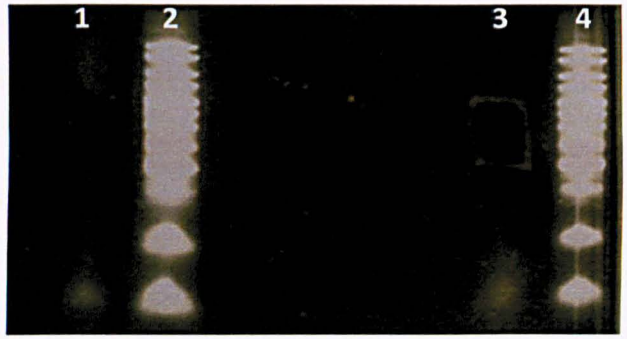

Lane 1 – cDNA from blank nanoparticle (55% $^{w}/_{w}$ PVP 25% $^{w}/_{w}$ Pluronic F127) exposed *S. aureus* SH1000, lanes 2 and 4 - DNA ladder HyperLadder™ V (Bioline), lane 3 - cDNA from DMSO exposed *S. aureus* SH1000.

C

Lane 1 – cDNA from uninhibited *S. aureus* SH1000, lane 2 - DNA ladder HyperLadder™ V (Bioline).

Figure 5.10 Size selection of cDNA product containing 100-200 nt material on Novex® 6% TBE-Urea 1 mM gels (Invitrogen).

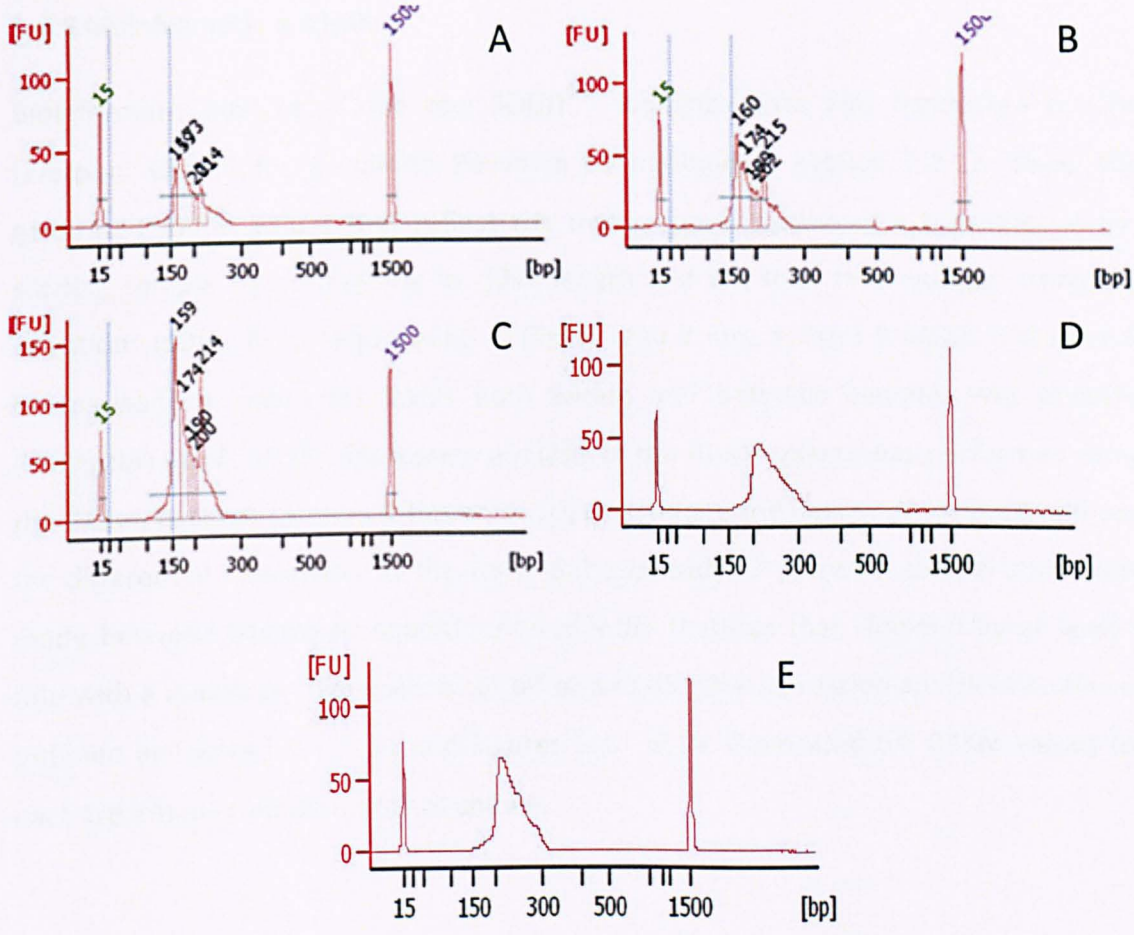

Figure 5.11. Size selected and amplified cDNA from: (A) nanoparticle (20% $^{w}/_{w}$ ciprofloxacin 55% $^{w}/_{w}$ PVP 25% $^{w}/_{w}$ pluronic F127 - 50.27.55) exposed *S. aureus* SH1000, (B) - DMSO dissolved ciprofloxacin exposed *S. aureus* SH1000, (C) - DMSO exposed *S. aureus* SH1000, (D) - blank nanoparticle (55% $^{w}/_{w}$ PVP 25% $^{w}/_{w}$ pluronic F127) exposed *S. aureus* SH1000, (E) - uninhibited *S. aureus* SH1000.

5.5.6 Bioinformatic analysis

Bioinformatic analysis of the raw SOLiD™ sequence data was conducted by The Liverpool Centre for Genomics Research as outlined in section 2.8.12. Using the generated RPKM values that reflect the molar concentration of a transcript in the starting sample by normalising for RNA length and the total read number using the equation: (10^9 x Exon read count) / (Total read count x Exon length), transparent comparisons of transcript levels both within and between samples was possible (Mortazavi *et al.*, 2008). Expression analysis of the RPKM values was performed using the DESeq package (Anders & Huber, 2010) to estimate the degree of variance and test for differential expression in the data. Subsequently, 7 pairwise comparisons were made between treatment conditions to identify features that changed by at least 2 fold with a maximum significance cut off at p=0.05. The expression analysis results are outlined in Tables 5.5 – 5.21 and Figures 5.12 -5.19. Generated full RPKM values for each treatment condition are not shown.

5.6 Comparisons of differential expression between treatment groups

5.6.1 Transcriptional response of *S. aureus* SH1000 to ciprofloxacin – comparisons of nanoparticle, DMSO dissolved ciprofloxacin and untreated cells.

At 20 minutes post treatment, 37 and 109 transcripts were significantly ($P \leq 0.05$) up and down regulated ≥2 fold, respectively, for nanoparticle ciprofloxacin treated compared with untreated cells (Tables 5.5, 5.6 and Fig 5.12). For DMSO dissolved ciprofloxacin compared with untreated cells, 31 and 107 transcripts were up and down regulated respectively (Tables 5.7, 5.8 and Fig 5.13). Common features both up and down regulated in nanoparticle ciprofloxacin and DMSO dissolved ciprofloxacin treated cells compared with untreated cells, accounted for 67% of the features identified as significant (Tables 5.5, 5.6, 5.7 and 5.8). Ciprofloxacin induced the expression of a variety of genes involved in DNA repair and replication, the majority of which were shared between treatment types. In particular: SAOUHSC_01363 a UmuC-like DNA damage repair protein, and the positive and negative regulators of the SOS response: SAOUHSC_01333 (*lexA*) the lexA repressor and SAOUHSC_01262 (*recA*) recombinase A, were all up-regulated with similar fold changes between treatments.

Ciprofloxacin induces double-stranded DNA breaks and stalled replication forks, which are processed to single stranded DNA. RecA forms filaments on the single stranded DNA and facilitates recombinational repair and binds the SOS gene repressor LexA, stimulating auto-proteolysis. This cleavage inactivates the LexA repressor and results in the induction of the SOS genes (Michel, 2005 ; Cirz *et al.*, 2007). In addition several genes that encode proteins involved in DNA metabolism are also part of the LexA regulon, including *uvrA* and *uvrB* that encode two subunits of the nucleotide excision repair (NER) endonuclease and they are co-transcribed and regulated via LexA binding to the *uvrB* promoter (Zou *et al.*, 2004 ; Cirz *et al.*, 2007). SAOUHSC_01342 (*sbcC*) and SAOUHSC_01341 (*sbcD*) are LexA regulated and encode the exonucleases SbcC and SbcD which process stalled replication forks (Connelly *et al.*, 1998).

Interestingly however, the DNA gyrase genes (*gyrA* and *gyrB*) were not shown to be significantly differentially expressed using the criteria outlined, in any treatment including ciprofloxacin. In the proposed mechanism of quinolone mode of action as

outlined in section 1.8.5 and Figure 1.6, DNA gyrase are thought to be primary targets for ciprofloxacin. This result may represent experimental variability; for example time of exposure and concentration of ciprofloxacin used to treat the cells.

The results presented in Table 5.9 compare the up-regulated features associated with DNA repair and replication identified in this study and those obtained by Cirz *et al.* (2007) when investigating the transcriptional response of *S. aureus* 8325 to ciprofloxacin in a microarray study. It is important to note however that the test conditions differ from those outlined in this work: water soluble ciprofloxacin HCl was added to early log phase *S. aureus* 8325 cultures (0.5 to 0.6 OD_{600}) at 0.8 $\mu g\ ml^{-1}$ and cells harvested at 30 min and 120 min post ciprofloxacin HCl addition. The up regulated features identified in this study at 20 min post ciprofloxacin addition either DMSO dissolved or nanoparticle formulated correlate well with the features that are classified as significant (≥2 fold change) at 30 min post ciprofloxacin addition in the Cirz *et al.* (2007) study. The genes *uvrB*, *uvrA*, *recA*, *lexA*, *sbcD* and the UmuC-like DNA damage repair feature SAOUHSC_01363 displayed up regulation in both studies. Although *dnaA* and *dnaN* displayed ≥2-fold change in RPKM value in each test condition, they were not considered statistically significant. Cirz *et al.* (2007) indicated that these features were down regulated at 30 min and displayed ≥2 fold up regulation at 120 min. Interestingly, the excinuclease ABC, B subunit (SAOUHSC_00776) and *sbcC* were shown to be up regulated ≥2 fold in this study but not in the Cirz *et al.* (2007) investigation at 30 min or 120 min. This is possibly explained by the different concentrations of ciprofloxacin or delivery methods used. Another noticeable feature identified in Table 5.9 was the similarity in the degree of up regulation between ciprofloxacin target genes and the delivery methods used in this study. However, two exceptions were identified. *nusA* was only shown to be up regulated (3.59 fold) in the pairwise comparison between nanoparticle formulated ciprofloxacin and blank nanoparticle treated cells. *sbcC* was shown to be up regulated (6.06 fold) in the DMSO dissolved ciprofloxacin compared with untreated cells however it was not identified as a statistically significant change. Whereas *sbcC* was considered statistically significantly up regulated in all other treatments containing ciprofloxacin. The degree of similarity in the fold changes observed in DNA repair and replication features, suggested that

ciprofloxacin delivery methods did not induce significant differential molecular targeting in known ciprofloxacin target genes. In addition to the common up-regulation of DNA repair and replication features in both delivery methods, similarities were observed in antibiotic resistance and virulence factor functional groups, such as SAOUHSC_01944 a probable beta-lactamase.

In the pairwise comparison between nanoparticle formulated ciprofloxacin and untreated cells, the antibiotic resistance associated feature, SAOUHSC_02418 that shares 100% homology with the EmrB and QacA subfamily in *S. aureus* JKD6008 and has a known function of drug resistance via transport processes was shown to be up regulated. QacA is a plasmid encoded multidrug efflux protein in *S. aureus* that confers high levels of resistance to commonly used antimicrobial agents (Hassan *et al.*, 2009). EmrB is a membrane protein with homology to the major facilitator super-family (MFS) transporters that couple the high energy stored in a cation gradient to the transport of molecules across the membranes of Gram-negative bacteria (Tanabe *et al.*, 2009). Also, the up regulation of the virulence associated cofactor staphylocoagulase (SAOUHSC_00192) that activates prothrombin and is linked to the initiation of blood clotting in the bacterial host, was identified (Friedrich *et al.*, 2003).

Similarities in the transcriptional down-regulation of genes between ciprofloxacin delivery methods were also observed (Tables 5.6 and 5.8) from a range of functional groups. These included the antibiotic resistance feature, SAOUHSC_01285 (*femC)* that is associated with resistance to meticillin (Gustafson *et al.*, 1994). Genes involved in a range of metabolic processes were identified, including those associated with electron transport, energy metabolism, co-factor and fatty acid metabolism; a large number of these genes were down regulated in both nanoparticle and DMSO dissolved ciprofloxacin treated cells, with 63% similarity between the treatment groups. No groupings of metabolic pathways were identified as showing differences when comparing features that were unique to individual treatments. Virulence factors mostly associated with capsular polysaccharides (*capB, C, D, E, H, J, K, L, N*) that reduce antigenic recognition and carotenoid biosynthesis features were also found to be down regulated. Most *S. aureus* strains produce one type of capsular polysaccharide belonging to either type 5 or type 8, which contributes to the pathogenesis of the

organism. The genes are organised as an operon in which the polycistronic message is controlled primarily by the promoter located at the beginning of the operon. It has been reported that the induction of the DNA repair genes *sbcCD* also acts as a repressor of *cap5* capsular polysaccharide genes (Chen *et al.*, 2007). These results correlate well with the features observed in this study that show an up-regulation of the exonucleases *sbcC* and *sbcD* but repression of a whole range of type 5 capsule production genes in both ciprofloxacin delivery methods. In the described model, activated RecA induced by the SOS response causes LexA to auto-cleave, depressing the SOS regulon inducing SbcCD. The increased SbcCD results in reduced capsular polysaccharide and repression of *cap5* promoter activity. These authors suggest two possible reasons for the repression of capsular polysaccharides by SOS induction: to save energy in order to perform DNA repair or to increase the adherence capability of *S. aureus*. The fibronectin binding protein gene *fnbB* has previously been shown to be repressed directly by LexA and is induced by the SOS response in the presence of ciprofloxacin. It is therefore likely that *fnbB* and *cap5* genes are regulated in a concomitant process upon induction of the SOS response to permit increased cell adherence and reduce the possibility of further cell interactions with DNA damaging agents, as a survival mechanism (Bisognano *et al.*, 2004 ; Chen *et al.*, 2007).

Table 5.5. *S. aureus* SH1000 genes up-regulated following treatment with nanoparticle formulated ciprofloxacin compared with untreated cells.

Group functions	*S. aureus* 8325 ORF	*S. aureus* 8325 Gene	*S. aureus* 8325 Gene Product	Fold Change Up Regulated	P-value
DNA Repair and Replication	SAOUHSC_00776		excinuclease ABC, B subunit	7.99	1.82E-03
	SAOUHSC_00779	*uvrB*	excinuclease ABC subunit B	7.04	2.45E-03
	SAOUHSC_00780	*uvrA*	excinuclease ABC subunit A	6.63	4.39E-03
	SAOUHSC_01262	*recA*	recombinase A	4.19	2.50E-02
	SAOUHSC_01333	*lexA*	lexA repressor	5.66	8.53E-03
	SAOUHSC_01341	*sbcD*	exonuclease SbcD	9.01	5.56E-04
	SAOUHSC_01342	*sbcC*	exonuclease SbcC	15.38	7.69E-05
	SAOUHSC_01363		DNA damage repair protein	64.20	1.82E-08
Antibiotic Resistance	SAOUHSC_01944		probable beta-lactamase	8.89	2.67E-02
	SAOUHSC_02418		drug resistance transporter, EmrB/QacA subfamily	4.14	1.99E-02
	SAOUHSC_02420		hypothetical protein	4.05	3.06E-02
Virulence factors	SAOUHSC_00192		staphylocoagulase	4.44	4.05E-02
	SAOUHSC_01365		deblocking aminopeptidase	8.57	1.14E-03

	SAOUHSC_01718		hypothetical protein	3.78	2.87E-02
	SAOUHSC_02313		K+-transporting ATPase	7.56	1.57E-02
	SAOUHSC_02416		hypothetical protein	3.96	3.34E-02
	SAOUHSC_02453		tagatose-6-phosphate kinase	8.00	1.30E-02
	SAOUHSC_02455	*lacA*	galactose-6-phosphate isomerase subunit LacA	5.43	1.61E-02
Hypothetical genes	SAOUHSC_00347		hypothetical protein	24.57	8.69E-06
	SAOUHSC_00409		hypothetical protein	5.95	9.19E-03
	SAOUHSC_00583		hypothetical protein	8.00	3.70E-02
	SAOUHSC_00825		hypothetical protein	5.85	6.28E-03
	SAOUHSC_01023		hypothetical protein	5.33	4.71E-02
	SAOUHSC_01139		hypothetical protein	3.53	3.56E-02
	SAOUHSC_01340		hypothetical protein	3.46	4.82E-02
	SAOUHSC_01334		hypothetical protein	49.42	8.93E-08
	SAOUHSC_01343		hypothetical protein	13.27	1.88E-04
	SAOUHSC_01344		hypothetical protein	20.44	5.63E-04
	SAOUHSC_01976		hypothetical protein	5.33	4.44E-02

	SAOUHSC_02002	hypothetical protein	4.14	1.91E-02
	SAOUHSC_02141	hypothetical protein	12.44	9.08E-03
	SAOUHSC_02144	hypothetical protein	34.50	1.01E-06
	SAOUHSC_02157	hypothetical protein	6.28	5.24E-03
	SAOUHSC_02294	hypothetical protein	6.88	2.96E-03
	SAOUHSC_02419	hypothetical protein	3.57	4.54E-02
	SAOUHSC_02424	hypothetical protein	4.08	2.76E-02
	SAOUHSC_02734	hypothetical protein	23.11	1.08E-03

Table 5.6 *S. aureus* SH1000 genes down-regulated following treatment with nanoparticle formulated ciprofloxacin compared with untreated cells.

Group functions	*S. aureus* 8325 ORF	*S. aureus* 8325 Gene	*S. aureus* 8325 Gene Product	Fold Change Down Regulated	P-value
Antibiotic resistance	SAOUHSC_01285	*femC*	factor involved in meticillin resistance	9.54	6.51E-04
	SAOUHSC_01948	*bcrA*	bacitracin transport ATP-binding protein bcrA	6.88	1.92E-03
Virulence factors	SAOUHSC_00114		capsular polysaccharide biosynthesis protein	9.88	5.02E-04
	SAOUHSC_00115	*capB*	capsular polysaccharide synthesis enzyme Cap5B	6.43	9.94E-03

	SAOUHSC_00116	*capC*	capsular polysaccharide synthesis enzyme Cap8C	8.36	3.44E-03
	SAOUHSC_00117	*capD*	capsular polysaccharide biosynthesis protein Cap5D	5.40	1.37E-02
	SAOUHSC_00118	*capE*	capsular polysaccharide biosynthesis protein Cap5E	4.08	4.76E-02
	SAOUHSC_00122	*capI*	capsular polysaccharide biosynthesis protein Cap5I	4.09	3.73E-02
	SAOUHSC_00123	*capJ*	capsular polysaccharide biosynthesis protein Cap5J	3.78	4.85E-02
	SAOUHSC_00127	*capN*	cap5N protein/UDP-glucose 4-epimerase	3.62	4.19E-02
	SAOUHSC_02466		truncated MHC class II analog protein	5.44	1.92E-02
	SAOUHSC_02669	*sarZ*	transcriptional regulator SarZ	6.77	2.81E-03
Stress response	SAOUHSC_02862	*clpC*	ATP-dependent Clp protease, ATP-binding subunit ClpC	7.50	3.02E-03
Cell division	SAOUHSC_00994		bifunctional autolysin	3.22	4.89E-02
	SAOUHSC_00736		hypothetical protein	3.18	4.68E-02
Protein synthesis					
Lantibiotic synthesis	SAOUHSC_01420		lantibiotic precursor	3.34	4.66E-02

	SAOUHSC_01947		hypothetical protein	5.37	1.31E-02
	SAOUHSC_01949		intracellular serine protease	6.19	1.09E-02
Carotenoid biosynthesis	SAOUHSC_01990		squalene desaturase	5.30	2.01E-02
	SAOUHSC_02881		hypothetical protein	6.53	6.37E-03
	SAOUHSC_02882		hypothetical protein	12.50	2.71E-04
Miscellaneous	SAOUHSC_00624		integrase/recombinase	4.78	8.87E-03
Metabolism	SAOUHSC_00187		formate acetyltransferase	5.87	3.47E-03
	SAOUHSC_00188		pyruvate formate-lyase 1 activating enzyme	3.46	3.78E-02
	SAOUHSC_00281		formate/nitrite transporter family protein	8.91	4.89E-04
	SAOUHSC_00285		ABC transporter permease protein	5.14	6.16E-03
	SAOUHSC_00287		ABC transporter ATP-binding protein	3.56	3.16E-02
	SAOUHSC_00608	*adhA*	alcohol dehydrogenase	5.06	1.27E-02

SAOUHSC_00634		manganese/iron transport system substrate-binding protein	3.54	4.18E-02
SAOUHSC_00637		manganese/iron transport system ATP-binding protein	3.44	4.66E-02
SAOUHSC_00706		hypothetical protein	3.95	2.79E-02
SAOUHSC_00707		fructose 1-phosphate kinase	4.22	2.05E-02
SAOUHSC_00708		fructose specific permease	3.42	4.56E-02
SAOUHSC_00738		proton-dependent Peptide Transporters	3.85	2.77E-02
SAOUHSC_00749		hypothetical protein	4.26	1.37E-02
SAOUHSC_00797	*tpiA*	triosephosphate isomerase	3.41	3.71E-02
SAOUHSC_00899		argininosuccinate synthase	4.50	2.67E-02
SAOUHSC_00923		hypothetical protein	5.20	2.08E-02
SAOUHSC_01013		phosphoribosylformylglycinamidine synthase II	4.81	2.10E-02
SAOUHSC_01014		amidophosphoribosyl transferase	4.31	3.08E-02
SAOUHSC_01016		phosphoribosylglycinamide formyltransferase	4.90	1.57E-02

SAOUHSC_01165		uracil permease	5.88	3.32E-03
SAOUHSC_01166	*pyrB*	aspartate carbamoyltransferase catalytic subunit	6.56	2.02E-03
SAOUHSC_01168	*pyrC*	dihydroorotase	5.85	3.65E-03
SAOUHSC_01169		carbamoyl phosphate synthase small subunit	5.71	4.04E-03
SAOUHSC_01170	*carB*	carbamoyl phosphate synthase large subunit	4.80	8.37E-03
SAOUHSC_01171		orotidine 5'-phosphate decarboxylase	3.46	3.34E-02
SAOUHSC_01172	*pyrE*	orotate phosphoribosyltransferase	4.06	1.74E-02
SAOUHSC_01275		hypothetical protein	3.72	3.37E-02
SAOUHSC_01278		aerobic glycerol-3-phosphate dehydrogenase	3.83	2.90E-02
SAOUHSC_01369		dihydrodipicolinate reductase	5.63	4.41E-02
SAOUHSC_01418	*sucA*	2-oxoglutarate dehydrogenase E1 component	3.57	3.93E-02
SAOUHSC_01884		proline dehydrogenase	4.76	2.11E-02
SAOUHSC_01991		ABC transporter permease	4.50	2.67E-02
SAOUHSC_02119		high affinity proline permease	3.58	3.91E-02

SAOUHSC_02270	ammonium transporter	15.75	4.08E-03
SAOUHSC_02387	hypothetical protein	3.57	2.84E-02
SAOUHSC_02400	PTS system mannitol-specific protein	4.19	3.43E-02
SAOUHSC_02402	PTS system mannitol-specific transporter subunit IIA	5.24	7.53E-03
SAOUHSC_02403	mannitol-1-phosphate 5-dehydrogenase	4.97	9.85E-03
SAOUHSC_02412	hypothetical protein	3.61	3.76E-02
SAOUHSC_02444	BCCT family osmoprotectant transporter	5.44	5.86E-03
SAOUHSC_02468	acetolactate synthase, catabolic	3.89	2.13E-02
SAOUHSC_02610	formimidoylglutamase	3.85	2.38E-02
SAOUHSC_02648	L-lactate permease	6.02	5.36E-03
SAOUHSC_02681	nitrate reductase, alpha subunit	5.40	2.07E-02
SAOUHSC_02684	assimilatory nitrite reductase [NAD(P)H] large subunit	4.08	4.76E-02
SAOUHSC_02772	glutamate dehydrogenase / hypothetical	4.19	1.82E-02
SAOUHSC_02830	D-lactate dehydrogenase	7.75	1.06E-03

	SAOUHSC_02836	phosphinothricin N-acetyltransferase	6.67	4.02E-03
	SAOUHSC_02848	PTS system glucose-specific transporter subunit IIABC	3.98	2.32E-02
	SAOUHSC_02875	D-lactate dehydrogenase	4.78	3.28E-02
Hypothetical genes				
	SAOUHSC_00065	hypothetical protein	3.54	3.12E-02
	SAOUHSC_00146	hypothetical protein	4.50	1.40E-02
	SAOUHSC_00257	hypothetical protein	3.53	3.00E-02
	SAOUHSC_00356	hypothetical protein	4.44	1.49E-02
	SAOUHSC_00358	hypothetical protein	4.19	2.14E-02
	SAOUHSC_00561	hypothetical protein	3.28	3.98E-02
	SAOUHSC_00619	hypothetical protein	3.33	4.25E-02
	SAOUHSC_00808	hypothetical protein	4.05	3.88E-02
	SAOUHSC_00820	hypothetical protein	4.47	1.64E-02
	SAOUHSC_00821	hypothetical protein	3.67	2.72E-02
	SAOUHSC_00826	hypothetical protein	8.56	7.34E-04
	SAOUHSC_00828	hypothetical protein	4.22	3.33E-02
	SAOUHSC_00962	hypothetical protein	14.00	7.02E-05

SAOUHSC_01024	hypothetical protein	5.57	4.62E-03
SAOUHSC_01403	hypothetical protein	2.90	2.30E-02
SAOUHSC_01458	hypothetical protein	3.43	4.66E-02
SAOUHSC_01819	hypothetical protein	4.76	1.35E-02
SAOUHSC_01945	hypothetical protein	4.99	1.09E-02
SAOUHSC_01987	hypothetical protein	3.46	4.51E-02
SAOUHSC_02332	hypothetical protein	4.46	1.39E-02
SAOUHSC_02391	hypothetical protein	4.41	1.70E-02
SAOUHSC_02401	mannitol operon activator, BglG family	5.94	4.11E-03
SAOUHSC_02442	hypothetical protein	3.71	2.58E-02
SAOUHSC_02443	hypothetical protein	4.06	2.09E-02
SAOUHSC_02572	hypothetical protein	3.70	3.51E-02
SAOUHSC_02650	hypothetical protein	3.97	2.34E-02
SAOUHSC_02685	sirohydrochlorin ferrochelatase	6.75	9.53E-03
SAOUHSC_02781	hypothetical protein	4.45	1.80E-02
SAOUHSC_02853	hypothetical protein	2.88	4.80E-02

SAOUHSC_02876	hypothetical protein	4.00	5.00E-02
SAOUHSC_02880	hypothetical protein	4.07	3.76E-02
SAOUHSC_02925	hypothetical protein	5.48	1.72E-02
SAOUHSC_02930	hypothetical protein	6.90	1.59E-03
SAOUHSC_02950	hypothetical protein	9.00	2.45E-02
SAOUHSC_03032	hypothetical protein	6.75	8.81E-03
SAOUHSC_03035	hypothetical protein	4.72	9.06E-03
SAOUHSC_A00354	hypothetical protein	7.09	2.05E-03

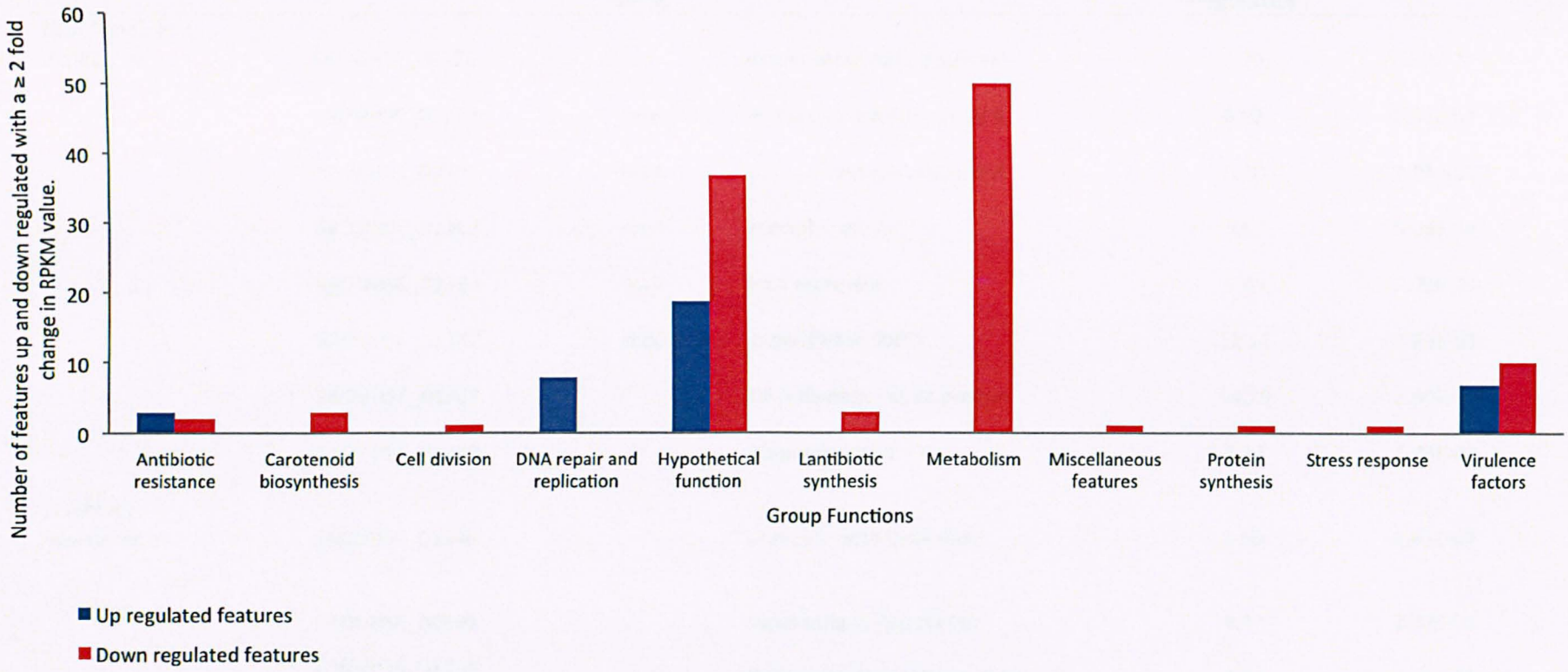

Figure 5.12 Number of features with a ≥ 2-fold change in RPKM value up and down regulated, following treatment with nanoparticle formulated ciprofloxacin compared with untreated cells.

Table 5.7 *S. aureus* SH1000 genes up-regulated following treatment with DMSO dissolved ciprofloxacin compared with untreated cells.

Group functions	*S. aureus* 8325 ORF	*S. aureus* 8325 Gene	*S. aureus* 8325 Gene Product	Fold Change Up Regulated	P-value
DNA Repair and Replication	SAOUHSC_00776		excinuclease ABC, B subunit	7.29	4.30E-04
	SAOUHSC_00779	*uvrB*	excinuclease ABC subunit B	6.83	6.35E-04
	SAOUHSC_00780	*uvrA*	excinuclease ABC subunit A	5.20	3.00E-03
	SAOUHSC_01262	*recA*	recombinase A	6.63	9.56E-04
	SAOUHSC_01333	*lexA*	lexA repressor	5.49	2.25E-03
	SAOUHSC_01342	*sbcC*	exonuclease SbcC	12.15	1.89E-05
	SAOUHSC_01363		DNA-damage repair protein	54.28	1.60E-10
	SAOUHSC_01443		ribonuclease HI	4.74	1.76E-02
Antibiotic Resistance	SAOUHSC_01944		probable beta-lactamase	7.99	2.43E-02
Virulence	SAOUHSC_00399		superantigen-like protein	4.77	1.72E-02
	SAOUHSC_02313		K+-transporting ATPase, F subunit	4.89	3.21E-02
Protein synthesis	SAOUHSC_01651		50S ribosomal protein L33	3.19	9.70E-03
Metabolism	SAOUHSC_00743	*nrdF*	ribonucleotide-diphosphate reductase subunit beta	3.01	5.57E-04
	SAOUHSC_01365		hypothetical protein	7.67	3.20E-04

Hypothetical genes	SAOUHSC_02416	hypothetical protein	2.96	9.44E-05
	SAOUHSC_00182	hypothetical protein	4.16	9.70E-03
	SAOUHSC_00205	hypothetical protein	4.44	4.58E-02
	SAOUHSC_00347	hypothetical protein	18.88	8.24E-07
	SAOUHSC_00580	hypothetical protein	3.59	4.66E-02
	SAOUHSC_00745	hypothetical protein	8.88	1.37E-02
	SAOUHSC_00825	hypothetical protein	4.68	1.09E-02
	SAOUHSC_01334	hypothetical protein	40.51	2.79E-09
	SAOUHSC_01340	hypothetical protein	3.07	4.78E-02
	SAOUHSC_01343	hypothetical protein	9.71	9.44E-05
	SAOUHSC_01344	hypothetical protein	15.55	5.57E-04
	SAOUHSC_01976	hypothetical protein	3.85	1.86E-20
	SAOUHSC_02144	hypothetical protein	33.37	9.73E-09
	SAOUHSC_02157	hypothetical protein	6.02	1.30E-03
	SAOUHSC_02294	hypothetical protein	7.23	4.52E-04
	SAOUHSC_02424	hypothetical protein	3.00	4.29E-02
	SAOUHSC_A01910	hypothetical protein	7.11	4.29E-02

Table 5.8 *S. aureus* SH1000 genes down-regulated following treatment with DMSO dissolved ciprofloxacin compared with untreated cells.

Group functions	*S. aureus* 8325 ORF	*S. aureus* 8325 Gene	*S. aureus* 8325 Gene Product	Fold Change Down Regulated	P-value
Antibiotic resistance	SAOUHSC_01285	*femC*	factor involved in meticillin resistance	3.27	2.67E-02
	SAOUHSC_01948	*bcrA*	bacitracin transport ATP-binding protein bcrA	4.07	1.05E-02
Virulence factors	SAOUHSC_00114		capsular polysaccharide biosynthesis protein	10.65	1.24E-04
	SAOUHSC_00115	*capB*	capsular polysaccharide synthesis enzyme Cap5B	7.51	2.65E-03
	SAOUHSC_00116	*capC*	capsular polysaccharide synthesis enzyme Cap8C	7.32	2.04E-03
	SAOUHSC_00117	*capD*	capsular polysaccharide biosynthesis protein Cap5D	6.75	2.93E-03
	SAOUHSC_00118	*capE*	capsular polysaccharide biosynthesis protein Cap5E	5.44	9.61E-03
	SAOUHSC_00119	*capF*	capsular polysaccharide synthesis enzyme Cap8F	4.50	1.59E-02
	SAOUHSC_00121	*capH*	capsular polysaccharide synthesis enzyme O-acetyl transferase Cap5H	4.17	2.13E-02

	SAOUHSC_00122	*capI*	capsular polysaccharide biosynthesis protein Cap5I	3.46	4.38E-02
	SAOUHSC_00123	*capJ*	capsular polysaccharide biosynthesis protein Cap5J	3.79	3.08E-02
	SAOUHSC_00124	*capK*	capsular polysaccharide biosynthesis protein Cap5K	3.70	3.47E-02
	SAOUHSC_00545	*sdrD*	sdrD protein	4.22	3.84E-02
	SAOUHSC_02669	*sarZ*	transcriptional regulator SarZ	4.28	6.66E-03
Cell division	SAOUHSC_00994		bifunctional autolysin	2.92	4.10E-02
Protein synthesis	SAOUHSC_00736		hypothetical protein	3.90	1.08E-02
	SAOUHSC_00767		ribosomal subunit interface protein	4.37	6.89E-03
Lantibiotic synthesis	SAOUHSC_01947		lantibiotic ABC transporter permease	4.65	1.13E-02
	SAOUHSC_01949		intracellular serine protease	4.50	1.59E-02
Carotenoid biosynthesis	SAOUHSC_01990		squalene desaturase	4.13	2.75E-02
	SAOUHSC_02879		squalene desaturase	3.91	2.03E-02
	SAOUHSC_02881		hypothetical protein	4.66	1.13E-02
	SAOUHSC_02882		hypothetical protein	10.23	2.50E-04

Stress response					
	SAOUHSC_02563	*ureF*	urease accessory protein UreF	3.25	3.95E-02
	SAOUHSC_02862	*clpC*	ATP-dependent Clp protease, ATP-binding subunit ClpC	6.43	2.38E-03
Miscellaneous	SAOUHSC_00624		integrase/recombinase	4.85	3.55E-03
Metabolism					
	SAOUHSC_00120		UDP-N-acetylglucosamine 2-epimerase	4.33	1.87E-02
	SAOUHSC_00152		hypothetical protein	3.65	1.70E-02
	SAOUHSC_00187		formate acetyltransferase	4.54	4.96E-03
	SAOUHSC_00188		pyruvate formate-lyase 1 activating enzyme	2.95	4.77E-02
	SAOUHSC_00285		ABC transporter permease protein	4.55	5.24E-03
	SAOUHSC_00287		ABC transporter ATP-binding protein	3.56	2.02E-02
	SAOUHSC_00556		proline/betaine transporter	3.02	3.58E-02
	SAOUHSC_00625		putative monovalent cation/H+ antiporter subunit A	3.07	3.31E-02
	SAOUHSC_00706		hypothetical protein	3.65	1.56E-02

SAOUHSC_00707	fructose 1-phosphate kinase	3.35	2.22E-02
SAOUHSC_00708	fructose specific permease	2.81	4.77E-02
SAOUHSC_00738	proton-dependent peptide transporters	2.95	3.87E-02
SAOUHSC_00747	Iron compound ABC uptake transporter permease protein	3.58	3.77E-02
SAOUHSC_00748	Iron compound ABC uptake transporter ATP binding protein	4.56	6.28E-03
SAOUHSC_00749	hypothetical protein	5.22	2.45E-03
SAOUHSC_00898	argininosuccinate lyase	3.55	3.10E-02
SAOUHSC_00899	argininosuccinate synthase	4.50	1.59E-02
SAOUHSC_00923	hypothetical protein	4.63	1.40E-02
SAOUHSC_01013	Phosphoribosylformylglycin-amidine synthase II	4.81	1.22E-02
SAOUHSC_01165	uracil permease	4.81	3.72E-03
SAOUHSC_01014	amidophosphoribosyl transferase	4.71	1.33E-02
SAOUHSC_01015	phosphoribosylaminoimidazole synthetase	4.71	1.33E-02

SAOUHSC_01016		phosphoribosylglycinamide formyltransferase	3.27	4.29E-02
SAOUHSC_01166	*pyrB*	aspartate carbamoyltransferase catalytic subunit	6.73	6.27E-04
SAOUHSC_01168	*pyrC*	dihydroorotase	5.55	1.67E-03
SAOUHSC_01169		carbamoyl phosphate synthase small subunit	4.50	5.11E-03
SAOUHSC_01170	*carB*	carbamoyl phosphate synthase large subunit	4.50	5.34E-03
SAOUHSC_01171		orotidine 5'-phosphate decarboxylase	4.10	8.59E-03
SAOUHSC_01172	*pyrE*	orotate phosphoribosyltransferase	3.66	1.46E-02
SAOUHSC_01416		dihydrolipoamide succinyltransferase	3.07	3.98E-02
SAOUHSC_01418	*sucA*	2-oxoglutarate dehydrogenase E1 component	4.14	1.35E-02
SAOUHSC_01884		proline dehydrogenase	3.26	4.90E-02
SAOUHSC_01886	*ribH*	6,7-dimethyl-8-ribityllumazine synthase	2.96	3.82E-02
SAOUHSC_01887		riboflavin biosynthesis protein	2.88	4.32E-02
SAOUHSC_01888		riboflavin synthase subunit alpha	3.00	3.59E-02

	SAOUHSC_01889	*ribD*	riboflavin biosynthesis protein RibD	3.00	3.66E-02
	SAOUHSC_01991		ABC transporter permease	4.13	2.25E-02
	SAOUHSC_02270		ammonium transporter	15.76	1.27E-03
	SAOUHSC_02402		PTS system mannitol-specific transporter subunit IIA	2.96	4.66E-02
	SAOUHSC_02444		BCCT family osmoprotectant transporter	5.79	1.34E-03
	SAOUHSC_02467		alpha-acetolactate decarboxylase	2.91	4.18E-02
	SAOUHSC_02490	*adk*	adenylate kinase	3.07	3.80E-02
	SAOUHSC_02610		formimidoylglutamase	2.84	4.65E-02
	SAOUHSC_02648		L-lactate permease	3.01	3.71E-02
	SAOUHSC_02830		D-lactate dehydrogenase	5.07	2.70E-03
	SAOUHSC_03054	*rnpA*	ribonuclease P	13.78	8.62E-06
Hypothetical genes	SAOUHSC_00134		hypothetical protein	3.73	1.33E-02
	SAOUHSC_00146		hypothetical protein	3.32	2.27E-02
	SAOUHSC_00253		hypothetical protein	4.95	1.38E-02

SAOUHSC_00257	hypothetical protein	3.01	3.74E-02
SAOUHSC_00358	hypothetical protein	3.10	3.39E-02
SAOUHSC_00371	hypothetical protein	4.06	9.29E-03
SAOUHSC_00609	hypothetical protein	6.19	1.56E-02
SAOUHSC_00619	hypothetical protein	3.30	2.34E-02
SAOUHSC_00806	hypothetical protein	3.43	3.55E-02
SAOUHSC_00807	hypothetical protein	5.63	8.31E-03
SAOUHSC_00808	hypothetical protein	4.50	1.56E-02
SAOUHSC_00820	hypothetical protein	3.41	2.05E-02
SAOUHSC_00821	hypothetical protein	3.22	2.94E-02
SAOUHSC_00826	hypothetical protein	4.41	6.93E-03
SAOUHSC_00828	hypothetical protein	4.22	2.06E-02
SAOUHSC_00924	hypothetical protein	4.50	2.02E-02
SAOUHSC_00925	hypothetical protein	4.22	3.84E-02
SAOUHSC_00962	hypothetical protein	3.70	1.36E-02
SAOUHSC_01817	hypothetical protein	3.71	1.66E-02
SAOUHSC_01819	hypothetical protein	6.06	1.11E-03

SAOUHSC_01853	hypothetical protein	3.03	4.81E-02
SAOUHSC_01918	hypothetical protein	4.78	1.24E-02
SAOUHSC_01919	hypothetical protein	5.32	7.92E-03
SAOUHSC_01945	hypothetical protein	3.02	4.54E-02
SAOUHSC_02145	hypothetical protein	3.27	2.87E-02
SAOUHSC_02442	hypothetical protein	3.35	2.61E-02
SAOUHSC_02443	hypothetical protein	4.33	7.50E-03
SAOUHSC_02650	hypothetical protein	3.82	1.19E-02
SAOUHSC_02774	hypothetical protein	3.16	2.87E-02
SAOUHSC_02925	hypothetical protein	4.88	1.14E-02
SAOUHSC_02930	hypothetical protein	5.43	1.96E-03
SAOUHSC_03032	hypothetical protein	3.68	3.40E-02
SAOUHSC_03035	hypothetical protein	3.59	1.61E-02
SAOUHSC_03048	hypothetical protein	64.54	4.23E-09
SAOUHSC_A01436	hypothetical protein	3.60	4.24E-02

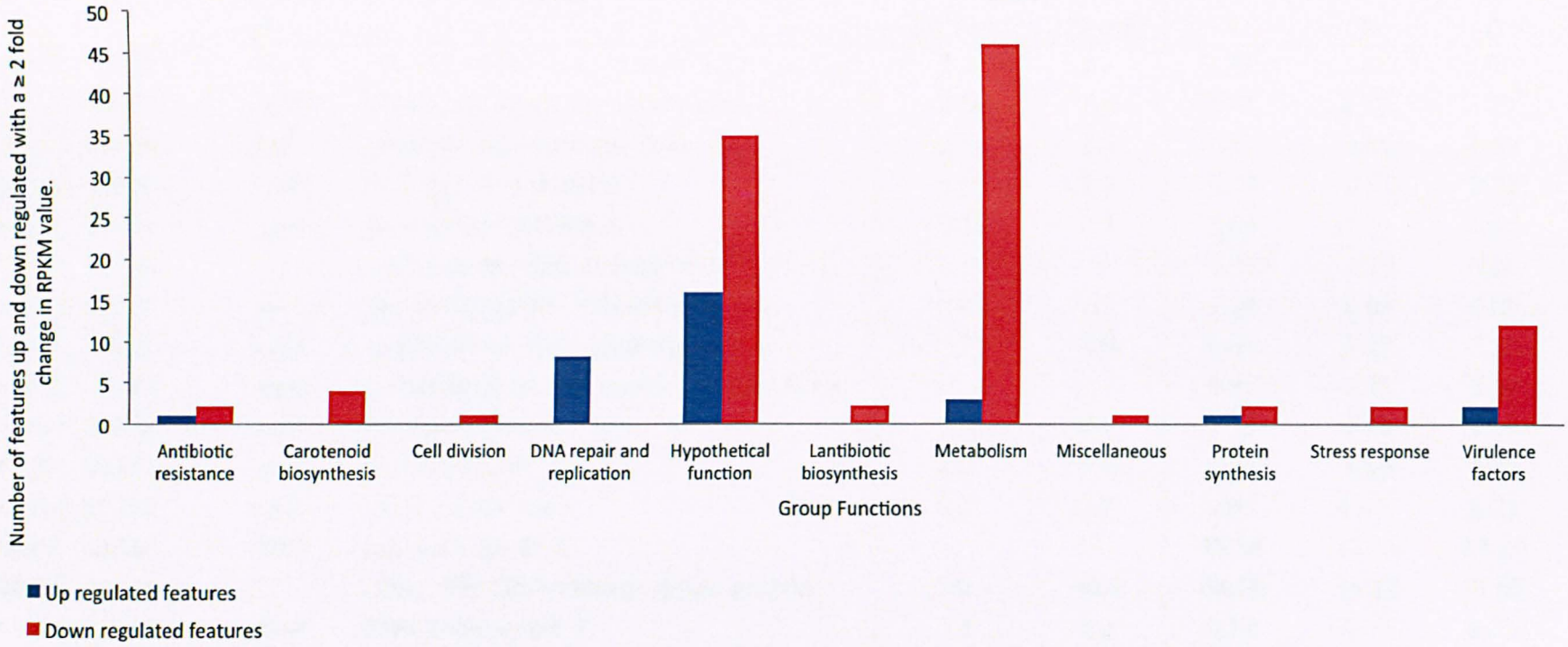

Figure 5.13 Number of features with a ≥ 2-fold change in RPKM value up and down regulated, following treatment with DMSO dissolved ciprofloxacin compared with untreated cells.

Table 5.9. Comparisons of the DNA repair and replication features that were up regulated following treatment with ciprofloxacin in *S. aureus* identified in this RNA-Seq study and the Cirz *et al.* (2007) microarray study.

S. aureus 8325 ORF	*S. aureus* 8325 gene	*S. aureus* 8325 Gene Product	Fold change up-regulated					
			Cirz *et al.* (2007) study		This study[1]			
			30 min	120 min	A	B	C	D
SAOUHSC_00001	*dnaA*	chromosomal replication initiation protein	-1.1	2.7	2.38*	2.66*	3.01*	3.62*
SAOUHSC_00002	*dnaN*	DNA polymerase III subunit beta	-1.0	2.6	2.02*	2.35*	2.00*	2.43*
SAOUHSC_00004	*recF*	recombination protein RecF	1.2	2.8	0.54	0.75	0.52	0.87
SAOUHSC_00005	*gyrB*	DNA gyrase subunit B	1.2	2.9	0.63	0.82	0.75	0.85
SAOUHSC_00006	*gyrA*	DNA gyrase subunit A	-1.0	2.4	1.04	1.07	0.88	1.28
SAOUHSC_00776		excinuclease ABC, B subunit	-	-	7.99	7.29	8.60	5.69
SAOUHSC_00779	*uvrB*	excinuclease ABC subunit B	2.8	2.5	7.04	6.83	6.89	6.18
SAOUHSC_00780	*uvrA*	excinuclease ABC subunit A	2.7	2.9	6.63	5.20	7.11	5.02
SAOUHSC_01243	*nusA*	transcriptional termination protein NusA	-	-	0.42	0.77	3.59	0.63
SAOUHSC_01262	*recA*	recombinase A	4.9	4.7	4.19	6.63	4.02	5.17
SAOUHSC_01333	*lexA*	lexA repressor	4.1	3.8	5.66	5.49	4.49	4.31
SAOUHSC_01341	*sbcD*	exonuclease SbcD	4.2	3.4	9.01	6.06*	8.21	8.72
SAOUHSC_01342	*sbcC*	exonuclease SbcC	-	-	15.38	12.15	14.23	16.17
SAOUHSC_01363		UmuC-like DNA damage repair protein	7.9	10.7	64.20	54.28	51.65	55.95
SAOUHSC_02111	*dinP*	DNA polymerase IV	-1.1	2.2	0.52	0.73	0.75	0.61

Table legend overleaf

[1]Full presented data sets and respective P-values for each treatment comparison with a ≥2 fold change in RPKM with maximum significance cut off at P=0.05 are outlined in Tables 5.5, 5.7, 5.14 and 5.16.

*Values that display ≥2 fold change in RPKM but P= >0.05, therefore deemed a statistically insignificant change

(-) Non-significantly differentially expressed features

A – *S. aureus* features up-regulated following treatment with nanoparticle formulated ciprofloxacin compared with untreated cells (completed data set presented in Table 5.5).

B – *S. aureus* features up-regulated following treatment with DMSO dissolved ciprofloxacin compared with untreated cells (completed data set presented in Table 5.7).

C - *S. aureus* features up-regulated following treatment with nanoparticle formulated ciprofloxacin compared with blank nanoparticle treated cells (completed data set presented in Table 5.14).

D - *S. aureus* features up-regulated following treatment with DMSO dissolved ciprofloxacin compared with DMSO treated cells (completed data set presented in Table 5.16).

5.6.2 *S. aureus* SH1000 transcriptional response to blank nanoparticles

Interestingly, exposure of *S. aureus* cells to equal concentrations of blank nanoparticle formulated excipients (PVP and pluronic F127) induced a transcriptional response with 33 and 19 transcripts up and down regulated respectively when compared to untreated cells (Tables 5.10 & 5.11 and Fig 5.14). Transcripts with hypothetical functions were most abundantly differentially expressed followed by metabolism related features. The types of features differentially expressed were markedly different and the fold changes in expression observed in this analysis were lower than those identified in the pairwise comparison between ciprofloxacin loaded nanoparticles and uninhibited cells.

Up regulated transcripts included: a cell wall hydrolase SAOUHSC_01219 that is associated with catabolic processes in peptidoglycan synthesis. The degree of peptidoglycan cross-linking ultimately determines how sensitive the cell wall is to degradation (Navarre & Schineewind, 1999). *sarV* (SAOUHSC_02532) was also up-regulated and is a member of the SarA protein family whose gene products play a role in regulating virulence associated genes and genes involved in autolysis. Hyper-expression of *sarV* in parental strains has been shown to result in a strain highly susceptible to TritonX-100 and penicillin induced lysis (Manna *et al.*, 2004). This would suggest that the blank nanoparticles enhanced the expression of features linked to the induced degradation of the cell wall and cell lysis processes that may act in a combined manner in the ciprofloxacin loaded nanoparticle preparation, resulting in enhanced antimicrobial activity. A range of metabolic associated features were also shown to be up-regulated. These included argininosuccinate lysase, which catalyses the reversible breakdown of argininosuccinate synthase; both enzymes are involved in urea cycling and argininosuccinate lysase in arginine synthesis (Emmett & Kloos, 1979). Up-regulation of arginine associated synthetic pathways, despite being a high consumer of ATP, might indicate an increased need for arginine during blank nanoparticle treatment and possibly a decreased efficiency of some amino acid driven systems. Similar trends were observed when *S. aureus* 8325 was heat shocked at 48°C in a microarray study (Fleury *et al.*, 2009). The camphor resistance gene *crcB* (SAOUHSC_01903) was also up-regulated; camphor has been suggested to cause

chromosomes to de-condense resulting in lethal effects within the cell. The increased expression of *crcA*, *crcB* and *cspE* has been shown to promote or protect chromosome folding through the re-condensation of the chromosomes resulting in increased resistance to camphor in *E. coli* (Hu *et al.*, 1996). Overall the treatment of *S. aureus* SH1000 with blank nanoparticles consisting of the polymer PVP and amphiphilic block co-polymer pluronic F127 which are described as inert materials, induced the up regulation (ca. 2-3 fold) of a whole host of features ranging from diverse cellular processes.

Down regulated genes were principally associated with metabolism and cell transporter mechanisms. SAOUHSC_00187 is a formate acetyltransferase part of the pyruvate metabolic pathway that can shunt pyruvate into the glyoxylate and dicarboxylate metabolic cycles and used for the synthesis of carbohydrates from simple carbon compounds. Alcohol dehydrogenase has multiple functions within cellular metabolism, but is principally associated with amino acid and carbohydrate metabolism, and SAOUHSC_2610 is a formimidoylglutamase within the histidine metabolic pathway that converts N-Formimino L-glutamate into L-glutamate. Although the fold changes to metabolic processes were relatively small (ca. 2-3 fold), the subtle changes observed in multiple pathways suggests that the blank nanoparticles force the cells to undergo transcriptional modifications to adapt to the treatment.

Table 5.10 *S. aureus* SH1000 genes up-regulated following treatment with blank nanoparticles (55% $^{w}/_{w}$ PVP 25% $^{w}/_{w}$ pluronic F127) compared with untreated cells.

Group functions	*S. aureus* 8325 ORF	*S. aureus* 8325 Gene	*S. aureus* 8325 Gene Product	Fold Change Up Regulated	P-value
Antibiotic resistance					
	SAOUHSC_01220		hypothetical protein	3.09	1.87E-03
	SAOUHSC_01903	*crcB*	camphor resistance protein CrcB	2.15	3.09E-02
Virulence factors					
	SAOUHSC_02532	*sarV*	transcriptional regulator SarV	2.53	1.01E-03
Carotenoid biosynthesis	SAOUHSC_01990		squalene desaturase	2.24	6.57E-03
	SAOUHSC_01991		ABC transporter permease	2.28	4.78E-03
Cell wall synthesis	SAOUHSC_01219		cell wall hydrolase	2.27	3.19E-02
Miscellaneous	SAOUHSC_01301		hypothetical protein - transposon related	2.27	9.56E-03
Metabolism					
	SAOUHSC_00898		argininosuccinate lyase	2.68	4.97E-04
	SAOUHSC_00899		argininosuccinate synthase	2.87	2.91E-04
	SAOUHSC_01726		(5-methylaminomethyl-2-thiouridylate)-methyltransferase	2.36	2.05E-03
	SAOUHSC_02360		thymidine kinase	2.19	4.72E-03

	SAOUHSC_02416	hypothetical protein	3.47	9.84E-06
	SAOUHSC_02793	phosphomannomutase	2.27	6.20E-03
Hypothetical genes	SAOUHSC_00440	hypothetical protein	6.13	1.24E-11
	SAOUHSC_00029	hypothetical protein	2.46	3.13E-03
	SAOUHSC_00316	hypothetical protein	2.23	1.37E-02
	SAOUHSC_00825	hypothetical protein	2.38	6.37E-03
	SAOUHSC_01230	hypothetical protein	2.67	7.68E-04
	SAOUHSC_01422	hypothetical protein	3.24	1.02E-04
	SAOUHSC_01484	hypothetical protein	3.27	2.03E-03
	SAOUHSC_01924	hypothetical protein	2.365	7.06E-03
	SAOUHSC_02115	hypothetical protein	2.73	4.43E-04
	SAOUHSC_02136	hypothetical protein	4.01	2.39E-03
	SAOUHSC_02290	hypothetical protein	2.57	3.25E-03
	SAOUHSC_02294	hypothetical protein	2.68	4.65E-04
	SAOUHSC_02534	hypothetical protein	2.35	2.26E-02
	SAOUHSC_02616	hypothetical protein	3.64	5.17E-06
	SAOUHSC_02646	hypothetical protein	2.13	1.03E-02

	SAOUHSC_02732	hypothetical protein	4.42	7.52E-08
	SAOUHSC_02817	hypothetical protein	2.74	1.71E-02
	SAOUHSC_02838	hypothetical protein	3.78	1.83E-04
	SAOUHSC_02950	hypothetical protein	3.19	3.07E-03
	SAOUHSC_A00354	hypothetical protein	2.16	5.32E-03

Table 5.11 *S. aureus* SH1000 genes down-regulated following treatment with blank nanoparticles (55% $^{w}/_{w}$ PVP 25% $^{w}/_{w}$ pluronic F127) compared with untreated cells.

Group functions	*S. aureus* 8325 ORF	*S. aureus* 8325 Gene	*S. aureus* 8325 Gene Product	Fold Change Down Regulated	P-value
Carotenoid biosynthesis	SAOUHSC_02882		hypothetical protein	2.39	2.22E-03
Metabolism	SAOUHSC_00097		purine nucleoside phosphorylase	3.88	5.25E-05
	SAOUHSC_00152		hypothetical protein	2.91	1.59E-04
	SAOUHSC_00187		formate acetyltransferase	2.59	5.31E-04
	SAOUHSC_00608	*adhA*	alcohol dehydrogenase	2.21	6.52E-03
	SAOUHSC_02270		ammonium transporter	2.68	4.53E-02
	SAOUHSC_02387	*ylbE*	oxidoreductase ylbE	2.02	1.07E-02
	SAOUHSC_02610		formimidoylglutamase	2.21	3.69E-03

	SAOUHSC_02671	nitrate/nitrite transporter	2.24	1.31E-02
	SAOUHSC_02684	assimilatory nitrite reductase [NAD(P)H] large subunit	2.08	2.44E-02
Hypothetical genes	SAOUHSC_00065	hypothetical protein	2.06	8.98E-03
	SAOUHSC_00396	hypothetical protein	3.44	1.37E-02
	SAOUHSC_00371	hypothetical protein	2.19	4.45E-03
	SAOUHSC_00561	hypothetical protein	2.04	9.10E-03
	SAOUHSC_00690	hypothetical protein	2.01	1.01E-02
	SAOUHSC_00841	hypothetical protein	2.17	4.49E-03
	SAOUHSC_01687	hypothetical protein	3.12	6.10E-04
	SAOUHSC_02685	hypothetical protein	2.87	2.46E-03
	SAOUHSC_02930	hypothetical protein	2.11	6.24E-03

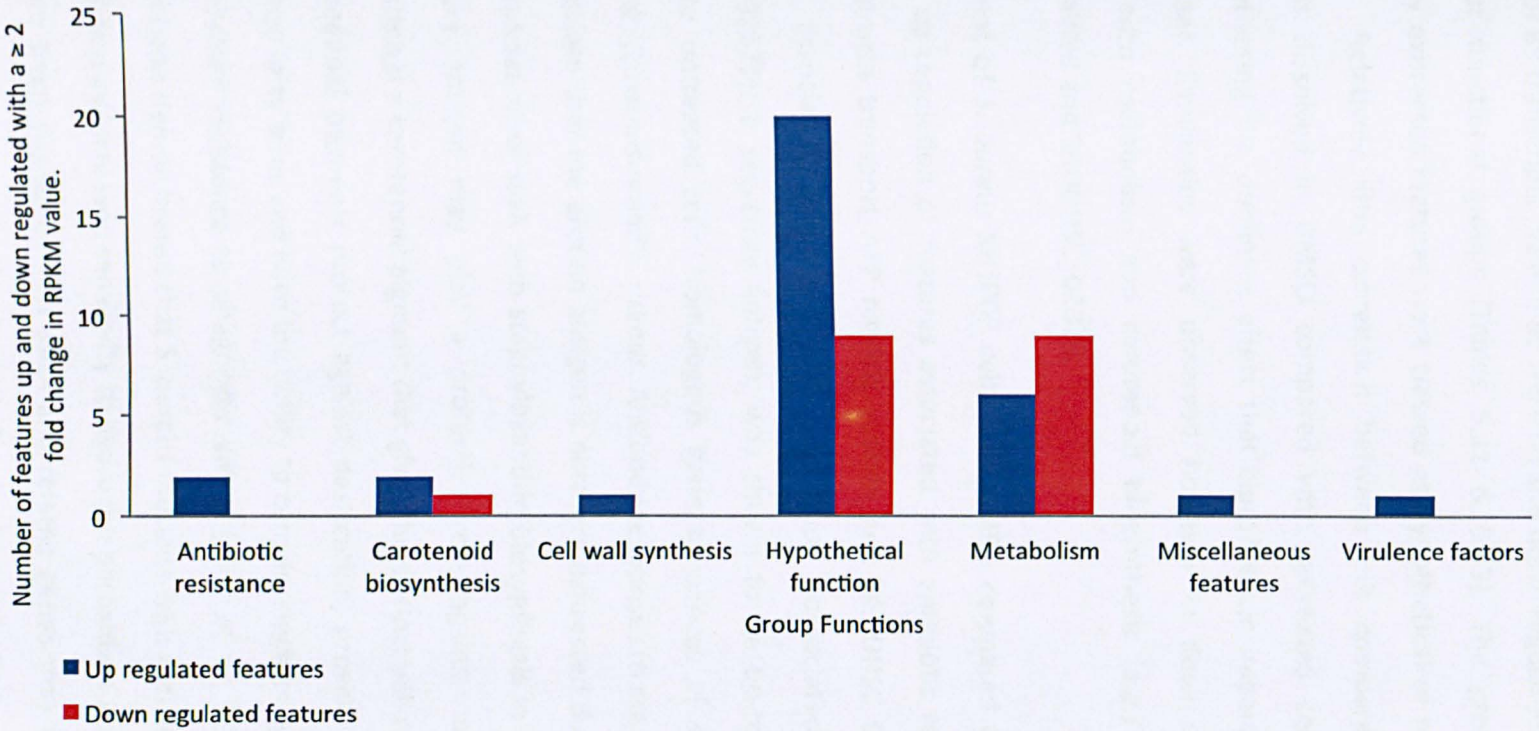

Figure 5.14 Number of features with a ≥ 2-fold change in RPKM value up and down regulated, following treatment with blank nanoparticles (55% $^{w}/_{w}$ PVP 25% $^{w}/_{w}$ pluronic F127) compared with untreated cells.

5.6.3 *S. aureus* SH1000 transcriptional response to DMSO

The exposure of *S. aureus* SH1000 to DMSO induced the significant differential expression of 88 transcripts (52 and 36 were up and down regulated respectively) from a variety of functional groups (Tables 5.12 & 5.13). The greatest numbers of differentially expressed features were classed as hypothetical or metabolism related (Fig 5.15). Relatively little correlation between this comparative analysis and ciprofloxacin dissolved in DMSO compared with untreated cells was apparent, probably reflecting the dominant effect that ciprofloxacin imparts on transcription when present. Similarities were observed however in down-regulated features associated with metabolism and carotenoid biosynthesis (*e.g.*) SAOUHSC_00188, SAOUHSC_00898 and SAOUHSC_02879.

The treatment of *S. aureus* SH1000 cells with DMSO compared to untreated cells, caused the up-regulation of features associated with antibiotic resistance including *bcrA* a bacitracin transport ATP binding protein and SAOUHSC_02420 a multidrug resistance associated protein. The virulence associated feature *ssaA* (SAOUHSC_02571), a secretory antigen, was shown to be up-regulated 2.14 fold compared to untreated cells. Homologous gene sequences of *ssaA* are found in *S. epidermidis, S. carnosus* and *S. aureus*. Antibody responses to ssaA in staphylococcal infection indicate that the protein antigen is normally expressed during infection. The apparent association of ssaA with staphyloxanthin biosynthesis in *S. aureus* suggests the secretory antigen may play a protective role against oxidative defences. Staphyloxanthin is a carotenoid pigment that gives the distinct yellow or orange colony colour. Carotenoid pigments protect against desiccation, provide resistance against long chain free fatty acids and have the ability to convert singlet oxygen to a non-toxic form that permits resistance to phagocytic killing (Lang *et al.*, 2000 ; Kenny *et al.*, 2009). It has been demonstrated that *S. aureus* mutants with reduced staphyloxanthin biosynthesis display increased sensitivity to hydrogen peroxidase (Kullik *et al.*, 1998). It has therefore been suggested that *ssaA* and related genes may be involved in the biosynthetic pathway associated with staphylococcal carotenoid formation (Lang *et al.*, 2000 ; Kenny *et al.*, 2009). DMSO treatment may therefore impart a stress on *S. aureus* that elaborates the expression of *ssaA* to provide a protective role. The up-regulation

of stress response related features, SAOUHSC_00133 a cobalt-zinc-cadmium resistance protein and *ureA* SAOUHSC_02557 a urea transporter, suggests possible loss of regulation over metal homeostasis or the need to protect against the damaging effects of heavy metals and urea toxicity imparted by DMSO. Linked to this is the up-regulation of a range of iron ABC uptake transporters, suggesting *S. aureus* SH1000 cells scavenge iron with the aim of intracellular accumulation. Other metabolic related features were also up-regulated including two spermidine / putrescine ABC transporter features. Polyamines (putrescine / spermidine / spermine) are associated with DNA metabolism and play important roles in cell proliferation and differentiation, and are essential for the growth and functioning of normal cells. Cellular polyamine content is regulated by biosynthesis, degradation and transport. The up-regulation of the associated ABC transporters for these features suggests the cells require to either take up or remove intracellular polyamines to maintain normal functioning of DNA metabolism (Wallace *et al.*, 2003).

Treatment of *S. aureus* SH1000 with DMSO caused the down-regulation of features linked with virulence. These included SAOUHSC_02241 and SAOUHSC_02243 that are associated with leukocidin and hemolysin toxin production. A range of metabolic features were also shown to be down-regulated including components of the gluconeogenesis pathway, SAOUHSC_00187 that converts pyruvate to Acetyl-CoA and SAOUHSC_00187 that converts acetaldehyde into Acetyl-CoA. This down-regulation of pathways would reduce the amount of available Acetyl-CoA to progress into the TCA cycle. Down-regulation of nitrate reduction was observed (SAOUHSC_02679, 02680 and 02681) the reduction of nitrate to nitrite ultimately leads to the formation of ammonia the down regulation of these features is likely to lead to the accumulation of nitrate. Components of amino acid metabolism were also shown to be down-regulated, *i.e.* SAOUHSC_01451 a threonine dehydratase associated with isoleucine biosynthesis and an arginine / ornithine antiporter. The metabolism of arginine is thought to be important for survival and pathogenesis (Zhu *et al.*, 2007).

Although DMSO treatment induced small reductions in growth (Fig 5.5) and inhibition of *S. aureus* SH1000 at increased concentrations, it caused alterations in transcription

profiles at growth limiting exposure periods and concentrations. In particular, a variety of metabolic pathways were shown to be altered due to DMSO treatment.

Table 5.12 *S. aureus* SH1000 genes up-regulated following treatment with DMSO compared with untreated cells.

Group functions	*S. aureus* 8325 ORF	*S. aureus* 8325 Gene	*S. aureus* 8325 Gene Product	Fold Change Up Regulated	P-value
Antibiotic resistance	SAOUHSC_01948	*bcrA*	bacitracin transport ATP-binding protein bcrA	2.87	9.85E-04
	SAOUHSC_02420		multidrug resistance protein B	2.16	1.34E-02
	SAOUHSC_02629		EmrB/QacA family drug resistance transporter	2.05	1.97E-02
Virulence factors	SAOUHSC_00668		bacitracin transport system permease protein	2.07	1.83E-02
	SAOUHSC_02466		truncated MHC class II analog protein	2.12	4.36E-02
	SAOUHSC_02571	*ssaA*	secretory antigen SsaA	2.14	1.24E-02
Lantibiotic synthesis	SAOUHSC_01949		intracellular serine protease	2.34	1.92E-02
Protein export	SAOUHSC_02989	*secY*	preprotein translocase subunit SecY	2.49	4.53E-02
Protein synthesis	SAOUHSC_01078		ribosomal protein L32	2.22	6.20E-03
Carotenoid biosynthesis	SAOUHSC_02882		hypothetical protein	2.21	1.53E-02

Stress response	SAOUHSC_00133		cobalt-zinc-cadmium resistance protein	2.074	3.82E-02
	SAOUHSC_02557	*ureA*	urea transporter	2.093	4.63E-02
Metabolism					
	SAOUHSC_00097		purine nucleoside phosphorylase	2.24	2.66E-02
	SAOUHSC_00152		hypothetical protein	2.97	6.77E-04
	SAOUHSC_00654		ferrichrome ABC transporter permease	2.07	2.39E-02
	SAOUHSC_00747		iron compound ABC uptake transporter permease protein	2.41	1.93E-02
	SAOUHSC_00748		iron compound ABC uptake transporter ATP-binding protein	3.31	2.36E-04
	SAOUHSC_00871		D-alanine--poly(phosphoribitol) ligase subunit 2	2.04	1.10E-02
	SAOUHSC_00989		N-acetyl-L,L-diaminopimelate aminotransferase	2.15	1.35E-02
	SAOUHSC_01048		spermidine/putrescine ABC transporter permease	2.36	6.91E-03
	SAOUHSC_01049		spermidine/putrescine ABC transporter	2.11	1.78E-02
	SAOUHSC_01168	*pyrC*	dihydroorotase	2.23	9.64E-03

	SAOUHSC_01169		carbamoyl phosphate synthase small subunit	2.60	2.12E-03
	SAOUHSC_01170	*carB*	carbamoyl phosphate synthase large subunit	2.26	8.53E-03
	SAOUHSC_01434		dihydrofolate reductase	2.40	3.82E-03
	SAOUHSC_01440		putative preQ0 transporter	37.50	1.08E-10
	SAOUHSC_01884		proline dehydrogenase	2.93	2.46E-03
	SAOUHSC_01886	*ribH*	6,7-dimethyl-8-ribityllumazine synthase	2.10	1.56E-02
	SAOUHSC_02722		hypothetical protein	2.10	3.23E-02
Hypothetical genes	SAOUHSC_00134		hypothetical protein	2.15	1.25E-02
	SAOUHSC_00238		hypothetical protein	2.73	1.09E-02
	SAOUHSC_00368		hypothetical protein	3.22	4.08E-02
	SAOUHSC_00396		hypothetical protein	3.52	1.30E-02
	SAOUHSC_00770		hypothetical protein	2.19	2.28E-02
	SAOUHSC_00826		hypothetical protein	2.18	5.55E-03
	SAOUHSC_00962		hypothetical protein	3.01	3.34E-04
	SAOUHSC_01230		hypothetical protein	2.15	2.93E-02

SAOUHSC_01315	hypothetical protein	2.44	4.01E-03
SAOUHSC_01439	hypothetical protein	5.51	2.20E-07
SAOUHSC_01458	hypothetical protein	2.74	5.72E-04
SAOUHSC_01687	hypothetical protein	2.34	1.86E-02
SAOUHSC_01823	hypothetical protein	2.40	5.08E-03
SAOUHSC_01898	hypothetical protein	2.47	2.49E-02
SAOUHSC_02145	hypothetical protein	2.25	4.02E-03
SAOUHSC_02157	hypothetical protein	2.12	1.94E-02
SAOUHSC_02332	hypothetical protein	2.77	1.71E-03
SAOUHSC_02842	hypothetical protein	2.77	3.23E-03
SAOUHSC_02853	hypothetical protein	2.07	1.70E-02
SAOUHSC_02888	membrane protein	2.39	1.35E-02
SAOUHSC_02925	hypothetical protein	2.18	3.17E-02
SAOUHSC_02930	hypothetical protein	3.04	4.03E-04
SAOUHSC_02944	hypothetical protein	2.23	1.40E-02

Table 5.13 *S. aureus* SH1000 genes down-regulated following treatment with DMSO compared with untreated cells.

Group functions	*S. aureus* 8325 ORF	*S. aureus* 8325 Gene	*S. aureus* 8325 Gene Product	Fold Change Down Regulated	P-value
Virulence factors	SAOUHSC_00284		5'-nucleotidase	2.45	1.62E-02
	SAOUHSC_02241		leukocidin/hemolysin toxin family protein	2.86	5.79E-03
	SAOUHSC_02243		leukocidin/hemolysin toxin family protein	2.65	1.42E-02
Stress response	SAOUHSC_02862	*clpC*	ATP-dependent Clp protease, ATP-binding subunit ClpC	2.17	1.58E-02
Carotenoid biosynthesis	SAOUHSC_01990		squalene desaturase	2.56	5.84E-03
	SAOUHSC_02877		squalene synthase	2.69	2.28E-03
	SAOUHSC_02879		squalene desaturase	3.02	6.28E-04
Protein synthesis	SAOUHSC_00483		hypothetical protein	2.08	1.92E-02
Metabolism	SAOUHSC_00113		bifunctional acetaldehyde-CoA/alcohol dehydrogenase	2.37	3.23E-02
	SAOUHSC_00187		formate acetyltransferase	2.65	1.32E-03
	SAOUHSC_00188		pyruvate formate-lyase 1 activating enzyme	5.63	8.44E-09

SAOUHSC_00189	hypothetical protein	3.58	6.26E-03
SAOUHSC_00317	glycerol-3-phosphate transporter	2.03	4.25E-02
SAOUHSC_00412	NADH dehydrogenase subunit 5	3.21	3.09E-04
SAOUHSC_00413	hypothetical protein	2.85	8.73E-04
SAOUHSC_00898	argininosuccinate lyase	5.38	1.50E-07
SAOUHSC_00899	argininosuccinate synthase	5.08	1.03E-06
SAOUHSC_01008	phosphoribosylaminoimid-azole carboxylase, catalytic subunit	3.13	5.48E-03
SAOUHSC_01009	phosphoribosylaminoimid-azole carboxylase ATPase subunit	2.30	2.05E-02
SAOUHSC_01396	dihydrodipicolinate synthase	2.13	4.46E-02
SAOUHSC_01397	dihydrodipicolinate reductase	3.29	4.46E-03
SAOUHSC_01398	2,3,4,5-tetrahydropyridine-2-carboxylate N-succinyltransferase	2.19	3.88E-02
SAOUHSC_01451	threonine dehydratase	2.93	1.19E-02
SAOUHSC_01452	alanine dehydrogenase	3.98	2.71E-02

	SAOUHSC_01991	ABC transporter permease	2.23	1.51E-02
	SAOUHSC_02679	respiratory nitrate reductase, delta subunit	5.21	5.79E-05
	SAOUHSC_02680	nitrate reductase, beta subunit	4.59	7.70E-05
	SAOUHSC_02681	nitrate reductase, alpha subunit	2.92	2.50E-03
	SAOUHSC_02682	uroporphyrin-III C-methyltransferase	3.54	3.01E-04
	SAOUHSC_02806	gluconate permease	2.37	1.36E-02
	SAOUHSC_02967	arginine/ornithine antiporter	2.28	3.24E-02
Hypothetical genes	SAOUHSC_00189	hypothetical protein	3.58	6.26E-03
	SAOUHSC_00580	hypothetical protein	2.07	3.82E-02
	SAOUHSC_00825	hypothetical protein	2.20	3.44E-02
	SAOUHSC_02880	conserved hypothetical protein	2.89	1.34E-03
	SAOUHSC_A02680	hypothetical protein	2.35	2.89E-02

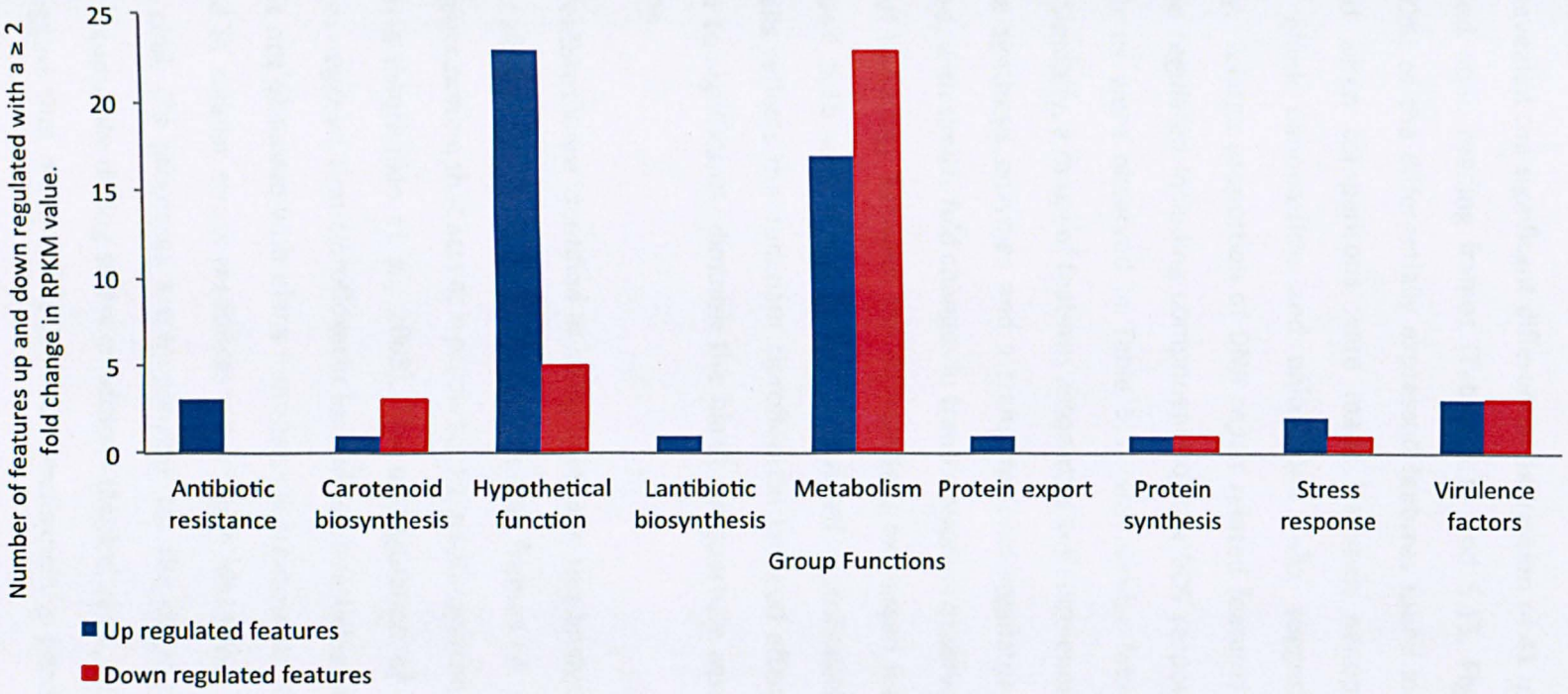

Figure 5.15 Number of features with a ≥ 2-fold change in RPKM value up and down regulated, following treatment with DMSO compared with untreated cells.

5.6.4 *S. aureus* SH1000 transcriptional response to nanoparticle formulated ciprofloxacin compared with blank nanoparticle treatment.

Comparative analysis of nanoparticle formulated ciprofloxacin with blank nanoparticle treated cells revealed the significant differential expression of 41 up regulated and 84 down regulated open reading frames (Tables 5.14 and 5.15, Figure 5.16). A large proportion (70%) of the differentially expressed features found in this analysis were also identified when comparisons were made between nanoparticle formulated ciprofloxacin, blank nanoparticle and uninhibited cells, suggesting good sample reproducibility. A large proportion of DNA repair related features were identified as significantly up regulated including components of the SOS response and nucleotide excision repair as were observed in Table 5.5, with similar fold changes between comparisons. Similarly, a range of features associated with virulence including capsular polysaccharide synthesis enzymes and a transcriptional regulator of virulence were down regulated, with similar fold changes in transcription as observed in Table 5.6. The large degree of homology between the differentially expressed features identified in Tables 5.14 and 5.15 with nanoparticle formulated ciprofloxacin compared with uninhibited cells reflects the dominant ciprofloxacin induced effects on transcription that appeared to significantly diminish the blank nanoparticle associated features in this comparison.

A number of features were identified as being unique to this analysis, including the up regulation of cell wall synthesis related open reading frames *i.e.* SAOUHSC_02423 a UDP-N-acetylglucosamine that acts as a precursor for peptidoglycan synthesis in Gram-positive bacteria (Mochalkin *et al.*, 2008). The up-regulation of cell wall synthesis related features suggests that ciprofloxacin loaded nanoparticles may induce cell wall damage that is not observed with blank nanoparticle treatment. The up-regulation of genes involved in cellular stress responses were again identified, including the CtsR regulon gene *clpB*. Clp proteases are responsible for the degradation of misfolded proteins that accumulate during stress conditions (Michel *et al.*, 2006). It is therefore possible to suggest that nanoparticle loaded ciprofloxacin is perceived by *S. aureus* SH1000 as a stressor.

The down regulation of several features unique to this comparative analysis were identified including SAOUHSC_01281 that encodes a host factor protein associated with RNA degradation processes and an antibiotic resistance feature *fmtB* that is associated with meticillin resistance, reduced sensitivity to oxacillin and Triton X-100 (Komatsuzawa *et al.*, 2000). Other features, principally virulence, carotenoid synthesis and antibiotic resistance related, were also identified as being down regulated in this comparative analysis and the comparison made between nanoparticle formulated ciprofloxacin and untreated cells.

Table 5.14 *S. aureus* SH1000 genes up-regulated following treatment with nanoparticle formulated ciprofloxacin compared with blank nanoparticle treated cells.

Group functions	*S. aureus* 8325 ORF	*S. aureus* 8325 Gene	*S. aureus* 8325 Gene Product	Fold Change Up Regulated	P-value
DNA repair and replication	SAOUHSC_00776		excinuclease ABC, B subunit	8.60	1.26E-03
	SAOUHSC_00779	*uvrB*	excinuclease ABC subunit B	6.89	2.27E-03
	SAOUHSC_00780	*uvrA*	excinuclease ABC subunit A	7.11	3.24E-03
	SAOUHSC_01243	*nusA*	transcription termination protein NusA	3.59	4.54E-02
	SAOUHSC_01262	*recA*	recombinase A	4.02	2.87E-02
	SAOUHSC_01333	*lexA*	lexA repressor	4.49	2.06E-02
	SAOUHSC_01341	*sbcD*	exonuclease SbcD	8.21	6.48E-04
	SAOUHSC_01342	*sbcC*	exonuclease SbcC	14.23	1.11E-04
	SAOUHSC_01363		DNA damage repair protein	51.65	5.57E-08
	SAOUHSC_02417		hypothetical protein	7.12	2.15E-03
Antibiotic resistance	SAOUHSC_02003		multidrug resistance ABC transporter ATP-binding and permease protein	3.53	3.48E-02
	SAOUHSC_02420		multidrug resistance protein B	4.88	1.42E-02

Cell wall synthesis					
	SAOUHSC_01866		putative choline kinase	3.62	4.47E-02
	SAOUHSC_02423		UDP-N-acetylglucosamine pyrophosphorylase	4.53	1.98E-02
Stress response					
	SAOUHSC_00912	*clpB*	ATP-dependent Clp protease, ATP-binding subunit ClpB	3.13	4.97E-02
Metabolism					
	SAOUHSC_01334		hypothetical protein	44.18	1.25E-07
	SAOUHSC_01365		deblocking aminopeptidase	6.77	3.09E-03
	SAOUHSC_01440		putative preQ0 transporter	3.77	3.88E-02
	SAOUHSC_02140		putative manganese-dependent inorganic pyrophosphatase	3.74	3.27E-02
	SAOUHSC_02399		glucosamine--fructose-6-phosphate aminotransferase	4.22	1.56E-02
	SAOUHSC_02403		mannitol-1-phosphate 5-dehydrogenase	6.20	1.93E-02
	SAOUHSC_02409		arginase	15.50	4.04E-03
	SAOUHSC_02452		tagatose 1,6-diphosphate aldolase	8.78	1.02E-02
	SAOUHSC_02453		tagatose-6-phosphate kinase	6.20	2.21E-02
	SAOUHSC_02454	*lacB*	galactose-6-phosphate isomerase	14.98	1.88E-03

Hypothetical genes

SAOUHSC_00347	hypothetical protein	27.67	4.89E-06
SAOUHSC_00409	hypothetical protein	4.73	1.90E-02
SAOUHSC_00772	hypothetical protein	4.24	4.62E-02
SAOUHSC_00907	hypothetical protein	3.22	4.43E-02
SAOUHSC_01023	hypothetical protein	12.40	7.86E-03
SAOUHSC_01141	hypothetical protein	3.51	3.58E-02
SAOUHSC_01331	hypothetical protein	39.26	7.12E-06
SAOUHSC_01343	hypothetical protein	9.80	7.97E-04
SAOUHSC_01344	hypothetical protein	11.88	2.01E-03
SAOUHSC_02141	hypothetical protein	7.23	1.80E-02
SAOUHSC_02144	hypothetical protein	26.73	3.57E-06
SAOUHSC_02157	hypothetical protein	4.81	1.50E-02
SAOUHSC_02419	hypothetical protein	3.94	2.92E-02
SAOUHSC_02424	hypothetical protein	6.83	2.86E-03
SAOUHSC_02734	hypothetical protein	5.37	2.75E-02
SAOUHSC_03024	hypothetical protein	4.23	2.45E-02

Table 5.15. *S. aureus* SH1000 genes down-regulated following treatment with nanoparticle formulated ciprofloxacin compared with blank nanoparticle treated cells.

Group functions	*S. aureus* 8325 ORF	*S. aureus* 8325 Gene	*S. aureus* 8325 Gene Product	Fold Change Down Regulated	P-value
DNA repair and replication	SAOUHSC_01281		host factor 1 protein	4.05	1.93E-02
Virulence factors	SAOUHSC_00114		capsular polysaccharide biosynthesis protein	8.57	1.59E-03
	SAOUHSC_00115	*capB*	capsular polysaccharide synthesis enzyme Cap5B	5.12	2.92E-02
	SAOUHSC_00116	*capC*	capsular polysaccharide synthesis enzyme Cap8C	8.44	4.53E-03
	SAOUHSC_00117	*capD*	capsular polysaccharide biosynthesis protein Cap5D	4.84	2.84E-02
	SAOUHSC_02669	*sarZ*	transcriptional regulator SarZ	6.00	5.53E-03
Stress response	SAOUHSC_02862	*clpC*	ATP-dependent Clp protease, ATP-binding subunit ClpC	4.84	2.52E-02
Antibiotic resistance	SAOUHSC_01285	*femC*	factor involved in meticillin resistance and Glutamine synthetase repressor	10.65	5.41E-04
	SAOUHSC_01948	*bcrA*	bacitracin transport ATP-binding protein bcrA	4.32	2.16E-02

	SAOUHSC_02404	*fmtB*	FmtB (Mrp) protein involved in meticillin resistance and cell wall biosynthesis	78.09	1.73E-08
Carotenoid biosynthesis	SAOUHSC_01990		squalene desaturase	11.75	9.54E-04
	SAOUHSC_02881		hypothetical protein	4.84	2.84E-02
	SAOUHSC_02882		hypothetical protein	5.16	2.42E-02
Lantibiotic synthesis	SAOUHSC_01950	*epiD*	flavoprotein, epiD	8.71	3.47E-02
Protein synthesis					
	SAOUHSC_00526		putative ribosomal protein L7Ae-like	2.83	1.87E-02
	SAOUHSC_00530		elongation factor Tu	3.35	2.08E-02
	SAOUHSC_02095		low molecular weight protein tyrosine phosphatase	4.46	2.15E-02
Miscellaneous genes	SAOUHSC_00624		integrase/recombinase	4.01	1.93E-02
	SAOUHSC_01288		hypothetical protein - transposon related	4.36	4.58E-02
	SAOUHSC_01292		hypothetical protein - transposon related	5.08	4.10E-02

Metabolism

SAOUHSC_00281	formate/nitrite transporter family protein	9.23	4.16E-04
SAOUHSC_00285	ABC transporter permease protein	3.49	3.60E-02
SAOUHSC_00556	proline/betaine transporter	3.63	3.08E-02
SAOUHSC_00634	manganese/iron transport system substrate-binding protein	4.74	1.76E-02
SAOUHSC_00738	proton-dependent Peptide Transporters	4.00	2.79E-02
SAOUHSC_00749	hypothetical protein	3.98	1.91E-02
SAOUHSC_00898	argininosuccinate lyase	6.71	2.28E-03
SAOUHSC_00899	argininosuccinate synthase	12.76	2.02E-04
SAOUHSC_00923	hypothetical protein	4.60	3.85E-02
SAOUHSC_00926	oligopeptide ABC transporter ATP-binding protein	5.08	4.10E-02
SAOUHSC_01014	amidophosphoribosyl-transferase	4.84	2.52E-02
SAOUHSC_01015	Phosphoribosylaminoimid-azole synthetase	4.49	3.39E-02
SAOUHSC_01016	Phosphoribosylglycinamide-formyltransferase	4.63	3.02E-02

SAOUHSC_01991		ABC transporter permease	10.12	8.51E-04
SAOUHSC_01165		uracil permease	5.59	4.42E-03
SAOUHSC_01166	*pyrB*	aspartate carbamoyltransferase catalytic subunit	8.76	5.67E-04
SAOUHSC_01168	*pyrC*	dihydroorotase	5.32	5.52E-03
SAOUHSC_01169		carbamoyl phosphate synthase small subunit	6.10	3.09E-03
SAOUHSC_01170	*carB*	carbamoyl phosphate synthase large subunit	4.89	8.39E-03
SAOUHSC_01171		orotidine 5'-phosphate decarboxylase	3.17	4.86E-02
SAOUHSC_01172	*pyrE*	orotate phosphoribosyltransferase	5.42	6.11E-03
SAOUHSC_01275		hypothetical protein	5.32	7.87E-03
SAOUHSC_01278		aerobic glycerol-3-phosphate dehydrogenase	4.39	2.16E-02
SAOUHSC_01287		glutamine synthetase, type I	4.49	1.98E-02
SAOUHSC_01394		aspartate kinase	6.45	2.43E-02
SAOUHSC_01395		aspartate semialdehyde dehydrogenase	5.57	3.12E-02

	SAOUHSC_01396	dihydrodipicolinate synthase	5.61	2.64E-02
	SAOUHSC_02119	high affinity proline permease	4.01	2.79E-02
	SAOUHSC_02397	ABC transporter ATP-binding protein	10.94	1.70E-04
	SAOUHSC_02400	PTS system mannitol-specific protein	8.62	2.08E-03
	SAOUHSC_02402	PTS system mannitol-specific transporter subunit IIA	3.87	3.48E-02
	SAOUHSC_02411	hypothetical protein	17.42	7.23E-04
	SAOUHSC_02412	hypothetical protein	23.53	8.53E-06
	SAOUHSC_02444	BCCT family osmoprotectant transporter	4.71	1.12E-02
	SAOUHSC_02648	L-lactate permease	5.60	9.24E-03
	SAOUHSC_02830	D-lactate dehydrogenase	5.02	7.07E-03
	SAOUHSC_02836	phosphinothricin N-acetyltransferase	5.74	1.24E-02
	SAOUHSC_02848	phosphotransferase system (PTS) system glucose-specific transporter subunit IIABC	3.65	3.94E-02
Hypothetical genes				
	SAOUHSC_00257	hypothetical protein	3.71	2.62E-02

SAOUHSC_00356	hypothetical protein	3.27	4.84E-02
SAOUHSC_00358	hypothetical protein	4.30	2.42E-02
SAOUHSC_00585	hypothetical protein	4.52	3.13E-02
SAOUHSC_00600	hypothetical protein	4.43	2.43E-02
SAOUHSC_00808	hypothetical protein	5.03	2.47E-02
SAOUHSC_00826	hypothetical protein	7.08	2.82E-03
SAOUHSC_00828	hypothetical protein	4.19	4.21E-02
SAOUHSC_00962	hypothetical protein	10.62	2.23E-04
SAOUHSC_01024	hypothetical protein	9.20	6.86E-04
SAOUHSC_01422	hypothetical protein	4.03	3.06E-02
SAOUHSC_01458	hypothetical protein	5.69	7.79E-03
SAOUHSC_01817	hypothetical protein	3.42	3.68E-02
SAOUHSC_02394	hypothetical protein	17.29	9.55E-05
SAOUHSC_02401	hypothetical protein	6.43	3.04E-03
SAOUHSC_02432	hypothetical protein	64.86	3.17E-05
SAOUHSC_02442	hypothetical protein	3.70	3.21E-02
SAOUHSC_02470	hypothetical protein	3.47	4.96E-02

SAOUHSC_02572	hypothetical protein	6.77	4.09E-03
SAOUHSC_02616	hypothetical protein	4.15	1.71E-02
SAOUHSC_02650	hypothetical protein	3.50	3.99E-02
SAOUHSC_02702	hypothetical protein	3.21	4.81E-02
SAOUHSC_02732	hypothetical protein	4.03	2.57E-02
SAOUHSC_02876	hypothetical protein	4.62	3.54E-02
SAOUHSC_02950	hypothetical protein	28.07	9.43E-04
SAOUHSC_A00354	hypothetical protein	15.15	2.98E-05

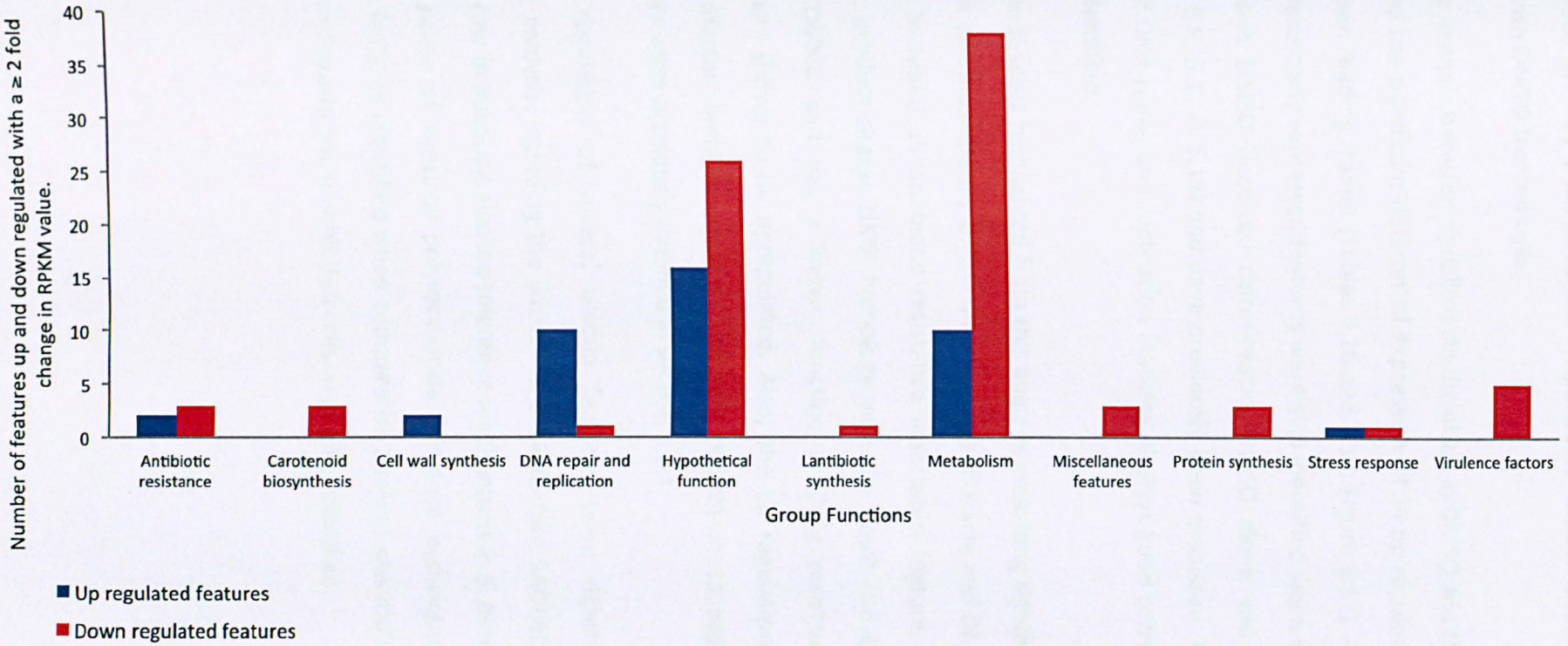

Figure 5.16 Number of features with a ≥ 2-fold change in RPKM value up and down regulated, following treatment with nanoparticle formulated ciprofloxacin compared with blank nanoparticle treated cells.

5.6.5 *S. aureus* SH1000 transcriptional response to DMSO dissolved ciprofloxacin compared with DMSO treated cells.

Comparative analysis between ciprofloxacin dissolved in DMSO and DMSO only treated cells revealed the significant differential expression of 34 up regulated and 105 down regulated open reading frames (Tables 5.16 and 5.17, Figure 5.17). A large proportion (68%) of differentially expressed features were also identified when comparisons were made between DMSO dissolved ciprofloxacin, DMSO alone and uninhibited cells (Tables 5.7, 5.8, 5.12 & 5.13) and have previously been discussed. The degree of up-regulation of DNA repair and replication features displays good correlation with those previously identified.

Several features were highlighted from this analysis indicating significant fold changes in expression when comparing DMSO dissolved ciprofloxacin and DMSO alone treated cells. These included an antibiotic resistance associated feature, SAOUHSC_02418 whose gene product shares 100% homology with the EmrB and QacA subfamily in *S. aureus* JKD6008 and has a known function of drug resistance via transport processes, was shown to be upregulated. Also, the up regulation of the virulence associated cofactor staphylocoagulase (SAOUHSC_00192) was identified. The details of these features were previously outlined in section 5.6.1.

The down regulation of several unique features were determined from this comparative analysis, including the stress response feature SAOUHSC_02441 (*asp23*) that plays a role in initiating alkaline tolerance mechanisms in *S. aureus* (Kuroda *et al.*, 1995). The range of capsular polysaccharide virulence associated and carotenoid biosynthesis features identified when comparative analysis was made between DMSO dissolved ciprofloxacin and uninhibited cells were also identified.

Table 5.16 *S. aureus* SH1000 genes up-regulated following treatment with DMSO dissolved ciprofloxacin compared with DMSO treated cells.

Group functions	*S. aureus* 8325 ORF	*S. aureus* 8325 Gene	*S. aureus* 8325 Gene Product	Fold Change Up Regulated	P-value
DNA repair and replication	SAOUHSC_00776		excinuclease ABC, B subunit	5.69	1.98E-03
	SAOUHSC_00779	*uvrB*	excinuclease ABC subunit B	6.18	1.27E-03
	SAOUHSC_00780	*uvrA*	excinuclease ABC subunit A	5.02	3.73E-03
	SAOUHSC_01262	*recA*	recombinase A	5.17	1.57E-03
	SAOUHSC_01333	*lexA*	lexA repressor	4.31	7.97E-03
	SAOUHSC_01341	*sbcD*	exonuclease SbcD	8.72	1.81E-04
	SAOUHSC_01342	*sbcC*	exonuclease SbcC	16.17	4.11E-06
	SAOUHSC_01363		DNA damage repair protein	55.95	3.17E-10
Antibiotic resistance	SAOUHSC_02418		drug resistance transporter, EmrB/QacA subfamily	3.13	4.08E-02
	SAOUHSC_02420		multidrug resistance protein B	4.32	8.15E-03
Virulence factors	SAOUHSC_00192		staphylocoagulase	3.87	4.92E-02
	SAOUHSC_02571	*ssaA*	secretory antigen SsaA	3.43	2.42E-02
Protein synthesis	SAOUHSC_01078		ribosomal protein L32	2.49	3.07E-02

Metabolism	SAOUHSC_01651	*rpmG*	50S ribosomal protein L33	2.71	3.59E-02
	SAOUHSC_01365		deblocking aminopeptidase	7.84	3.37E-04
	SAOUHSC_01824		thiamine biosynthesis protein ThiI	3.06	3.90E-02
Hypothetical genes					
	SAOUHSC_00182		hypothetical protein	4.01	1.13E-02
	SAOUHSC_00347		hypothetical protein	27.93	7.20E-08
	SAOUHSC_00368		hypothetical protein	4.32	3.71E-02
	SAOUHSC_00396		hypothetical protein	5.09	2.01E-02
	SAOUHSC_00583		hypothetical protein	7.12	3.82E-02
	SAOUHSC_00745		hypothetical protein	10.17	9.33E-03
	SAOUHSC_01331		hypothetical protein	28.99	5.79E-05
	SAOUHSC_01334		hypothetical protein	38.66	2.72E-09
	SAOUHSC_01340		hypothetical protein	3.29	2.87E-02
	SAOUHSC_01343		hypothetical protein	16.21	3.95E-06
	SAOUHSC_01344		hypothetical protein	17.80	4.45E-04
	SAOUHSC_01823		hypothetical protein	3.53	2.06E-02
	SAOUHSC_01976		hypothetical protein	4.41	4.04E-02

	SAOUHSC_02144	hypothetical protein	38.21	5.93E-09
	SAOUHSC_02157	hypothetical protein	12.47	2.08E-05
	SAOUHSC_02294	hypothetical protein	6.38	1.06E-03
	SAOUHSC_02853	hypothetical protein	2.46	1.72E-02
	SAOUHSC_03024	hypothetical protein	4.55	6.37E-03

Table 5.17 *S. aureus* SH1000 genes down-regulated following treatment with DMSO dissolved ciprofloxacin compared with DMSO treated cells.

Group functions	*S. aureus* 8325 ORF	*S. aureus* 8325 Gene	*S. aureus* 8325 Gene Product	Fold Change Down Regulated	P-value
Antibiotic resistance	SAOUHSC_01285	*femC*	factor involved in meticillin resistance and Glutamine synthetase repressor	3.91	1.07E-02
Stress response	SAOUHSC_00204		globin domain-containing protein	3.70	2.14E-02
	SAOUHSC_02441	*asp23*	alkaline shock protein 23	3.49	1.67E-02
	SAOUHSC_02862	*clpC*	ATP-dependent Clp protease, ATP-binding subunit ClpC	14.25	2.28E-05
Carotenoid biosynthesis	SAOUHSC_01990		squalene desaturase	10.81	4.89E-04
	SAOUHSC_02877		squalene synthase	7.43	6.90E-04

	SAOUHSC_02879		squalene desaturase	12.08	3.37E-05
	SAOUHSC_02882		hypothetical protein	4.74	2.14E-02
	SAOUHSC_02881		hypothetical protein	5.55	8.80E-03
Virulence factors					
	SAOUHSC_00114		capsular polysaccharide biosynthesis protein	7.94	1.47E-03
	SAOUHSC_00115	*capB*	capsular polysaccharide synthesis enzyme Cap5B	8.36	3.43E-03
	SAOUHSC_00116	*capC*	capsular polysaccharide synthesis enzyme Cap8C	9.34	1.41E-03
	SAOUHSC_00117	*capD*	capsular polysaccharide biosynthesis protein Cap5D	10.32	8.21E-04
	SAOUHSC_00118	*capE*	capsular polysaccharide biosynthesis protein Cap5E	9.83	1.68E-03
	SAOUHSC_00119	*capF*	capsular polysaccharide synthesis enzyme Cap8F	7.24	3.21E-03
	SAOUHSC_00121	*capH*	capsular polysaccharide synthesis enzyme O-acetyl transferase Cap5H	5.21	1.56E-02
	SAOUHSC_00122	*capI*	capsular polysaccharide biosynthesis protein Cap5I	3.78	4.53E-02
	SAOUHSC_02669	sarZ	transcriptional regulator SarZ	3.15	3.59E-02

Protein synthesis	SAOUHSC_00736		hypothetical protein	3.12	3.71E-02
	SAOUHSC_00767		ribosomal subunit interface protein	2.90	4.78E-02
Metabolism					
	SAOUHSC_00120		UDP-N-acetylglucosamine 2-epimerase	5.75	8.09E-03
	SAOUHSC_00188		pyruvate formate-lyase 1 activating enzyme	16.98	2.80E-06
	SAOUHSC_00187		formate acetyltransferase	12.29	2.35E-05
	SAOUHSC_00285		ABC transporter permease protein	3.29	3.29E-02
	SAOUHSC_00287		ABC transporter ATP-binding protein	3.67	2.26E-02
	SAOUHSC_00608	*adhA*	alcohol dehydrogenase	3.55	2.73E-02
	SAOUHSC_00625		putative monovalent cation/H+ antiporter subunit A	4.17	9.63E-03
	SAOUHSC_00626		putative monovalent cation/H+ antiporter subunit B	3.50	2.21E-02
	SAOUHSC_00627		putative monovalent cation/H+ antiporter subunit C	4.04	1.14E-02

SAOUHSC_00628		putative monovalent cation/H+ antiporter subunit D	3.68	1.78E-02
SAOUHSC_00629		putative monovalent cation/H+ antiporter subunit E	3.18	3.35E-02
SAOUHSC_00632		putative monovalent cation/H+ antiporter subunit G	3.01	4.26E-02
SAOUHSC_00708		fructose specific permease	3.81	1.51E-02
SAOUHSC_00738		proton-dependent Peptide Transporters	3.28	3.03E-02
SAOUHSC_00749		hypothetical protein	3.53	2.44E-02
SAOUHSC_00796	*pgk*	phosphoglycerate kinase	2.67	4.23E-02
SAOUHSC_00797	*tpiA*	triosephosphate isomerase	3.56	6.82E-03
SAOUHSC_00798		phosphoglyceromutase	2.73	3.75E-02
SAOUHSC_00898		argininosuccinate lyase	19.51	1.32E-06
SAOUHSC_00899		argininosuccinate synthase	23.41	8.09E-07
SAOUHSC_00926		oligopeptide ABC transporter ATP-binding protein	7.62	6.90E-03
SAOUHSC_01010		phosphoribosylaminoimidazole-succinocarboxamide synthase	3.98	2.59E-02

SAOUHSC_01011	*purS*	phosphoribosylformylglycinamidine synthase, PurS protein	5.02	1.92E-02
SAOUHSC_01012		phosphoribosylformylglycinamidine synthase I	4.70	1.47E-02
SAOUHSC_01013		phosphoribosylformylglycinamidine synthase II	5.54	1.13E-02
SAOUHSC_01014		amidophosphoribosyl-transferase	5.09	1.60E-02
SAOUHSC_01015		phosphoribosylaminoimidazole synthetase	4.83	1.99E-02
SAOUHSC_01165		uracil permease	3.75	1.69E-02
SAOUHSC_01166	*pyrB*	aspartate carbamoyltransferase catalytic subunit	3.66	2.40E-02
SAOUHSC_01275		hypothetical protein	3.99	1.73E-02
SAOUHSC_01287		glutamine synthetase, type I	4.99	8.01E-04
SAOUHSC_01394		aspartate kinase	5.90	1.70E-02
SAOUHSC_01395		aspartate semialdehyde dehydrogenase	5.57	1.63E-02
SAOUHSC_01396		dihydrodipicolinate synthase	5.73	1.47E-02
SAOUHSC_01397		dihydrodipicolinate reductase	5.31	2.14E-02

SAOUHSC_01398		2,3,4,5-tetrahydropyridine-2-carboxylate N-succinyltransferase	4.48	2.92E-02
SAOUHSC_01416		dihydrolipoamide succinyltransferase	5.21	3.45E-03
SAOUHSC_01418	*sucA*	2-oxoglutarate dehydrogenase E1 component	5.82	3.12E-03
SAOUHSC_01601		alpha-D-1,4-glucosidase	4.75	2.84E-02
SAOUHSC_01709		acetyl-CoA carboxylase, biotin carboxylase	4.77	2.61E-02
SAOUHSC_01991		ABC transporter permease	9.42	6.10E-04
SAOUHSC_02244		succinyl-diaminopimelate desuccinylase	3.51	4.55E-02
SAOUHSC_02270		ammonium transporter	7.86	4.00E-02
SAOUHSC_02387	*ylbE*	oxidoreductase ylbE	3.19	3.33E-02
SAOUHSC_02402		PTS system mannitol-specific transporter subunit IIA	4.34	9.03E-03
SAOUHSC_02403		mannitol-1-phosphate 5-dehydrogenase	4.60	6.81E-03
SAOUHSC_02444		BCCT family osmoprotectant transporter	7.02	6.37E-04
SAOUHSC_02648		L-lactate permease	4.73	4.18E-03

	SAOUHSC_02679	respiratory nitrate reductase, delta subunit	6.01	9.48E-03
	SAOUHSC_02680	nitrate reductase, beta subunit	8.60	2.14E-03
	SAOUHSC_02681	nitrate reductase, alpha subunit	5.04	1.20E-02
	SAOUHSC_02682	uroporphyrin-III C-methyltransferase	6.12	3.80E-03
	SAOUHSC_02683	assimilatory nitrite reductase [NAD(P)H] small subunit	4.42	7.40E-03
	SAOUHSC_02684	assimilatory nitrite reductase [NAD(P)H] large subunit	4.07	3.31E-02
	SAOUHSC_02772	glutamate dehydrogenase	3.47	2.59E-02
	SAOUHSC_02830	D-lactate dehydrogenase	4.45	6.98E-03
	SAOUHSC_02836	phosphinothricin N-acetyltransferase	3.71	2.54E-02
	SAOUHSC_02848	phosphotransferase system (PTS) system glucose-specific transporter subunit IIABC	4.85	4.87E-03
Hypothetical genes				
	SAOUHSC_00189	hypothetical protein	5.16	2.69E-02
	SAOUHSC_00203	hypothetical protein	3.49	2.37E-02
	SAOUHSC_00253	hypothetical protein	4.13	4.93E-02
	SAOUHSC_00358	hypothetical protein	3.43	2.00E-02

SAOUHSC_00405	hypothetical protein	3.35	3.88E-02
SAOUHSC_00609	hypothetical protein	5.41	4.39E-02
SAOUHSC_00807	hypothetical protein	7.74	3.52E-03
SAOUHSC_00808	hypothetical protein	4.59	2.68E-02
SAOUHSC_00820	hypothetical protein	3.09	3.87E-02
SAOUHSC_00821	hypothetical protein	3.26	3.25E-02
SAOUHSC_00828	hypothetical protein	4.18	3.28E-02
SAOUHSC_00923	hypothetical protein	4.26	3.48E-02
SAOUHSC_00924	hypothetical protein	6.64	1.13E-02
SAOUHSC_00925	hypothetical protein	6.39	1.29E-02
SAOUHSC_01707	hypothetical protein	4.26	3.48E-02
SAOUHSC_01708	LamB/YcsF family protein	5.44	1.04E-02
SAOUHSC_01819	hypothetical protein	3.56	2.10E-02
SAOUHSC_01851	hypothetical protein	4.26	4.10E-02
SAOUHSC_01945	hypothetical protein	3.23	4.43E-02
SAOUHSC_02097	hypothetical protein	3.05	4.13E-02
SAOUHSC_02401	hypothetical protein	3.62	2.01E-02

SAOUHSC_02442	hypothetical protein	4.60	1.26E-03
SAOUHSC_02443	hypothetical protein	5.39	1.02E-03
SAOUHSC_02604	hypothetical protein	4.56	6.82E-03
SAOUHSC_02771	hypothetical protein	3.42	2.80E-02
SAOUHSC_02880	conserved hypothetical protein	8.23	5.69E-04
SAOUHSC_03032	hypothetical protein	4.38	2.88E-02

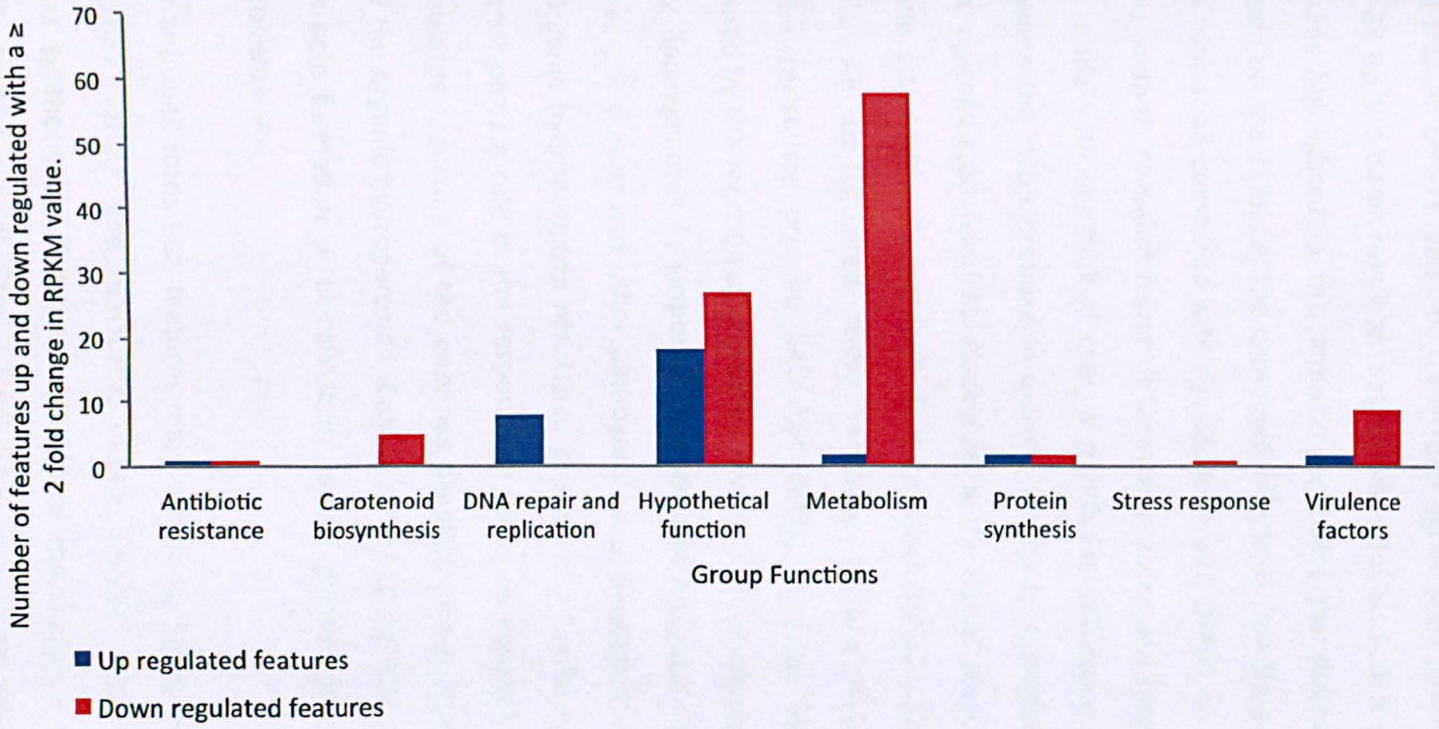

Figure 5.17 Number of features with a ≥ 2-fold change in RPKM value up and down regulated, following treatment with DMSO dissolved ciprofloxacin compared with DMSO treated cells.

5.6.6 *S. aureus* SH1000 transcriptional response to nanoparticle formulated ciprofloxacin compared with DMSO dissolved ciprofloxacin.

Comparative analysis of nanoparticle formulated ciprofloxacin and DMSO dissolved ciprofloxacin treated cells revealed 62 transcripts significantly differentially expressed, with 29 and 33 up and down regulated respectively (Tables 5.18 & 5.19 and Fig 5.18). The differences highlighted in this analysis represent the holistic effects of each delivery system on the cells, *i.e.* the combined effects of ciprofloxacin, excipients and nanoparticle formation compared with ciprofloxacin and DMSO on *S. aureus* SH1000. Although this analysis revealed fewer differentially expressed features compared to the analysis made with uninhibited cells, a significant difference in expression was evident between the two ciprofloxacin delivery methods. Nanoparticle formation of ciprofloxacin up-regulated features associated with: stress response, cell division, virulence factors and primarily metabolic features over DMSO dissolved ciprofloxacin treated cells. An up-regulated stress response feature included an organic hydroperoxide resistance protein, SAOUHSC_01831. Organic hydroperoxides are oxidants formed by the reaction of molecular oxygen with unsaturated fatty acids and catalysed by lipoxygenases in response to pathogen infection. To counteract this oxidative stress, *S. aureus* and other pathogens have developed various antioxidant pathways. Organic hydroperoxide resistance protein is a Cys-based thiol dependent peroxidase that plays a role in the response to peroxide induced stress. Peroxidase activation requires reduction of the enzymes disulfide group formed upon catalytic reduction of the organic hydroperoxide (Cussiol *et al.*, 2010). This result may suggest that nanoparticle formation of ciprofloxacin causes greater cell stress induced by organic hydroperoxides.

Cell division and wall formation features were shown to be up-regulated, including SAOUHSC_01827 (*ezrA)* and SAOUHSC_01142 (*mraZ).* EzrA is required for peptidoglycan synthesis and for the assembly of the divisome at the mid-cell in cytokinesis. In *Bacillus subtilis,* EzrA is involved in preventing aberrant formation of FtsZ rings. It has therefore been suggested that EzrA is essential for growth and cell division in *S. aureus* (Steele *et al.*, 2011). MraZ is also associated with cell division and cell wall biosynthesis. Up-regulation of such features may suggest that the cells are

increasingly required to repair and synthesise cell wall and peptidoglycan in response to nanoparticle ciprofloxacin exposure compared to DMSO dissolved ciprofloxacin exposure.

Other prominent up-regulated features were associated with metabolism, in particular metabolic processes involving lactose metabolism *i.e.* the galactose-6-phosphate isomerases (*lacA* and *lacB*), tagatose 1,6-diphosphate aldolase (SAOUHSC_02452) and tagatose-6-phosphate kinase (SAOUHSC_02453). Assimilation of lactose in *S. aureus* results in the intracellular accumulation of galactose-6-phosphate. This phosphorylated carbohydrate acts as the intracellular inducer of lactose (*lac*) genes and is metabolised to triose phosphates in the glycolytic pathway via tagatose phosphate intermediates, therefore increasing the available substrates for the glycolysis pathway (Rosey *et al.*, 1991). A feature associated with iron uptake and transport, SAOUHSC_02840 was also shown to be up-regulated suggesting nanoparticle formation of ciprofloxacin may encourage intracellular accumulation of iron. There is an intimate link between metabolic processes and virulence gene expression in *S. aureus* to allow for survival and proliferation (Lan *et al.*, 2010). Interestingly, this analysis did not indicate significant differential expression of ciprofloxacin related target features, such as *lexA*, *recA*, and exonucleases. This therefore suggests that nanoparticle formation of ciprofloxacin does not significantly enhance the actions of the antimicrobial agent within the multi-component nanoparticle system. However, these results combined with those observed in Tables 5.5 and 5.6 suggest that nanoparticle formulated ciprofloxacin can reach the intracellular molecular target sites that are associated with ciprofloxacin and other 4-quinolones (Fisher *et al.*, 1989). This therefore suggested that nanoparticle formation may not enhance the bioavailability of ciprofloxacin to *S. aureus* as differential expression in key ciprofloxacin target genes would be anticipated.

The down-regulation of 33 features was observed when comparing nanoparticle formulated ciprofloxacin with DMSO dissolved ciprofloxacin. The leukocidin / hemolysin toxin production associated feature, SAOUHSC_02243, and the superantigen – like protein, SAOUHSC_00399 that is associated with the non-specific activation of T-cells and massive cytokine release (DeLeo & Chambers, 2009 ; Fraser &

Proft, 2008) which is produced as a defense mechanism against the host immune system, were found to be significantly down-regulated. This suggests that metabolic expenditure on such virulence factors may not be required when the cells are treated with nanoparticle formulated ciprofloxacin compared to DMSO dissolved ciprofloxacin.

A range of metabolic features were also found to be significantly differentially expressed, including features associated with energy processing, components of the glycolysis pathway and citric acid cycle. For example: alcohol dehydrogenase, SAOUHSC_00608 that coverts ethanol to acetaldehyde ; L-lactate dehydrogenase, SAOUHSC_00206 that converts lactate to pyruvate and L-lactate permease, SAOUHSC_02648 are all components that produce products which feed into the glycolysis pathway that ultimately lead into the citric acid cycle. The down-regulated response to the increased cell damage induced by nanoparticle formation of ciprofloxacin therefore appears to be focused on virulence factors and processes involved in cellular respiration. Although differential expression was demonstrated between the treatment conditions, the type of features identified are unlikely to account for the enhanced efficacy attributed to using nanoparticle delivery.

Table 5.18 *S. aureus* SH1000 genes up-regulated following treatment with nanoparticle formulated ciprofloxacin compared with DMSO dissolved ciprofloxacin treated cells.

Group functions	*S. aureus* 8325 ORF	*S. aureus* 8325 Gene	*S. aureus* 8325 Gene Product	Fold Change Up Regulated	P-value
Stress response					
	SAOUHSC_01831		organic hydroperoxide resistance protein	13.40	1.04E-11
	SAOUHSC_02381		hypothetical protein	2.26	3.02E-03
Cell division					
	SAOUHSC_01142	*mraZ*	cell division protein MraZ	2.04	2.23E-02
	SAOUHSC_01827	*ezrA*	septation ring formation regulator EzrA	3.47	1.71E-05
Virulence factors					
	SAOUHSC_00668		bacitracin transport system permease protein	2.60	8.69E-04
Protein synthesis	SAOUHSC_01829	*rpsD*	30S ribosomal protein S4	85.24	7.76E-42
Metabolism					
	SAOUHSC_00167		peptide ABC transporter ATP-binding protein	2.04	3.64E-02
	SAOUHSC_00748		iron compound ABC uptake transporter ATP-binding protein	2.08	2.18E-02
	SAOUHSC_02451		PTS system lactose-specific transporter subunit IIA	3.50	3.25E-02

	SAOUHSC_02452		tagatose 1,6-diphosphate aldolase	5.67	2.84E-03
	SAOUHSC_02453		tagatose-6-phosphate kinase	6.00	1.67E-03
	SAOUHSC_02454	*lacB*	galactose-6-phosphate isomerase subunit LacB	9.67	3.58E-06
	SAOUHSC_02455	*lacA*	galactose-6-phosphate isomerase subunit LacA	7.86	4.79E-07
	SAOUHSC_02840		L-serine dehydratase, iron-sulfur-dependent, beta subunit	2.44	6.29E-03
	SAOUHSC_02841		transcriptional regulator pfoR	2.62	6.00E-04
Hypothetical genes					
	SAOUHSC_00409		hypothetical protein	2.29	9.02E-03
	SAOUHSC_00772		hypothetical protein	2.05	4.48E-02
	SAOUHSC_00807		hypothetical protein	2.50	3.84E-02
	SAOUHSC_01122		hypothetical protein	2.40	8.09E-03
	SAOUHSC_01331		hypothetical protein	2.00	1.98E-02
	SAOUHSC_02002		hypothetical protein	3.01	9.64E-05
	SAOUHSC_02105		hypothetical protein	2.71	6.97E-03

	SAOUHSC_02115	hypothetical protein	2.61	1.52E-03
	SAOUHSC_02425	hypothetical protein	2.06	1.28E-02
	SAOUHSC_02534	hypothetical protein	2.50	1.62E-02
	SAOUHSC_02535	hypothetical protein	2.18	2.62E-02
	SAOUHSC_02734	hypothetical protein	5.20	2.40E-04
	SAOUHSC_02813	hypothetical protein	2.29	3.69E-03
	SAOUHSC_A02811	hypothetical protein	9.00	2.21E-02

Table 5.19 *S. aureus* SH1000 genes down-regulated following treatment with nanoparticle formulated ciprofloxacin compared with DMSO dissolved ciprofloxacin treated cells.

Group functions	*S. aureus* 8325 ORF	*S. aureus* 8325 Gene	*S. aureus* 8325 Gene Product	Fold Change Down Regulated	P-value
Antibiotic resistance	SAOUHSC_01285	*femC*	factor involved in meticillin resistance and Glutamine synthetase repressor	2.92	1.16E-04
Virulence factors	SAOUHSC_00399		superantigen-like protein	2.15	3.17E-02
	SAOUHSC_00817		hypothetical protein	2.19	2.16E-02
	SAOUHSC_01456	*piuB*	uncharacterized iron-regulated membrane protein Iron-uptake factor PiuB	2.56	7.68E-04

	SAOUHSC_02243		leukocidin/hemolysin toxin family protein	3.75	2.04E-02
	SAOUHSC_02887		immunodominant antigen A	2.18	1.54E-02
Lantibiotic synthesis					
	SAOUHSC_01953		lantibiotic precursor	2.14	4.29E-02
Protein synthesis					
	SAOUHSC_01678	*rpsU*	30S ribosomal protein S21 / small subunit ribosomal protein S21	2.07	2.19E-02
Metabolism					
	SAOUHSC_00206		L-lactate dehydrogenase	2.23	9.79E-03
	SAOUHSC_00281		formate/nitrite transporter family protein	3.50	1.51E-04
	SAOUHSC_00608	*adhA*	alcohol dehydrogenase	2.28	2.23E-02
	SAOUHSC_00962		hypothetical protein	3.79	1.29E-05
	SAOUHSC_01265		hypothetical protein	2.00	1.71E-02
	SAOUHSC_01287		glutamine synthetase, type I	2.42	2.21E-03
	SAOUHSC_01828		GAF domain-containing protein	10.01	1.34E-16
	SAOUHSC_01830		glycerophosphoryl diester phosphodiesterase	2.76	4.70E-03
	SAOUHSC_02412		hypothetical protein	3.10	5.18E-04

	SAOUHSC_02648	L-lactate permease	2.00	1.10E-02
	SAOUHSC_02681	nitrate reductase, alpha subunit	3.20	2.83E-02
	SAOUHSC_02821	membrane spanning protein	2.11	2.77E-02
	SAOUHSC_02836	phosphinothricin N-acetyltransferase	2.50	1.37E-02
Hypothetical genes	SAOUHSC_00537	hypothetical protein	2.65	7.42E-04
	SAOUHSC_00561	hypothetical protein	2.78	2.99E-04
	SAOUHSC_00962	hypothetical protein	3.79	1.29E-05
	SAOUHSC_01024	hypothetical protein	2.67	6.45E-04
	SAOUHSC_01608	hypothetical protein	2.27	2.71E-02
	SAOUHSC_02391	hypothetical protein	3.06	6.06E-05
	SAOUHSC_02401	hypothetical protein	2.24	1.88E-02
	SAOUHSC_02572	hypothetical protein	2.23	3.67E-03
	SAOUHSC_02685	hypothetical protein	3.40	1.82E-02
	SAOUHSC_02853	hypothetical protein	3.51	2.00E-04
	SAOUHSC_02872	hypothetical protein	2.43	1.72E-02
	SAOUHSC_A00354	hypothetical protein	2.90	2.38E-03

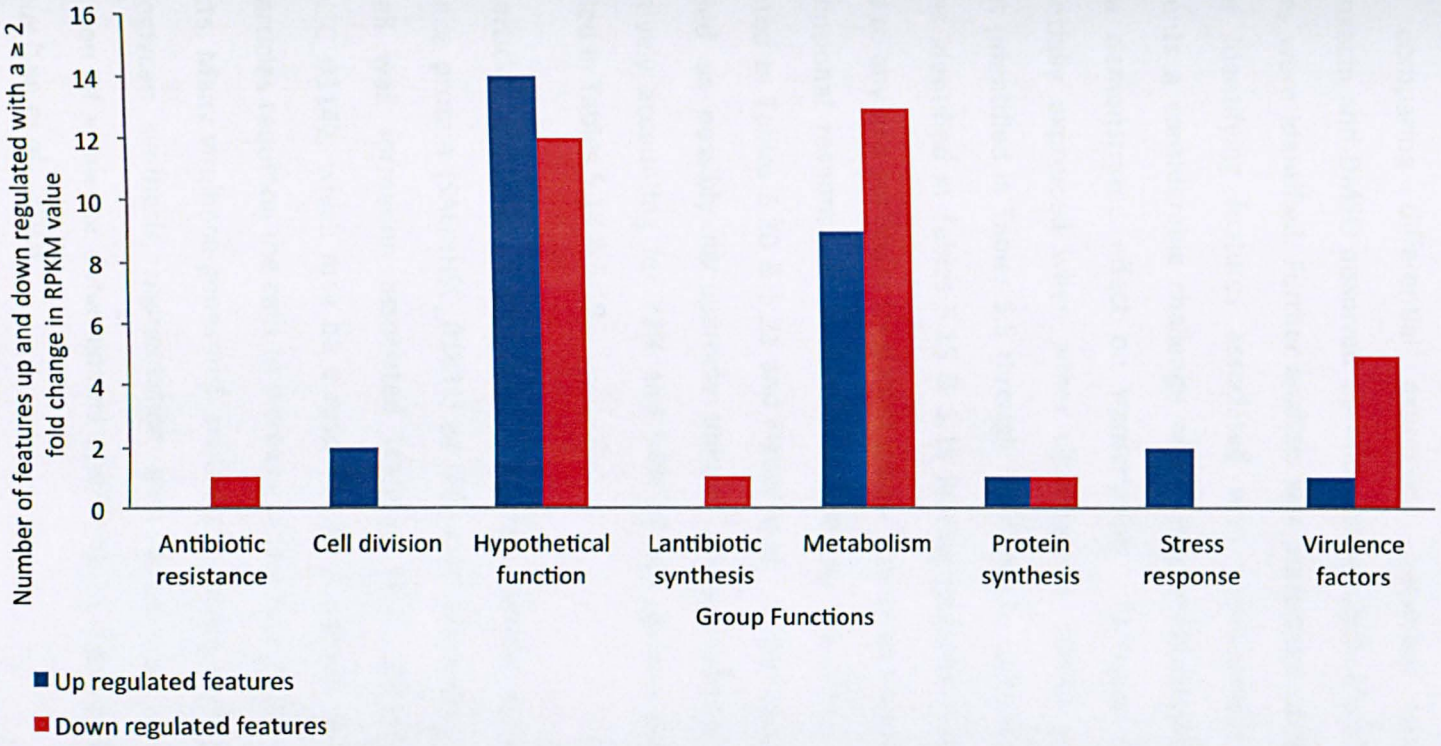

Figure 5.18 Number of features with a ≥ 2-fold change in RPKM value up and down regulated, following treatment with nanoparticle formulated ciprofloxacin compared with DMSO dissolved ciprofloxacin treated cells.

5.6.7 Transcriptional response of *S. aureus* SH1000 to nanoparticle formulated ciprofloxacin compared with DMSO dissolved ciprofloxacin treated cells, with only unique features associated with nanoparticle formation identified.

When comparing differential expression between nanoparticle formulated ciprofloxacin and DMSO dissolved ciprofloxacin treated cells (Tables 5.18 & 5.19), 62 features were identified. Further analysis was performed using the dataset with the aim of identifying features associated with nanoparticle formation only. This represents a considerable challenge when using multi-component systems that all have a demonstrated effect on transcription. Features that were persistently differentially expressed when either ciprofloxacin, DMSO or the excipients were present (identified in Tables 5.5 through Tables 5.17), were removed from the list of features identified in Tables 5.18 & 5.19 leaving features that could not be directly related to any one particular treatment group. The unique features, thought to be the transcriptional response of *S. aureus* SH1000 to the effect of nanoparticles, are presented in Tables 5.20 & 5.21 and Figure 5.19. In this analysis, 39 features were identified as possibly nanoparticle unique, 21 and 18 up and down regulated respectively accounting for 72% and 54% of the up and down-regulated features identified in Tables 5.18 & 5.19.

Nanoparticle associated up-regulated features include an organic hydroperoxide resistance protein (SAOUHSC_01831) as discussed previously. Also, the cell division and cell wall formation associated features EzrA, SAOUHSC_01827 and MraZ, SAOUHSC_01142, which may be a response to increased cell damage imparted by nanoparticles requiring the cells to increase production of cell wall and peptidoglycan products. Many virulence genes in *S. aureus* are co-regulated so that genes affecting peptidoglycan synthesis, pigmentation and metabolism may also influence the production of virulence determinants and have an impact on the pathogenesis of *S. aureus* (Lan *et al.*, 2010).

Some metabolic features also appear to be linked with nanoparticle insult on *S. aureus,* including the lactose metabolism feature *lacA* (SAOUHSC_02455) a galactose-6-phosphate isomerase as described in section 5.6.6. A feature associated with iron

uptake and transport, SAOUHSC_00748 and a feature associated with the conversion of serine to pyruvate that forms part of the gluconeogenesis pathway, SAOUHSC_02840 was also up-regulated. Significant up-regulation (85.24 fold) of the gene *rpsD* (SAOUHSC_01829) also appears to be a nanoparticle associated effect. This 30S ribosomal protein has been characterised in *E. coli* and found to have a range of functions: it is one of two assembly initiator proteins for the 30S subunit and binds directly to 16S rRNA where it nucleates assembly of the 30S subunit; with S5 and S12 it plays an important role in translational accuracy; protein S4 is a translational repressor protein, it controls the translation of the alpha-operon by binding to its mRNA, and it functions as a rho-dependent anti-terminator of rRNA transcription increasing the synthesis of rRNA under conditions of excess protein and permitting a more rapid return to homeostasis (Torres *et al.*, 2001 ; Takyar *et al.*, 2005). Up-regulated features are principally based on: stress response, cell wall synthesis and cell division, aspects of cellular metabolism and a ribosomal protein associated with transcriptional and translational processing events.

A range of down-regulated genes were identified as being associated with nanoparticle formation (Table 5.21). Interestingly, all the down-regulated virulence associated features identified when comparing nanoparticle formulated ciprofloxacin with DMSO dissolved ciprofloxacin treated cells can be attributed to the effects of nanoparticle insult on the cells. This includes the leukocidin / hemolysin associated feature, SAOUHSC_02243 and the superantigen like protein, SAOUHSC_00399, as described in the previous section. The down-regulation of the iron uptake factor *piuB* also appears to be a nanoparticle induced feature. The 30S ribosomal protein S21, SAOUHSC_01678 (*rpsU*) that is required for the initiation of protein synthesis (Versalovic *et al.*, 1993) was shown to be associated with nanoparticle induced effects on the cells. Down-regulation of features were principally associated with: virulence; metabolic energy production and processing.

Table 5.20 *S. aureus* SH1000 genes up-regulated following treatment with nanoparticle formulated ciprofloxacin compared with DMSO dissolved ciprofloxacin treated cells. The transcriptional effects of ciprofloxacin, blank nanoparticle and DMSO were removed, leaving only unique features identified as nanoparticle formation effects.

Group functions	*S. aureus* 8325 ORF	*S. aureus* 8325 Gene	*S. aureus* 8325 Gene Product	Fold Change Up Regulated	P-value
Stress response	SAOUHSC_01831		organic hydroperoxide resistance protein	13.40	1.04E-11
	SAOUHSC_02381		hypothetical protein	2.26	3.02E-03
Cell division	SAOUHSC_01142	*mraZ*	cell division protein MraZ	2.04	2.23E-02
	SAOUHSC_01827	*ezrA*	septation ring formation regulator EzrA	3.47	1.71E-05
Virulence factors	SAOUHSC_00668		bacitracin transport system permease protein	2.60	8.69E-04
Protein synthesis	SAOUHSC_01829	*rpsD*	30S ribosomal protein S4	85.24	7.76E-42
Metabolism	SAOUHSC_00167		peptide ABC transporter ATP-binding protein	2.04	3.64E-02
	SAOUHSC_00748		iron compound ABC uptake transporter ATP-binding protein	2.08	2.18E-02

	SAOUHSC_02451		PTS system lactose-specific transporter subunit IIA	3.50	3.25E-02
	SAOUHSC_02455	*lacA*	Galactose-6-phosphate isomerase subunit LacA	7.86	4.79E-07
	SAOUHSC_02840		L-serine dehydratase, iron-sulfur-dependent, beta subunit	2.44	6.29E-03
Hypothetical genes	SAOUHSC_01122		hypothetical protein	2.40	8.09E-03
	SAOUHSC_02002		hypothetical protein	3.01	9.64E-05
	SAOUHSC_02105		hypothetical protein	2.71	6.97E-03
	SAOUHSC_02115		hypothetical protein	2.61	1.52E-03
	SAOUHSC_02425		hypothetical protein	2.06	1.28E-02
	SAOUHSC_02534		hypothetical protein	2.50	1.62E-02
	SAOUHSC_02535		hypothetical protein	2.18	2.62E-02
	SAOUHSC_02813		hypothetical protein	2.29	3.69E-03
	SAOUHSC_02841		transcriptional regulator pfoR	2.62	6.00E-04
	SAOUHSC_A02811		hypothetical protein	9.00	2.21E-02

Table 5.21 *S. aureus* SH1000 genes down-regulated following treatment with nanoparticle formulated ciprofloxacin compared with DMSO dissolved ciprofloxacin treated cells. The transcriptional effects of ciprofloxacin, blank nanoparticle and DMSO were removed, leaving only unique features identified as nanoparticle formation effects.

Group functions	*S. aureus* 8325 ORF	*S. aureus* 8325 Gene	*S. aureus* 8325 Gene Product	Fold Change Down Regulated	P-value
Virulence factors	SAOUHSC_00399		superantigen-like protein	2.15	3.17E-02
	SAOUHSC_00817		hypothetical protein	2.19	2.16E-02
	SAOUHSC_01456	*piuB*	uncharacterized iron-regulated membrane protein Iron-uptake factor PiuB	2.56	7.68E-04
	SAOUHSC_02243		leukocidin/hemolysin toxin protein family	3.75	2.04E-02
	SAOUHSC_02887		immunodominant antigen A	2.18	1.54E-02
Lantibiotic synthesis	SAOUHSC_01953		lantibiotic precursor	2.14	4.29E-02
Protein synthesis	SAOUHSC_01678	*rpsU*	30S ribosomal protein S21 / small subunit ribosomal protein S21	2.07	2.19E-02
Metabolism	SAOUHSC_00206		L-lactate dehydrogenase	2.23	9.79E-03
	SAOUHSC_01265		hypothetical protein	2.00	1.71E-02
	SAOUHSC_01828		GAF domain-containing protein	10.01	1.34E-16

	SAOUHSC_01830	glycerophosphoryl diester phosphodiesterase	2.76	4.70E-03
	SAOUHSC_02821	membrane spanning protein	2.11	2.77E-02
Hypothetical genes				
	SAOUHSC_00537	hypothetical protein	2.65	7.42E-04
	SAOUHSC_00561	hypothetical protein	2.78	2.99E-04
	SAOUHSC_01608	hypothetical protein	2.27	2.71E-02
	SAOUHSC_02391	hypothetical protein	3.06	6.06E-05
	SAOUHSC_02685	hypothetical protein	3.40	1.82E-02
	SAOUHSC_02872	hypothetical protein	2.43	1.72E-02

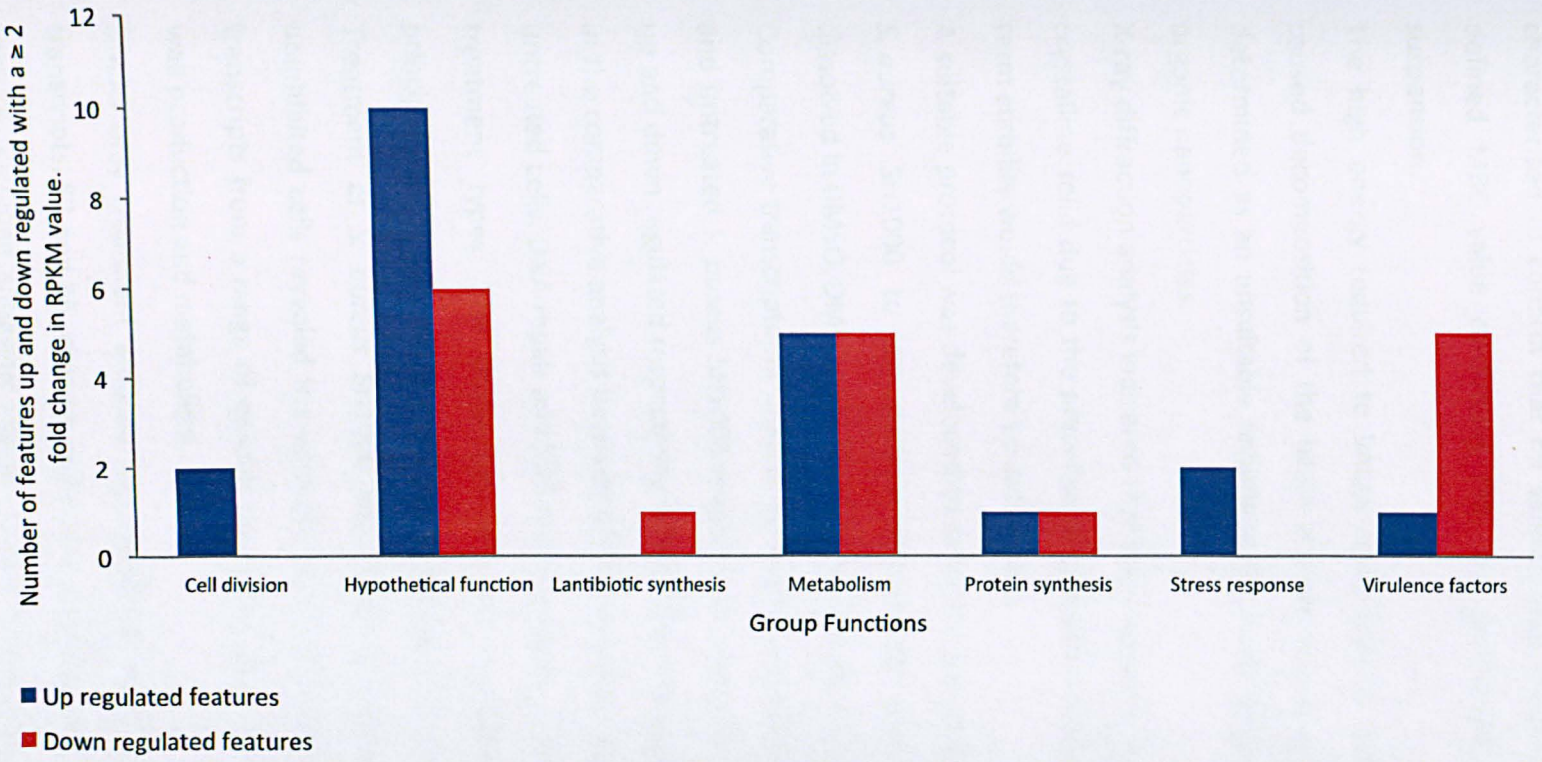

Figure 5.19 Number of features with a ≥ 2-fold change in RPKM value up and down regulated, following treatment with nanoparticle-formulated ciprofloxacin compared with DMSO dissolved treated cells. The transcriptional effects of ciprofloxacin, blank nanoparticle and DMSO were removed, leaving only unique features identified as nanoparticle formation effects.

5.7 Key points

- The ciprofloxacin loaded nanoparticle preparation (50/27/55) was further characterised to confirm that no spontaneous micellisation occurred at the defined MBC value confirming that the preparation was a nanoparticle suspension.
- The high energy required to image small organic nanoparticles using SEM caused decomposition of the labile organic compounds and was therefore determined as an unsuitable technique for morphological characterisation of organic nanoparticles.
- X-ray diffraction analysis indicated that the nanoparticle preparation exists as a crystalline solid due to the presence of ciprofloxacin and pluronic F127; long-term stability would therefore be anticipated.
- A suitable protocol was developed to ascertain the transcriptional response of *S. aureus* SH1000 to nanoparticle formulated ciprofloxacin, ciprofloxacin dissolved in DMSO, DMSO only, blank nanoparticles and uninhibited cells.
- Comparative transcriptomic analysis between nanoparticle loaded ciprofloxacin and untreated *S. aureus* SH1000 revealed 37 and 109 transcripts significantly up and down regulated respectively; 67% of these features were also identified in the comparative analysis between DMSO dissolved ciprofloxacin treated and untreated cells. DNA repair and SOS response genes were up-regulated in both treatment types. The down-regulation of virulence associated features principally linked to capsular polysaccharide biosynthesis were also noted.
- Treatment of *S. aureus* SH1000 with blank nanoparticles compared with uninhibited cells revealed the up-regulation of 33 and down-regulation of 19 transcripts from a range of cellular processes, principally associated with cell wall production and metabolism.
- DMSO only treatment induced the significant differential expression of 88 transcripts, 52 and 36 were up and down regulated respectively. Up-regulated features included antibiotic resistance (*bcrA*) and virulence (*ssaA*) associated components. The leukocidin / hemolysin toxin associated features and

metabolic processes including parts of the gluconeogenesis pathway and amino acid cycles were shown to be down-regulated.

- Comparative analysis between ciprofloxacin loaded and blank nanoparticles revealed the differential expression of 41 and 84 up and down regulated transcripts respectively. The dominant effects of ciprofloxacin on expression appeared to diminish blank nanoparticle associated features. However, unique cell wall synthesis and cell stress related transcripts were shown to be up-regulated, possibly suggesting that nanoparticle loaded ciprofloxacin is perceived by *S. aureus* SH1000 as a stressor.
- Comparative analysis between DMSO dissolved ciprofloxacin and DMSO treated cells revealed significant differential expression of 34 and 105 up and down regulated transcripts. Up-regulated features include antibiotic resistance and virulence associated transcripts. The stress response feature *asp23* that plays a role in alkaline tolerance was down regulated in this comparative analysis.
- Comparative analysis between nanoparticle formulated ciprofloxacin and DMSO dissolved ciprofloxacin represented the holistic effects of each delivery system on *S. aureus* SH1000. In this analysis, 29 and 33 transcripts were up and down regulated respectively suggesting differences in expression between the two ciprofloxacin delivery methods. No significant differential expression was observed in ciprofloxacin related features, suggesting nanoparticle formation of ciprofloxacin does not significantly enhance the actions of the antimicrobial compared to the solvent dissolved delivery. Nanoparticle formation of ciprofloxacin induced the up-regulation of transcripts associated with stress response, cell division, cell wall formation, virulence factors and metabolic pathways linked with lactose assimilation compared to DMSO dissolved delivery.
- Virulence associated features were found to be down regulated in response to nanoparticle loaded ciprofloxacin. Although nanoparticle formation caused no differential expression in ciprofloxacin targets, a number of stress response, virulence, cell division and metabolic pathways were differentially expressed.

However it is unlikely that the differential expression of these features is likely to account for the enhanced antimicrobial activity caused by the nanoparticle preparation.

- 39 nanoparticle unique open reading frames as outlined in section 5.6.7 were identified, with 21 and 18 up and down regulated respectively. Nanoparticle associated up-regulated transcripts included the organic hydroperoxide resistance protein and cell wall formation features, suggesting the presence of nanoparticles induces stress responses and may cause cell wall damage in which the cell is required to increase production of cell wall and peptidoglycan precursors and products to maintain cell integrity. Down-regulated responses to nanoparticles principally included the virulence associated features, possibly suggesting energy expenditure on such components when the cells are exposed to nanoparticles is not required.
- This analysis highlights the transcriptional complexity of cells as they respond to chemical stimulus comprising of multi-component systems. The investigation suggests nanoparticle delivery causes differences in expression compared to a conventional delivery method and has indicated that nanoparticle exposure alone induces transcriptional differences. However, it is unlikely that the identified differentially expressed features found in this study accounts for the observed enhanced efficacy when utilising ciprofloxacin organic nanoparticles. The results in Table 5.9 also indicated similar fold changes in DNA repair and replication genes between ciprofloxacin delivery methods. Based on these results it is suggested that differential molecular targeting does not account for the enhanced antimicrobial activity exhibited when using nanoparticle formulated ciprofloxacin.
- This research represents the first transcriptomic analysis of antimicrobial loaded organic nanoparticle treated bacteria. The data indicates that the hydrophobic antimicrobial ciprofloxacin can be processed into stable nanoparticles for aqueous delivery. The potential advantages of utilising such antimicrobial delivery platforms include enhanced efficacy of inhibition compared to conventional delivery, the ability to use a reduced dose for comparable antimicrobial activity, and the ability to use an organic solvent free

delivery system. The findings could have wider implications for the development of nano-medicine and should provide a useful resource for future studies on the use of organic nanoparticles as drug delivery vehicles.

Chapter 6

General Discussion

Nanotechnology is an emerging field seeking to exploit distinct technological advances gained by controlling the structure of materials at reduced dimensional scales. The manipulation of materials at the nano-scale is expected to be a critical driver of economic growth and development in this century (Venugopal *et al.*, 2008). The high surface area to volume ratios of nanomaterials is thought to contribute to effective antimicrobial activities (Weir *et al.*, 2008). Large numbers of antimicrobial candidates are falling into class II of the biopharmaceutical classification system. These materials exhibit high permeability but low solubility that results in inadequate bioavailability, pharmacokinetics and stability (Lipinski, 2000 ; Rabinow, 2004 ; Kingsley *et al.*, 2006). Nanoparticle formation can increase the therapeutic efficacy of antimicrobial compounds because their biodistribution follows that of the carrier rather than depending on the physiochemical properties of the active molecule itself. Key pharmacokinetic characteristics of antibiotics including improved solubility, controlled release, and site specific targeting can be achieved by employing appropriate nano-carriers (Allaker & Ren, 2008 ; Mora-Huetas *et al.*, 2010). Nanoparticles have been shown to exhibit a higher intracellular uptake compared with microparticles. The rate of uptake can also be manipulated through changes made to the composition of the nanoparticle (Pinto *et al.*, 2006). Nanotechnology is at the forefront of developing efficient drug delivery systems and is beginning to address many of the shortcomings of traditional drugs currently on the market. Nanoparticles have the ability to improve the biocompatibility of compounds for the treatment of numerous diseases and infections (Patel *et al.*, 2010). The term 'nanoantibiotics' has recently been coined to describe nano-materials that increase the effectiveness of antibiotics (Huh & Kwon, 2011).

This thesis further developed the work conducted by Zhang *et al.* (2008a) that reported a generic method for producing organic nanoparticles using a modified emulsion-templating and freeze drying process to produce aqueous nanodispersions of Triclosan. The nanoparticle formulated antimicrobial was shown to produce lower MIC values than co-solvent dissolved Triclosan when tested against *Corynebacterium* (Zhang *et al.*, 2008a). A variant of this novel technology was utilised as outlined in section 2.4 to produce nanoparticle preparations of poorly water-soluble antifungals, biocides and an antibiotic. The nanoparticles were subsequently characterised and tested for inhibitory activity against a range of Gram-negative and Gram-positive bacteria, and fungi as appropriate. The results suggested that nanoparticles produced using the aforementioned technique, were usually more inhibitory than the antimicrobials delivered by conventional means. Increasing numbers of methodologies and applications of nanoparticle technologies are evident in the published literature using both inorganic and organic systems (Morones *et al.*, 2005 ; Cousins *et al.*, 2007 ; Esmaeili *et al.*, 2007 ; Kisich *et al.*, 2007 ; Peng *et al.*, 2008 ; Jeong *et al.*, 2008 ; Haggstrom *et al.*, 2010). However, the technology used in this study has been shown to be applicable to a range of antimicrobials rather than simply being tested in a single system.

The antimicrobial activity of the nanoparticle preparations was shown to be significantly dependent upon design, a conclusion that has also been identified in previous studies (Das *et al.*, 2010 ; Bozkir & Saka, 2005 ; Dillen *et al.*, 2004). MIC values ranging from 2.86 $\mu g\ ml^{-1}$ to > 500 $\mu g\ ml^{-1}$ were observed through modifications to the choice of excipient used in the nanoparticle composition, despite the antimicrobial loading ratio remaining constant at 10% $^{w}/_{w}$. The data obtained from a generic materials screen were subsequently utilised in the computer-based application Design of Experiment (DOE MODDE^{TM}). Although the model's significance weighting was reduced due to problems with formulating the suggested nanoparticle preparations, several trends were identified: increased dichlorophen and gelatin loading ratios generally increased MIC values and increased SDS and hydroxy propyl methyl cellulose ratios generally decreased MIC values (Fig 4.2.). However different trends were observed when *E. coli* was used as the test organism compared to *S. aureus* SH1000,

MRSA-252 and *C. albicans*. This is likely to be a reflection of the differences in the organism's sensitivity to the individual components of the nanoparticle and to its cell wall composition. To determine if modifications to nanoparticle design influenced the physical characteristics of the nanosuspension, each preparation was sized and zeta potential determined as outlined in 2.5.1. It has previously been suggested that reducing particle size enhances efficacy because of increased dissolution rates and therefore bioavailability (Hu *et al.*, 2004 ; Belesti *et al.*, 2005 ; Jiang *et al.*, 2008). No correlation between the size of the prepared nanoparticles and antimicrobial efficacy was observed in this study. The loading ratio of drugs used in the nanoparticle preparation was previously shown not to influence nanoparticle size when prepared using techniques different to those used in this study (Pereira *et al.*, 2008 ; Joo *et al.*, 2008). However, Quintanar *et al.* (1998) and Stella *et al.* (2007) suggested that increased drug loading ratio caused an increase in nanoparticle size. This study identified no correlation between antimicrobial loading ratio and nanoparticle size. Zeta potential mainly depends on the chemical nature of the excipients and the pH of the dispersion medium. No specific trends were observed regarding zeta potential behaviour and efficacy of the nanoparticle suspensions, a feature that has also been identified in the published literature (Mora-Huertas *et al.*, 2010). The variation in observed inhibitory activity between formulations could not therefore be linked to the expressed nanoparticle characteristics. Some possible explanations for such variability in efficacy include the degree of antimicrobial partitioning that may have enabled increased drug concentration at the site of action. This explanation was used by Haas *et al.* (2009) to justify the observed increased quinine concentration in red blood cells when quinine was nano-encapsulated. Differences in nanoparticle number may explain differences in activity. Reduced loading ratio of antimicrobial and increased loading ratio of excipients are suggested to increase the number of particles produced. Increased particle number potentially increases the rate of antimicrobial dissolution and therefore bioavailability. However, a balance between the advantages gained with increased particle number and the availability of sufficient antimicrobial to initiate an antimicrobial affect would be anticipated. As previously outlined, nanoparticle number studies were not possible here due to the small size of the particles used in the investigation. Generic trends were however evident from the modeling data

against the organisms investigated. It is suggested that fine-tuned optimisation can only be achieved through gradual stepwise modifications in the type and loading ratios of antimicrobial and excipient materials. Nanoparticles should be designed specifically for their intended target organism and method of application to achieve greatest efficacy.

This study has shown that no correlation exists between the antimicrobial activity of the blank nanoparticles and the antimicrobial loaded equivalents (Tables 3.6, 4.2 & 4.5). Examination of a series of defined controlled materials prepared for one formulation also confirmed that the nanoparticle preparation was more inhibitory than a micellisation and unprocessed feedstock solution (Table 4.5), even though low MIC values were obtained when these controls were tested against *C. albicans* and *S. aureus*. The same MIC values were obtained when both the micellisation and feedstock controls were tested against *S. aureus*. This would suggest that a synergy between the water stirred dichlorophen, SDS and HPMC had occurred in the micellisation control. However, the same trends were not replicated when the micellisation and feedstock controls were tested against *E. coli* and *C. albicans* and therefore enhanced efficacy attributed to synergy can only be suggested.

A potential synergy between the antimicrobials and the excipients used in the nanoparticle preparations may exist. The synergistic effects between the surfactant and the antimicrobial are likely to be most dominant within the system. For example, phenols and substituted phenols such as pentachlorophenol and dichlorophen induce physical disruption and partial solubilisation of the cell wall and membrane (Gilbert & McBain, 2003). Anionic surfactants such as SDS and sodium lauryl ether sulphate reduce surface and interfacial tensions by accumulating at the interface of immiscible components and increasing the mobility and solubility of hydrophobic components. Surfactants can therefore interact with microbial proteins and modify enzyme conformation that alters activity, stability and specificity (Singh *et al.*, 2007). It is less likely that a synergistic effect between non-ionic surfactants and antimicrobials exists, for example, in the ciprofloxacin and Pluronic F127 preparations as reduced membrane disruption imparted by the surfactant would be anticipated. However, the RNA-Seq

results indicated significant differential expression (ca. 2-3 fold changes) due to exposure to blank nanoparticles suggesting the material combinations do impart changes within the cell at a molecular level that may act synergistically with the actions of ciprofloxacin.

Collectively, the control results suggest a synergistic effect between the materials may account for some of the improvements in inhibitory efficacy. However, the nanoparticle formulation of the materials appeared to further enhance the antimicrobial properties of dichlorophen compared to un-processed equivalents.

The data discussed above indicate interesting observational features of the novel nanoparticle formulations, and previous studies albeit using alternative technologies have highlighted the advantageous properties of using a nanoparticle approach. Little research has however been focused on explaining or demonstrating why nanoparticles are more inhibitory than their bulk material equivalents. The difficulty of investigating and effectively quantifying nanoparticle-cell interactions is the most likely explanation for this limited understanding. However, the already widespread introduction of products containing some form of nanotechnology, raises concerns regarding the possibility of unexpected toxicity issues and uncertainties surrounding environmental impact and persistence. Further research into the interactions of nanoparticles with both prokaryotes and eukaryotes are essential (Ju-Nam & Lead, 2008 ; Nagarajan, 2008 ; Seaton *et al.*, 2010).

The failure to firmly identify correlations between physical nanoparticle characteristics and inhibitory activity, suggested an alternative approach was required. Rather than studying biochemical and biophysical interactions, determining the molecular response of bacteria to nanoparticle exposure and comparing this to the response to an organic co-solvent dissolved antimicrobial was identified as a viable approach. Although some studies offer details about the molecular-cell response to inorganic nanoparticles (Lok *et al.*, 2006 ; Pelletier *et al.*, 2010), no such studies were identified in the published literature regarding organic systems. This thesis presented the development of novel ciprofloxacin organic nanoparticles. Physical characterisation and molecular mode of

action analyses were subsequently performed to identify if differences in inhibitory activity between treatment conditions could be attributed to differential gene expression.

Next-generation high-throughput DNA sequencing techniques have opened up a range of new opportunities in life sciences and biomedicine (Hall, 2007 ; Wilhelm, 2009). The sequencing technologies can be exploited not only to analyse static genomes but also dynamic transcriptomes via the application of RNA-Seq (Marguerat & Bahler, 2010). Examples of digital transcriptomics using RNA-Seq are becoming increasingly evident in the published literature (Yoder-Himes *et al.*, 2009 ; Isabella & Clark 2011). RNA-Seq was identified as a suitable technique to determine if differential expression existed between ciprofloxacin organic nanoparticle and solvent dissolved ciprofloxacin treated cells.

Following the sequencing of five *S. aureus* transcriptomes, seven pairwise comparisons of the generated RPKM values revealed that all treatment conditions induced differential expression within the parameters set. The greatest fold changes were observed when ciprofloxacin was present regardless of delivery method. The results indicated 67% similarity in differentially expressed features between ciprofloxacin delivery methods when compared with untreated cells. The pairwise comparative analysis between nanoparticle formulated ciprofloxacin and DMSO dissolved ciprofloxacin did however reveal differential expression of 62 open reading frames. The most noticeable of these included the up regulation of the stress response feature SAOUHSC_01831, an organic hydroperoxide resistance protein. Organic hydroperoxides are oxidants normally formed by the host in response to pathogen infection (Cussiol *et al.*, 2010). The cell wall and cell division genes *mraZ* and *ezrA* were also up regulated. The antibiotic resistance gene *femC* and the virulence-associated feature SAOUHSC_02243 linked with leukocidin / hemolysin toxin production were shown to be down regulated. Further analysis of the data set identified that 63% of these open reading frames were thought to be uniquely expressed due to nanoparticle exposure and included the previously outlined features except *femC*. However, differential expression was observed indicating variations in molecular mode of action

between ciprofloxacin delivery methods. The types of genes identified as differentially expressed, are unlikely to account for the enhanced efficacy attributed to nanoparticle delivery of ciprofloxacin.

The results presented in Table 5.9 which compare up-regulated DNA repair and replication genes that are known ciprofloxacin targets (Drlica & Zhao, 1997 ; Drlica *et al.*, 2008) indicated similar fold changes in expression between delivery methods. Ciprofloxacin must entre bacterial cells before it can exert an antimicrobial effect (Berlanga *et al.*, 2004). It can be deduced that nanoparticle formulated ciprofloxacin causes inhibition of *S. aureus* via the conventional target genes *i.e.* nanoparticle formulation does not restrict antimicrobial availability to target sites and nanoparticles primarily do not exert their inhibitory effect using alternative mechanisms compared to solvent dissolved delivered ciprofloxacin. This therefore suggests that ciprofloxacin is effective as a nanoparticle even when the molecular target site for the antimicrobial is intracellular. It is possible that nanoparticle formation of ciprofloxacin promotes the interaction of the antimicrobial with the cell surface, thus permitting increased penetration of ciprofloxacin into the cell and therefore enhanced efficacy. The large size of the ciprofloxacin nanoparticles, relative to *S. aureus* cells means the bulk nanomaterial is unlikely to entre the cell. The use of radiolabeled *e.g.* ^{14}C or ^{3}H ciprofloxacin could be used to investigate if nanoparticle formation enhanced the intracellular accumulation of ciprofloxacin compared to DMSO delivered ciprofloxacin in *S. aureus*. However, accurate quantification of accumulation is likely to be technically challenging and the radiolabeling of the antimicrobial may alter how ciprofloxacin interacts with the cell. Another method to investigate nanoparticle-cell interaction could combine imaging with the use of chemically florescent or quantum dot labelled ciprofloxacin nanoparticles. This could be used to identify where the nanoparticles are accumulating and whether the material entres the cell.

The RNA-Seq results suggested that from a molecular perspective increased bioavailability due to reduced particle size, increased particle number, or increased antimicrobial partitioning that is thought to increase the local concentration of ciprofloxacin, is unlikely to be the explanation for the enhanced efficacy attributed to

ciprofloxacin nanoparticle delivery. This was suggested because of the similarity in expression levels of known ciprofloxacin targets between the treatments tested, *i.e.* if increased ciprofloxacin bioavailability was observed then greater up-regulation of ciprofloxacin target genes would be anticipated. These findings therefore contrast with those identified in previous studies that suggested increased efficacy was attributed to increased bioavailability due to nanoparticle delivery (Hu *et al.*, 2004 ; Haas *et al.*, 2009 ; Kanaujia *et al.*, 2011). The RNA-seq results also contrast with those presented in Figure 4.3 that indicated enhanced dissolution of dichlorophen when nanoparticle formulated, compared to a water stirred dichlorophen and excipient mixture. However, to develop a more conclusive assessment of the link between bioavailability, efficacy of inhibition and differential molecular targeting, a dissolution test comparing the ciprofloxacin preparation 50.27.55 and a DMSO dissolved dissolution assay would be required. Also evident from the Cirz *et al.* (2007) study was the similarity in the type of up regulated DNA repair and replication genes at 30 min post treatment addition compared to this study even though an alternative experimental protocol and method of gene expression assessment were used.

As previously outlined, limited investigation has been conducted on the molecular mechanisms that account for the bacterial response to organic nanoparticles. Pelletier *et al.* (2010) performed microarray analysis to elucidate the global transcriptomics of *E. coli* upon exposure to CeO_2 nanoparticles. It was reported that CeO_2 nanoparticles were inhibitory to *E. coli* and that inhibitory activity decreased with increased nanoparticle size. However growth comparisons were not made with the unformulated cerium chloride. In the microarray experiments it was reported that there was no significant differential gene expression between CeO_2 nanoparticle and the cerium chloride treated *E. coli.* Only eight genes were significantly differentially expressed, the majority involved in sulphur metabolism. However, different concentrations of CeO_2 and cerium chloride were used in the microarray experiment and therefore a treatment concentration affect needs to be considered when interpreting the results (Pelletier *et al.*, 2010). Lok *et al.* (2006) performed a proteomic analysis on the mode of action of silver nanoparticles in *E. coli.* Silver nanoparticles were found to be more inhibitory than unprocessed silver nitrate when tested against *E. coli*, but there were

no dramatic global changes in the proteomes of *E. coli* between treatment conditions. However, the expressions of eight proteins were specifically stimulated in the silver nanoparticle treated cells. Analysis revealed alterations in the expression of cell envelope and heat shock proteins. Envelope proteins are induced during stress conditions and guard against the entry of foreign substances. The heat shock proteins expressed have chaperone functions against stress induced protein denaturation. However, different concentrations of silver nanoparticles and silver nitrate were used to treat the *E. coli* cells and therefore again concentration differences must be considered. It was also shown that silver nanoparticles induced loss of intracellular potassium and thus loss of proton motive force and reduction in ATP levels. (Lok *et al.*, 2006). Collectively, the findings presented by Pelletier *et al.* 2010 and Lok *et al.* 2006 indicate that nanoparticle treatment utilising inorganic systems, does not induce significant differential expression in the bacterial transcriptome or proteome compared to conventional or unformulated equivalents. The results presented in this thesis highlighted differential gene expression between the nanoparticle formulated and DMSO dissolved ciprofloxacin treated *S. aureus* SH1000. However, it is suggested that differential molecular targeting is unlikely to account for the enhanced efficacy attributed to nanoparticle delivery, due to the types of genes identified.

Attempts to resolve the problems associated with antimicrobial resistance have focused on discovering new antimicrobials and the chemical modification of existing compounds. The challenging and dynamic pattern of infectious disease and the emergence of strains resistant to many conventionally available antimicrobials means that there is an increasing demand for long-term solutions to these problems (Taylor *et al.*, 2002). The design, discovery and delivery of antimicrobial compounds with improved efficacy and avoidance of resistance acquisition are therefore highly sought after (Turos *et al.*, 2007). The use of nanoparticles for the delivery of antimicrobial compounds in overcoming resistant pathogens has been identified as a possible alternative to current approaches (Allaker & Ren, 2008). One method is to incorporate more than one antimicrobial into the same nanoparticle for concomitant delivery (Zhang *et al.*, 2010b). Another approach is to combine antibiotics with antimicrobial nanoparticles. For example, the antibacterial activities of ampicillin, kanamycin and

chloramphenicol were increased in the presence of silver nanoparticles when tested against *Salmonella typhi, E. coli, S. aureus* and *Micrococcus luteus*. The authors suggested increased antimicrobial efficacy was attributed to the synergistic effect of the silver nanoparticle – antibiotic complex leading to increased cell damage (Fayaz *et al.*, 2010). It has become evident that overcoming antibiotic resistance by developing more powerful antibiotics can only lead to limited and temporary success and eventually contributes to the development of greater resistance. Nanoparticles enable the combination of multiple independent and potentially synergistic materials on the same platform in order to enhance antimicrobial activity and potentially limit resistance acquisition to antibiotics (Huh & Kwon, 2011).

A detailed understanding of the *in-vivo* biodistribution of nanoparticles will be required in the elucidation of efficacy and safety of such delivery systems in humans and animals (Almeida *et al.*, 2011). Nanoparticles can improve the pharmacokinetics and pharmacodynamics of drugs and may be particularly useful for increasing the circulation time for rapidly excreted drugs. However, the complexity of *in-vivo* systems imposes multiple barriers that can potentially inhibit efficacy of nanoparticle delivery systems. Limited penetration across the vascular endothelium and uptake by the reticuloendothelial system potentially impedes the effectiveness of nanoparticle delivery. Current nanodelivery systems rely on passive transvascular exchange and tissue accumulation. Physical properties such as nanoparticle size, morphology, surface chemistry and charge influence the biodistribution profile and pharmacokinetics of nanoparticles (Chrastina *et al.*, 2011). For example, increased nanoparticle size displayed a positive correlation with increased adsorption to the surface, and uptake of nanoparticles by macrophages (Fang *et al.*, 2006; Owens & Peppas, 2006).

The kinetics of nanoparticle clearance from circulation is related to the ability of nanoparticles to clear the drug and will impact on the drug level in the blood and the uptake of the drug into particular tissue compartments. Therefore, nanoparticle clearance has a direct influence on therapeutic effect. For systemic delivery, the delay of reticuloendothelial system clearance of nanoparticles from circulation would improve pharmacokinetics of drug delivery. In particular it would increase the mean

residence time, area under curve (AUC) and elimination half-life of the drug loaded nanoparticles. Increasing residence time in the blood will statistically increase the chance of the drug reaching the target, potentially elevating uptake in the target tissue compartment leading to improved therapy (Chrastina *et al.*, 2011).

There remains limited and conflicting information in the published literature on the *in-vivo* immunological response to nanoparticles. Characterising the cellular level distribution of nanoparticles in the liver, spleen and lymph nodes will better elucidate particle *in-vivo* toxicity and permit greater understanding of the inflammatory or immune suppression properties of the nanomaterial. Further understanding of the immune response to nanomaterials will be essential as a number of preparations have displayed promising vaccine carrier properties, owing to their interactions with dendritic and other antigen presenting cells (Klippstein & Pozo, 2010; Almeida *et al.*, 2011).

The results presented in this thesis have potential significance for Iota NanoSolutions in the targeting and future development of the nanoparticle technology. The most significant findings from the study were: the improvement in inhibitory efficacy attributed to nanoparticle formation compared to conventional organic co-solvent dissolved delivery for most of the antimicrobials investigated, and the variability in the inhibitory efficacy attributed to the design of the nanoparticles. The results suggested that step-wise modification of nanoparticle design and the tailoring of each preparation to the required application of the nanosuspension were likely to be the most successful route for optimisation of nanoparticle efficacy. The results from the RNA-Seq experiments highlighted 62 differentially expressed features between the nanoparticle and DMSO dissolved ciprofloxacin preparations. However, the differential expression of a number of features within particular groups (*e.g.*) stress response were not identified. This combined with the observation that gene expression levels in known ciprofloxacin targets were not shown to be significantly altered between treatment types suggested that nanoparticle formation of ciprofloxacin did not induce differential molecular targeting. This finding has potential significance for Iota NanoSolutions. If the nanoparticles induce no identifiable modification to the mode of

action related to the active compound, fewer barriers will potentially exist in developing ciprofloxacin or other active pharmaceutical ingredients using the same technology, for clinical trials and ultimately developing a product for market. Although not investigated in this study, issues related to mammalian cell cytotoxicity, drug accumulation, distribution, metabolism and excretion would require investigation prior to clinical trials. These studies may also suggest why the nanoparticle formulated antimicrobial exhibited greater efficacy compared with the co-solvent dissolved equivalent.

Nanotechnology presents significant opportunity for economic and technological development in a range of sectors (Defra, 2007). It is anticipated that the sale of products employing nanotechnology will reach $1 trillion per annum by 2015 with medically related products alone occupying $53 billion in this market (Teow *et al.*, 2011). However, there remains little data on the toxicity of nanoparticles as carriers for functional compounds. The absence of meaningful toxicity data for nanoparticles has fostered a perception that many nanoparticulate preparations are inherently hazardous. As a consequence, the success of nanotechnology will require assurances that the products or applications being developed are safe from a health, safety and environmental standpoint (Warheit, 2010). This will require continued concerted evaluations of such aspects by scientists funded by government departments, the research councils, and industry (Defra, 2007).

The advantageous features of the novel organic nanoparticle technology compared to conventional delivery methods are evident throughout this thesis. The most significant of these are greater potency and the ability to use an aqueous medium to deliver hydrophobic compounds. The approaches taken in this investigation to elucidate nanoparticle mode of action are valid and challenge some current understandings. However, the study was unable to resolve the mechanisms underpinning the enhanced efficacy attributed to nanoparticle delivered antimicrobials. Future work could investigate if antimicrobial nanoparticles induce cell lysis that may account for increased efficacy. This could be performed using bacterial viability assays combined with cell imaging. The *in-vivo* assessment of antimicrobial nanoparticle activity would

also represent an interesting line of inquiry. The findings described in this thesis provide a useful resource for future studies investigating the design, application and mode of action of organic nanoparticles.

Chapter 7

References

Abarca, M. L., Accensi, F., Cano, J. & Cabanes, F. J. (2004). Taxonomy and significance of black aspergilli. *Antonie Van Leeuwenhoek* **86**, 33-49.

Adam, O., Badot, P. M., Degiorgi, F. & Crini, G. (2009). Mixture toxicity assessment of wood preservative pesticides in the freshwater amphipod *Gammarus pulex* (L.). *Ecotoxicol Environ Saf* **72**, 441-449.

Allaker, R. P. & Ren, G. (2008). Potential impact of nanotechnology on the control of infectious diseases. *Trans R Soc Trop Med Hyg* **102**, 1-2.

Allen Jr, L. V. (2008). Dosage form design and development. *Clinical Therapeutics* **30**, 2102-2111.

Almeida, J. P., Chen. A. L., Foster, A. & Drezek, R. (2011). *In vivo* biodistribution of nanoparticles. *Nanomedicine* **6**, 815-835.

Amsterdam, D. (1990). Assessing cidal activity of antimicrobial agents: problems and pitfalls. *ANNLDO* **7**, 49-56.

Anders, S. & Huber, W. (2010). Differential expression analysis for sequence count data. *Genome Biology* **11**, R106.

Andrews, J. M. (2001). Determination of minimum inhibitory concentrations. *Journal of Antimicrobial Chemotherapy* **48**, 5-16.

Ansorge, W. J. (2009). Next-generation DNA sequencing techniques. *N Biotechnol* **25**, 195-203.

Applied Biosystems (2010). SOLiD™ Total RNA-Seq Kit protocol manual.

Arnold, M. M., Gorman, E. M., Schieber, L. J., Munson, E. J. & Berkland, C. (2007). NanoCipro encapsulation in monodisperse large porous PLGA microparticles. *J Control Release* **121**, 100-109.

Asrar, J., Ding, Y., La Monica, R. E. & Ness, L. C. (2004). Controlled release of tebuconazole from a polymer matrix microparticle: release kinetics and length of efficacy. *J Agric Food Chem* **52**, 4814-4820.

Badreshia, S. & Marks, J. G., Jr. (2002). Iodopropynyl butylcarbamate. *Am J Contact Dermat* **13**, 77-79.

Baker, M. D. & Acharya, K. R. (2004). Superantigens: structure-function relationships. *Int J Med Microbiol* **293**, 529-537.

Bax, R., Mullan, N. & Verhoef, J. (2000). The millennium bugs-the need for and development of new antibacterials. *Int J Antimicrob Agents* **16**, 51-59.

Bayer CropScience website: www.bayercropscience.co.uk
Accessed January 2011.

Belesti, A., Panagi, Z. & Avgoustakis, K. (2005). Biodistribution properties of nanoparticles based on mixtures of PLGA with PLGA-PEG diblock copolymers. *Int J Pharmaceutics* **298**, 233-241.

Berlanga, M., Montero, M. T., Hernandez-Borrell, J. & Vinas, M. (2004). Influence of the cell wall on ciprofloxacin susceptibility in selected wild-type Gram-negative and Gram-positive bacteria. *Int J Antimicrob Agents* **23**, 627-630.

Bioconductor – open souce software for bioinformatics
website: www.bioconductor.org
Accessed January 2011.

Bisognano, C., Kelley, W. L., Estoppey, T., Francois, P., Schrenzel, J., Li, D., Lew, D.P., Hooper, D.C., Cheung, A.L. & Vaudaux, P. (2004). A recA-LexA-dependent pathway mediates ciprofloxacin-induced fibronectin binding in *Staphylococcus aureus. J Biol Chem* **279**, 9064-9071.

Boucher, Helen W., Talbot, George H., Bradley, John S., Edwards, John E., Gilbert, D., Rice, Louis B., Scheld, M., Spellberg, B. & Bartlett, J. (2009). Bad Bugs, No Drugs: No ESKAPE! An Update from the Infectious Diseases Society of America. *Clinical Infectious Diseases* **48**, 1-12.

Bozkir, A. & Saka, O.M. (2005). Formulation and investigation of 5-FU nanoparticles with factorial design-based studies. *Farmaco* **60**, 840-846.

Brazma, A., Hingamp, P., Quackenbush, J., Sherlock, G., Spellman, P., Stoeckert, C., Aach, J., Ansorge, W., Ball, C. A., Causton, H. C., Gaasterland, T., Glenisson, P., Holstege, F. C., Kim, I. F., Markowitz, V., Matese, J. C., Parkinson, H., Robinson, A., Sarkans, U., Schulze-Kremer, S., Stewart, J., Taylor, R., Vilo, J., Vingron, M. (2001). Minimum information about a microarray experiment (MIAME)-toward standards for microarray data. *Nat Genet* **29**, 365-371.

Brown, A. J. P., Odds, F. C. & Gow, N. A. R. (2007). Infection-related gene expression in *Candida albicans. Current Opinion in Microbiology* **10**, 307-313.

Bruschi, M. L., Lara, E. H., Martins, C. H., Vinholis, A. H., Casemiro, L. A., Panzeri, H. & Gremiao, M. P. (2006). Preparation and antimicrobial activity of gelatin microparticles containing propolis against oral pathogens. *Drug Dev Ind Pharm* **32**, 229-238.

Bystrzejewska-Piotrowska, G., Golimowski, J. & Urban, P. L. (2009). Nanoparticles: Their potential toxicity, waste and environmental management. *Waste Management* **29**, 2587-2595.

Calderone, R. A. & Fonzi, W. A. (2001). Virulence factors of *Candida albicans*. *Trends Microbiol* **9**, 327-335.

Cao, G. (2004). In *Nanostructures and Nanomaterials: synthesis, properties and applications*. Imperial College Press; London.

Chandra, J., Kuhn, D. M., Mukherjee, P. K., Hoyer, L. L., McCormick, T. & Ghannoum, M. A. (2001). Biofilm Formation by the Fungal Pathogen *Candida albicans*: Development, Architecture, and Drug Resistance. *J Bacteriol* **183**, 5385-5394.

Chen, Z., Luong, T. T. & Lee, C. Y. (2007). The *sbcDC* locus mediates repression of type 5 capsule production as part of the SOS response in *Staphylococcus aureus*. *J Bacteriol* **189**, 7343-7350.

Chen, C.-R., Malik, M., Snyder, M. & Drlica, K. (1996). DNA Gyrase and Topoisomerase IV on the Bacterial Chromosome: Quinolone-induced DNA Cleavage. *Journal of Molecular Biology* **258**, 627-637.

Chen, X. & Schluesener, H. J. (2008). Nanosilver: a nanoproduct in medical application. *Toxicol Lett* **176**, 1-12.

Cheung, W., Pontoriero, F., Taratula, O., Chen, A. M. & He, H. (2010). DNA and carbon nanotubes as medicine. *Adv Drug Deliv Rev* **62**, 633-649.

Chrastina, A., Massey, K. A. & Schnitzer, J. E. (2011). Overcoming *in vivo* barriers to targeted nanodelivery. *Nanomed and Nanobiotechnol* **3**, 421-437.

Christoffersen, R. E. (2006). Antibiotics - an investment worth making? *Nat Biotech* **24**, 1512-1514.

Cirz, R. T., Jones, M. B., Gingles, N. A., Minogue, T. D., Jarrahi, B., Peterson, S. N. & Romesberg, F. E. (2007). Complete and SOS-mediated response of *Staphylococcus aureus* to the antibiotic ciprofloxacin. *J Bacteriol* **189**, 531-539.

Connelly, J. C., Kirkham, L. A. & Leach, D. R. (1998). The SbcCD nuclease of *Escherichia coli* is a structural maintenance of chromosomes (SMC) family protein that cleaves hairpin DNA. *Proc Natl Acad Sci U S A* **95**, 7969-7974.

Costa, V., Angelini, C., De Feis, I. & Ciccodicola, A. (2010). Uncovering the complexity of transcriptomes with RNA-Seq. *J Biomed Biotechnol* **2010**, 853916-353935.

Cousins, B., Allison, H., Doherty, P., Edwards, C., Garvey, M., Martin, D. & Williams, R. (2007). Effects of a nanoparticulate silica substrate on cell attachment of *Candida albicans*. *Journal of Applied Microbiology* **102**, 757-765.

Cowen, L. E. (2001). Predicting the emergence of resistance to antifungal drugs. *FEMS Microbiology Letters* **204**, 1-7.

Cowen, L. E. (2008). The evolution of fungal drug resistance: modulating the trajectory from genotype to phenotype. *Nat Rev Microbiol* **6**, 187-198.

Cox, P. J., Foote, N. M. & MacManus, S. M. (2004). Solid state study of hydrogen bonding in dichlorophen crystals. *International Journal of Pharmaceutics* **269**, 15-18.

Cullum, R., Alder, O. & Hoodless, P. A. (2011). The next generation: using new sequencing technologies to analyze gene regulation. *Respirology* **16**, 210-222.

Cussiol, J. R. R., Alegria, T. G. P., Szweda, L. I. & Netto, L. E. S. (2010). Ohr (Organic Hydroperoxide Resistance Protein) Possesses a Previously Undescribed Activity, Lipoyl-dependent Peroxidase. *Journal of Biological Chemistry* **285**, 21943-21950.

Das, S, Suresh, P.K. & Desmukh, R. (2010). Design of Eudragit RL 100 nanoparticles by nanoprecipitation method for ocular drug delivery. *Nanomedicine* **6**, 318-323.

De Lucca, A. J. (2007). Harmful fungi in both agriculture and medicine. *Rev Iberoam Micol* **24**, 3-13.

Dearden, J. C. (1985). Partitioning and lipophilicity in quantitative structure-activity relationships. *Environ Health Perspect* **61**, 203-228.

DeLeo, F. R. & Chambers, H. F. (2009). Reemergence of antibiotic-resistant *Staphylococcus aureus* in the genomics era. *J Clin Invest* **119**, 2464-2474.

Denning, D. W. & Hope, W. W. (2010). Therapy for fungal diseases: opportunities and priorities. *Trends in Microbiology* **18**, 195-204.

Denyer, S. P. & Stewart, G. S. A. B. (1998). Mechanisms of action of disinfectants. *International Biodeterioration & Biodegradation* **41**, 261-268.

Department for Environment, Farming and Rural Affairs (2005). Characteristing the potential risks posed by engineered nanoparticles - A first UK Government research report, pp. 1-15 and 29-38. Edited by DEFRA: www.defra.co.uk Crown Copyright.

Department for Environment, Farming and Rural Affairs (2007). Characteristing the potential risks posed by engineered nanoparticles - A second UK Government research report, pp. 1-41. Edited by DEFRA: www.defra.co.uk Crown Copyright.

Department for Environment, Farming and Rural Affairs website:
www.defra.gov.uk/environment/quality/nanotech
Accessed December 2010.

Dillen, K., Bridts, C., Van der Veken, P., Cos, P., Vandervoort, J., Augustyns, K., Stevens, W. & Ludwig, A. (2008). Adhesion of PLGA or Eudragit/PLGA nanoparticles to *Staphylococcus* and *Pseudomonas*. *Int J Pharm* **349**, 234-240.

Dillen, K., Vandervoort, J., Van den Mooter, G. & Ludwig, A. (2006). Evaluation of ciprofloxacin-loaded Eudragit RS100 or RL100/PLGA nanoparticles. *Int J Pharm* **314**, 72-82.

Dillen, K., Vandervoort, J., Van den Mooter, G., Verheyden, L. & Ludwig, A. (2004). Factorial design, physicochemical characterisation and activity of ciprofloxacin-PLGA nanoparticles. *Int J Pharm* **275**, 171-187.

Dobrindt, U. (2005). (Patho-)Genomics of *Escherichia coli*. *Int J Med Microbiol* **295**, 357-371.

Donaldson, K., Stone, V., Gilmour, P. S., Brown, D. M. & MacNee, W. (2000). Ultrafine particles: mechanisms of lung injury. *Philosophical Transactions of the Royal Society of London Series A: Mathematical, Physical and Engineering Sciences* **358**, 2741-2749.

Drlica, K., Malik, M., Kerns, R. J. & Zhao, X. (2008). Quinolone-mediated bacterial death. *Antimicrob Agents Chemother* **52**, 385-392.

Drlica, K. & Zhao, X. (1997). DNA gyrase, topoisomerase IV, and the 4-quinolones. *Microbiol Mol Biol Rev* **61**, 377-392.

Drulis-Kawa, Z. & Dorotkiewicz-Jach, A. (2010). Liposomes as delivery systems for antibiotics. *International Journal of Pharmaceutics* **387**, 187-198.

Dubes, A., Parrot-Lopez, H., Abdelwahed, W., Degobert, G., Fessi, H., Shahgaldian, P. & Coleman, A. W. (2003). Scanning electron microscopy and atomic force microscopy imaging of solid lipid nanoparticles derived from amphiphilic cyclodextrins. *Eur J Pharm Biopharm* **55**, 279-282.

Duncalf, D.J., Foster, A.J., Long, J., Rannard, S.P. & Wang, D. (2008). Improvements Relating to Biocidal Compositions. *Patent number: WO2008006714*.

Elan drug technologies
website: www.elandrugtechnologies.com/nanocrystal_technology
Accessed January 2011.

Emmett, M. & Kloos, W. E. (1979). The nature of arginine auxotrophy in cutaneous populations of staphylococci. *J Gen Microbiol* **110**, 305-314.

Eriksson, L., Johansson, E., Kettaneh-Wold, N., Wikström.,C. & Wold, S. (2008). Design of Experiments – Principles and Applications 3rd eddition. Umetricks Academy.

Esmaeili, F., Hosseini-Nasr, M., Rad-Malekshahi, M., Samadi, N., Atyabi, F. & Dinarvand, R. (2007). Preparation and antibacterial activity evaluation of rifampicin-loaded poly lactide-co-glycolide nanoparticles. *Nanomedicine* **3**, 161-167.

Fang, C., Shi, B., Pei, Y. Y., Hong, M. H., Wu, J. & Chen, H. Z. (2006). Influence of particle size and MePEG molecular weight on *in vitro* macrophage uptake and *in vivo* long circulating of stealth nanoparticles in rats. *Eur J Pharm Sci* **27**, 27-36.

Farokhzad, O. C. & Langer, R. (2009). Impact of Nanotechnology on Drug Delivery. *ACS Nano* **3**, 16-20.

Fayaz, A. M., Balaji, K., Girilal, M., Yadav, R., Kalaichelvan, P. T. & Venketesan, R. (2010). Biogenic synthesis of silver nanoparticles and their synergistic effect with antibiotics: a study against gram-positive and gram-negative bacteria. *Nanomedicine* **6**, 103-109.

Fisher, L. M., Lawrence, J. M., Josty, I. C., Hopewell, R., Margerrison, E. E. & Cullen, M. E. (1989). Ciprofloxacin and the fluoroquinolones. New concepts on the mechanism of action and resistance. *Am J Med* **87**, 2S-8S.

Fleury, B., Kelley, W. L., Lew, D., Gotz, F., Proctor, R. A. & Vaudaux, P. (2009). Transcriptomic and metabolic responses of *Staphylococcus aureus* exposed to supra-physiological temperatures. *BMC Microbiol* **9**, 76.

Fog Nielsen, K. (2003). Mycotoxin production by indoor molds. *Fungal Genetics and Biology* **39**, 103-117.

Foster, T. J. (2005). Immune evasion by staphylococci. *Nat Rev Microbiol* **3**, 948-958.

Fraser, J. D. & Proft, T. (2008). The bacterial superantigen and superantigen-like proteins. *Immunological Reviews* **225**, 226-243.

Frauen, M., Steinhart, H., Rapp, C. & Hintze, U. (2001). Rapid quantification of iodopropynyl butylcarbamate as the preservative in cosmetic formulations using high-performance liquid chromatography-electrospray mass spectrometry. *J Pharm Biomed Anal* **25**, 965-970.

Friedrich, R., Panizzi, P., Fuentes-Prior, P. Richter, K., Verhamme, I., Anderson, P.J., Kawabata, S., Huber, R., Bode, W. & Bock, P.E. (2003). Staphylocoagulase is a prototype for the mechanism of cofactor-induced zymogen activation. *Nature* **425**, 535-539.

Fu, X., Fu, N., Guo, S., Yan, Z., Xu, Y., Hu, H., Menzel, C., Chen, W., Li, Y., Zeng, R. & Khaitovich, P. (2009). Estimating accuracy of RNA-Seq and microarrays with proteomics. *BMC Genomics* **10**, 161-170.

Futi, V. (2009). Preparation of Ciprofloxacin Nanoparticles. *Iota Nanosolutions Ltd - Internal Research Report* (IN/IR/09 002).

Gilbert, P., Beveridge, E. G. & Crone, P. B. (1977). The lethal action of 2-phenoxyethanol and its analogues upon *Escherichia coli* NCTC 5933. *Microbios* **19**, 125-141.

Gilbert, P., Beveridge, E. G. & Crone, P. B. (1980). Effect of 2-phenoxyethanol upon RNA, DNA and protein biosynthesis in *Escherichia coli* NCTC 5933. *Microbios* **28**, 7-17.

Gilbert, P. & McBain, A. J. (2003). Potential impact of increased use of biocides in consumer products on prevalence of antibiotic resistance. *Clin Microbiol Rev* **16**, 189-208.

Greenwood, D., Finch, R. & Davey, P. (2007). In *Antimicrobial Chemotherapy.* Oxford University Press; USA.

Gustafson, J., Strässle, A., Hächler, H., Kayser, F. H. & Berger-Bächi, B. (1994). The *femC* locus of *Staphylococcus aureus* required for methicillin resistance includes the glutamine synthetase operon. *J Bacteriol* **176**, 1460-1467.

Haas, S. E., Bettoni, C. C., de Oliveira, L. K., Guterres, S. S. & Dalla Costa, T. (2009). Nanoencapsulation increases quinine antimalarial efficacy against *Plasmodium berghei in- vivo. International Journal of Antimicrobial Agents* **34**, 156-161.

Haggstrom, J. A., Klabunde, K. J. & Marchin, G. L. (2010). Biocidal properties of metal oxidenanoparticles and their halogenadducts. *Nanoscale* **2**, 399-405.

Hall, N. (2007). Advanced sequencing technologies and their wider impact in microbiology. *J Exp Biol* **210**, 1518-1525.

Hansen, K. D., Brenner, S. E. & Dudoit, S. (2010). Biases in Illumina transcriptome sequencing caused by random hexamer priming. *Nucleic Acids Res* **38**, e131.

Hassan, K. A., Xu, Z., Watkins, R. E., Brennan, R. G., Skurray, R. A. & Brown, M. H. (2009). Optimized production and analysis of the staphylococcal multidrug efflux protein QacA. *Protein Expr Purif* **64**, 118-124.

Hassellöv, M., Readman, J., Ranville, J. & Tiede, K. (2008). Nanoparticle analysis and characterization methodologies in environmental risk assessment of engineered nanoparticles. *Ecotoxicology* **17**, 344-361.

Heerklotz, H. (2008). Interactions of surfactants with lipid membranes. *Q Rev Biophys* **41**, 205-264.

Hinton, J. C., Hautefort, I., Eriksson, S., Thompson, A., Rhen, M. (2004). Benefits and pitfalls of using microarrays to monitor bacterial gene expression during infection. *Curr Opin Microbiol* **7**, 277-282.

Hiramatsu, K. (2001). Vancomycin-resistant *Staphylococcus aureus*: a new model of antibiotic resistance. *Lancet Infect Dis* **1**, 147-155.

Ho, Y. P. & Leong, K. W. (2010). Quantum dot-based theranostics. *Nanoscale* **2**, 60-68.

Horn, D. & Rieger, J. (2001). Organic Nanoparticles in the Aqueous Phase - Theory, Experiment, and Use. *Angewandte Chemie International Edition* **40**, 4330-4361.

Hu, J., Johnston, K. P. & Williams, R. O., 3rd (2004). Nanoparticle engineering processes for enhancing the dissolution rates of poorly water soluble drugs. *Drug Dev Ind Pharm* **30**, 233-245.

Hu, K. H., Liu, E., Dean, K., Gingras, M., DeGraff, W. & Trun, N. J. (1996). Overproduction of three genes leads to camphor resistance and chromosome condensation in *Escherichia coli*. *Genetics* **143**, 1521-1532.

Huh, A. J. & Kwon, Y. J. (2011). "Nanoantibiotics": A new paradigm for treating infectious diseases using nanomaterials in the antibiotics resistant era. *J Control Release* doi:10.1016/j.jconrel.2011.07.002.

Hutchings, G. J., Brust, M. & Schmidbaur, H. (2008). Gold--an introductory perspective. *Chem Soc Rev* **37**, 1759-1765.

Imbuluzqueta, E., Elizondo, E., Gamazo, C., Moreno-Calvo, E., Veciana, J., Ventosa, N. & Blanco-Prieto, M. J. (2011). Novel bioactive hydrophobic gentamicin carriers for the treatment of intracellular bacterial infections. *Acta Biomater* **7**, 1599-1608.

Iota NanoSolutions™ website: www.iotanano.com
Accessed January 2011.

Isabella, V. M. & Clark V. L. (2011). Deep sequencing-based analysis of the anaerobic stimulon in *Neisseria gonorrhoeae*. *BMC Genomics* **12,** 51.

Ito, T., Katayama, Y. & Hiramatsu, K. (1999). Cloning and Nucleotide Sequence Determination of the Entire mec DNA of Pre-Methicillin-Resistant *Staphylococcus aureus* N315. *Antimicrob Agents Chemother* **43**, 1449-1458.

Jarrard, H. E., Delaney, K. R. & Kennedy, C. J. (2004). Impacts of carbamate pesticides on olfactory neurophysiology and cholinesterase activity in coho salmon (*Oncorhynchus kisutch*). *Aquat Toxicol* **69**, 133-148.

Jeong, Y. I., Na, H. S., Seo, D. H., Kim, D. G., Lee, H. C., Jang, M. K., Na, S. K., Roh, S. H., Kim, S. I. & Nah, J. W. (2008). Ciprofloxacin-encapsulated poly(DL-lactide-co-glycolide) nanoparticles and its antibacterial activity. *Int J Pharm* **352**, 317-323.

Jiang, W., Kim, B. Y., Rutka, J. T. & Chan, W. C. (2008). Nanoparticle-mediated cellular response is size-dependent. *Nat Nanotechnol* **3**, 145-150.

Joo, H. H., Lee, H. Y., Guan, Y. S. & Kim, J.C. (2008). Colloidal stability and *in vitro* permeation study of poly(ε-caprolactone) nanocapsules containing hinokitiol. *J Indust Eng Chemistry* **14,** 608-613.

Ju-Nam, Y. & Lead, J. R. (2008). Manufactured nanoparticles: An overview of their chemistry, interactions and potential environmental implications. *Science of The Total Environment* **400**, 396-414.

Kabanov, A. V., Batrakova, E. V. & Alakhov, V. Y. (2002). Pluronic block copolymers as novel polymer therapeutics for drug and gene delivery. *J Control Release* **82**, 189-212.

Kabanov, A. V., Batrakova, E. V., Sriadibhatla, S., Yang, Z., Kelly, D. L. & Alakov, V. Y. (2005). Polymer genomics: shifting the gene and drug delivery paradigms. *J Control Release* **101**, 259-271.

Kanaras, A. G., Wang, Z., Brust, M., Cosstick, R. & Bates, A. D. (2007). Enzymatic disassembly of DNA-gold nanostructures. *Small* **3**, 590-594.

Kanaujia, P., Lau, G., Ng, W. K., Widjaja, E., Hanefeld, A., Fishbach, M., Maio, M. & Tan, R. B. (2011). Nanoparticle formation and growth during *in vitro* dissolution of ketoconazole solid dispersion. *J Pharm Sci* **100**, 2876-2885.

Kanehisa, M. & Goto, S. (2000). KEGG: Kyoto Encyclopedia of Genes and Genomes. *Nucleic Acids Res* **28**, 27-30.

Kaneko, J. & Kamio, Y. (2004). Bacterial two-component and hetero-heptameric pore-forming cytolytic toxins: structures, pore-forming mechanism, and organization of the genes. *Biosci Biotechnol Biochem* **68**, 981-1003.

Kang, S., Herzberg, M., Rodrigues, D. F. & Elimelech, M. (2008). Antibacterial Effects of Carbon Nanotubes: Size Does Matter! *Langmuir* **24**, 6409-6413.

Kaper, J. B., Nataro, J. P. & Mobley, H. L. (2004). Pathogenic *Escherichia coli. Nat Rev Microbiol* **2**, 123-140.

Karkowska-Kuleta, J., Rapala-Kozik, M. & Kozik, A. (2009). Fungi pathogenic to humans: molecular bases of virulence of *Candida albicans, Cryptococcus neoformans* and *Aspergillus fumigatus. Acta Biochim Pol* **56**, 211-224.

Kenny, J. G., Ward, D., Josefsson, E., Jonsson, I. M., Hinds, J., Rees, H. H., Lindsay, J. A., Tarkowski, A. & Horsburgh, M. J. (2009). The *Staphylococcus aureus* response to unsaturated long chain free fatty acids: survival mechanisms and virulence implications. *PLoS One* **4**, e4344.

Khan, Z. U., Chandy, R. & Metwali, K. E. (2003). *Candida albicans* strain carriage in patients and nursing staff of an intensive care unit: a study of morphotypes and resistotypes. *Mycoses* **46**, 479-486.

Kingsley, J. D., Dou, H., Morehead, J., Rabinow, B., Gendelman, H. E. & Destache, C. J. (2006). Nanotechnology: a focus on nanoparticles as a drug delivery system. *J Neuroimmune Pharmacol* **1**, 340-350.

Kipp, J. E. (2004). The role of solid nanoparticle technology in the parenteral delivery of poorly water-soluble drugs. *Int J Pharm* **284**, 109-122.

Kircher, M. & Kelso, J. (2010). High-throughput DNA sequencing-concepts and limitations. *Bioessays* **32**, 524-536.

Kisich, K. O., Gelperina, S., Higgins, M. P., Wilson, S., Shipulo, E., Oganesyan, E. & Heifets, L. (2007). Encapsulation of moxifloxacin within poly(butyl cyanoacrylate) nanoparticles enhances efficacy against intracellular *Mycobacterium tuberculosis. Int J Pharm* **345**, 154-162.

Klippstein, R. & Pozo, D. (2010). Nanotechnology-based manipulation of dendritic cells for enhanced immunotherapy strategies. *Nanomedicine* **6**, 23-529.

Kocbek, P., Baumgartner S. & Kristl, J. (2006). Preparation and evaluation of nanosuspensions for enhancing the dissolution of poorly soluble drugs. *Int J Pharm* **312**, 179-186.

Komatsuzawa, H., Ohta, K., Sugai, M., Fujiwara, T., Glanzmann, P., Berger-Bächi, B. & Suginaka, H. (2000). Tn551-mediated insertional inactivation of the *fmtB* gene encoding a cell wall-associated protein abolishes methicillin resistance in *Staphylococcus aureus. Journal of Antimicrobial Chemotherapy* **45**, 421-431.

Kreuter, J. (1991). Liposomes and nanoparticles as vehicles for antibiotics. *Infection* **19 Suppl 4**, S224-228.

Kullik, I., Giachino, P. & Fuchs, T. (1998). Deletion of the alternative sigma factor sigmaB in *Staphylococcus aureus* reveals its function as a global regulator of virulence genes. *J Bacteriol* **180**, 4814-4820.

Kuroda, M., Ohta, T. & Hayashi, H. (1995). Isolation and the gene cloning of an alkaline shock protein in methicillin resistant *Staphylococcus aureus*. *Biochem Biophys Res Commun* **207**, 978-984.

Kvaal, C., Lachke, S. A., Srikantha, T., Daniels, K., McCoy, J. & Soll, D. R. (1999). Misexpression of the opaque-phase-specific gene PEP1 (SAP1) in the white phase of *Candida albicans* confers increased virulence in a mouse model of cutaneous infection. *Infect Immun* **67**, 6652-6662.

Lan, L., Cheng, A., Dunman, P. M., Missiakas, D. & He, C. (2010). Golden pigment production and virulence gene expression are affected by metabolisms in *Staphylococcus aureus*. *J Bacteriol* **192**, 3068-3077.

Landfester, K. (2009). Miniemulsion Polymerization and the Structure of Polymer and Hybrid Nanoparticles. *Angewandte Chemie International Edition* **48**, 4488-4507.

Lang, S., Livesley, M. A., Lambert, P. A., Littler, W. A. & Elliott, T. S. (2000). Identification of a novel antigen from *Staphylococcus epidermidis*. *FEMS Immunol Med Microbiol* **29**, 213-220.

Leo, E., Brina, B., Forni, F. & Vandelli, M.A. (2004). *In vitro* evaluation of PLA nanoparticles containing a lipophilic drug in water-soluble or insoluble form. *Int J Pharm* **278**, 133-141.

Levy, S. B. (2000). Antibiotic and antiseptic resistance: impact on public health. *Pediatr Infect Dis J* **19**, S120-122.

Li, B., Ruotti, V., Stewart, R. M., Thomson, J. A. & Dewey, C. N. (2010). RNA-Seq gene expression estimation with read mapping uncertainty. *Bioinformatics* **26**, 493-500.

Li, N., Wang, J., Yang, X. & Li, L. (2011). Novel nanogels as drug delivery systems for poorly soluble anticancer drugs. *Colloids Surf B Biointerfaces* **83**, 237-244.

Lindsay, J. A. & Holden, M. T. G. (2004). *Staphylococcus aureus*: superbug, super genome? *Trends Microbiol* **12**, 378-385.

Lipinski, C. A. (2000). Drug-like properties and the causes of poor solubility and poor permeability. *J Pharmacol Toxicol Methods* **44**, 235-249.

Lok, C.-N., Ho, C.-M., Chen, R., He, Q.-Y., Yu, W.-Y., Sun, H., Tam, P. K.-H., Chiu, J.-F. & Che, C.-M. (2006). Proteomic Analysis of the Mode of Antibacterial Action of Silver Nanoparticles. *Journal of Proteome Research* **5**, 916-924.

Lupetti, A., Danesi, R., Campa, M., Del Tacca, M. & Kelly, S. (2002). Molecular basis of resistance to azole antifungals. *Trends Mol Med* **8**, 76-81.

Lvov, Y. M., Pattekari, P., Zhang, X. & Torchilin, V. (2010). Converting Poorly Soluble Materials into Stable Aqueous Nanocolloids. *Langmuir*, DOI: 10.1021/la1041635.

Malvern Instruments UK Ltd. (2003). Zetasizer Nano Series product manual.

Manna, A. C., Ingavale, S. S., Maloney, M., van Wamel, W. & Cheung, A. L. (2004). Identification of *sarV* (SA2062), a new transcriptional regulator, is repressed by *SarA* and *MgrA* (SA0641) and involved in the regulation of autolysis in *Staphylococcus aureus*. *J Bacteriol* **186**, 5267-5280.

Mardis, E. R. (2008). Next-generation DNA sequencing methods. *Annu Rev Genomics Hum Genet* **9**, 387-402.

Marguerat, S. & Bahler, J. (2010). RNA-seq: from technology to biology. *Cell Mol Life Sci* **67**, 569-579.

Masters, K. (1985). In *Spray drying handbook* 4th eddition.
Longman Scientific & Technical ; Harlow, England.

McCarron, P. A., Donnelly, R. F., Canning, P. E., McGovern, J. G. & Jones, D. S. (2004). Bioadhesive, non-drug-loaded nanoparticles as modulators of candidal adherence to buccal epithelial cells: a potentially novel prophylaxis for candidosis. *Biomaterials* **25**, 2399-2407.

Meneau, I. & Sanglard, D. (2005). Azole and fungicide resistance in clinical and environmental *Aspergillus fumigatus* isolates. *Med Mycol* **43 Suppl 1**, 307-311.

Meng, X., Tang, F., Peng, B. & Ren, J. (2010). Monodisperse Hollow Tricolor Pigment Particles for Electronic Paper. *Nanoscale Research Letters* **5**, 174-179.

Metzker, M. L. (2010). Sequencing technologies the next generation. *Nat Rev Genet* **11**, 31-46.

Michel, B. (2005). After 30 years of study, the bacterial SOS response still surprises us. *PLoS Biol* **3**, e255.

Michel, A., Agerer, F., Hauck, C. R., Herrmann, M., Ullrich, J., Hacker, J. & Ohlsen, K. (2006). Global regulatory impact of *ClpP* protease of *Staphylococcus aureus* on regulons involved in virulence, oxidative stress response, autolysis, and DNA repair. *J Bacteriol* **188**, 5783-5796.

Mochalkin, I., Lightle, S., Narasimhan, L., Bornemeier, D., Melnick, M., Vanderroest, S. & McDowell, L. (2008). Structure of a small-molecule inhibitor complexed with GlmU from *Haemophilus influenzae* reveals an allosteric binding site. *Protein Sci* **17**, 577-582.

Mohammadi, G., Valizadeh, H., Barzegar-Jalali, M., Lotfipour, F., Adibkia, K., Milani, M., Azhdarzadeh, M., Kiafar, F. & Nokhodchi, A. (2010). Development of azithromycin-PLGA nanoparticles: Physicochemical characterization and antibacterial effect against *Salmonella typhi*. *Colloids and Surfaces B: Biointerfaces* **80**, 34-39.

Mora-Huertas, C.E., Fessi, H. & Elaissari, A. (2010). Polymer-based nanocapsules for drug delivery. *Int J Pharm* **385**, 113-142.

Morones, J. R., Elechiguerra, J. L., Camacho, A., Holt, K., Kouri, J. B., Ramirez, J. T. & Yacaman, M. J. (2005). The bactericidal effect of silver nanoparticles. *Nanotechnology* **16**, 2346-2353.

Morrison, I.D. & Ross, S. (2002). In *Colloidal Dispersions – Suspensions, Emulsions and Foams.* John Wiley & Sons, Inc; New York.

Mortazavi, A., Williams, B. A., McCue, K., Schaeffer, L. & Wold, B. (2008). Mapping and quantifying mammalian transcriptomes by RNA-Seq. *Nat Methods* **5**, 621-628.

Muller, R. H. & Keck, C.M. (2004). Challenges and solutions for the delivery of biotech drugs-a review of drug nanocrystal technology and lipid nanoparticles. *J Biotechnol* **113**, 151-170.

Mycota® website: www.mycota.co.uk
Accessed January 2011.

Nagarajan, R. (2008). Nanoparticles: Synthesis, Stabilization, Passivation, and Functionalization. In *Nanoparticles: Building Blocks for Nanotechnology*, pp. 2-14. ACS Symposium Series, American Chemical Society; Washington, D.C.

Naglik, J. R., Challacombe, S. J. & Hube, B. (2003). *Candida albicans* secreted aspartyl proteinases in virulence and pathogenesis. *Microbiol Mol Biol Rev* **67**, 400-428.

Nataro, J. P. & Kaper, J. B. (1998). Diarrheagenic *Escherichia coli*. *Clin Microbiol Rev* **11**, 142-201.

Navarre, W. W. & Schneewind, O. (1999). Surface proteins of gram-positive bacteria and mechanisms of their targeting to the cell wall envelope. *Microbiol Mol Biol Rev* **63**, 174-229.

Nirmal, M. & Brus, L. (1998). Luminescence Photophysics in Semiconductor Nanocrystals. *Accounts of Chemical Research* **32**, 407-414.

Nishiyama, N. & Kataoka, K. (2006). Current state, achievements, and future prospects of polymeric micelles as nanocarriers for drug and gene delivery. *Pharmacology & Therapeutics* **112**, 630-648.

Norrby, S. R., Nord, C. E. & Finch, R. (2005). Lack of development of new antimicrobial drugs: a potential serious threat to public health. *The Lancet Infectious Diseases* **5**, 115-119.

Novick, R. P. & Geisinger, E. (2008). Quorum Sensing in Staphylococci. *Annual Review of Genetics* **42**, 541-564.

Nowack, B. & Bucheli, T. D. (2007). Occurrence, behavior and effects of nanoparticles in the environment. *Environ Pollut* **150**, 5-22.

Nucci, M. & Anaissie, E. (2001). Revisiting the source of candidemia: skin or gut? *Clin Infect Dis* **33**, 1959-1967.

Odds, F. C., Brown, A. J. & Gow, N. A. (2003). Antifungal agents: mechanisms of action. *Trends Microbiol* **11**, 272-279.

Overbeek, R., Begley, T., Butler, R. M., Choudhuri, J. V., Chuang, H. Y., Cohoon, M., de Crecy-Lagard, V., Diaz, N., Disz, T., Edwards, R., Fonstein, M., Frank, E. D., Gerdes, S., Glass, E. M., Goesmann, A., Hanson, A., Iwata-Reuyl, D., Jensen, R., Jamshidi, N., Krause, L., Kubal, M., Larsen, N., Linke, B., McHardy, A. C., Meyer, F., Neuweger, H., Olsen, G., Olson, R., Osterman, A., Portnoy, V., Pusch, G. D., Rodionov, D. A., Ruckert, C., Steiner, J., Stevens, R., Thiele, I., Vassieva, O., Ye, Y., Zagnitko, O. & Vonstein, V. (2005). The Subsystems Approach to Genome Annotation and its Use in the Project to Annotate 1000 Genomes. *Nucleic Acids Research* **33**, 5691-5702.

Owens, D. E. & Peppas, N. A. (2006). Opsonization, biodistribution, and pharmacokinetics of polymeric nanoparticles. *Int J Pharm* **307**, 93-102.

Page-Clisson, M. E., Pinto-Alphandary, H., Ourevitch, M., Andremont, A. & Couvreur, P. (1998). Development of ciprofloxacin-loaded nanoparticles: physicochemical study of the drug carrier. *J Control Release* **56**, 23-32.

Pandey, R., Ahmad, Z., Sharma, S. & Khuller, G. K. (2005). Nano-encapsulation of azole antifungals: potential applications to improve oral drug delivery. *Int J Pharm* **301**, 268-276.

Passalacqua, K. D., Varadarajan, A., Ondov, B. D., Okou, D. T., Zwick, M. E. & Bergman, N. H. (2009). Structure and complexity of a bacterial transcriptome. *J Bacteriol* **191**, 3203-3211.

Patel, N. R., Damann, K., Leonardi, C. & Sabliov, C. M. (2010). Itraconazole-loaded poly(lactic-co-glycolic) acid nanoparticles for improved antifungal activity. *Nanomedicine (Lond)* **5**, 1037-1050.

Paulo, C. S., Vidal, M. & Ferreira, L. S. (2010). Antifungal nanoparticles and surfaces. *Biomacromolecules* **11**, 2810-2817.

Payne, D. J., Gwynn, M. N., Holmes, D. J. & Pompliano, D. L. (2007). Drugs for bad bugs: confronting the challenges of antibacterial discovery. *Nat Rev Drug Discov* **6**, 29-40.

Pel, H. J., de Winde, J. H., Archer, D. B., Dyer, P. S., Hofmann, G., Schaap, P. J., Turner, G., de Vries, R. P., Albang, R., Albermann, K., Andersen, M. R., Bendtsen, J. D., Benen, J. A., van den Berg, M., Breestraat, S., Caddick, M. X., Contreras, R., Cornell, M., Coutinho, P. M., Danchin, E. G., Debets, A. J., Dekker, P., van Dijck, P. W., van Dijk, A., Dijkhuizen, L., Driessen, A. J., d'Enfert, C., Geysens, S., Goosen, C., Groot, G. S., de Groot, P. W., Guillemette, T., Henrissat, B., Herweijer, M., van den Hombergh, J. P., van den Hondel, C. A., van der Heijden, R. T., van der Kaaij, R. M., Klis, F. M., Kools, H. J., Kubicek, C. P., van Kuyk, P. A., Lauber, J., Lu, X., van der Maarel, M. J., Meulenberg, R., Menke, H., Mortimer, M. A., Nielsen, J., Oliver, S. G., Olsthoorn, M., Pal, K., van Peij, N. N., Ram, A. F., Rinas, U., Roubos, J. A., Sagt, C. M., Schmoll, M., Sun, J., Ussery, D., Varga, J., Vervecken, W., van de Vondervoort, P. J., Wedler, H., Wosten, H. A., Zeng, A. P., van Ooyen, A. J., Visser, J. & Stam, H. (2007). Genome sequencing and analysis of the versatile cell factory *Aspergillus niger* CBS 513.88. *Nat Biotechnol* **25**, 221-231.

Pelletier, D. A., Suresh, A. K., Holton, G. A., McKeown, C. K., Wang, W., Gu, B., Mortensen, N. P., Allison, D. P., Joy, D. C., Allison, M. R., Brown, S. D., Phelps, T. J. & Doktycz, M. J. (2010). Effects of engineered cerium oxide nanoparticles on bacterial growth and viability. *Appl Environ Microbiol* **76**, 7981-7989.

Peng, H. S., Liu, X. J., Lv, G. X., Sun, B., Kong, Q. F., Zhai, D. X., Wang, Q., Zhao, W., Wang, G. Y., Wang, D. D., Li, H. L., Jin, L. H. & Kostulas, N. (2008). Voriconazole into PLGA nanoparticles: improving agglomeration and antifungal efficacy. *Int J Pharm* **352**, 29-35.

Pereira, M. A., Mosqueira, V. C., Vilela, J. M., Andrade, M. S., Ramaldes, G. A. & Cardoso, V. M. (2008). PLA-PEG nanocapsules radiolabeled with 99m Technetium-HMPAO: release properties and physicochemical characterization by atomic force microscopy and photon correlation spectroscopy. *Eur J Pharm Sci* **33**, 42-51.

Petrikkou, E., Rodriguez-Tudela, J. L., Cuenca-Estrella, M., Gomez, A., Molleja, A. & Mellado, E. (2001). Inoculum Standardization for Antifungal Susceptibility Testing of Filamentous Fungi Pathogenic for Humans. *J Clin Microbiol* **39**, 1345-1347.

Petros, R. A. & DeSimone, J. M. (2010). Strategies in the design of nanoparticles for therapeutic applications. *Nat Rev Drug Discov* **9**, 615-627.

Pillai, R. R., Somayaji, S. N., Rabinovich, M., Hudson, M. C. & Gonsalves, K. E. (2008). Nafcillin-loaded PLGA nanoparticles for treatment of osteomyelitis. *Biomed Mater* **3**, 034114.

Pinto, C., Neufeld, R.J., Ribeiro, A.J. & Veiga, F. (2006). Nanoencapsulation I. Methods for preparation of drug-loaded polymeric nanoparticles. *Nanomedicine* **2**, 8–21.

Pissuwan, D., Cortie, C. H., Valenzuela, S. M. & Cortie, M. B. (2010). Functionalised gold nanoparticles for controlling pathogenic bacteria. *Trends Biotechnol* **28**, 207-213.

Plata, K., Rosato, A. E. & Wegrzyn, G. (2009). *Staphylococcus aureus* as an infectious agent: overview of biochemistry and molecular genetics of its pathogenicity. *Acta Biochim Pol* **56**, 597-612.

Poole, K. (2002). Mechanisms of bacterial biocide and antibiotic resistance. *J Appl Microbiol* **92**, 55-64.

Quintanar, D., Allémann, E., Doelker, E. & Fessi, H. (1998). Preparation and characterization of nanocapsules from preformed polymers by a new process based on emulsification–diffusion technique. *Pharm Res* **15**, 1056–1062.

Rabinow, B. E. (2004). Nanosuspensions in drug delivery. *Nat Rev Drug Discov* **3**, 785-796.

Rai, M., Yadav, A. & Gade, A. (2009). Silver nanoparticles as a new generation of antimicrobials. *Biotechnology Advances* **27**, 76-83.

Ramage, G., Saville, S. P., Thomas, D. P. & Lopez-Ribot, J. L. (2005). Candida biofilms: an update. *Eukaryot Cell* **4**, 633-638.

Ray, J. (2009). Nanotechnology: Organic Nanoparticles and their Formation. Unpublished Internal Research Report (IN/IR/09 003). Iota NanoSolutions Ltd.

Robinson, J. T., Thorvaldsdóttir, H., Winckler, W., Guttman, M., Lander, E. S., Getz, G. & Mesirov, P. V. (2011). Integrative Genomics Viewer. *Nature Biotechnology* **29**, 24-26.

Rooijakkers, S. H., van Kessel, K. P. & van Strijp, J. A. (2005). Staphylococcal innate immune evasion. *Trends Microbiol* **13**, 596-601.

Rosey, E. L., Oskouian, B. & Stewart, G. C. (1991). Lactose metabolism by *Staphylococcus aureus*: characterization of *lacABCD*, the structural genes of the tagatose 6-phosphate pathway. *J Bacteriol* **173**, 5992-5998.

Russell, A. D. & McDonnell, G. (2000). Concentration: a major factor in studying biocidal action. *Journal of Hospital Infection* **44**, 1-3.

Rutherford, K., Parkhill J., Crook J., Horsnell T., Rice P., Rajandream M. A. & Barrell B. (2000). Artemis: sequence visualization and annotation. *Bioinformatics* **16**, 944-945.

Salem, I. I., Flasher, D. L. & Düzgünes, N. (2005). Liposome-Encapsulated Antibiotics. In *Methods in Enzymology*, pp. 261-291. Academic Press.

Sanglard, D., Ischer, F., Calabrese, D., Micheli, M. & Bille, J. (1998). Multiple resistance mechanisms to azole antifungals in yeast clinical isolates. *Drug Resist Updat* **1**, 255-265.

Schaller, M., Borelli, C., Korting, H. C. & Hube, B. (2005). Hydrolytic enzymes as virulence factors of *Candida albicans*. *Mycoses* **48**, 365-377.

Schuster, E., Dunn-Coleman, N., Frisvad, J. C. & Van Dijck, P. W. (2002). On the safety of *Aspergillus niger*--a review. *Appl Microbiol Biotechnol* **59**, 426-435.

Seaton, A., Tran, L., Aitken, R. & Donaldson, K. (2010). Nanoparticles, human health hazard and regulation. *J R Soc Interface* **7**, 119-129.

Sekhon, B. S. & Kamboj, S. R. (2010). Inorganic nanomedicine--part 2. *Nanomedicine* **6**, 612-618.

Serrano, E., Rus, G. & García-Martínez, J. (2009). Nanotechnology for sustainable energy. *Renewable and Sustainable Energy Reviews* **13**, 2373-2384.

Sheetz, T., Vidal, J., Pearson, T. D. & Lozano, K. (2005). Nanotechnology: Awareness and societal concerns. *Technology in Society* **27**, 329-345.

Shukla, S. K. (2005). Community-associated methicillin-resistant *Staphylococcus aureus* and its emerging virulence. *Clin Med Res* **3**, 57-60.

Singh, A., Van Hamme, J. D. & Ward, O. P. (2007). Surfactants in microbiology and biotechnology: Part 2. Application aspects. *Biotechnol Adv* **25**, 99-121.

Smith & Nephew website: www.smith-nephew.com
Accessed Januray 2011.

Soppimath, K. S., Aminabhavi, T. M., Kulkarni, A. R. & Rudzinski, W. E. (2001). Biodegradable polymeric nanoparticles as drug delivery devices. *J Control Release* **70**, 1-20.

Steele, V. R., Bottomley, A. L., Garcia-Lara, J., Kasturiarachchi, J. & Foster, S. J. (2011). Multiple essential roles for *EzrA* in cell division of *Staphylococcus aureus*. *Molecular Microbiology* **80**, 542-555.

Stella, B., Arpicco, S., Rocco, F., Marsaud, V., Renoir, J.M., Cattel, L. & Couvreur, P. (2007). Encapsulation of gemcitabine lipophilic derivatives into polycyanoacry-late nanospheres and nanocapsules. *Int J Pharm* **344**, 71–77.

Strange, R. N. & Scott, P. R. (2005). Plant disease: a threat to global food security. *Annu Rev Phytopathol* **43**, 83-116.

Takyar, S., Hickerson, R. P. & Noller, H. F. (2005). mRNA Helicase Activity of the Ribosome. *Cell* **120**, 49-58.

Tanabe, M., Szakonyi, G., Brown, K. A., Henderson, P. J., Nield, J. & Byrne, B. (2009). The multidrug resistance efflux complex, EmrAB from *Escherichia coli* forms a dimer in vitro. *Biochem Biophys Res Commun* **380**, 338-342.

Taylor, P. W., Stapleton, P. D. & Paul Luzio, J. (2002). New ways to treat bacterial infections. *Drug Discov Today* **7**, 1086-1091.

Teki, R., Datta, M. K., Krishnan, R., Parker, T. C., Lu, T.-M., Kumta, P. N. & Koratkar, N. (2009). Nanostructured Silicon Anodes for Lithium Ion Rechargeable Batteries. *Small* **5**, 2236-2242.

Teow, Y., Asharani, P. V., Hande, M. P. & Valiyaueettil, S. (2011). Health impact and safety of engineered nanomaterials. *Chem Commun* **47**, 7025-7038.

The National Nanotechnology Initiative (NNI) (2008). Strategy for Nanotechnology – Related Environmental, Health, & Safety Research, pp. 1-8. Eddited by The National Science and Technology Council (NSTC), U.S. Government.

The R Project for Statistical Computing website www.r-project.org
Accessed January 2011

Tomlin, C. (1995). In *The Pesticide Manual*, 10th Edition. British Crop Protection Publications; UK.

Torres, M., Condon, C., Balada, J.-M., Squires, C. & Squires, C. L. (2001). Ribosomal protein S4 is a transcription factor with properties remarkably similar to NusA, a protein involved in both non-ribosomal and ribosomal RNA antitermination. *EMBO J* **20**, 3811-3820.

Turos, E., Shim, J. Y., Wang, Y., Greenhalgh, K., Reddy, G. S., Dickey, S. & Lim, D. V. (2007). Antibiotic-conjugated polyacrylate nanoparticles: new opportunities for development of anti-MRSA agents. *Bioorg Med Chem Lett* **17**, 53-56.

Ulrich, A. S. (2002). Biophysical Aspects of Using Liposomes as Delivery Vehicles. *Bioscience Reports* **22**, 129-150.

van Vliet, A. H. (2010). Next generation sequencing of microbial transcriptomes: challenges and opportunities. *FEMS Microbiol Lett* **302**, 1-7.

Venne, A., Li, S., Mandeville, R., Kabanov, A. & Alakhov, V. (1996). Hypersensitizing effect of pluronic L61 on cytotoxic activity, transport, and subcellular distribution of doxorubicin in multiple drug-resistant cells. *Cancer Res* **56**, 3626-3629.

Venugopal, J., Prabhakaran, M. P., Low, S., Choon, A. T., Zhang, Y. Z., Deepika, G. & Ramakrishna, S. (2008). Nanotechnology for nanomedicine and delivery of drugs. *Curr Pharm Des* **14**, 2184-2200.

Veronese, F. M. & Mero, A. (2008). The Impact of PEGylation on Biological Therapies. *BioDrugs* **22**, 315-329.

Versalovic, J., Koeuth, T., Britton, R., Geszvain, K. & Lupski, J. R. (1993). Conservation and evolution of the rpsU-dnaG-rpoD macromolecular synthesis operon in bacteria. *Molecular Microbiology* **8**, 343-355.

Wallace, H. M., Fraser, A. V. & Hughes, A. (2003). A perspective of polyamine metabolism. *Biochem J* **376**, 1-14.

Wang, Z., Gerstein, M. & Snyder, M. (2009). RNA-Seq: a revolutionary tool for transcriptomics. *Nat Rev Genet* **10**, 57-63.

Warheit, D. B. (2010). Debunking Some Misconceptions about Nanotoxicology. *Nano Lett* **10**, 4777-4782.

Webb, M. S., Boman, N. L., Wiseman, D. J., Saxon, D., Sutton, K., Wong, K. F., Logan, P. & Hope, M. J. (1998). Antibacterial efficacy against an in vivo *Salmonella typhimurium* infection model and pharmacokinetics of a liposomal ciprofloxacin formulation. *Antimicrobial Agents and Chemotherapy* **42**, 45-52.

Weir, E., Lawlor, A., Whelan, A. & Regan, F. (2008). The use of nanoparticles in anti-microbial materials and their characterization. *Analyst* **133**, 835-845.

Wertheim, H. F. L., Melles, D. C., Vos, M. C., van Leeuwen, W., van Belkum, A., Verbrugh, H. A. & Nouwen, J. L. (2005). The role of nasal carriage in *Staphylococcus aureus* infections. *The Lancet Infectious Diseases* **5**, 751-762.

Wick, L. M., Qi, W., Lacher, D. W. & Whittam, T. S. (2005). Evolution of genomic content in the stepwise emergence of *Escherichia coli* O157:H7. *J Bacteriol* **187**, 1783-1791.

Wilhelm, B. T. & Landry J. R. (2009). RNA-Seq-quantitative measurement of expression through massively parallel RNA-sequencing. *Methods* **48**, 249-257.

Williams, R.O. & Vaughn., J.M. (2006). Nanoparticle Engineering. In *Encyclopedia of Pharmaceutical Technology*, pp. 2384-2398. Informa Healthcare.

Wilson, W. W., Wade, M. M., Holman, S. C. & Champlin, F. R. (2001). Status of methods for assessing bacterial cell surface charge properties based on zeta potential measurements. *J Microbiol Methods* **43**, 153-164.

Yoder-Himes, D. R., Chain, P. S., Zhu, Y., Wurtzel, O., Rubin, E. M., Tiedje, J. M. & Sorell, R. (2009). Mapping the *Burkholderia cenocepacia* niche response via high-throughput sequencing. *Proc Natl Acad Sci U S A* **106**, 3976-3981.

Yu, L. (2001). Amorphous pharmaceutical solids: preparation, characterization and stabilization. *Adv Drug Deliv Rev* **48**, 27-42.

Zhang, Y., Bai, Y. & Yan, B. (2010a). Functionalized carbon nanotubes for potential medicinal applications. *Drug Discov Today* **15**, 428-435.

Zhang, L., Gu, F. X., Chan, J. M., Wang, A. Z., Langer, R. S. & Farokhzad, O. C. (2008b). Nanoparticles in medicine: therapeutic applications and developments. *Clin Pharmacol Ther* **83**, 761-769.

Zhang, H., Hussain, I., Brust, M., Butler, M. F., Rannard, S. P. & Cooper, A. I. (2005). Aligned two- and three-dimensional structures by directional freezing of polymers and nanoparticles. *Nat Mater* **4**, 787-793.

Zhang, L., Pornpattananangkul, D., Hu, C. M. & Huang, C. M. (2010b). Development of nanoparticles for antimicrobial drug delivery. *Curr Med Chem* **17**, 585–594.

Zhang, H., Wang, D., Butler, R., Campbell, N. L., Long, J., Tan, B., Duncalf, D. J., Foster, A. J., Hopkinson, A., Taylor, D., Angus, D., Cooper, A. I. & Rannard, S. P. (2008a). Formation and enhanced biocidal activity of water-dispersable organic nanoparticles. *Nat Nanotechnol* **3**, 506-511.

Zheng, W., Chung, L. M. & Zhao, H. (2011). Bias detection and correction in RNA-Sequencing data. *BMC Bioinformatics* **12**, 290-304.

Zhou, X., Park, J.-Y., Huang, S., Liu, J. & McEuen, P. L. (2005). Band Structure, Phonon Scattering, and the Performance Limit of Single-Walled Carbon Nanotube Transistors. *Physical Review Letters* **95**, 146805-146809.

Zhu, Y., Weiss, E. C., Otto, M., Fey, P. D., Smeltzer, M. S. & Somerville, G. A. (2007). *Staphylococcus aureus* biofilm metabolism and the influence of arginine on polysaccharide intercellular adhesin synthesis, biofilm formation, and pathogenesis. *Infect Immun* **75**, 4219-4226.

Zou, Y., Ma, H., Minko, I. G., Shell, S. M., Yang, Z., Qu, Y., Xu, Y., Geacintov, N. E. & Lloyd, R. S. (2004). DNA damage recognition of mutated forms of UvrB proteins in nucleotide excision repair. *Biochemistry* **43**, 4196-4205.

Appendix 1

Average determined MIC values in *S. aureus* SH1000 against average nanoparticle ciprofloxacin size and zeta potential.

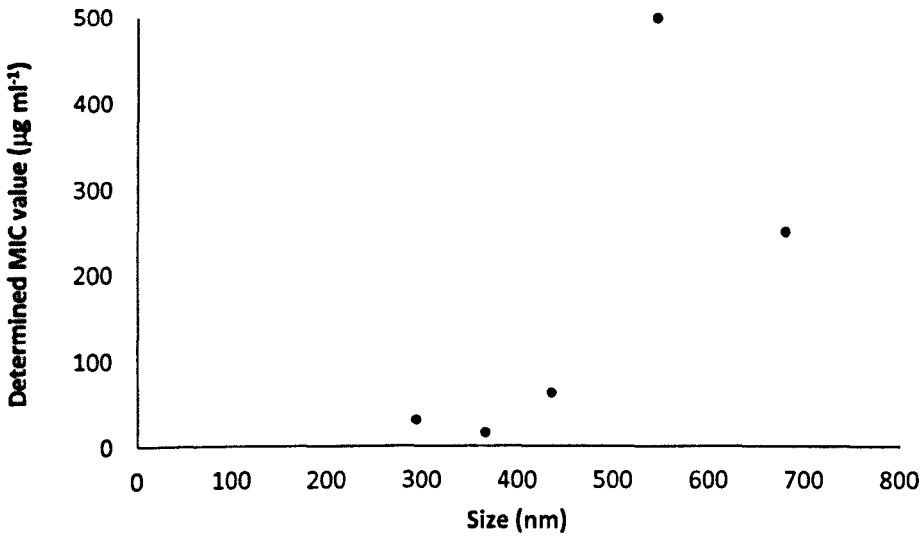
Determined MIC value (μg ml-1)
500
400
300
200
100
0
0
100
200
300
400
500
600
700
800
Size (nm)

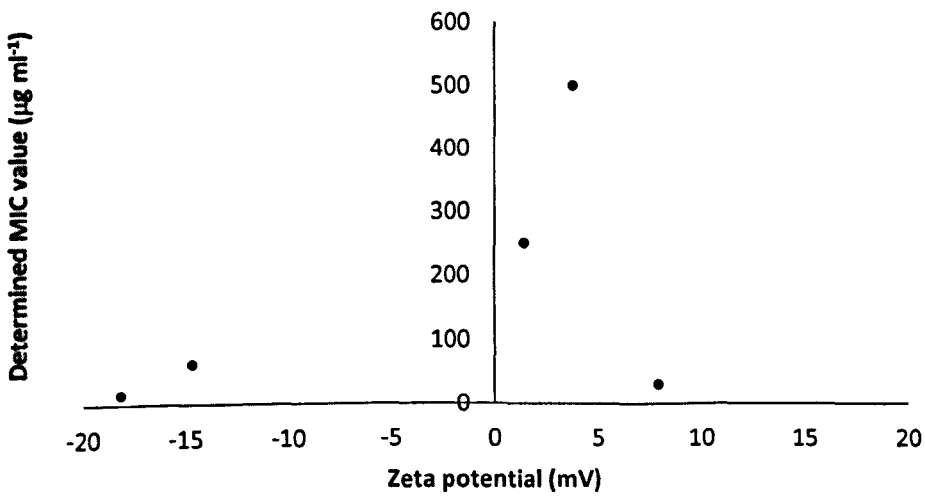
Determined MIC value (μg ml-1)
600
500
400
300
200
100
0
-20
-15
-10
-5
0
5
10
15
20
Zeta potential (mV)

Appendix 2

Average determined MIC values in *S. aureus* SH1000, MRSA-252, *C. albicans* and *E. coli* against average nanoparticle dichlorophen size and zeta potential.

S. aureus SH1000

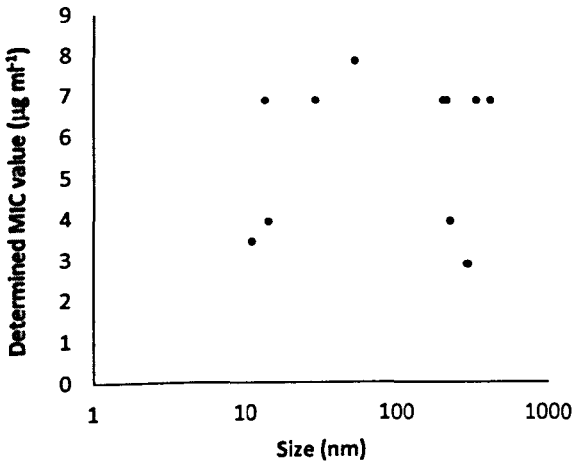

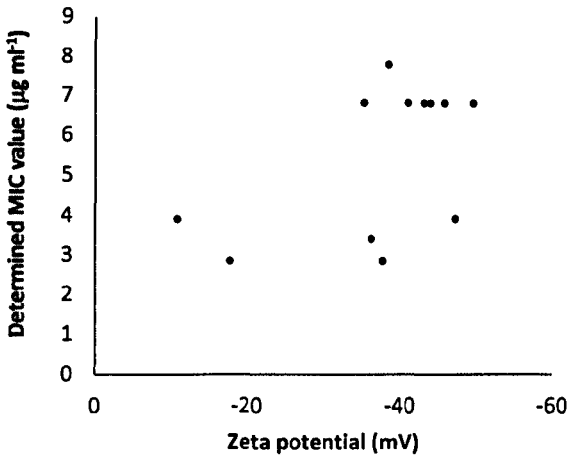

MRSA-252

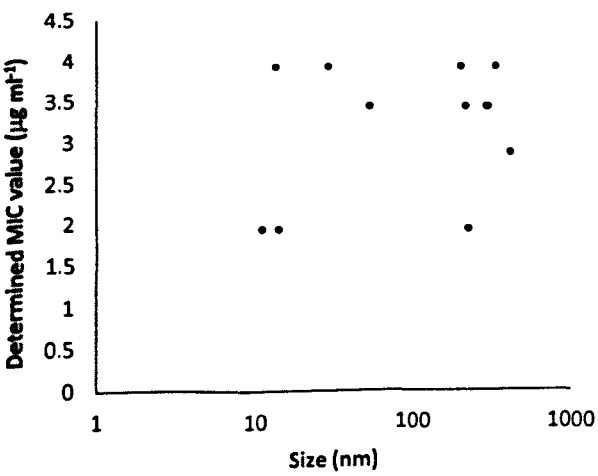

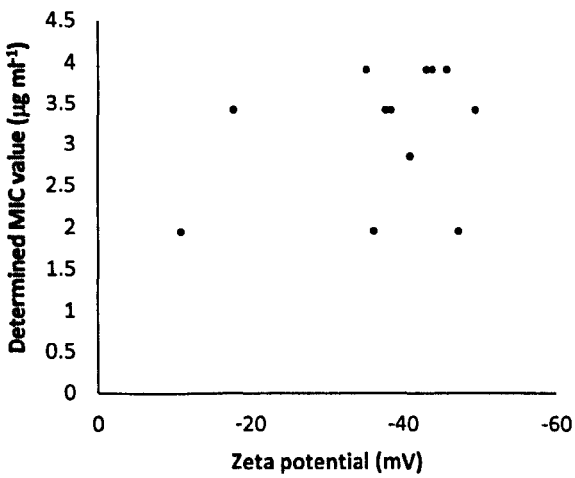

C. albicans

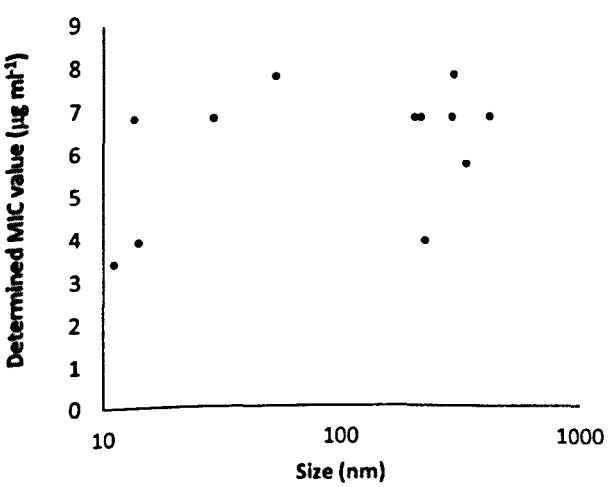

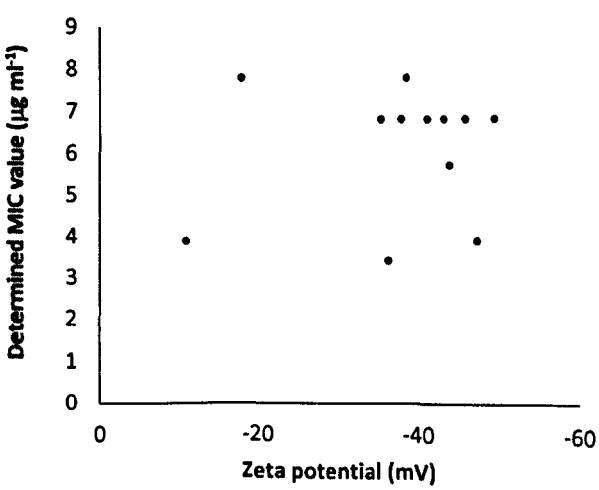

E. coli

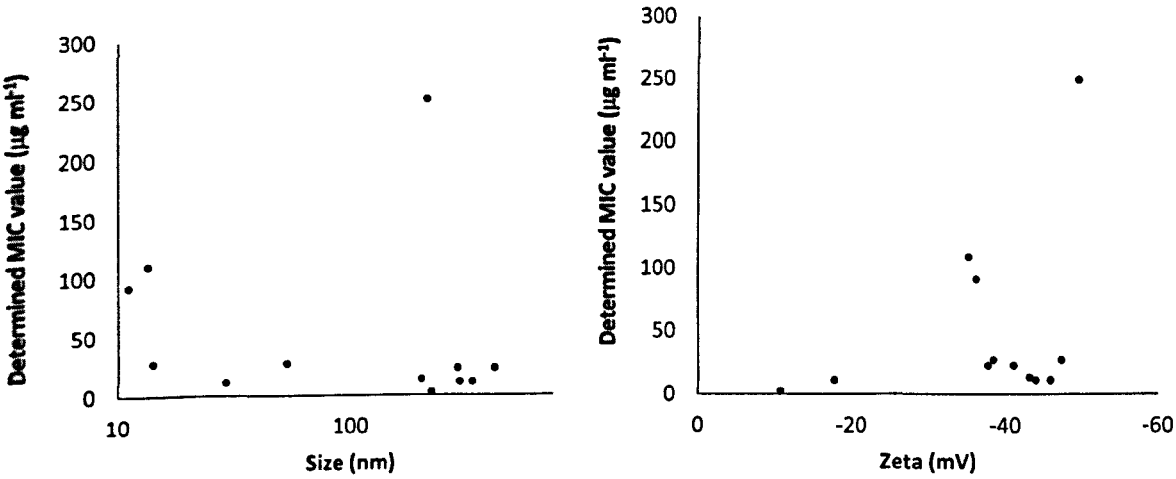
Determined MIC value (µg ml-1)
300
250
200
150
100
50
0
10
100
Size (nm)
Determined MIC value (µg ml-1)
300
250
200
150
100
50
0
0
-20
-40
-60
Zeta (mV)